UNIVERSITY OF
LINCOLN

School of Architecture and the Built Environment

Impact of Urban Built Form and Urban Density on Building Energy Performance in Different Climates

Ehsan Ahmadian

A thesis submitted in partial fulfilment of the requirements of the University of Lincoln for the degree of Doctor of Philosophy

July 2021

Abstract

Cities are recognized as the main consumers of energy on the planet, and to optimize their energy consumption and enhance the potential of using renewable energy sources, built form and density are considered highly influential factors. The energy efficiency of compact built forms has been debated by many studies. Meanwhile, urban density, as an attribute of urban form, has yet to be well defined due to the diversity of density indicators used in literature. Hence, there is a lack of integrated guidelines for urban density indicators and their relationships with urban built forms in urban energy studies.

This thesis establishes a framework to demonstrate the inter-correlation of urban built form, density and energy for residential buildings, and the impact of climate as an influential parameter is investigated by adopting a mixed methods research approach. It primarily identifies the relationship between the urban built form and density by introducing a novel indicator of urban form termed the *Form Signature*. It demonstrates the simultaneous correlation of two selected density indicators with influential variables developed from the geometry of four selected urban built forms. An urban energy simulation software package, CitySim, is adopted to conduct sensitivity analyses. The simulation models are validated against data from a known building group. An energy indicator, termed *Energy Equity*, is also introduced that simultaneously considers the amount of building energy demand as well as energy generation by building-mounted PVs.

Cross case study analysis is undertaken to examine the impact of climate on urban energy performance, where four cities (London, Singapore, Helsinki and Phoenix) are chosen based on the specific climatic criteria. Meteonorm software is adopted to generate climate file relating to each case study. The investigation is further complemented by analysing future scenarios to examine the impact of climate change and technological developments (i.e. the penetration of EVs into the transportation sector) on the energy efficiency of urban areas of the future.

Graphical results of the *Form Signature* indicator prove that the term ‘high density’ is crucially dependent on the definition of the density indicator. The resulting graphs provide a robust platform for the analysis of contexts such as climate, economy, social issues and energy. Overlaying results of building energy simulations over the *Form Signature* graphs indicates the relationship of energy with urban built form and density.

Results show that buildings with a greater number of storeys and greater plan depth (equivalent to low values of plot ratio and variable values of site coverage) have lower energy demand. When PV generation is also considered, low number of storeys and great plan depth can improve the energy performance of buildings (equivalent to low plot ratio and high site coverage). Having identical geometric variables, tunnel-court form (that is introduced in this study) provides the greatest density while pavilion form provides the lowest (~80% lower than tunnel-court). The energy performance of tunnel-court form is also the highest in all considered climates, while pavilion form shows the lowest energy performance (between 27% and 67% for cooling-dominated buildings and between 7% and 32% for heating-dominated buildings). Nevertheless, if density remains constant and geometric variables are changed, the opposite becomes true. An important conclusion is that the site plans with similar built forms and densities may have different energy performance since the same value of density can be achieved by different combinations of geometrical variables.

Increasing the cut-off angle reduces building energy demand in cooling-dominated buildings (i.e. in Singapore and Phoenix) between 6% and 56%, while increase building energy demand in heating-dominated buildings (i.e. in London and Helsinki) between 2% and 16.5%. Therefore, increasing density through cut-off angle is not always energy efficient as it depends on climate. In general, building energy demand in London is the lowest among the case studies, while it is the highest in Singapore (up to 219% higher than London). London also shows the highest value of Energy Equity (demonstrating the best energy performance) and Helsinki shows the lowest (up to 51% lower than London). Considering future scenarios, the total building energy demand in 2050 will be 48% higher than at present, on average. A recommendation for future urban planning in London, for instance, is that court and tunnel-court forms will be more energy efficient, and possessing a lower number of storeys, small cut-off angle and greater plan depth will further improve their energy performance and reduce their emissions.

The holistic outcome of this study provides urban energy planning guidelines that can be used by various stakeholders in the built environment.

Acknowledgement

I would like to deeply thank my supervisory team, Prof. Behzad Sodagar, Prof. Chris Bingham and Dr Amira Elnokaly, for their continuous support and insightful guidance during my PhD. I must also thank my ex-supervisors Prof Glen Mills and Dr Argyrios Zolotas who played key roles during their supervisory period, specifically Prof Glen Mills who continued his support after his return to South Africa. All of them made an eminent contribution to my research career that along with their impressively kind and respectful behaviour made me feel to be one of the luckiest students in the world.

Acknowledgement is also dedicated to Dr Phil Ashheton from the Math and Statistics Centre (Mash) of the University of Lincoln for his contribution to developing the MATLAB codes required for computer simulations.

I would also appreciate Prof. Hugh Byrd for his valuable advice at the beginning of my PhD that helped me to kick off my PhD journey.

Finally, I would like to thank my lovely family and proudly dedicate this thesis to my late mother's soul for her endless love, support, and the sacrifices that she has made on my behalf. As a teacher, she was always keen on education and would have been proud of her son awarded a PhD degree. She strongly founded the basis of success in every aspect of my life. I am greatly indebted to her and yearning to have her with me at this moment, though I always feel her presence in every big moment of my life.

List of publications stemming from work undertaken in this thesis

Journal papers

- Ahmadian E, Sodagar B, Bingham C, Elnokaly and Mills G (2021). Effect of urban built form and density on building energy performance in temperate climates, *Energy and Buildings*. In press.

- Ahmadian E, Sodagar B, Mills G, Byrd H, Bingham C and Zolotas A. (2019). Sustainable cities: The relationships between urban built forms and density indicators, *Cities*. 95.

- Ahmadian E, Byrd H, Sodagar B, Matthewman S, Kenney C and Mills G. (2019). Energy and the form of cities: the counterintuitive impact of disruptive technologies. *Architectural Science Review*. 62, 145-151.

Conference papers and presentations

- Ahmadian E, Sodagar B, Mills G and Bingham C. (2019). Correlation of urban built form, density and energy performance. *Journal of Physics: Conference Series,* 1343. *CISBAT 2019* | *Climate Resilient Cities – Energy Efficiency & Renewables in the Digital Era.* 4-6 September 2019, EPFL Lausanne, Switzerland

- Ahmadian E, Sodagar B, Mills G and Bingham C. (2019). Sustainable cities: a platform for connecting density with energy performance of urban areas. Presentation and abstract *in proceeding of 8th Global Conference on Global Warming (GCGW-2019)*. 22-25 April 2019, Doha, Qatar

Table of Contents

List of Figures

List of Tables

Chapter 1: Introduction

1.1 Background and problem identification

More than 50% of the world's population live in urban areas, and this is predicted to reach 66% by 2050 (United Nations, 2014). This rate of urbanization requires a city the size of Birmingham (UK) to be built each week for the next 20 years across the globe (Farrell, 2014).

Cities are the main consumers of energy on earth, amounting to 78% of total consumption and contributing to more than 60% of greenhouse gas emissions (United Nations). This is considered the main contributor to global temperature increases that is leading to extreme weather events (such as drought, heat waves, heavy rain and wildfires) (Houghton, 2009, Masson-Delmotte et al., 2018), acid rains, loss of habitable lands (Mann, 2009), famine, and pushing more than 100 million people into poverty (Lekwot et al., 2012, Masson-Delmotte et al., 2018). Hence, action has to be taken to mitigate the harmful effects of this massive amount of energy consumption.

Energy consumption in cities is due to a variety of factors, such as transportation, building (domestic and non-domestic), industry (e.g. food production), service and commercial activities. Their energy demands vary depending largely on climate, energy technologies and urban form. Hence, the form of the city has an impact on its energy usage (Delmastro et al., 2015, Rickwood et al., 2008, Steemers, 2003). However, urban form has a variety of attributes such as density, compactness, diversity, green areas, connectivity, orientation, shading and passivity that influence energy utilisation (Silva et al., 2017). In identifying the relationship between energy and urban form, the primary parameter analysed by researchers is density (Bhiwapurkar, 2014, Resch et al., 2016, Steemers, 2003). Rafiee et al. (2019) used density to show that buildings with higher numbers of housing units and less exposed perimeters have lower heating demand. Leng et al. (2020) adopted some of density indicators to illustrate the relationships of urban morphology with building heating demand. Mauree et al. (2017) demonstrated that building density can significantly impact on wind speed and air temperature in an urban setup that influence building energy demand. In addition to density, there is another urban parameter that can influence building energy demand, which is urban built form. Urban built form represents shape of buildings (e.g. pavilion, court etc.) (March, 1972) which affects environmental performance of buildings (Ratti et al., 2003). Therefore, it is crucial to

consider the urban built form and its impact on microclimatic conditions (Emmanuel and Steemers, 2018) that consequently affect building energy consumption (Lee and Jeong, 2017). There is currently a lack of a unified set of guidelines to communicate urban density indicators and their relationships with urban built forms (Morganti et al., 2012) to investigate their simultaneous correlation with energy (Ahmadian et al., 2019c).

To understand cities, they must not simply be viewed as places in space, but as systems of networks and flows. Flows add up to what happened at locations; therefore, *the whole is more than sum of its parts* (Batty, 2013). Each city can be considered as a complex ecosystem that is a far-from-equilibrium structure (Batty, 2017), which indicates the unstable nature of cities that needs a variety of parameters to be considered simultaneously if they are to be analysed. Parameters such as economy, culture, climate, energy, urban built form and density are all interrelated. They present situations in which several quantities are all varying simultaneously that make cities to be problems in organized complexity (Jacobs, 1961). To accommodate such complexity for future planning of cities, the intercorrelations of all parameters need to be investigated. As Radlin and Hemani (2019) write, '*We have underestimated the complexity of urban areas and treated them as clocks to be mended rather than organisms to be healed*.' This complexity requires holistic planning to facilitate the transition to future energy efficient and low carbon cities (Jank, 2017).

Figure 1.1 shows a '*seed diagram'* to highlight several of these elements (providing network in cities), though there are additional contributions that could also be added (e.g. population). Parameters such as climate, culture and economy historically have influenced the form of traditional cities (Chen et al., 2008, Khalili and Amindeldar, 2014, Stewart, 1999), while they have a direct influence on each other as well. Nevertheless, urban built form and density affect energy consumption (Leng et al., 2020), renewable energy generation (Hargreaves et al., 2017), and even microclimatic conditions (Salvati et al., 2020). Therefore, urban built form and density correlate with a variety of factors, while they both are tightly intercorrelated themselves (Ahmadian et al., 2019c).

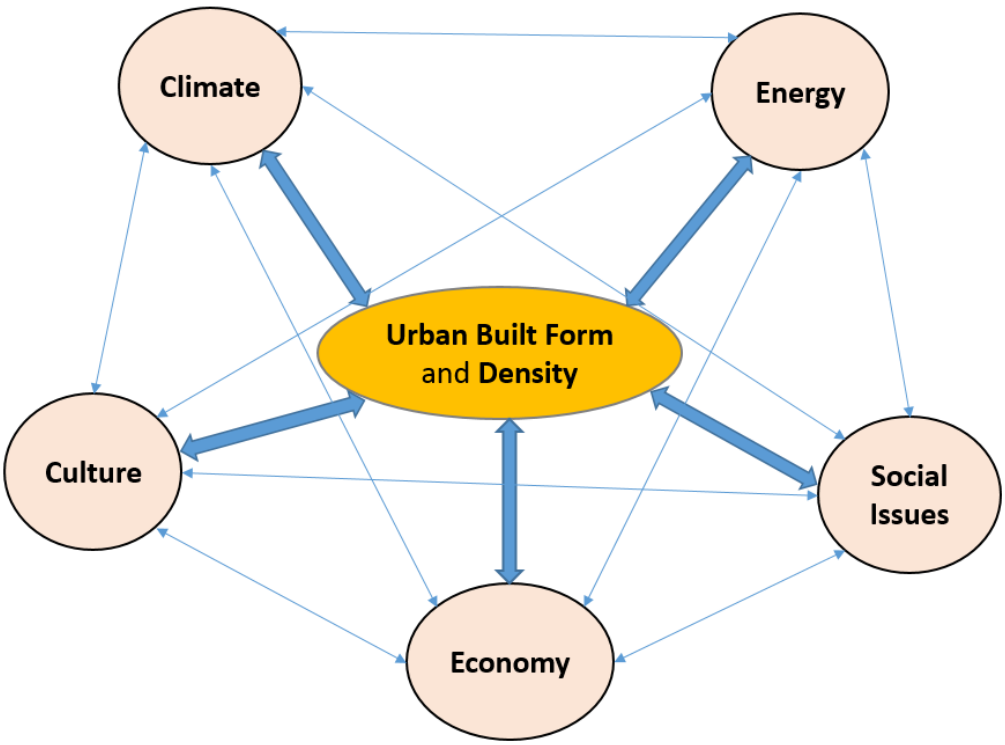

Figure 1.1: Seed diagram showing the correlation of urban built form and density with other elements

As shown in Figure 1.1, many of these parameters are interconnected which escalates the degree of complexity of urban studies and makes it challenging to explore the independent contribution of each element with urban built form. For instance, climatic conditions affect urban energy consumption/generation in urban areas. Tsirigoti and Tsikaloudaki (2018) showed that climate can significantly change the balance of heating and cooling demand of urban blocks, although it does not significantly alter the effect of urban form on energy performance (however, the climate zones of their two case studies were not geographically far from each other). Berger and Worlitschek (2019) demonstrated the impact of future climate change on the pattern of energy consumption in buildings and showed that Heating Degree Days (HDDs) will decrease and Cooling Degree Days (CDDs) will increase in future for a case study in Switzerland. Meanwhile, the economy remains an influential factor on other elements. Delmastro et al. (2015) showed the impact of social and economic inhabitation on the building energy saving potential. The correlation of culture and building energy consumption has also been acknowledged by several studies. Lin et al. (2016) investigated the impact of cultural background on the occupants' energy consumption behavior by adopting eco-feedback technologies, and Stephenson et al. (2010) proposed an Energy Cultures framework for analyzing this relationship. Soflaei et al. (2017) addressed the influence of socio-cultural aspects such as historical

context, language, religions, folk beliefs, values, norms, customs, ideologies, symbols, and even everyday lifestyle on the spatial organization of the traditional courtyard houses. Although many published studies investigated these possible interactions individually, a more comprehensive analysis is required to consider all the elements simultaneously and take into consideration their interconnected influence.

Acknowledging the interconnectivity of these parameters, this study specifically investigates the correlation between urban built form, density, energy and climate. A framework for investigating the impact of climate, economy and social issues on built form and density is proposed in Chapter 3 (section 3.6.2).

It has been reported that compact built form uses less energy both in building (Steadman et al., 2014, Steemers, 2003) and transport sectors (Newman and Kenworthy, 1989b) compared to dispersed cities. Steemers (2003) showed that increasing urban density increases energy use of office buildings because of the reduced availability of daylight. By using the LT method, he shows a sharply increasing trend of lighting energy demand against increasing cut-off angle that makes a significant change in the trend of the total energy balance of the building. Nevertheless, it seems that this result can be argued due to the recent technological development in the lighting industry that has provided high-efficiency lighting systems. Therefore, the contribution of lighting energy demand to the total energy balance of the building is going to be less significant. Steadman et al. (2014) used some indicators of density to demonstrate correlation of urban built form with gas and electricity consumption in buildings, though the definition of density has not been clearly determined in their study. Internationally this has resulted in encouraging compact cities since sprawl is seen as a high energy consumer (Ewing and Rong, 2008, Güneralp et al., 2017). Intuitively, these arguments for a compact urban form appear logical. Reducing the surface area to volume ratio of a building reduces heat loss and hence energy usage of buildings and lowering travel distances results in a reduction of fuel consumption. Combined, these two arguments present a robust case for introducing policies for shaping compact urban form.

Nevertheless, there is emerging evidence challenging these assumptions. Considering the energy supply side in addition to the energy demand side could definitely change the balance of this research area, because by utilization of renewable energy sources as the energy supply, a dispersed urban form can be more beneficial (Byrd et al., 2013). Urban areas are increasingly generating their own

energy from renewable energy sources (Sawin et al., 2013) which require a large surface area that cannot be achieved by compact buildings, such as building mounted PVs (Byrd, 2017, Mohajeri et al., 2016), ground source heat pumps (Echenique et al., 2012, Hargreaves et al., 2017) and biomass (Ghosh et al., 2006). Mohajeri et al. (2016) showed that the potential of building integrated PVs in dispersed neighborhoods is 15% and 17% higher for roofs and facades compared with compact neighborhoods in Switzerland. Hence, in some places the sprawl structure of city has greater advantages compared to the dense urban form due to reachability of renewable energy sources.

Studies on transportation energy consumption have traditionally focused on internal combustion engine vehicles (ICEVs). However, the proliferation of electric vehicles (EVs) and Plug-in Hybrid Electric Vehicles (PHEVs), which are significantly more energy efficient, are replacing ICEVs. The assumption has historically been that the energy supply for both fuel and electricity is from a centralized network rather than generated at point of use sites like photovoltaics (PVs) and solar thermal collectors (STC). There is the possibility of charging EVs from urban roof-mounted PVs (Byrd et al., 2013), which requires larger surface areas provided by roof/wall surfaces in sprawl forms for greater solar energy harvesting.

As shown in Figure 1.2, the majority of the previously discussed studies can be categorized into two main groups i) urban form versus energy demand ii) urban form versus renewable energy generation. The two sides of the energy flows (supply and demand) should not be considered in isolation as they both simultaneously play key roles in the equilibrium, and each side may become more significant as a result of geographical location, climate (Berger and Worlitschek, 2019) and economic situations (Delmastro et al., 2015).

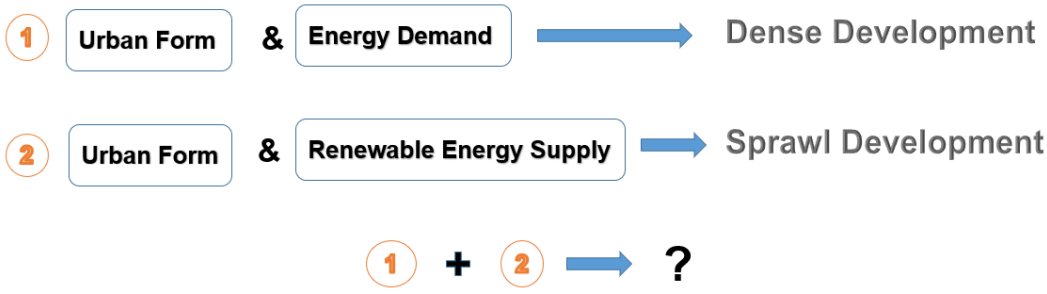

Figure 1.2: Categorization of the studies on urban form and energy

There has been considerable reported research regarding the correlation of energy and urban form. However, there remains issues that require further investigation, for instance:

1. Although density seems to be the most noticeable attribute of urban form in the literature, it has been described in variety of incompatible definitions such as site coverage (Cheng et al., 2006), plot ratio (Rode et al., 2014), volume-area ratio (Javanroodi et al., 2018), building density (Javanroodi and Nik, 2019), open space ratio (Cheng, 2009), BPRU index/compactness index (Steadman, 2014a), surface to volume ratio (Ratti et al., 2005), urban entropy (Mohajeri et al., 2016), form factor (Coccolo et al., 2016) and habitable rooms per hectare (Gordon et al., 2016). This becomes challenging when attempting to compare and contrast the results of different studies (Resch et al., 2016). For instance, Javanroodi and Nik (2019) adopted site coverage and building density for analysing building energy performance in urban areas, while You and Kim (2018) used plot ratio for the same purpose. Therefore, due to different definitions of the adopted density indicators, the comparison of their results is not possible. This is discussed in Chapter 2 (section 2.3). Hence, density needs to be defined in more comprehensive manner, and a single indicator cannot truly determine the definition of urban density (Ahmadian et al., 2019c). Furthermore, no study has examined the effect of urban built form at the same time with density and energy holistically (Ahmadian et al., 2019c). Hence, the relationship of density with urban built form needs to be established in a standard way to acquire a unique structure for future investigations in the relationship of energy and urban form. This is the subject of Chapter 3.
2. Whilst several studies link energy generation to energy demand their analyses are either restricted to ‘building’ scale (Cao et al., 2016, Ferrara et al., 2019), or when considering an ‘urban’ scale they do not focus on the impact of urban built form and density on building energy performance (Kazas et al., 2017, Murray et al., 2020). There are also several studies that focus on the impact of urban form (i.e. density) on building energy consumption (Leng et al., 2020, You and Kim, 2018) or renewable energy generation (Hachem et al., 2011, Hargreaves et al., 2017) separately, and there is little notable research which considers the two simultaneously. In fact, many studies consider cities to be solely energy consumers (Rafiee et al., 2019) and not energy generators,

although not all, for instance (Perera et al., 2019, Waibel et al., 2019), albeit the latter do not consider the effect of ‘urban built form’ and its influential geometrical variables along with density (including more than one indicator with intercorrelation) in their analysis. Therefore, there is a lack of a structure in the literature that is able to connect all the identified parameters with building energy performance and address their simultaneous intercorrelations.

3. Previously reported models have been based on the prevalence of existed technologies and currently available energy sources. There are very few studies that consider the effect of urban form on both building and transportation energy of the cities at the same time, and if so, they considered ICEVs (Hukkalainen et al., 2017, Resch et al., 2016). However, as disruptive technologies like EVs are penetrating into normal life in the cities, it is arguable that the policy on urban form should be based on the technologies of the future rather than the present and past. Disruptive technologies are either a new technology or a new combination of existing technologies that can cause major technology product paradigm shifts or create entirely new ones (Kostoff et al., 2004).

In this study, the intercorrelation of urban built form, density, energy and climate will be explored in detail. In addition, the effect of disruptive technologies on future city forms is examined. Furthermore, a structure is proposed for future studies on other elements such as economic and social issues. This will provide more insight to the current study and facilitate the achievement of sustainable cities.

1.2 Research hypothesis and question

The hypothesis is that energy use is not simply the sum of energy flows in the various parts of a city but that urban form has an energy signature. Hence, the main research question is:

What is the relationship between urban built form, density and energy flows in cities with different climates?

Answering this question will be vital in the future shape of our cities as they are growing rapidly as a result of further urbanization (United Nations, 2014) and their energy consumption is sharply increasing (Sugahara and Bermont, 2016). Hence, it is crucial to design new buildings/districts in an energy efficient manner.

1.3 Aim and objectives

The aim of this study is to establish a framework to demonstrate the intercorrelation between urban built form, density and energy in different climates. In light of the identified aim the objectives of this study are:

1. To critically identify the relationship between the urban built form and density
2. Identification of the influence of urban built form and density on the overall energy consumption in the city
3. Identification of the potential of utilizing renewable energies in the areas with different urban built forms and densities
4. To identify the effect of climate on the above-mentioned parameters
5. To assess the impact of future scenarios such as climate change and penetration of EVs on the energy consumption and form of the cities

Finally, the developed models provide a decision-making tool/guideline to assist city planners and policy makers to design new urban districts in an energy efficient manner. The final result is a graphical model to illustrate the inter-dependencies between urban built form, density and energy. The outcome has a potential of becoming digital with the intention of making it internationally available for further research.

1.4 Methodology

The study adopts a mixed research method approach (Creswell and Tashakkori, 2007) composed of qualitative, empirical/correlational and quantitative techniques, as shown in Figure 1.3.

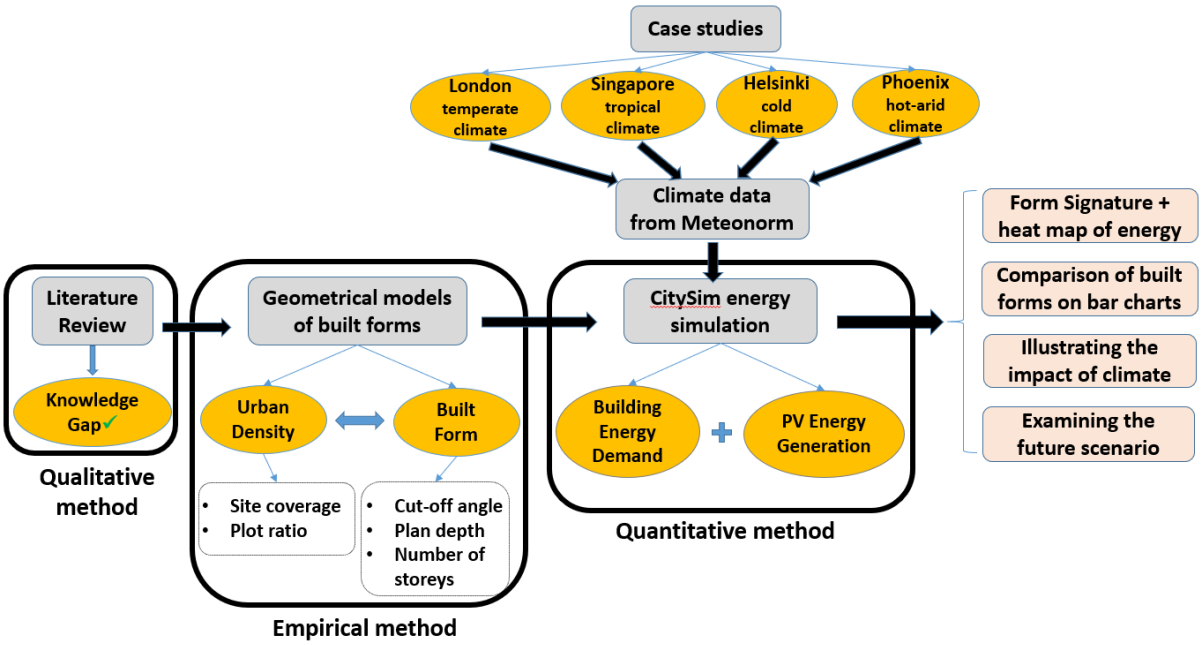

Figure 1.3: Methodological scheme of the study

Initially, a critical literature review is undertaken to compare and challenge previous studies in the literature. This is the qualitative part of the methodology as in some cases the outcomes are reproduced in this study whilst considering more recent condition and technological development. Furthermore, a comprehensive literature review on the 'urban density indicators' used in previous studies on the relationships of energy and urban form, is done. It not only demonstrates the effect of choice of density indicator on the outcome of the study, but also investigates the mathematical and physical relations of different indicators in order to select the two most appropriate ones for this PhD. These are highlighted in Chapter 2.

The empirical part of the method is made in Chapter 3 to establish the correlation of urban built form and density. The study analyses four different urban built forms (i.e. pavilion, terrace, court and tunnel-court form) to develop the geometrical models of them and derive their governing equations. The equations relate built forms geometrical variables (i.e. building plan depth, number of floors and cut-off angle) to two selected density indicators (i.e. site coverage and plot ratio). Excel spreadsheets are developed from the equations to generate underpinning data for each case. The output data is presented in a suite of graphs, called *Form Signature*, which demonstrates the correlation of each urban built form with urban density. This is a correlational method to critically inspect the relationship of the influential variables that relates geometry of built form to urban density. To demonstrate the practicality and validity of the proposed *Form Signature* tool, 32 case studies from 19 cities around the

world were selected. They were shortlisted from variety of climatic conditions aiming to determine the possible correlation of climate with form and density of built environments. The form and density of selected case studies were recognized and calculated, and the equivalent point of each case was identified on the *Form Signature* graphs. It not only proves the validity of the tool, but also proposes a procedure for future statistical analysis to explore the relationships between climate, urban built form and density.

The quantitative method of this study is done using simulation studies in Chapters 5, 6 and 7. The logic of choosing simulations is to conduct sensitivity analyses in order to separately clarify the influence of each parameter on the outcome of the analysis. It facilitates a *real* comparison of site plans with different forms and densities. In this way, the effect of other factors such as building type, size and age, people behavior, single, double and triple glazed window, and building energy system (centralized or decentralized, air-conditioning or solely heating, DHN and so on) is eliminated. While in case of using a monitored consumption data, there are many factors that undeniably affect the results of this comparison. Moreover, simulation expedites the study of future scenarios. For the simulation trials, the standard energy demand of a building is considered instead of considering the fuel consumption. For the purpose of this study, the type of all buildings is solely equivalently considered to be housing, since residential buildings have the biggest contribution of building energy demand worldwide (Abergel et al., 2019, Kalua, 2020). It should be noted however, that the same method can be used for analysing non-domestic buildings with different occupancy and usage profiles. The selected software for this study is CitySim, which is an 'urban energy simulation package'. It was selected due to its capabilities to perform energy analysis at an urban level rather than building level. It is able to consider parameters such as shadowing effects as well as inter-reflection between external surfaces in built environment. The simulation model is validated against a group of buildings located in Gainsborough (UK) and the results compared with those from the Standard Assessment Procedure (SAP), a national procedure widely used in the UK (see section 4.2.3).

Cross case study analysis is undertaken to examine the impact of climate on urban energy performance, where four cities with different climatic conditions are considered as case studies. They are selected primarily based on the classification of the world climate zones. To this end, the Köppen climate classification system (Peel et al., 2007)

is chosen which divides the earth into five main climatic zones (i.e. Tropical, dry, temperate, cold and polar). The proposed cities are selected so as to represent each of the main climate zones, which are London (temperate), Singapore (tropical), Helsinki (cold) and Phoenix (hot-arid). The second criteria for choosing the case studies is the availability of data as well as magnitude and importance of the city. All are big cities (including three capital cities) with considerable potential of energy optimization for current and future developments. They are outlined in Chapter 6. Meteonorm software is adopted to generate climate and horizon files for each case study. The software considers 10 years average temperature data and 20 years average radiation data for any specific location on the earth.

CitySim simulates building energy demand (heating, cooling, lighting and appliances) as well as solar energy generation (from roof-mounted PVs). To accommodate the parameters simultaneously, an energy indicator called *Energy Equity* is introduced showing the ratio between PV energy generations over building energy consumption. In case of having *Energy Equity* equal to one, the building (or district) is energetically self-sufficient.

Models of each urban built form with different densities (which is changed by changing geometrical variables) are drawn in AutoCAD. This provides a variety of site plans for input to energy analyses. The AutoCAD files are imported into CitySim. Simulations trials are executed for each of the models of the selected urban built forms, while for each case study, its specific climate and location data is used (see Figure 1.3). MATLAB code is written to analyze the simulation data derived from CitySim. The generated data is stored in an Excel sheet. Custom MATLAB code is written to generate ‘heat maps’ on the graphs from the previous analyses. This heat map shows the intensity of energy consumption/generation by buildings on the *Form Signature* graphs. Hence, existing patterns of energy consumption/supply versus built form and density in these cities are identified. Furthermore, the comparison of the energy performance of the selected built forms are presented in bar charts and tables.

The final part of the study explores the influence of future scenarios such as global warming, penetration of electric vehicles in the market and charging EVs by roof-mounted PVs, on the form of the urban areas. To predict future energy performance of the cities, global warming scenarios defined by IPCC are generated by Meteonorm software that are inserted into CitySim as climate files.

1.5 Innovation and contribution to knowledge

The notion that energy flows can be related to overall urban form is a new area of research that requires further investigation. This study offers a novel way of analyzing urban built form and density that will integrate building energy use, renewable energy supply and account for disruptive technologies by considering penetration of EVs into the market. It also challenges the assumptions that are built into these current models.

The novel contributions presented in this thesis are as follows:

- Establishing the correlation of urban built form and density (using two density indicators) by taking into consideration all the influential geometric parameters; namely plan depth, cut-off angle and number of storeys by introducing a new indicator called *Form Signature*.
- Introducing a built form termed 'tunnel-court' that is able to reach highest density compared to other selected built forms while achieving a high energy performance.
- Introducing an energy indicator termed *Energy Equity* representing the self-sufficiency of buildings.
- Simultaneous consideration of both supply and demand sides of energy flows in the city in relation to urban built form and density.
- Investigating the effect of future scenarios on the urban built form and density instead of current situation. This takes into consideration the impact of 'disruptive technologies' such as photovoltaics, electric vehicles, smart grids and blockchain energy supply. This leads to the recommendation of the best built form and geometry for the future of London to reach the highest energy performance.

The models correlate urban built form, density and energy by considering such variables as: building height, plan depth, cut-off angle, site coverage, plot ratio, extent of PVs, climatic conditions, EVs market penetration and many other factors concerning energy supply and demand. Finally, the models can be used by researchers, local government, urban designers/planners and engineers in order to contribute to a wider debate on the form of sustainable cities.

1.6 Structure of the thesis

This thesis consists of eight chapters and Figure 1.4 illustrates a holistic view of the thesis structure:

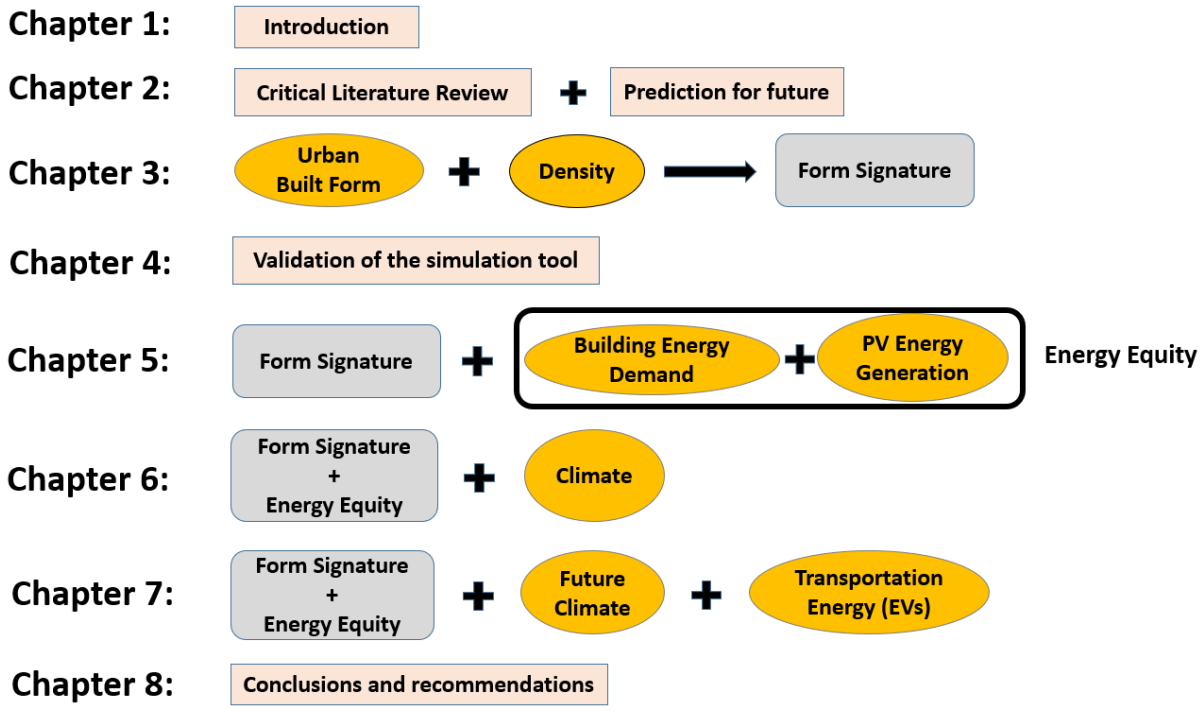

Figure 1.4: The structure of the thesis

Chapter 2: An extensive literature review that shows the gap in existing knowledge including many references for different aspects of this research to show the reliability of the study. This chapter reviews the historical research that has led to widespread policies on compact urban form, in particular, residential development, and collates evidence that demonstrates that dispersed urban form may be more energy efficient than compact form. The increased use of distributed energy generation in urban areas (generally roof-mounted PVs), the growth in ownership of electric vehicles and the potential introduction of smart and micro-grids and the possibility of virtual power plants is changing the impact that energy has on built form. Moreover, it is shown that how choosing a variety of density indicators by different studies makes it challenging to compare and interpret their results.

Chapter 3: Introduces a novel indicator of urban built form termed *Form Signature*. Generic models of four urban built forms are developed including pavilion, terrace, court and a newly introduced tunnel-court which are used to compare and contrast their land-use performance and density characteristics. The simultaneous relationship to each of the considered urban built forms with the two chosen density indicators is shown graphically with the three geometric parameters as the variables. For existing urban areas, the resulting graphs provide a robust tool for statistical analysis of contexts such as climate, economy, energy and crime potential and establish their relationship to built form and density. To show the value of the contribution, 32 case

studies from 19 cities in different global locations are analysed. For the planning of future urban areas, the resulting relationships provide an application-oriented urban planning tool to facilitate the most effective land-use method for promoting more sustainable cities. Examples showing the potential of the tool for future statistical energy and social analysis of urban areas are provided.

Chapter 4: This chapter explains the selection criteria for choosing the urban energy simulation tool (CitySim software) and discuss its advantages and limitations. It also demonstrates the validity of using CitySim for these studies by comparing its outputs against the available energy data of four buildings obtained by SAP analysis.

Chapter 5: Having developed the *Form Signature* graphs in Chapter 3, energy analysis is performed on geometrical models using CitySim. The City of London, representing a temperate climate, is considered as a case study to enter its climate file into the simulation software. An energy indicator called *Energy Equity* is introduced in this chapter which represent the ratio between PV energy generations over building energy consumption. The analysis is undertaken for all the built forms presented in Chapter 3. Graphical results provide urban planning guidelines to facilitate the identification of the most energy-efficient built form and density.

Chapter 6: The influence of climatic conditions on the relationship of energy with urban built form and density is taken into account in this chapter by considering three other cities with different climates, namely Singapore (hot and humid climate), Phoenix (hot and arid climate) and Helsinki (cold climate).

Chapter 7: This chapter considers the future climatic conditions in 2050, according to IPCC scenarios, along with the penetration of EVs into the transportation system due to the technological developments. To cater for future scenarios, it is assumed that people use EVs for transportation and charge them from building-mounted PVs using blockchain technology. The results, showing the impact of the future scenario on building energy performance, urban built form and density, are compared with the results obtained in Chapter 5 to identify the difference of the current and future scenarios. A recommendation for the efficient built form and density in the future of London is provided.

Chapter 8: Presents conclusions from the thesis and recommendations for urban planning/policymaking and also for future work.

Chapter 2: Review of current literature and prediction of future

2.1 Introduction

This chapter focusses on energy as a determinant of built and urban form and challenges the idea that a compact urban form is more energy efficient and that the results can be almost universally applied. There are other reasons for development of cities with compact urban form, such as the loss of agricultural land, loss of wildlife habitats, cost of infrastructure or topographical reasons. However, these tend to be specific to a given location.

The energy use of a city is dependent on both buildings and transport (Rickwood et al., 2008, Steemers, 2003) in varying amounts depending largely on climate, energy technologies and urban form. Traditionally this has focused on the heat loss from the fabric of buildings and internal combustion engine vehicles (ICVEs). The assumption has been that the energy supply for both electricity and fuel is from a centralized network rather than generated at point of use, and the logical conclusion of these assumptions has been that a compact city will consume less energy than a dispersed city. This is because buildings will use less energy as there is a reduced ratio of surface area to volume of the building fabric where energy flows from (Ewing and Rong, 2008, Joiner, 2010, Rode et al., 2014) and travel distances will be less (Guhathakurta and Williams, 2015, Newman and Kenworthy, 1989b).

As a result, compact urban areas have been extensively promoted (Breheny, 1995). This impacts on urban form since compactness normally requires containment at the peripheries that often result in built forms of greater height (which is not always the case, as will be further discussed). Therefore, urban form may have two basic shapes: compact cities, which tend to expand upwards, while dispersed cities expand outwards. Cities that expand upwards generally have a higher population density than cities that expand outwards (sprawl). In fact, cities are affected by two main forces which are ‘centrifugal forces’ (e.g. using private vehicles) and ‘cohesive forces’ (e.g. access to central facilities) (Margalit, 2016). There are secondary considerations for urban form that impact on energy use such as the density of sprawl, the proximity of buildings to each other and whether a city is mono or polycentric.

Furthermore, some studies confused ‘built form’ with ‘building type’ which questions the validity of the comparison they made to investigate the relationship between energy and urban form.

This chapter also shows the different urban form attributes and shows that only one of them is density. Then, it describes a variety of density indicators. Comparative analysis of the indicators demonstrates that they can be a source of confusion in the studies investigating the relationship of urban form and energy. Therefore, it is recommended in this chapter that more than one density indicator should be used to provide a comprehensive structure for urban energy analysis.

It should be mentioned that building energy performance and its correlation with urban form is affected by climate. Therefore, attention should be paid to generalising the results from different studies. This will be extensively examined in Chapter 5 and 6 by investigating the case studies from different climates. In this chapter, the climate category of the important studies from the literature are mentioned to avoid confusion.

2.1.1 Urban form, building type and building height

Case studies on housing in different countries are discussed below to compare energy use with the height of residential buildings (see section 2.2.1). The studies do not practically compare energy with density simply because a site plan with higher buildings does not necessarily achieve higher density as this depends on many factors such as plan depth and distance between buildings (that is defined by cut-off angle) (see Chapter 3). This is a field that requires further investigation but is complicated since greater density can be achieved by reducing housing unit sizes. Going upward or outward has an implicit assumption that residential unit sizes will be approximately the same in both cases. However, relatively high density can be achieved with low/medium rise, compact buildings and further evidence on energy use of large samples of these buildings is required. The results of the '*High-Rise Buildings: Energy and Density'* research project show that higher office buildings consume more gas and electricity, while higher residential buildings only consume more gas that is mainly used for heating in the UK (Godoy-Shimizu et al., 2018, Hamilton et al., 2017). They used actual annual metered consumption data of the selected buildings in England and Wales, which may result in having less control on the other influential geometric parameters, such as plan depth and cut-off angle. To have suitable control on these parameters, in this thesis, a simulation method is used for conducting energy analysis.

Furthermore, in the above-mentioned project, it was demonstrated that achieving higher density is not necessarily realised by having high-rise buildings, it can also be achieved by low-rise buildings by changing their built form. This is extensively investigated in Chapter 3 by considering the simultaneous impact of the built form and urban geometric variables on urban density and consequently energy use.

Furthermore, many studies consider 'building types' for comparison (e.g. Heinonen and Junnila (2014)). Again, this neither means urban form nor density. Urban form has a variety of attributes of which density is only one. This will be discussed in section 2.3. Building type is identified in two kinds of similarities according to Steadman et al. (2014); i) similarities of 'use' and 'activity' (e.g. housing, school) ii) and similarities of 'forms' (e.g. pavilion or terrace built form). '*Space is a shape, and function is what we do in it'* (Hillier, 2007). Some studies compare buildings such as detached, semi-detached and high-rise and name them as building types; although they are definitely not classed as built form (or even urban form) since each detached, semi-detached and high-rise building may have pavilion or any other form. The difference can be dimensions and the number of units inside them (e.g. apartments). Hence, a multi-unit building is a building with more than two units inside regardless of the built form. Then, if it is residential, it is called an apartment.

2.1.2 Intuitive and counter-intuitive impacts

Intuitively, the arguments for a compact urban form appear logical. Reducing the surface area to volume ratio of a building reduces heat loss and hence energy usage of the buildings, and reduced travel distances result in a reduction of fuel consumption. Combining these two arguments presents a robust case for introducing policies that promote compact urban form.

However, there is emerging evidence that this is not necessarily the case and that a dispersed urban form may be more energy efficient (Hargreaves et al., 2017). This chapter reviews both the historical research supporting compact urban form policy and also reviews more recent research that provides opposing evidence.

The case against compact buildings is essentially twofold. Firstly, that surface area to volume ratio (and equivalently the heat loss from the fabric of buildings) might not be longer a good indicator of energy usage in a building. This is based on improved insulation standards, biased assumptions in the modelling of energy usage (i.e. the glazing ratio) and a shift in energy usage within buildings towards more electrical

appliances (Lomas, 2010). Secondly, the increasing relevance and evidence of energy used in common areas of compact buildings (Finch et al., 2010, Heinonen and Junnila, 2014) along with the increase in wind shear (Hamilton et al., 2017) in tall buildings, that may not be adequately addressed in modelling energy use, results in higher energy consumption by tall buildings (though having tall buildings does not necessarily mean higher density as will be discussed in Chapter 3). Combining two above-mentioned points indicates that there is little difference in energy use between building types. This evidence is now being supported by empirical evidence of actual energy use from large samples of different building types from warm (Myors et al., 2005), temperate (Hamilton et al., 2017) and cold (Heinonen and Junnila, 2014) climates. However, when the possibility of generating energy on a roof with photovoltaics (PVs) is considered, the net energy flow in a residential building favours non-compact building types with a large roof to floor area ratio: detached buildings perform better than multi-unit buildings. The importance of research on large samples of buildings is that the results tend to be less distorted due to the social effects on energy use. For example, energy use is not only related to the characteristics of a building but also to household income, occupancy patterns and comfort standards. The larger the sample for a given building type, the more likely the energy use results reflect the mean characteristics of them (Hildon and Byrd, 1984).

The case against compact urban form due to transport energy use is based on the introduction and widespread growth of electric vehicles (EVs). EVs are significantly more energy efficient than ICE vehicles but their energy use (and carbon production) is dependent on how they are charged. If they are charged by PVs mounted on building roofs, then the energy is comparatively clean and free. Furthermore, smart grids and micro-grids allow for the energy generated to be directed away from the building so that a vehicle need not be at the point of generation in order to benefit. Alternatively, the energy could be directed towards electrically powered public transport.

When these disruptive technologies are taken into account, both energy use by buildings and transport favour lower density, non-compact urban form that shows the counterintuitive impact of these technologies. Therefore, it is argued that policy on urban form should be based on technologies of the future rather than the past.

Throughout this chapter, there are figures that all relate energy (y-axis) to an index of urban form (x-axis): building height (as a measure of ‘up’) and urban density (as a measure of ‘out’). The figures are indicative only and the importance is in their relative,

rather than absolute values (i.e. qualitative rather than quantitative). Hence the units of measurement and values are not included. However, absolute values can be obtained by referring to the body of work that is cited in the respective figure captions.

2.1.3 Sustainable and smart city

The work presented in this thesis will certainly contribute to the theory of sustainable cities. Sustainable city is determined as a city that meets environmental, social, cultural and political needs, alongside economic and physical objectives, while it ensures equitable access to all services by residents, without draining the resources of other cities and the region (Rogers, 1997). Nevertheless, there are several other definitions of sustainable city in the literature that cause various contradictions in its definition (Hassan and Lee, 2015).

While in many countries urban policy is based on the development of compact cities as a sustainable urban development (Arundel and Ronald, 2017), many consider the expansion of these characteristics to all aspects of sustainability. These vitally important aspects include environmental quality, social equity, economic viability, life satisfaction (Du et al., 2017), land use and infrastructure and energy. Alternative studies exist on the perceived advantages of compact cities (Dieleman and Wegener, 2004). Matsumoto et al. (2012) report that compact cities are energetically sustainable since they reduce the energy consumption in the cities (Ewing and Rong, 2008). Considering key technologies of future energy sustainability, compact cities show a relatively low capacity to utilize renewable energy sources (Ahmadian et al., 2019a, Cheng et al., 2006, Ghosh et al., 2006).

Meanwhile, low energy consumption of compact cities has been adopted as a criterion for smart cities (Albino et al., 2015). However, the definition of smart city is vague (Albino et al., 2015) and policy makers and governments define it according to their intention (Mandal and Byrd, 2017). Smart cities may be achieved by a variety of attributes such as efficient utilities, safety and security and financial sustainability (Chatterjee and Kar, 2015) where co-benefit with human wellbeing is a critical aspect (Güneralp et al., 2017). Although a general goal of smart cities is enhancing sustainability with help of technologies such as smart grid, autonomous mobility and wide range of functional sensors (Ratti and Claudel, 2016), there remains a large gap between smart and sustainable city frameworks (Ahvenniemi et al., 2017), and a post-

anthropocentric approach is required in practice and policymaking in order to develop true smart and sustainable cities (Yigitcanlar et al., 2019).

2.2 Energy and urban form

2.2.1 Urban form and building energy demand

Urban form has a significant relationship with the energy demand in buildings (Lee and Jeong, 2017) and in whole cities (Silva et al., 2017). Urban sprawl increases energy consumption for residential buildings (Boukarta and Berezowska, 2017). Detached houses consume more energy compared to attached tall buildings (Ewing and Rong, 2008). Overall energy use in cities may be reduced by achieving both higher density urban development (Güneralp et al., 2017, Resch et al., 2016) and higher population density (Osorio et al., 2016). According to Rode et al. (2014), both higher building densities and taller buildings can significantly increase heating energy efficiency while, conversely, Steadman et al. (2017) believe that high-rise buildings are more energy-intensive than low-rise buildings, and a case study in Sydney (a semi-subtropical climate) (Myors et al., 2005) found that high-rise residential buildings consumed more energy than medium rise which, in turn, consumed less than low rise.

The energy consumption assessment in a city is complicated due to the variety of building applications (activities) such as domestic, offices and industrial buildings. In order to increase density of domestic buildings, solutions such as higher degree of compactness, building depth and height, are suggested. Steemers (2003) believes only increasing the compactness will lead to higher energy efficiency. Meanwhile, he shows that increasing urban density has a negative effect on office buildings and boosts their energy usage simply because it reduces the available daylight. Bhiwapurkar (2014) notes that mixed-use urban development can reduce urban energy use intensity as it provides opportunities to live and work in close proximity.

Another urban factor that influences building energy demand is the Urban Heat Island (UHI) effect that leads to buildings needing more energy for cooling in summer and less energy for heating in winter. It is difficult to find a general agreement regarding the relationship of UHI with city configuration. Although it was traditionally believed that high-density urban development is the main cause of UHI intensity (Oke and East, 1971), some recent studies paradoxically show that sprawl urban area has more contribution in the formation of UHI (Stone Jr and Rodgers, 2001). However, the result established by Debbage and Shepherd (2015) illustrates that no matter if the city is

dense or sprawl, the main reason for UHI intensity is the spatial contiguity of urban development. The effect of UHI is considered in the energy simulation part of this thesis in Chapters 5, 6 and 7.

This study solely considers the operational energy of urban areas; however, different urban built forms and densities have different embodied energy (and carbon). This needs to be investigated using a life cycle assessment, which is out of the scope of this study.

Early research into energy and built form (March, 1972, Rickaby, 1987, Steadman and Brown, 1987) related energy use of buildings to the ratio of surface area to volume of buildings. Since heat loss from a building is proportional to its surface area and respective material heat flow properties (U-values), optimization of built form focusses on minimizing the ratio of surface area to volume ratio resulting in compact built form (Steemers, 2003). Although Steadman et al. (2009) note that there should be a maximum threshold for building depth in order to avoid artificial ventilation and lighting (i.e. higher energy consumption) that is required once the depth of rooms exceeds the 'passive zone'.

The assumption that heat loss from the envelope is the most relevant index of energy performance has prevailed over time. For example, almost 40 years after March's 'elementary model of Built Form' (1972), Joiner (2010) in an argument for urban intensification, suggests that, '*By joining houses together or otherwise clustering them, the external envelope of each house can be reduced, with consequent reductions in heat losses.*' The logical conclusion of this assumption is that housing is more energy efficient if its built form is compact. Given building requirements for natural ventilation and daylight, this might mean that more vertical forms (high-rise apartments) are more energy efficient than detached houses, unless specific built form like 'cruciform' (March, 1972) can help to increase density without going up.

This was the basis of the research of Rode et al. (2014) on the relationship between the urban morphology and residential heat demand. The results appear to provide evidence (as well as recommending policy) that tall buildings are an optimum form due to their relatively low surface to volume ratio and, hence, heat loss. Rode et al (2014) used the standard heat loss model of $E \propto (Ui \cdot Ai)$ (where E is the heat loss, U is the envelope material U-values and A is the respective area of the envelope materials). However, this type of analysis becomes a self-fulfilled prophecy that a low surface area to volume ratio will be the optimum since the U-values were kept constant

in the analysis. The result, adapted from Rode et al. (2014), is conceptually illustrated in Figure 2.1 and indicates an almost inverse-square law. Their results indicated that a two-storey building typically has a heat loss of twice that of a ten-storey building.

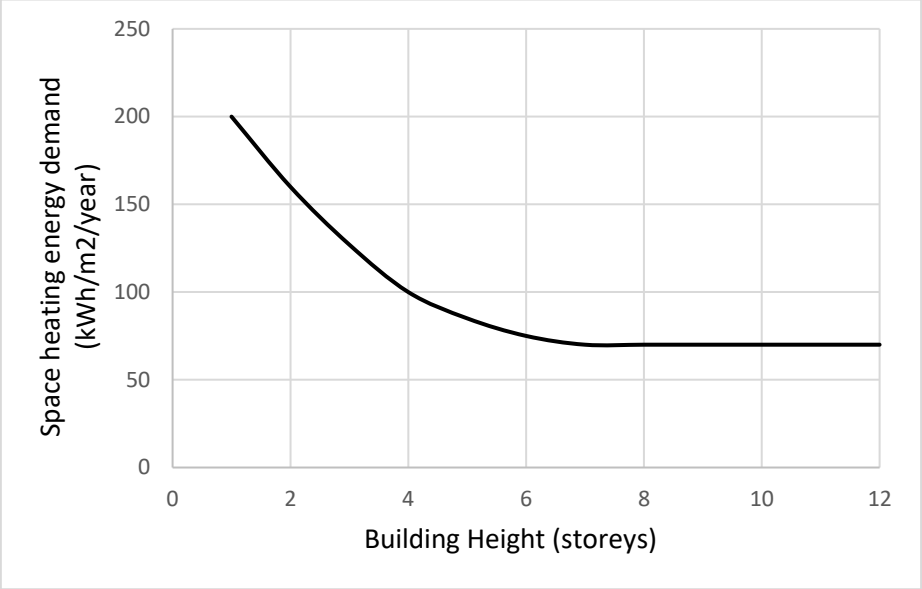

Figure 2.1: Indicative trend of energy consumption for space heating by increasing the number of storeys. (Adapted from Rode et al, 2014)

However, there are a number of assumptions that undermine this assertion. Firstly, the U-values of the existing buildings were outdated and up to 8 times worse than U.K. building regulations (a minimum legal requirement). This has a profound effect on modelling since, as insulation standards increase, the relative amount of energy used for heating decreases. Hypothetically, as an extreme example, if a material could be found which does not allow heat to flow through it, then surface area, and hence shape of a building, would not be relevant. Secondly, the assumption that all building types (detached, high-rise and types between) have the same elevational proportion of glazing, skews the results. For a fair comparison, the same size living unit (detached or multi-unit like apartment) has the same daylighting needs and should have the same area of glazing. Assuming that the amount of glazing should be proportional to the exposed external wall area can result in about twice as much glass in a detached building. The reason is that all around a detached building is exposed to environment, while in multi-unit building (E.g. apartment) only two of maximum three walls are exposed.

Added to this is the assumption that there is no heat transfer between adjacent properties in a multi-unit development. Unoccupied units, partial heating and variations in set temperatures all result in greater heat loss from compact housing that does not

occur in detached housing. However, by compacting housing into blocks, another aspect of energy use becomes more prominent: the heating, lighting and servicing of communal spaces. Lighting and heating corridors, machinery for lifts, ventilation and lighting for car parks, external lighting, mechanical ventilation, pumps, illuminated signage and others amount to significant energy consumption. Assessments of these have ranged between about 10% of overall energy use (when heating is included) (Ho, 2012) to around 20% (Finch et al., 2010) in colder climates. Furthermore, over time the insulation standards of building fabric have improved, and an increasing proportion of energy is now used for household appliances and entertainment (Lomas, 2010). This begins to challenge the idea that fabric heat loss is a representative indicator of a building's whole energy usage, particularly building types with communal areas. When all the above assumptions are adjusted (U-values, %glazing, heat transfer between units and energy use in common areas), modelling results indicate little correlation between building height and energy use (Figure 2.2).

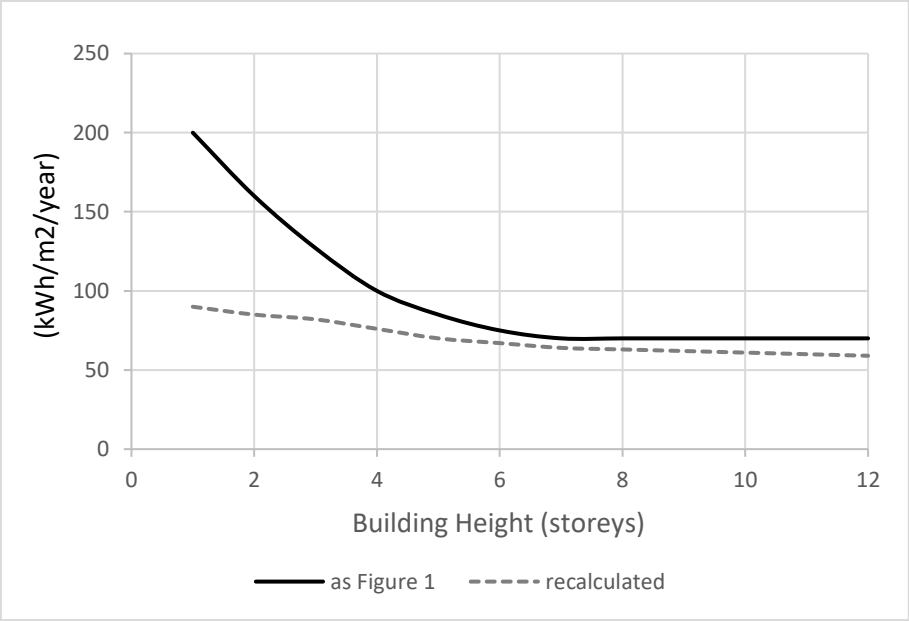

Figure 2.2: Relative energy use compared to building height for the original research (Figure 2.1) and recalculated to include upgraded insulation standards and energy use in common areas.

However, empirical data from a large sample may give a more reliable picture. This was demonstrated in a report by Myors et al. (2005) which analysed, using actual energy records, the energy use of a sample of 3854 house of differing types in Sydney, Australia (temperate climate). The results showed that, when energy use in common areas and for common services are taken into account, high-rise can be the least energy efficient building type, leaving detached buildings as more energy efficient.

This is indicated in Figure 2.3 and the results, being empirical rather than theoretical, from such a large sample upset the idea that high-rise built form is more energy efficient. Results of the Sydney study, based on actual energy readings, indicate almost exactly the opposite to the 'Cities and Energy' study results (Rode et al. 2014) shown in Figure 2.1. While the building type considered are not exactly the same in the studies, and the climate in Sydney is generally warmer than the European climate, the difference in the results is clearly evident.

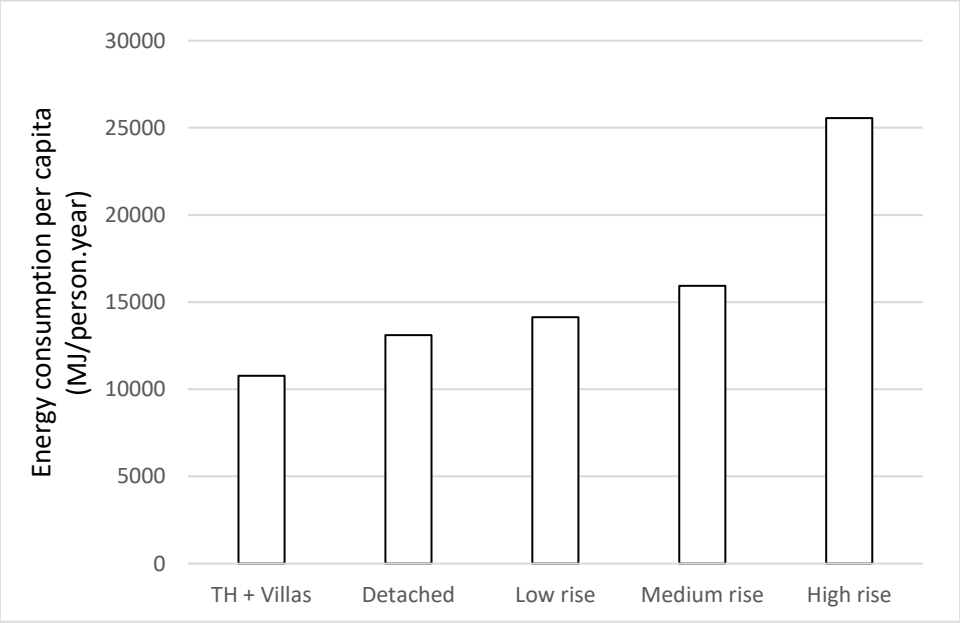

Figure 2.3: Relative energy consumption in different building types (empirical results from Sydney). (Adapted from Myors et al, 2005)

Similar research in Finland's cold climate (Heinonen and Junnila, 2014), again based on actual energy use, also identifies the same characteristic: detached houses using less overall energy than apartments on a per capita occupancy basis with building size normalized (Figure 2.4).

It should be noted that the categorizations of the buildings shown in Figure 2.3 and Figure 2.4 are neither based on density nor built form. Particularly in Figure 2.4, a built form (i.e. terrace) is compared with a building activity type (i.e. apartment) that basically is not a correct comparison (see discussion in section 2.1.1). A building with terrace form can be composed of many apartments inside depending on the block length and its number of storeys. On the other hand, an apartment can be inside a building with any built form (e.g. pavilion, terrace or court) or even inside a big detached house (as considered as a separated category in Figure 2.4). Therefore,

these comparisons require more detailed investigation to discover the relationship of energy with urban built from and density.

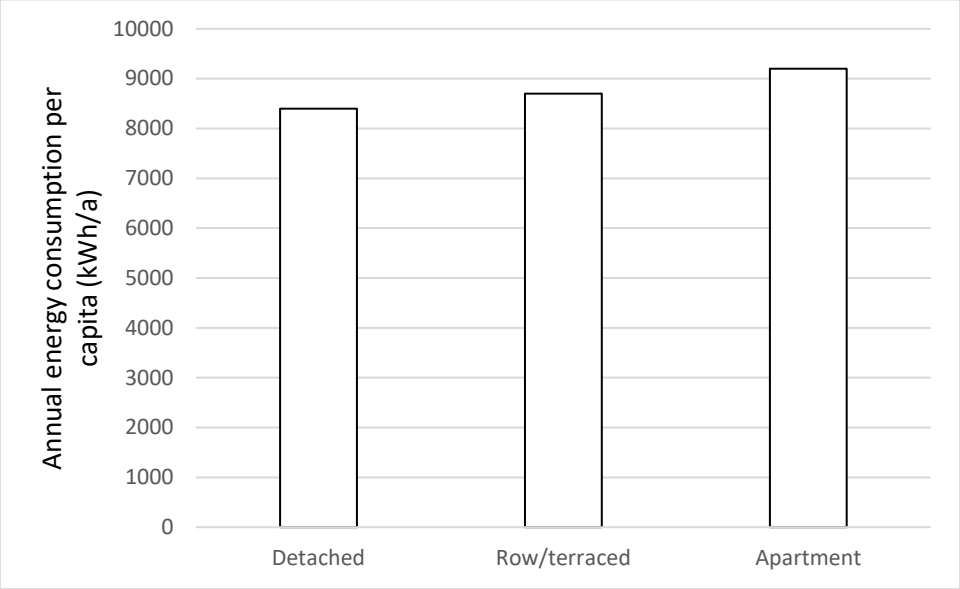

Figure 2.4: Average per capita energy use in different building types. (Adapted from Heinonen and Junnila, 2014)

A similar result was also identified by research on actual energy use on a large sample of London's housing stock (temperate climate)**.** This concluded that high-rise buildings are more energy-intensive than low-rise buildings, "*areas of city with lower buildings will use less energy than areas of tall buildings*" (Hamilton et al., 2017).

2.2.2 The impact of renewable energy supply on urban form

Recently, more research has been undertaken on the possibility of utilizing renewable energy sources in cities, specifically the potential for solar energy (Mohajeri et al., 2016, Sarralde et al., 2015).

Since the significant uptake of PVs on the roofs of houses, analysis of optimum built forms for reducing energy use now needs to consider not only energy losses from buildings but also energy generated by PVs on those buildings. The area of PV array that can be installed on a roof becomes the important criteria for generating energy. Hence, to compare the merits of different built forms, the ratio of PV area to floor area is considered as the indicator of energy analysis in some urban studies. Moreover, PVs can be installed on building facades as well as other locations on-site (such as car park roofs and bus stations) that can expand the potential of solar energy harvesting. For example, Cheng et al. (2011) identified that "*medium to low density housing may in some cases enable a greater saving in CO2 emissions than higher*

density development because of the greater amount of space for collection of renewable energy".

Not only do lower housing densities result in better solar access for PVs, compact development reduces solar access for both PVs and passive solar gains. For example, research by Mohajeri et al. (2016) observed that, "*When passing from dispersed to compact neighborhoods, the BIPV (building integrated photovoltaics) potential for facades decreases from 20% to 3%, whereas for roofs the BIPV potential decreases from 94% to 79%*".

High-rise is disadvantaged because the effective roof area is small compared to the floor area beneath, whereas low-rise buildings have a high roof area to floor area ratio and can provide a significant amount of electricity for their own needs.

This was demonstrated in research on a cross-section of building types across a city (Byrd et al., 2013). The energy generated by PVs on a building was compared with energy consumption of various built forms. While there is some potential for PVs to be mounted on non-residential buildings, suburban housing offered the greatest potential for PVs. This is indicated in Figure 2.5 which illustrates a cross-section through Auckland (NZ), and both the energy generated and consumed as a bar chart below (negative values indicate energy generated). Low-density, low-rise buildings in the suburbs not only produce enough energy for their own use but also produce an excess that can be exported. Conversely, high-rise consumes considerably more energy than it produces.

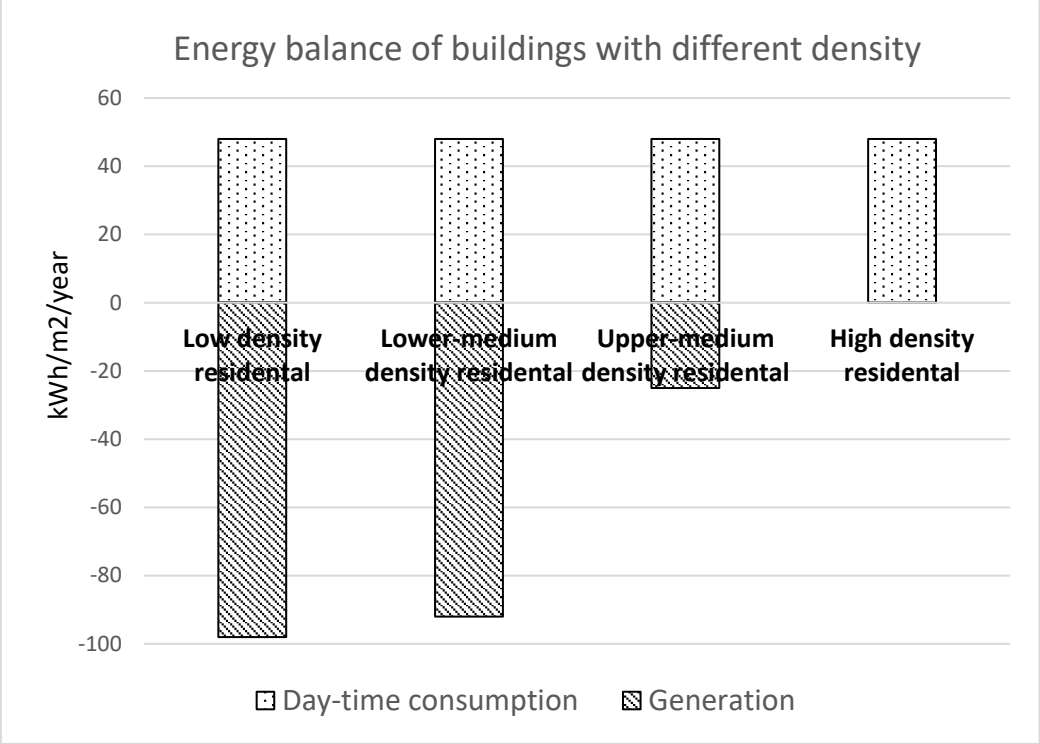

Figure 2.5: Comparing the potential energy generated from PVs with the energy consumed by the building. (Adapted from Byrd et al., 2013)

The net energy balance when urban areas have extensive energy generation from rooftop PVs varies from a considerable surplus in low-density suburbia to an emphatic deficit in high density areas.

Other studies have also demonstrated that in addition to solar energy, other types of renewable energy sources such as ground sourced heat pumps (Echenique et al. 2012; Hargreaves et al. 2017) as well as biomass (Ghosh et al., 2006) also have higher potential in lower density urban development.

The evidence above, based on actual energy use indicates that, irrespective of climate, urban form that goes ‘up’ is likely to result in greater energy consumption than urban form that goes ‘out’. However, these conclusions are made mainly based on a building scale analysis, while it is very crucial that an urban scale analysis is undertaken to consider the urban geometric parameters that influence urban density. This consideration assists to make a more precise estimation of building energy performance because it is affected by the factors such as shadowing effect and inter-reflected radiation between external walls in the built environment (Ahmadian et al., 2021). Therefore, it is also very important that how far is a building from its neighbours, regardless of being low-rise or high-rise, which is controlled and investigated by the

cut-off angle between buildings (see Chapter 3). It is possible to go ‘out’ without reducing density.

Modelling energy use of urban form on the basis of ratio of surface area to volume alone is no longer the only indicator of energy performance of buildings. However, when energy generated by PVs is considered, low-rise buildings are more energy efficient. Decentralized energy generation on rooftops combined with its efficient distribution through ‘feed-in’ to the main grid or to micro-grids results in low-density, low-rise housing becoming more energy efficient (IEA, 2009). Increasing urban density reduces the contribution of solar energy (Margalit, 2016) and high-rise urban development may even result in greater energy consumption.

It should be noted that sustainable design of buildings, particularly Passivhaus design, is an important factor that should be considered in the modern design of buildings. Using passive design strategies considerably reduces the energy load of the building that is advantageous for achieving a net-zero energy target. To this end, the Form Factor (defined as the ratio of thermal envelope surface area to the treated floor area) is a key indicator. This is an indicator of the heat loss from the envelope that aims to be lower than 3 for Passivhaus buildings (Burrell, 2015).

The proportion of energy used for heating and cooling as well as the energy generated by PVs will vary depending on climate (see Chapter 6). However, the overall trend is a gradual warming and research in the UK by Lomas (2010) has indicated that for every 1°C average warming, the national energy consumption by housing will decrease by about 4.6%.

2.2.3 Urban form and transportation energy

There are many studies in the literature that investigate the correlation of transportation energy consumption with urban form. Some researchers conclude that denser urban areas definitely incur less consumption of transportation energy (Ewing and Rong, 2008, Große et al., 2016), while others believe that it is highly dependent on social and economic aspects and it might reduce the amount of journey in the city (Banister et al., 1997). Doherty et al. (2009) indicates that compactness could influence other aspects of sustainability like social networks and community interactions. The very first justification for increase of transportation energy consumption in case of urban sprawl (Guhathakurta and Williams, 2015) is that people should commute longer distance in a sprawling neighborhood.

Historically, research into the relationship between energy use and urban density was intensified after Newman and Kenworthy (1989b)'s publication that graphically illustrates an almost inverse-square relationship between energy use (*E*) and population density (*d*) such that $E \propto 1/d^n$ as illustrated in Figure 2.6.

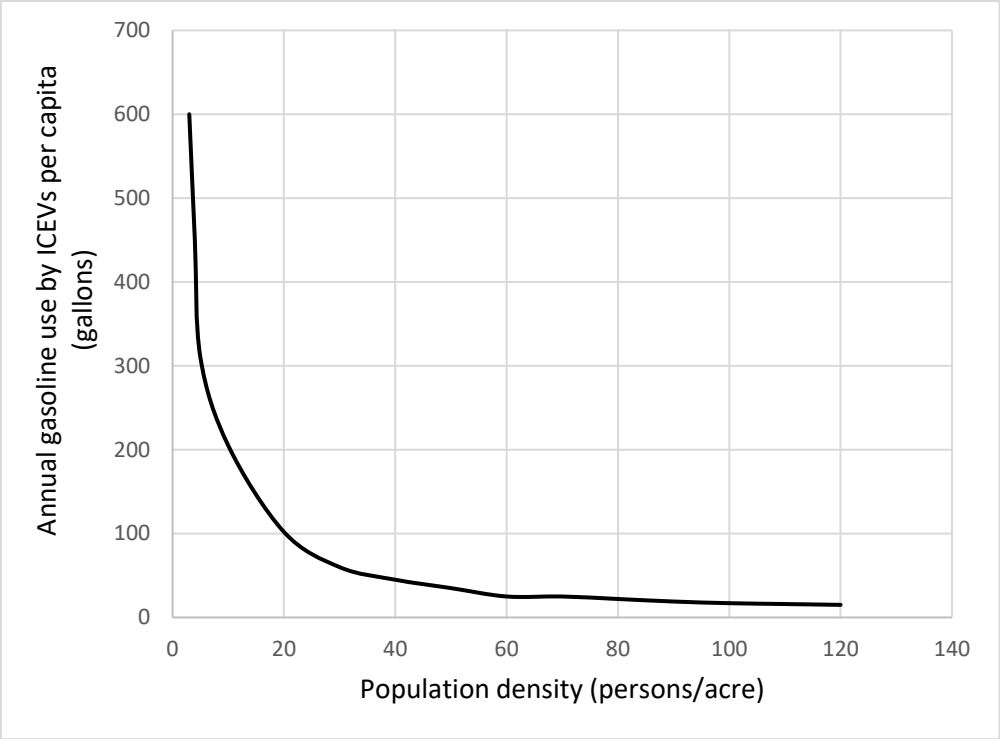

Figure 2.6: Gasoline use per capita versus population density. (Adapted from (Newman and Kenworthy, 1989a))

This research attracted some criticism. For instance, the difference in fuel prices between the cities was not considered (Gomez-Ibanez, 1991) and that it assumes a mono-centric city form (Gordon et al., 1991). In polycentric cities, despite sprawl, trips are normally shorter, and people can walk or cycle to work in ideal cases (Lefèvre, 2009). It has also been criticised by Breheny (1995) who suggests that the evidence of transport energy use does not support the theory of the inverse square relationship proposed by Newman and Kenworthy: "*Over the last 30 years decentralization has made a trivial contribution to additional energy consumption, implying that efforts to prevent further decentralization – if successful, which is doubtful - will also be trivial in their effect*".

However, Breheny still considers that Newman and Kenworthy's correlation is correct but that its magnitude is incorrect. Although it is not quantified, the conclusion might be that the relationship between transport energy and urban density is closer to $E \propto 1/d$ instead of $E \propto 1/d^n$.

More recent research on the relationship of transport energy and urban density has considered the use of EVs powered by decentralized energy supplies (Byrd, 2017). Based on data on existing vehicle travel patterns combined with potential solar energy available on rooftops, it is possible to calculate the extent to which electricity from PVs can displace hydrocarbon-based fuels. However, it should be noted that this research was based on a high penetration of PVs that is more likely to occur after the middle of this century. The research identified that there is an inverse correlation between urban density and transport energy consumption. That is to say that building roof-mounted PVs in lower density urban areas can potentially generate more energy than is required for building consumption. The excess of this generated energy can be used for transport needs in urban areas. Suburbia can effectively power transport in a city. This does not necessarily mean that the vehicles need to stay at home to be charged. There are various options of distributing renewable energy that is generated by distributive means including the possibility of peer to peer or micro-grids (Appavou et al., 2017). This system promotes 'prosumer' concept, where consumers are both buyers and sellers (Jones et al., 2019). The future use of virtual power plants (VPPs) will also make it possible to utilise energy stored throughout an urban area to be directed towards electrically powered public transport (Nikonowicz and Milewski, 2012).

This is the diametrically opposite to the relationship of energy and built form that Newman and Kenworthy (1989) proposed; such that $E \propto -1/d^n$. This is illustrated in Figure 2.7. While EVs have not penetrated the market to that extent as yet, the graph indicates a more likely future than a continued reliance on fossil fuel for transport. Hence, this is a very simple illustration of a predictive model of future transportation and many other impacting variables are excluded such as percentage of EV penetration, technology development, public transportation improvement and people choices.

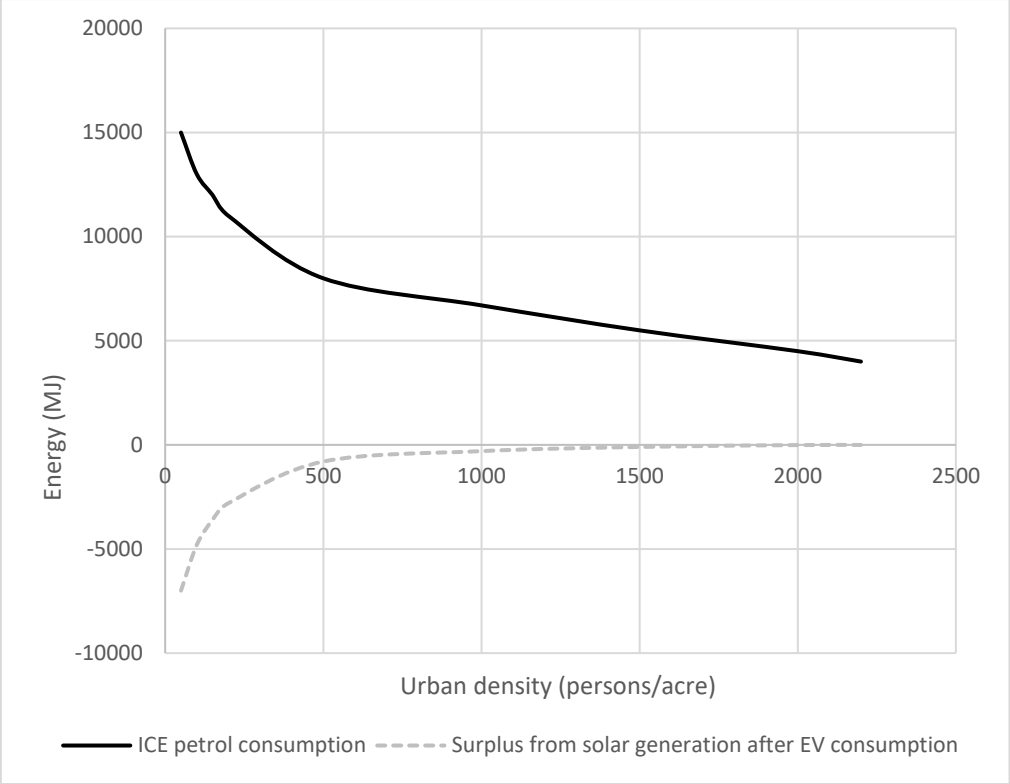

Figure 2.7: Comparison of transportation energy consumption in case of using ICEVs and EVs. (Adapted from Byrd et al, 2013)

2.3 Determining urban form and density

As described in previous sections, for identifying the relationship between energy and urban form, the main parameter analysed by researchers is density (Bhiwapurkar, 2014, Resch et al., 2016, Steemers, 2003). It means most of the studies on energy and urban form immediately discuss density and sprawl. Meanwhile, other studies investigated building types (e.g. apartment) or height of buildings (e.g. low-rise, high-rise) that should not be mistaken with urban form.

According to literature, many parameters contribute to urban form, including density (Güneralp et al., 2017), compactness, diversity, green areas, orientation, shading, passivity, connectivity, accessibility and centrality and so on (Jabareen, 2006, Silva et al., 2017). Therefore, urban form and density should be distinguished. It is also useful to establish the relationship between them. However, before that, it is essential to determine consistent definitions. Debating the correlation between urban form and density, different researchers have used a variety of indicators to define the density of urban form, leading to confusion. In some cases, opaqueness between the terms density and compactness also arises. While some studies distinguish between the two (Silva et al., 2017), others use the same indicators to define either compactness (Mohajeri et al., 2016) or density (Sarralde et al., 2015).

This study categorizes density indicators into two main groups, as follows:

1. Indicators that deal with the physical/geometrical aspects of urban form:
    - Site coverage: Total built area (covered by buildings) in a neighbourhood divided by total area of a neighbourhood, or simply the ratio of the building footprint area to its site area. It is also called ground space index (GSI) (Berghauser Pont and Haupt, 2007) or building footprint.
    - Plot ratio: Total floor area in a neighbourhood divided by total area of a neighbourhood. It is also called floor area ratio (FAR) (Rode et al., 2014) or floor space index (FSI) (Berghauser Pont and Haupt, 2007).
    - Volume-area ratio: Total building volume in a neighbourhood divided by total area of a neighbourhood (Javanroodi et al., 2018, Perera et al., 2021).
    - Building density: Total number of buildings per unit of area (dwellings/ha) (Mohajeri et al., 2016) or the ratio of the built-up area and the overall campus area (Remmen et al., 2018).
    - Open space ratio: Describes the intensity of use of the non-built ground (which is the inverse measure of site coverage) (Cheng, 2009) and indicates the amount of open space available in the site (Berghauser Pont and Haupt, 2007).
    - Height of buildings: Number of storeys which is a very basic indicator.
    - Nearest-neighbour ratio: "*The average distance between buildings from centroids normalised by the total area of a neighbourhood"* which is an indication of horizontal distribution of buildings (Mohajeri et al., 2016).
    - Degree of equal distribution: Measured by Gini coefficient (Tsai, 2005).
    - Degree of clustering: Measured by Moran coefficient (Tsai, 2005).
    - BPRU (Building Performance Research Unit) index: Also termed compactness index and takes the length of perimeter of a given plan and compares it with the perimeter of the same area with the circle shape (Steadman, 2014a). Steadman (2014a) modified this for his analysis and took the perimeter of a square of equal area to the given plan divided by the actual area of the plan. Lower values mean less compact shape and the perfectly square plan scores one.
    - Surface to volume ratio: The ratio of total surface of a building (except floor) over its volume (Ratti et al., 2005, Ratti et al., 2003, Steadman et al., 2009).
    - Volume wall area ratio: (Steadman, 2014a, Steadman et al., 2009) which is the opposite of surface to volume ratio.

- Urban entropy: "*It is a quantitative measure of size distributions of various indicators (e.g. areas, perimeter, height, and volumes) of the buildings. It measures the dispersal or spreading of the probability distributions of the various building geometry*" (Mohajeri et al., 2016).
- Form factor: It is calculated by dividing the summation of wall, roof and ground area to the gross area of the building (Coccolo et al., 2016).
- Habitable rooms per hectare: Number of habitable rooms per hectare (Gordon et al., 2016).
- Area of roof to floor area ratio: Roof area divided to the total floor area of the building (Byrd et al., 2013). It can represent the proportion of solar energy generation from roof-top panels with respect to total building energy demand.
- Number of housing units per building (Rafiee et al., 2019)

2. Indicators considering population and people behaviour/expectations in addition to physical aspects, thereby bringing social aspects into consideration:
    - Population density: Total number of people per unit area.
    - Population-weighted density: Since density is not constant in all areas of a city and the distribution pattern of people or buildings can vary, a more precise method of defining density is population-weighted density (Nick R, 2014). It shows the density profile of the city which refers to a series of density measurements based on a reference location that shows the amount of population living in a specific density. Density profile has been adopted in the UK as the basis for rural definition. In the UK rural classification system, density profile is calculated based on land area enclosed by a series of concentric circles of 200m, 400m, 800m and 1600m radii (Cheng, 2009). Moreover, density gradient is defined as another indicator that shows the rate at which density falls (according to distance) from the location of reference. The density gradient is usually derived from densities measured in a series of concentric rings at a 10m or 20m width, radiating out from the location of the reference (Longley and Mesev, 2002). For example, the average population density of Hong Kong is about 6300 persons per square kilometre, while the distribution of the population is very uneven, ranging from 780 to 52,000 people per square kilometer (Hing-wang, 2007).

- Perceived density: Defined as an "*individual's perception and estimate of the number of people present in a given area, the space available and its organization"*, so the same density can be perceived and evaluated in very different ways, by different people, under different circumstances, in different cultures and countries (Rapoport, 1975). Perceived density addresses the relative relationships between individual and space as well as between individuals in the space. So, it is divided into two concepts. First the perception of density with respect to the relationship among spatial elements such as height, spacing and juxtaposition (spatial density), and secondly the interaction between people (social density) (Cheng, 2009).
- Crowding: Defined as the subjective evaluation by an individual that a given density and perceived density is negative (Churchman, 1999).
- Living density: Defined as a density inside home (Churchman, 1999).
- Occupancy density: "*Ratio of the number of occupants to the floor area of an individual habitable unit. It is an important measure in building services design as it provides an indicator for estimating the services required*" (Cheng, 2009). It is the inverse measure of occupancy rate. For example, higher occupancy rate means larger habitable area for each occupant.
- Gross re-urbanization density depicts the number of residents and number of employed persons per hectare (Greenberg, 1991). This measure of density shows the balance of mix land use in certain area (Churchman, 1999).
- Jobs per land area, which is simply the number of jobs per unit of area (GLAEconomics, 2005).

Comparing results of different case studies using such a diversity of indicators can be challenging (Resch et al., 2016) and indicates the high complexity of cities. Moreover, sets of indicators tend to closely correlate through basic linear relationships. For example, volume-area ratio can be obtained by multiplying plot ratio and the height of each storey. Schwarz (2010) empirically analysed the correlation between urban indicators and found seven exhibiting the lowest cross-correlation. Peponis et al. (2007) considered four measures of density (streets, connectivity, population and different building category) for their analysis on the city of Atlanta.

There are also cases of having different indicators being referred to by the same or similar properties. For instance, the term 'high density' can mean either high building

density or high population density. However, higher building density does not necessarily mean higher population density as it depends on other parameters such as building type, mixed land use and the culture of people. In this context, take a small household size case with a large dwelling size, the higher plot ratio may lead to lower occupancy density which means more habitable area for individuals that consequently mitigate the crowding condition (Cheng, 2009). Specifically in case of energy analysis, results based on the population density (Arbabi and Mayfield, 2016, Chen et al., 2018, Nichols and Kockelman, 2015) are not sufficient to show the precise relationship of urban density and form with energy since most calculations of population density are based on an assumption of the average number of people per dwelling (Jenks et al., 2005). Meanwhile, according to parameters to do with culture and economic conditions, the number of people per unit area is not consistent in different parts of the world.

To eliminate the effects of people behaviour and social aspects that are evidently a source of uncertainty in energy analyses (Clevenger and Haymaker, 2006), indicators from the group 1 above are used in this study (see Chapter 3) as they are a more reliable choice to identify the authentic relationship between urban form and density.

As an indicator from group 1, building density may be calculated as either gross density (number of dwellings per hectare of a given land area, including public infrastructure such as roads, open space and in some instances non-residential development) or net density (number of dwellings per hectare on land devoted solely to residential development ; excluding roads, parks and other public lands). This is an important indicator for making planning policy (Cheng, 2009). In the UK, for instance, the government has set a residential density of 30 dwellings per hectare as the national indicative minimum for new housing developments (DCLG, 2006). This may not however be an optimum density indicator for urban energy analysis (Hamilton et al., 2017) because it does not take into account the form and shape of the buildings that influence the results.

Establishing whether any of the aforementioned indicators represents the true definition of density can be challenging given that none of those discussed above are sufficiently comprehensive to individually show the density of urban form. Hence, a set of indicators should be chosen to define density, and they should have the lowest possible correlation between them. The majority of the aforementioned studies have

considered only one indicator to show urban density. Even when more than one indicator is analysed, no study has examined the effect of urban built form simultaneously with density and energy. Resch et al. (2016) adopted five density indicators, however, not only the impact of the population was included in the definition of the indicators that led to providing the energy use results per capita (instead of per m^2), but also, the effect of urban built form was not considered in their study. They also excluded the UHI effect and solar irradiance that are important parameters in urban energy analysis. It is crucial to give information about urban built form as it alters the microclimatic conditions (Emmanuel and Steemers, 2018) that consequently affect building energy consumption (Lee and Jeong, 2017). There remains a lack of integrated guidelines to communicate urban density indicators and their relationships with urban built forms (Bhiwapurkar, 2014). Providing such guidelines is an important contribution of this thesis, which is developed in Chapter 3.

2.4 Discussion and limitations

In the introduction, the impact of climate on building energy consumption was mentioned but still requires further consideration (this will be investigated in Chapter 6). The evidence that compact built form consistently performs worse over differing climates does not necessarily mean that climate is not a factor. Nevertheless, the case studies mentioned above in Australia, Finland and the UK have contrasting climates but broadly similar results that do not favour compact buildings. However, solar energy availability will vary considerably between these climates.

Climate change will also have an impact with average temperatures likely to continue to rise resulting in less heat loss in colder climates, more overheating in warmer climates and consequent increased use of air-conditioning (unless more passive technologies advent). The combination of increasing internal heat gains, inadequate design for solar protection or natural ventilation, continued climate change as well as market forces promoting air-conditioning, has led to a shift in energy use from winter to summer in temperate climates (Byrd, 2012). While this can be partially addressed by improved building design, it tends to be multi-unit and high-rise buildings that do not shade fenestration or allow for cross-ventilation. The impact of this was highlighted in research in warmer climates (Mandal and Byrd, 2017) and it is not unreasonable to speculate that air-conditioning will spread further in urban areas in

temperate climates as average temperatures increase. If this occurs, it is likely that this new electricity load in temperate climates will be driven by compact building types.

A further important argument that is relevant to the relationship of energy and urban form is that of ‘resilience’; in particular mitigating the impact of electricity blackouts. Tall buildings are inherently more vulnerable to electricity blackouts. Pumps, lifts, emergency lighting and security systems can make this building type almost uninhabitable in a blackout (Byrd and Matthewman, 2014). Whereas building types that are low-rise and have reasonable roof to floor area ratio are less vulnerable and, with self-generation of electricity, can become partially autonomous for energy supply.

The argument for compaction of urban form in order to minimize impact on agricultural land is also an area requiring further research. Not all land is suitable for crop growth, and some forms of agricultural production have an adverse environmental impact. For example, in New Zealand (where compact urban form is partially argued on grounds of loss of productive land) recent statistics (Ministry for the Environment, 2018) have shown that urban growth is only 2.6% that of the growth of dairy land (with significant adverse impacts) and 5.9% of the area of land given to ‘lifestyle blocks’ (non-commercial hobby farms for the elite). In the UK, only 5.9% of total land area is built on, though each single area has bigger/smaller built on area as indicated by an ‘interactive online tool’ developed by Easton (2017). While the impact of urban form on energy is quite universal, issues around land use are local. Regardless of above-mentioned technical aspects, it is acknowledged that sprawl can occupied animal habitats and endanger biodiversity, which is certainly against sustainable development.

Another important issue is the rate at which new technologies will impact on urban form. Disruptive technologies are introduced and evolve over a matter of years while urban form may take decades or centuries to adapt. The evidence that is beginning to be revealed about the relationship between urban form and disruptive technologies is unlikely to have a significant impact on established urban form but is an important contribution to planning policy for new developments and the continuing debate of the compaction of cities. The impact of disruptive technologies is relatively recent and, until they are more widely distributed and adopted within the built environment, caution should be taken in extrapolating the results. However, what the results are showing so

far is that previous compact city theory needs to be reviewed and that radical changes may be required when shaping or designing urban development policies.

Finally, urban form does not solely mean density of urban area. Density is an attribute of urban form. It can be determined by variety of indicators, which do not have the same definitions. Hence, performing similar analyses with different density indicators can lead to different outcomes. It also causes inconsistency in the outcome of different studies that makes it difficult to do comparative analysis. This was found as a significant gap in the studies of energy and urban form that is targeted for investigation in Chapter 3 by introducing a new indicator as a combination of two density indicators.

2.5 Conclusion

The fundamental discussion of the relationship between urban form and energy is concerned with compaction: compaction of individual buildings (‘up’) and compaction of the spread of buildings (‘out’). Intuition combined with previous research results has indicated that buildings with a low ratio of surface area to volume lose less heat and that containment of urban spread (sprawl) results in less transport energy. The simple conclusion from this is that ‘up’ is better than ‘out’ for reducing energy consumption.

Subsequent research reviewed in this chapter has demonstrated that heat loss from building fabric may not be a good indicator of whole-building energy use. When other factors are accounted for (common area energy use, occupancy, energy use for non-space heating) the correlation between urban form and energy use is shown to be weak. Case studies in different climates using actual energy data have indicated that tall buildings perform worse than low-rise buildings. Furthermore, when energy generated on a building is considered, the net energy balance of a building strongly favours low-rise buildings rather than high-rise.

Research on the relationship between transport energy and urban form has focussed on vehicles with internal combustion engines. Again, the conclusion of this is that urban form should not go ‘out’ but should be contained by going ‘up’. However, as car manufacturers shift production to EVs combined with incentives to assist purchase, these vehicles are likely to dominate the market in years to come. It is relatively simple to then charge these vehicles from electricity generated on rooftops. The result is that suburbia becomes an energy generator and that travel distance within an urban area has little impact on resource depletion or carbon production. The

future use of VPPs will also make it possible to utilize energy stored throughout an urban area to be directed towards electrically powered public transport.

One of the main reasons for this counterintuitive result is the influence of disruptive technologies. The distributed generation of electricity that has the possibility of being directed towards the charging of EVs, for private or public use, changes the assumptions previously made in this field of research.

To derive any credible assessments, the correlation of urban form and density should be formally established. This should be considered as a basic requirement for studies of energy, urban form and density in order to avoid confusion in comparative analyses. Meanwhile, using set of density indicators gives more comprehensive nature to the analysis.

Current policies on compaction of urban areas have been influenced, among other things, on research that has not taken account of these technological changes. The shape of urban areas of the future should not be determined by the technologies of the past but by the technologies of the future. However, the trends illustrated in this chapter are long term and, in wealthier nations, changes in building stock are slow and technologies may change even faster. This highlights the need for continued research in this field and to challenge intuitive assumptions that persist.

Chapter 3: Urban built form and density (*Form Signature*)

3.1 Introduction

Cities are one of the most complex artefacts ever produced by humans. This is what makes them difficult to describe and understand. New models are needed to unpack urban complexity. This chapter contributes to urban science, which tackles cities as dynamic, non-equilibrium systems and networks. The concept of sustainable urban development has emerged to ensure sustainability in all the key roles of this complexity. It requires appropriate urban planning and land-use management considering environmental, social and economic assessment.

The systemic complexity of urban built form is often neglected when policies are formulated. For example, policies with interrelated variables such as density, movement, energy and so on tend to be considered sequentially. This results in 'policy silos' that are rarely synthesized and therefore the reality of cities as complex networks of networks, or systematic ecosystems, are unintentionally missed. This has been recognized by several city analysts and observers. For instance: "*The point is that planners do not sit above the system, bending it to their will: cities are complex, emergent patterns that result from the interaction of a huge number of variables, including society's norms and values, the working of markets and the impact of technology. Planning is just one of the inputs to the system, and probably not the most important one*" (Radlin and Hemani, 2019). The importance of the work described in this chapter is two-fold. Firstly, the ease of using a proposed graphical tool for future planning and policies that address the balance between influential variables, and following existing restrictions, is inherent in the concept of *Form Signature*. Secondly, the developed tool can be adopted as a baseline for future urban assessments, specifically for investigating relationships of energy with density and built form in order to advise policy makers on, for example, energy-oriented urban planning for sustainable cities. '*Planning decisions we make today determine the scope of choices we will have tomorrow'* (Ratti and Claudel, 2016).

Due to the complexity of relationships between form, density and energy, there is no one-size-fits-all solution for optimization (Doherty et al., 2009). Hence, the aim of this study is to develop a series of guidelines to provide a comprehensive relationship of density with four generic (theoretical) urban built forms in order to assist urban planners on the choice of the most appropriate built form and density according to

urban policies of cities in different parts of the world. In addition, a new type of urban built form, termed the ‘tunnel-court’, is introduced that provides an opportunity for achieving the highest urban density and demonstrates the potential for future compact city developments.

This chapter considers two physical/geometric density indicators (see Chapter 2, section 2.3); site coverage and plot ratio, plus three geometric variables; number of storeys, plan depth and cut-off angle (obstruction angle) that doubtlessly influence the above-mentioned indicators. These three geometric variables are enough to fully govern the geometry of urban areas and provide the opportunity of deriving the relevant equations. The geometric parameters significantly affect the energy demand for heating and cooling (Tsirigoti and Tsikaloudaki, 2018) particularly by altering urban microclimate as they affect UHI intensity (Boccalatte et al., 2020). Site coverage and plot ratio are chosen because not only they are the most popular and practical indicators in the literature, but also, the majority of the other density indicators can be obtained by a simple linear relationship with any of these two. Although some common developers use plots per hectare as an indicator, it cannot be an appropriate choice for this study because this indicator does not give any information neither about the form of the buildings nor about the geometrical characteristics of the urban area. Therefore, it certainly is not a reasonable indicator for sensitive urban energy analysis. The analytical and graphical expression of the extensive relationships between these five factors contributes to the future enhancement of this area of study. Analytical models of the different urban built forms considering their land-use performance are developed to investigate their inter-relationships with density. The outcome of the analysis allows a direct comparison of the relative attributes of different urban built forms in terms of density through the introduction of the *Form Signature*, an indicator of the relationship between density and urban built form. The absence of such an indicator is a gaping hole in current literature specifically for urban energy optimization. This comprehensive index not only proposes a tool for urban design and policy, but also opens a door for future statistical analysis on the complex relationship of a variety of parameters such as energy, climate, family wealth and crime with density and urban built form simultaneously.

Although energy analysis is the key feature in this study, a procedure is identified for integrating other parameters such as climate, economy and social issues that constitute cities as complex ecosystems (Newman and Jennings, 2012).

3.2 Geometrical parameterization of urban built forms

For this study, generic models of four urban built forms are developed in order to define the real relationship of 'urban built form' and 'density' for various cases. Three of them (pavilion, terrace and court form) are the elementary forms developed by (March, 1972), and since then widely used by many authors (Huang et al., 2008, Ratti et al., 2003). They may be found in different places of the world albeit slightly amended with reference to culture and climatic conditions. The fourth built form, termed a 'tunnel-court', is developed in this study, based on an amended and practical version of the 'cruciform' developed by March (1972). These theoretical models drive the equations that govern the correlation between indicators.

A site with generic area, *Z*, is considered to set a threshold for the built area (Figure 3.1).

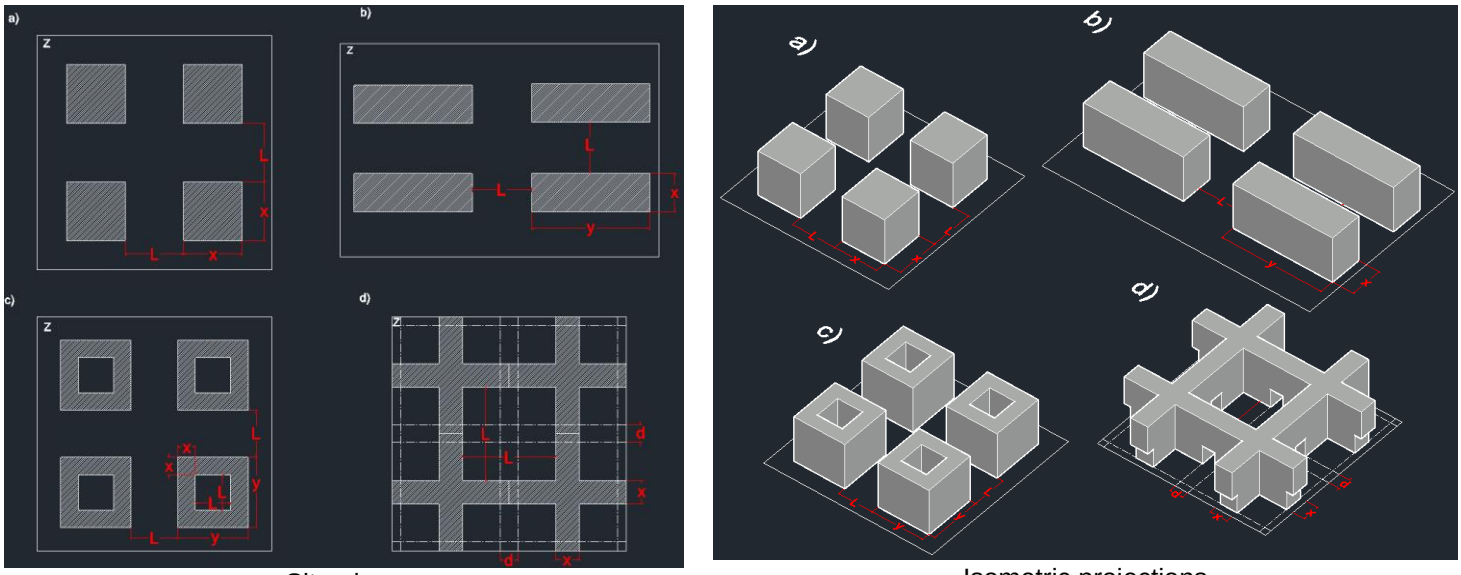

Site plans Isometric projections

Figure 3.1: Generic urban built forms a) pavilion, b) terrace, c) court and d) tunnel-court

The density gradient (which shows the rate at which density falls from the location of reference) of the whole site is zero since the buildings are considered to be evenly distributed over the entire area.

Parameters that can affect the results of subsequent analysis are:

- Number of storeys (*n*)
- Storey height (*h*)
- Cut-off angle or obstruction angle (θ) (is the angle between the ground and the line joining the roofline of one façade to the base of another façade) (Figure 3.2)
- Plan depth (*x*)
- Distance with adjacent building (*L*)

The height of building is simply calculated using Eqn (3.1),

$$H = nh \tag{3.1}$$

The cut-off angle is calculated using Eqn (3.2) (see Figure 3.2),

$$tan\,\theta = \frac{nh}{L} \tag{3.2}$$

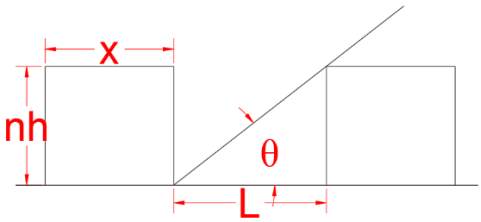

Figure 3.2: Building height, cut-off angle and distance between buildings

Hence, the distance between two buildings (*L*) is dependent on cut-off angle, as follows:

$$L = \frac{nh}{tan\,\theta} \tag{3.3}$$

3.2.1 Pavilion, terrace and court forms

From Figure 3.1, the number of building blocks (m_b) is calculated by dividing the whole area of site (*Z*) by the area that each building and its adjacent free space occupy. This is given by Eqns (3.4), (3.5*)* and (3.6*)* for the pavilion, terraced and court cases, respectively.

The main indicators to be examined are:

- Site coverage (*C*): defined as $\frac{total\ built\ area\ (covered\ by\ buildings)}{total\ area\ of\ site}$
- Plot ratio (*P*): defined as $\frac{total\ floor\ area}{total\ area\ of\ site}$
- Volume-area ratio (*V*): defined as $\frac{total\ buildings\ volume}{total\ area\ of\ site}$
- Surface to volume ratio (*S*): defined as $\frac{total\ exposed\ surface\ area\ of\ building}{total\ volume\ of\ building}$

Table 3.1: Equations showing mathematical models of different built forms based on their geometry

Pavilion		**Terrace**		**Court**	
$m_b = \frac{Z}{(x+L)^2}$	(3.4)	$m_b = \frac{Z}{(x+L)(y+L)}$	(3.5)	$m_b = \frac{Z}{(y+L)^2} = \frac{Z}{(2x+2L)^2}$ [1]	(3.6)
$C = \frac{m_b x^2}{Z} = \frac{x^2}{(x+L)^2}$	(3.7)	$C = m_b \frac{xy}{Z} = \frac{xy}{(x+L)(y+L)} = \frac{9x^2}{(x+L)(9x+L)} = \frac{9x^2}{9x^2+10xL+L^2}$ [2]	(3.8)	$C = m_b \frac{2xy+2xL}{Z} = \frac{2x}{(y+L)} = \frac{x}{x+L}$	(3.9)
$P = nC = n\frac{m_b x^2}{Z} = \frac{nx^2}{(x+L)^2}$	(3.10)	$P = nC = \frac{9nx^2}{9x^2+10xL+L^2}$	(3.11)	$P = nC = nm_b \frac{2xy+2xL}{Z} = \frac{nx}{x+L}$	(3.12)
$V = \frac{m(nh)x^2}{Z} = nhC = hP = \frac{nhx^2}{(x+L)^2}$	(3.13)	$V = nhC = hP = \frac{9nhx^2}{9x^2+10xL+L^2}$	(3.14)	$V = nhC = HC = hP = \frac{nhx}{x+L}$	(3.15)
$S = \frac{x^2+4nhx}{nhx^2} = \frac{x+4nh}{nhx}$	(3.16)	$S = \frac{xy+2nhx+2nhy}{nhxy} = \frac{9x^2+2nhx+18nhx}{9nhx^2} = \frac{9x+20nh}{9nhx}$	(3.17)	$S = \frac{2xy+2Lx+4nhy+4nhL}{2nhxy+2nhlx} = \frac{4x^2+4xL+8nhx+8nhL}{4nhx^2+4nhLx} = \frac{(2x+4nh)(2x+2L)}{2nhx(2x+2L)} = \frac{x+2nh}{nhx}$	(3.18)

Site coverage shows the percentage of total buildings footprint in the whole site area and based on the model shown in Figure 3.1, is obtained from Eqns (3.7*)*, (3.8*)* and (3.9*)* for pavilion, terrace and court, respectively. Since *Z* is eliminated from the final equation, the magnitude of site area does not have any effect on the results of this analysis, hence, the results are valid for any generic site area with any dimensions as long as the layout assumptions/patterns are adhered to.

Assuming all buildings have the same number of storeys and that all storeys have the same floor area, the plot ratio of the site is obtained by multiplication of site coverage to the number of storeys showing in Eqns (3.10*)*, (3.11*)* and (3.12*)* for the pavilion, terrace and court, respectively.

Volume-area ratio is a rarely used indicator mentioned by Mohajeri et al. (2016). Assuming all the buildings have the same height, this indicator is obtained from Eqns (3.13*)*, (3.14*)* and (3.15*)* for pavilion, terrace and court, respectively. The results show

[1] Considering y=2x+L
[2] Considering y=9x

that this is simply the product of plot ratio and the storey height (*h*) which is constant. Hence, basically any result obtained for plot ratio can be readily obtained for volume-area ratio by simple multiplication.

Surface to volume ratio is used as an indicator that affects the amount of heat loss from the exposed surfaces (roof and facades) as well as thermal performance of the building (Ratti et al., 2003). Based on the literature, the higher the surface to volume ratio, the higher is the heat loss from building (Philipp et al., 2011). The value of this indicator is obtained from Eqns (3.16*)*, (3.17*)* and (3.18*)* for pavilion, terrace and court, respectively.

There is an extra parameter, 'y', in the geometry of terrace and court models that makes them different from the others--see Figure 3.1. It can be simplified for court model according to its geometry, as mentioned in Eqn (3.6). In the case of terrace model, it represents the length of terrace building and it is essential to give appropriate values in order to provide the related site plans as input for energy simulations. Since no general rule for the value of 'y' has been found, an experimental analysis is made to define suitable values. The aim was to establish a relationship between plan depth of terrace buildings (*x*) and their length (*y*). To this end, an extensive exploration on the London map (Source: Google Maps 2020) was made to identify terrace housing examples as case studies. 25 cases, as shown in Table 3.2, were selected and their plan depths and lengths measured from Google Maps. The last column of Table 3.2 shows the ratio of plan length to depth, where all the numbers were rounded to be integers. Notably, a diverse range of ratios are apparent, ranging between 3 and 27.

Table 3.2: Case studies of terrace housing in London and their dimensions

Case study		Depth (m)	Length (m)	Length/Depth	Map
1	Mitre Rd	11.8	100	8	
2	Collinson Walk	7	38	5	
3	Pilton Pl	8	38	5	
4	Beaconsfield Rd	8	66	8	
5	Trafalgar Ave	8.7	113	13	
6	Fentiman Rd	10.20	192	19	
7	Ballater Rd	12.5	150	12	
8	Midmoore Rd	17.2	217	13	
9	Louisville Rd	16.4	438	27	
10	Gassiot Rd	16.2	260	16	
11	Tildesley Rd	9.9	67	7	
12	Waldemar Ave	14.4	183	13	
13	Wilsham St	9	83	9	
14	Ixworth Pl	12.1	43	4	
15	Couthurst Rd	11.1	139	13	
16	Fairlawn Ct	9.8	80	8	
17	Brabazon St	9	35.4	4	

18	Devons Rd	7.7	57.5	7	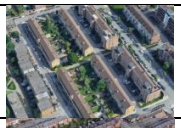
19	Lymington Ave	15	137	9	
20	Upper Belgrave St	15.2	90	6	
21	Musbudy St	12.3	51	4	
22	Shadwell Gardens	9.4	29	3	
23	Wenlock St	17.2	53	3	
24	Linton St	9	37	4	
25	Raleigh St	8.9	34	4	

To select the most appropriate ratio for this study, the average ratio of all cases is calculated, which is equal to 9. Hence, in this study, the value of terrace length is chosen to be nine times more than plan depth, as shown in Eqn (3.19).

$$y = 9x \qquad (3.19)$$

This value was used in Eqn (3.8) in order to obtain the site coverage formula of terraced built form model.

This is solely a mathematical calculation according to the geometry of the existed terraced buildings in London, which provides sufficient credibility to be used in this study. Changing this ratio could result in longer or shorter terrace form buildings that affects surface to volume ratio of the block (see Eqn (3.17)). It impacts energy waste from the envelope, as well as the roof area of building block, which consequently influences the energy demand of the building as well as the amount of solar energy generation by changing the area available for installation of PV panels.

3.2.2 Tunnel-court form

The tunnel-court built form is similar to the cruciform (Martin and March, 1972) with an additional modification to Martin's model. In the original model, the roads for transportation were not clear (Steadman, 2014b). Hence, in the tunnel-court model roads pass from the intersection of crosses and make short tunnel passages in the buildings. These so-called tunnels eliminate two storeys of the buildings in their path and the distance reserved for roads is denoted by *d* (road reserve). Based on Figure 3.1 (d), the number of building blocks (crosses in this case) in the site (m_b) is calculated by dividing whole area of site by the area occupied by each cross, as in Eqn (3.20).

For this specific case, the site coverage for 1 and 2 storey buildings is lower than the cases with higher number of storeys as there is no coverage of the roads for 1 and 2 storey buildings. Hence, there is a contribution that is subtracted from the nominator of Eqn (3.21).

This difference is also relevant for calculating the plot ratio, since the floor area of 1 and 2 storeys are smaller than the floor area of higher storey counterparts. Assuming all buildings have the same number of storeys, the plot ratio is then obtained from Eqn (3.22).

Since volume-area ratio is obtained by simple multiplication of storey height to plot ratio, it can be calculated using Eqn (3.23).

Due to the different shape of tunnel-court built form for 1 and 2 storey buildings, two separated equations were derived for this built form, given in Eqn (3.24) a) and b).

Table 3.3: Equations showing the mathematical model of tunnel-court built form based on its geometry

Tunnel-court		
$m_b = \frac{Z}{(x+L)^2}$		(3.20)
$C = m_b \frac{x(x+L)+xL-2xd[n\leq 2]^3}{Z} = \frac{x^2+2xL-2xd[n\leq 2]}{(x+L)^2}$		(3.21)
$P = nC - m_b \frac{4xd[n>2]}{Z} = \frac{n(x^2+2xL-2xd[n\leq 2])-4xd[n>2]}{(x+L)^2}$		(3.22)
$V = hP = nhC - \frac{4hxd[n>2]}{(x+L)^2} = \frac{nh(x^2+2xL-2xd[n\leq 2])-4xd[n>2]}{(x+L)^2}$		(3.23)
$S = \frac{x^2+1.2Lx+4nhx+2.4nhL}{nhx^2+1.2nhLx}$ [4] $S = \frac{x^2+2.8Lx+4nhL+24x-9.6L}{nhx^2+2nhLx-4.8Lx}$	*a) For 1 and 2 storey buildings* *b) For more than 2 storey buildings*	(3.24)

[3] Iverson bracket
[4] Considering d=0.4L

The complexity of the shape of tunnel-court form can be observed from Eqn (3.24). Unlike the other built forms, the variable '*L*' (distance between buildings) is included in Eqn (3.24), which brings the impact of cut-off angle into the calculation of the surface to volume ratio. Moreover, '*d*' (road width) was also included in Eqn (3.24), which was eliminated by being substituted with an equivalent value of '*L*': *d=0.4L*, obtained from the data in Table 3.4.

3.3 Site coverage and plot ratio Vs number of storeys

To establish the relationship between indicators and selected variables, an Excel spreadsheet tool is developed for each built form using the developed equations. It allows simultaneous analysis of all the influential variables. A screenshot of the tool is shown in Figure 3.3.

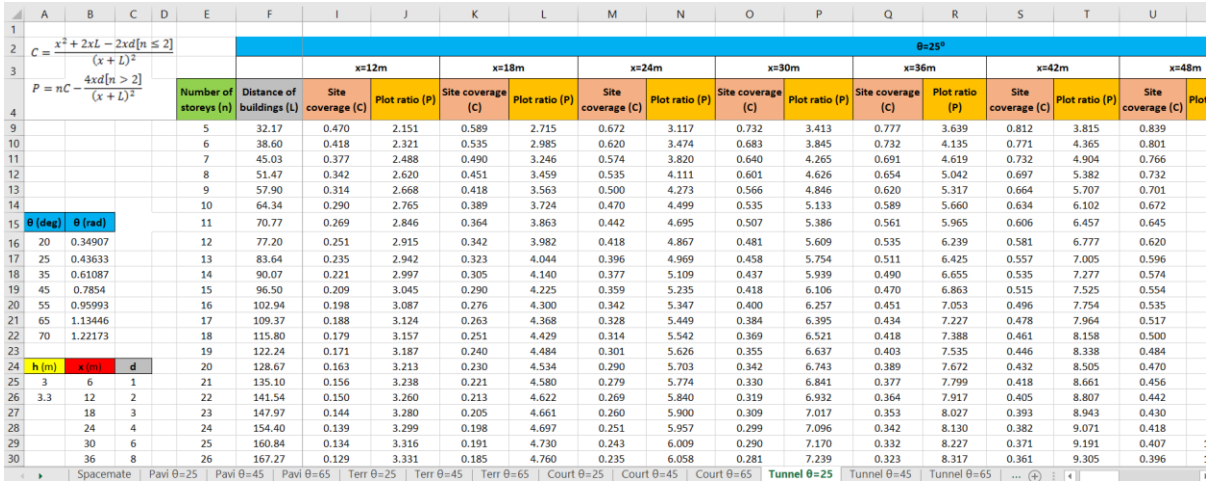

$$C = \frac{x^2 + 2xL - 2xd[n \le 2]}{(x+L)^2}$$

$$P = nC - \frac{4xd[n > 2]}{(x+L)^2}$$

θ=25°																	
		x=12m		x=18m		x=24m		x=30m		x=36m		x=42m		x=48m			
Number of storeys (n)	Distance of buildings (L)	Site coverage (C)	Plot ratio (P)	Site coverage (C)	Plot ratio (P)	Site coverage (C)	Plot ratio (P)	Site coverage (C)	Plot ratio (P)	Site coverage (C)	Plot ratio (P)	Site coverage (C)	Plot ratio (P)	Site coverage (C)	Plot		
5	32.17	0.470	2.151	0.589	2.715	0.672	3.117	0.732	3.413	0.777	3.639	0.812	3.815	0.839			
6	38.60	0.418	2.321	0.535	2.985	0.620	3.474	0.683	3.845	0.732	4.135	0.771	4.365	0.801			
7	45.03	0.377	2.488	0.490	3.246	0.574	3.820	0.640	4.265	0.691	4.619	0.732	4.904	0.766			
8	51.47	0.342	2.620	0.451	3.459	0.535	4.111	0.601	4.626	0.654	5.042	0.697	5.382	0.732			
9	57.90	0.314	2.668	0.418	3.563	0.500	4.273	0.566	4.846	0.620	5.317	0.664	5.707	0.701			
10	64.34	0.290	2.765	0.389	3.724	0.470	4.499	0.535	5.133	0.589	5.660	0.634	6.102	0.672			
11	70.77	0.269	2.846	0.364	3.863	0.442	4.695	0.507	5.386	0.561	5.965	0.606	6.457	0.645			
12	77.20	0.251	2.915	0.342	3.982	0.418	4.867	0.481	5.609	0.535	6.239	0.581	6.777	0.620			
13	83.64	0.235	2.942	0.323	4.044	0.396	4.969	0.458	5.754	0.511	6.425	0.557	7.005	0.596			
14	90.07	0.221	2.997	0.305	4.140	0.377	5.109	0.437	5.939	0.490	6.655	0.535	7.277	0.574			
15	96.50	0.209	3.045	0.290	4.225	0.359	5.235	0.418	6.106	0.470	6.863	0.515	7.525	0.554			
16	102.94	0.198	3.087	0.276	4.300	0.342	5.347	0.400	6.257	0.451	7.053	0.496	7.754	0.535			
17	109.37	0.188	3.124	0.263	4.368	0.328	5.449	0.384	6.395	0.434	7.227	0.478	7.964	0.517			
18	115.80	0.179	3.157	0.251	4.429	0.314	5.542	0.369	6.521	0.418	7.388	0.461	8.158	0.500			
19	122.24	0.171	3.187	0.240	4.484	0.301	5.626	0.355	6.637	0.403	7.535	0.446	8.338	0.484			
20	128.67	0.163	3.213	0.230	4.534	0.290	5.703	0.342	6.743	0.389	7.672	0.432	8.505	0.470			
21	135.10	0.156	3.238	0.221	4.580	0.279	5.774	0.330	6.841	0.377	7.799	0.418	8.661	0.456			
22	141.54	0.150	3.260	0.213	4.622	0.269	5.840	0.319	6.932	0.364	7.917	0.405	8.807	0.442			
23	147.97	0.144	3.280	0.205	4.661	0.260	5.900	0.309	7.017	0.353	8.027	0.393	8.943	0.430			
24	154.40	0.139	3.299	0.198	4.697	0.251	5.957	0.299	7.096	0.342	8.130	0.382	9.071	0.418			
25	160.84	0.134	3.316	0.191	4.730	0.243	6.009	0.290	7.170	0.332	8.227	0.371	9.191	0.407			
26	167.27	0.129	3.331	0.185	4.760	0.235	6.058	0.281	7.239	0.323	8.317	0.361	9.305	0.396			

θ (deg)	θ (rad)
20	0.34907
25	0.43633
35	0.61087
45	0.7854
55	0.95993
65	1.13446
70	1.22173

h (m)	x (m)	d
3	6	1
3.3	12	2
	18	3
	24	4
	30	6
	36	8

Spacemate | Pavi θ=25 | Pavi θ=45 | Pavi θ=65 | Terr θ=25 | Terr θ=45 | Terr θ=65 | Court θ=25 | Court θ=45 | Court θ=65 | Tunnel θ=25 | Tunnel θ=45 | Tunnel θ=65

Figure 3.3: A screenshot from the Excel spreadsheet tool.

Values assigned to the variables are chosen based on the methodology and assumptions given below:

- Number of storeys vary between 1 and 40.
- The storey height is considered to be 3 m (*h*=3m) corresponding to the normal height of storeys in residential buildings (Muhaisen, 2006). This can be a number from 2 to 4.5 m (Steadman, 2014a) that can change the total energy demand of building.
- The distance between buildings is obtained from Eqn (3.3), and since *n* varies between 1 and 40; the value of *L* is consequently changed.
- Plan depth is investigated with four different values in order to consider its influence on site coverage (*x*=6m, *x*=12m, *x*=18m, *x*=24 m).
- The cut-off angle is given three different values (*θ*=25°, *θ*=45°, *θ*=65°).

The range of plan depth choice is twofold; firstly, to accommodate shallow to deep scenarios, and secondly as a means of modelling possible passive zones (light and ventilation) in the buildings. Since the minimum plan depth to achieve a passive zone is twice the storey height (i.e. typically 6 m) (Steadman et al., 2009), the value is 6 m. For cases having windows both sides, the passive zone remains up to 12 m. The rest of the plan depth values are chosen to be a factor of 6 in order to have an idea of the passive to non-passive ratio which is an applicable indicator for the energy analysis of buildings (Ratti et al., 2005). Regarding the cut-off angle, a lower bound of 25° is selected to provide a longer distance between buildings and ensure sufficient solar radiation and avoid excessive over shading on the building facades. Increasing the cut-off angle allows for reduced solar radiation received by the facades, and while it is unlikely that θ exceeds 45° in modern residential buildings (Steadman, 2014b), an angle of 65° is also considered to identify the trends of changing indicators when buildings are very close to one another. (however, a typical cut-off angle of office skyscrapers is 75º (Steadman, 2014a)). Notably, building height, cut-off angle and plan depth are varied according to urban planning policies (themselves derived from climate, geography, culture and other factors) in different parts of the world. Hence, a comprehensive assessment over a wide range of values to cover a variety of different locations on the earth is considered. For brevity here, only results based on sample values are shown.

Note: There is an additional consideration in case of tunnel-court due to the presence of variable road width (*d*) in the equations. Table 3.4 shows the assumptions for the road width for calculating site coverage, plot ratio and volume-area ratio.

Table 3.4: Road width in tunnel-court built form based on building distances and number of storeys

L (m)	d (m)	Number of storeys (θ=25º)	Number of storeys (θ=45º)	Number of storeys (θ=65º)
1 - 2	1	_	_	1
2 - 5	2	_	1	2 - 3
5 - 7	3	1	2	4 - 5
8 - 11	4	2	3	6 - 8
12 - 18	6	3	4 - 5	9 - 13
19 - 35	8	4 - 5	6 - 8	14 - 25
35 - 50	10	6 – 8	9 - 18	26 - 36
51 - 80	16	9 - 12	19 - 26	37 - 40
80 upward	22	13 - 40	27 - 40	–

3.3.1 Effect of plan depth, cut-off angle and number of storeys

Figure 3.4 shows the trend of site coverage and plot ratio versus number of storeys for the case of keeping cut-off angle at 25° and varying the plan depth from 6 to 24m (top), and for the case of having a constant plan depth of 12m and varying the cut-off angle from 25° to 65° (bottom).

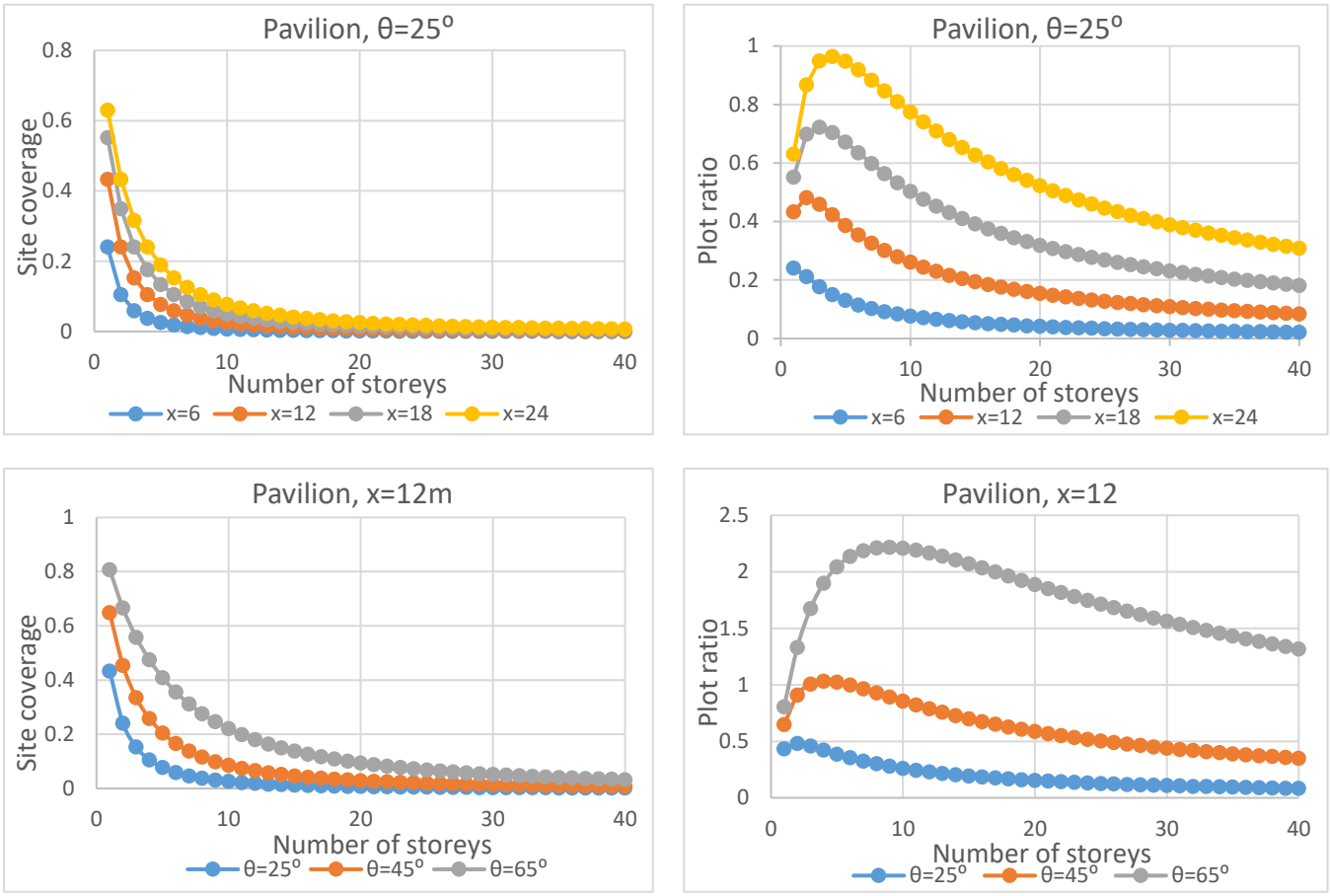

Figure 3.4: Trends of changing site coverage and plot ratio with increasing number of storeys for pavilion form in case of θ=25° (top) in case of x=12m (bottom)

From Figure 3.4 (top), it can be seen that higher plan depths generally provide greater site coverage and plot ratio. However, a more general conclusion is that regardless of the value of plan depth, as number of storeys increases, the rate of change of site coverage and plot ratio significantly reduces, and ultimately becomes tangential. Figure 3.4 (bottom) shows that higher values of cut-off angle considerably increase the site coverage of buildings, while substantially increasing the plot ratio (specifically, at higher numbers of storeys), indicating its importance as an influential parameter for these indicators. Notably, the trend curve is more acute in cases of higher cut-off angle. These conclusions are valid for all types of urban built forms considered in this study.

3.3.2 Comparison of built forms

Results for site coverage and plot ratio of the built forms are now integrated in Figure 3.5 to provide greater insight.

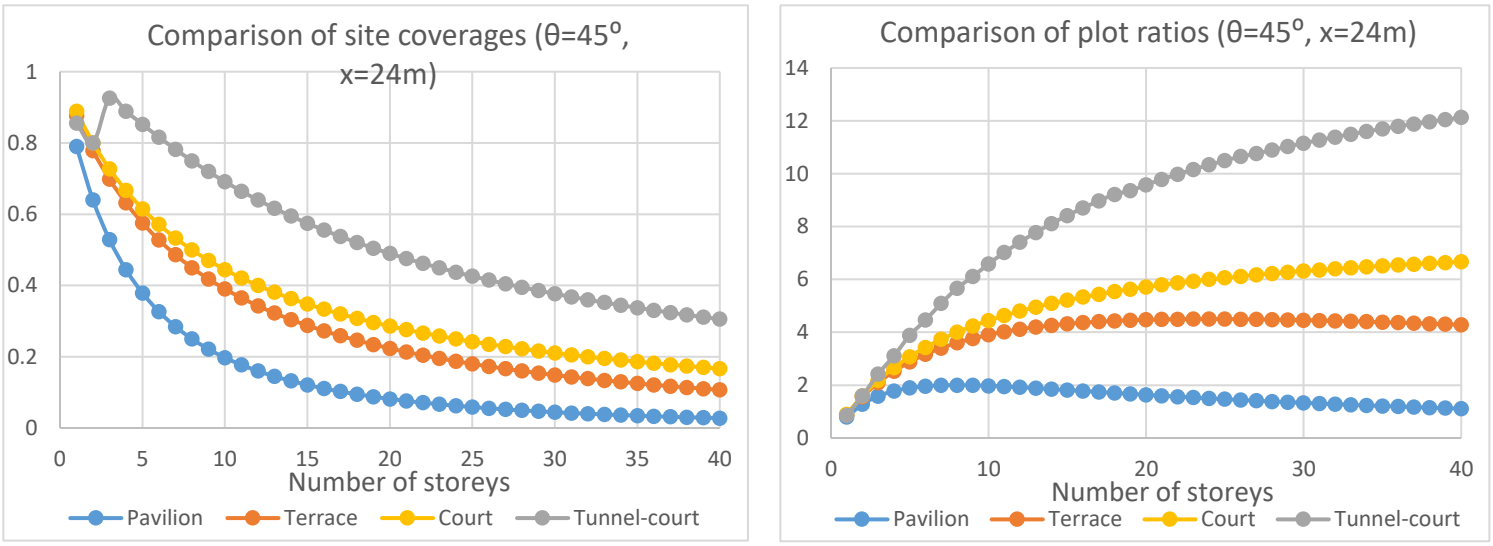

Figure 3.5: Comparison of site coverage and plot ratio of pavilion, terrace, court and tunnel-court forms in case of θ=45°, x=24m

From the graph, and for the same *x* and *θ*, the pavilion form always has the lowest site coverage and plot ratio regardless of number of storeys. Terrace and court forms are in the middle, while court form shows higher values. The value of plot ratio for pavilion at its peak is around half that of the terrace and court. Tunnel-court provides the greatest site coverage, and its plot ratio is much higher than the others, while its difference with other forms increases with increasing number of storeys. A peculiarity of tunnel-court form is the anomalous characteristics of the trend lines for 1 and 2 storey buildings that are due to the additional component (*2xd, [n≤2]*) in Eqn (3.21), which accommodate the difference in the plan of the first two storeys as a result of the roads passing from the buildings. Other values of *x* and *θ* indicate similar trends.

Of particular note is the peak depicted on the trend lines of plot ratio of pavilion and terrace forms. This shows that there is an optimum number of storeys that gives the highest possible plot ratio. The reason is that for pavilion and terrace forms, as the number of storeys increases the distance between buildings increase in four directions (with respect to neighbour buildings). Exceeding a certain number of storeys means the buildings are too far from each other resulting in the emergence of large open areas leading to lower plot ratio and site coverage. This is not the case for court and tunnel-court forms that depict a continuous ascending trend in their characteristics (see Figure 3.5). That is because the parameter '*L*' presents inside the geometry of

the court/tunnel-court building blocks. Hence, by increasing the distance between buildings, the inner yard of the block is extended too that increases the floor area of the buildings.

3.3.3 Practical cases of constant distance between adjacent buildings

As emphasised, the descending trend of plot ratio after the peak in the pavilion/terrace cases is due to the increase in the distance between buildings in all directions as the number of storeys increases. For the same reason, the amount of site coverage tends to zero for high-rise buildings ($n \geq 20$). This only occurs in theory as in practical cases this rule is rarely respected, at least in the horizontal direction. In different cities in the world, and based on their policies, the horizontal distance between buildings is usually kept constant and only the distance of buildings in different rows increases with respect to increasing height. For example, in hot-arid climates the distance between adjacent buildings can be considered narrow (e.g. 6 m) in order to benefit from shadow and shield direct sunlight. In these cases, both site coverage and plot ratio of pavilion/terrace building forms are much higher than the theoretical situation above. It is also the case for court form if the distance from the adjacent block is kept constant. The results of this alternative assessment in the case of L=6m (in horizontal direction) are shown in Figure 3.6.

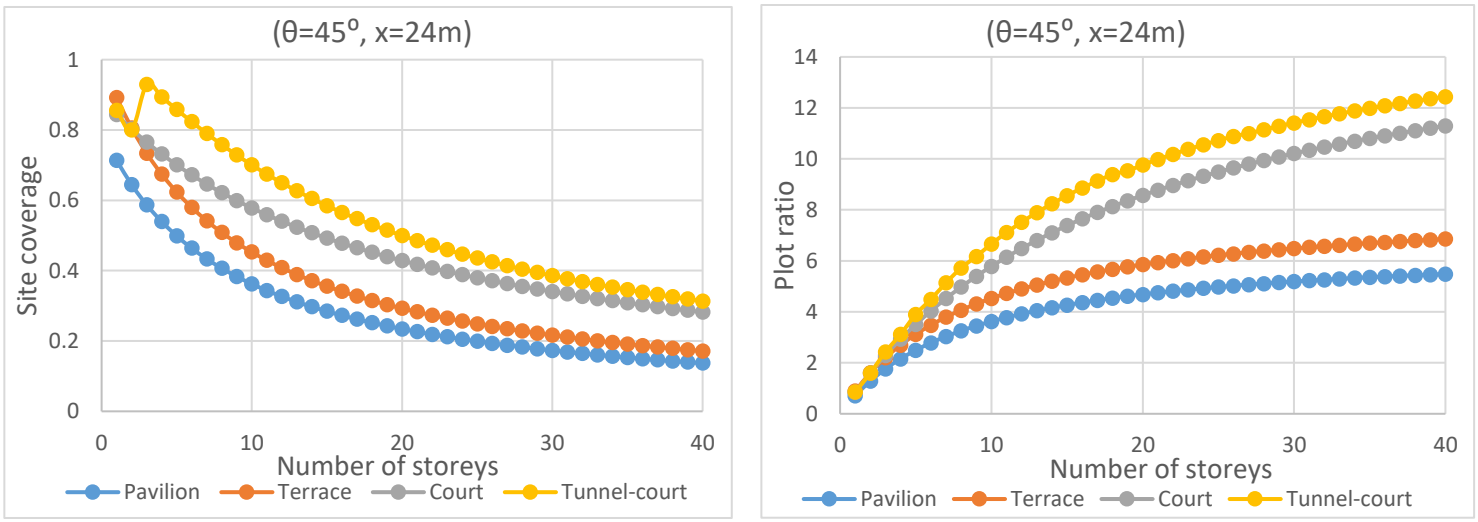

Figure 3.6: Comparison of site coverage and plot ratio of urban built forms in case of constant distance (6m) with adjacent buildings for (θ=25°, x=12m) and (θ=45°, x=24m)

It can be seen that the pavilion form still occupies the lowest site coverage and plot ratio, while the difference with the terrace form is not as significant as in the previous analyses. In this case, court form still acquires higher site coverage and plot ratio compared to the terrace form, although it has some overlap with terrace form

when the number of storeys is 1 or 2. The highest possible density can be still achieved by tunnel-court form. Moreover, there is no peak in the trend curve of pavilion and terrace forms and their plot ratio is always ascending with *n*. Hence, the presented methodology can also be applied alternative assumptions (e.g. in this case *L* is kept constant in the horizontal direction) to tailor the results according to specific requirements.

The results of analysing volume-area ratio are excluded from this study because it has a positive linear correlation with plot ratio (simply by multiplying plot ratio to storey height). Therefore, all trendlines show similar characteristics to the plot ratio.

3.4 Surface to volume ratio vs. number of storeys

This indicator has been used in many studies as a representative of the amount of heat transfer from/to building fabric (Ascione et al., 2013, Mutani et al., 2016) that is directly related to the thermal transmittance of the envelope. It indicates the magnitude of the surface areas exposed to outdoor environment compared to the volume of building. Hence, the higher this indicator the higher is the exposed surface area and the higher is the heat loss from building. This indicator has even been used as a measure of compactness in some studies (Le Guen et al., 2018). Having undertaken a similar analysis here, the trends of changing surface to volume ratio against number of storeys for four urban built forms are shown in Figure 3.7.

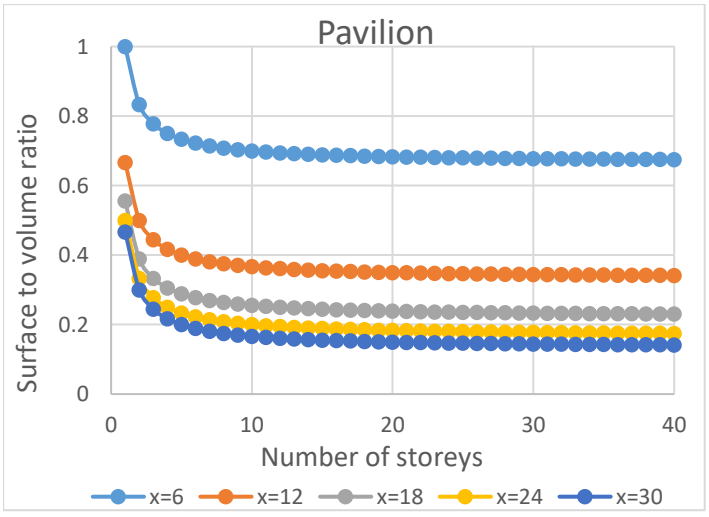

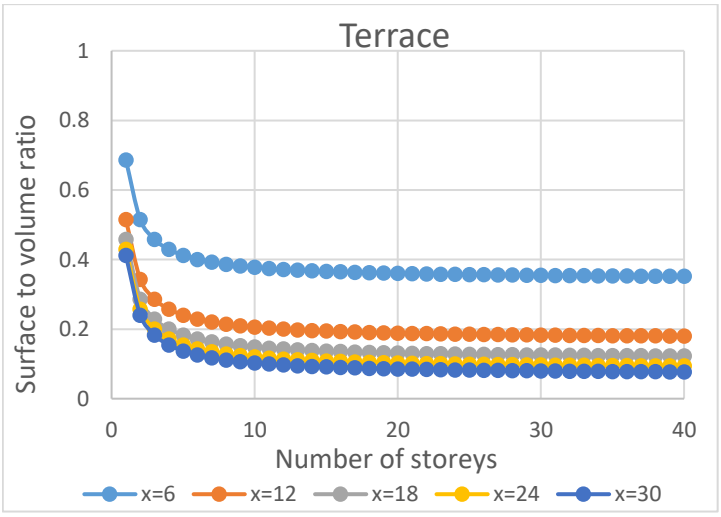

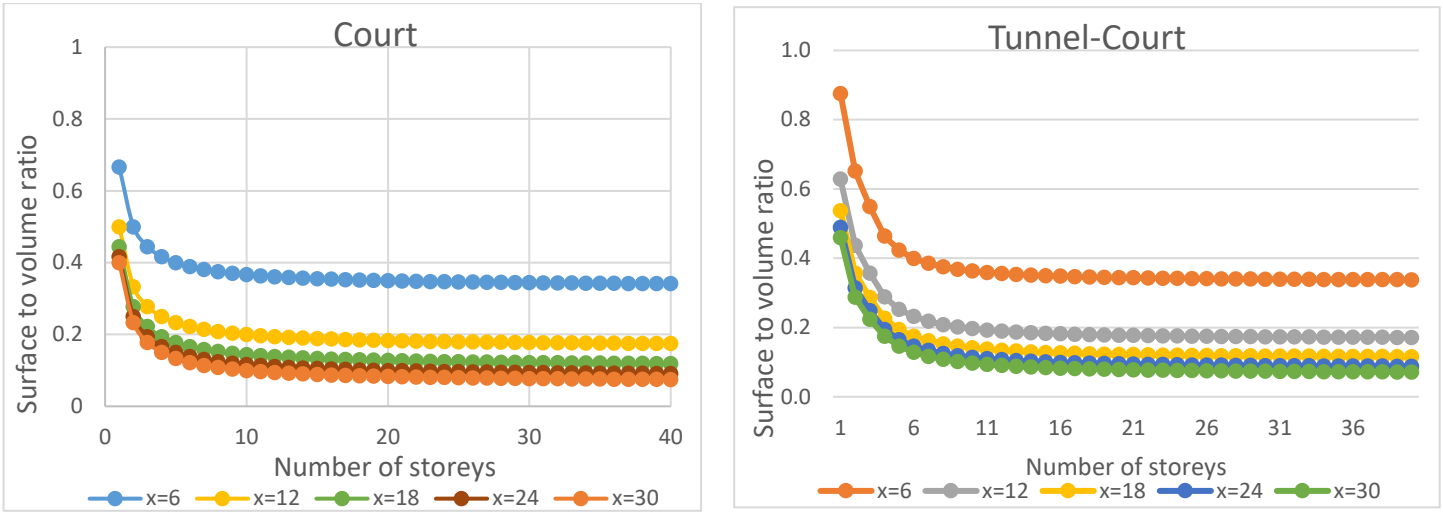

Figure 3.7: Trend of surface to volume ratio of different urban built forms with respect to the number of storeys

The results show a descending trend of surface to volume ratio with increasing number of storeys. Also, it indicates that by using greater plan depths, the building achieves lower surface to volume ratio. This means that there are lower losses from the buildings that are taller and deeper in depth. Attention should be paid to the slope of the curves which indicate that after a particular number of storeys (approximately 10), the characteristic is almost tangential. Hence, constructing buildings higher than this threshold does not have significant effect on heat loss reduction, and increasing the number of storeys should have other justifications. Nevertheless, as discussed in Chapter 2, building higher may cause negative effects on overall energy performance of the building. This will be extensively investigated in Chapter 5.

It should be note that in case of tunnel-court form, the cut-off angle does have a minor influence on the magnitude of surface to volume ratio. However, it is of low significance and doesn't impact on the overall trend. Hence, the average trend of this indicator for cut-off angle of 45º for tunnel-court form is used for comparison purpose.

For direct comparison purposes of the examined urban built forms, Figure 3.8 shows the results combined, and indicate that the highest values of surface to volume ratio are obtained by pavilion form, while the other three built forms show better performance with limited relative performance improvements.

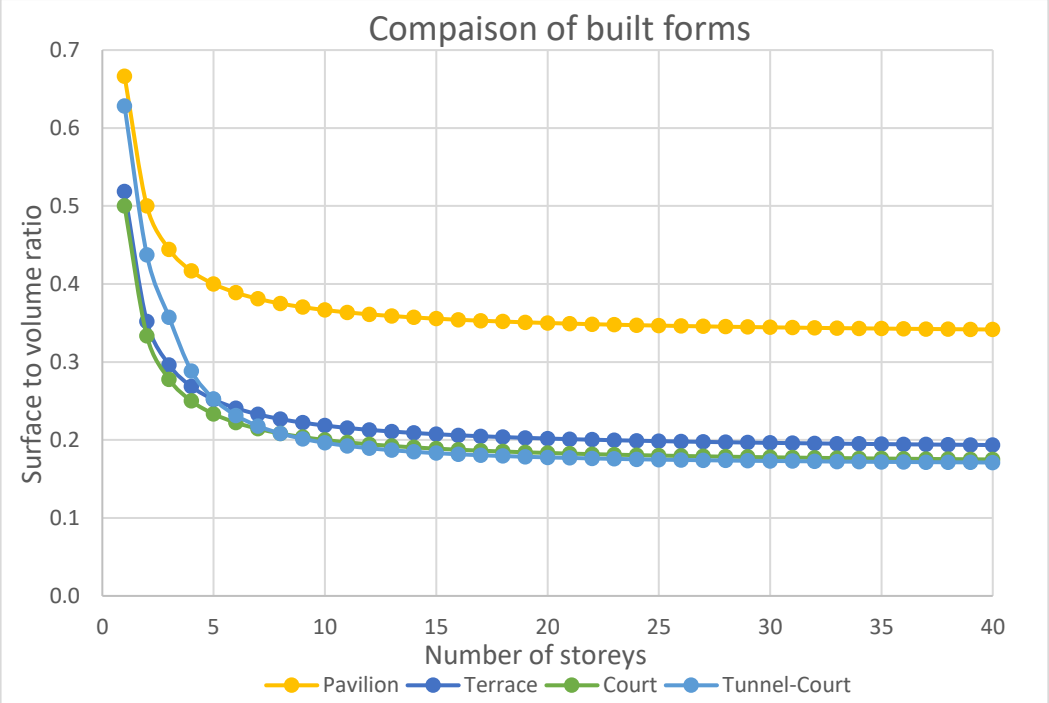

Figure 3.8: Comparing the change in the values of surface to volume ratio of pavilion, terrace, court and tunnel-court forms

For buildings having less than eight floors the lowest surface to volume ratio belongs to court form, while, for buildings with more than eight number of floors, tunnel-court form shows lowest surface to volume ratio. Therefore, in case of solely considering building fabric heat loss, court (for less than eight storeys) and tunnel-court (for more than eight storeys) forms are better choices, though making more holistic conclusions about energy performance of building needs to consider other influential parameters.

3.5 Combining the density indicators in a single diagram

3.5.1 Selection criteria for indicators

It is of particular interest to investigate the relative importance of indicators for best describing urban density. As discussed in Chapter 2, a set of density indicators should be employed to give a more comprehensive definition because they may or may not show similar trends in urban analyses. Here in this study, volume-area ratio is disregarded as it can be obtained with a simple linear relationship with plot ratio. Meanwhile, since both plot ratio and surface to volume ratio have been used many times in the literature to represent buildings density/compactness, their relationship is shown in Figure 3.9.

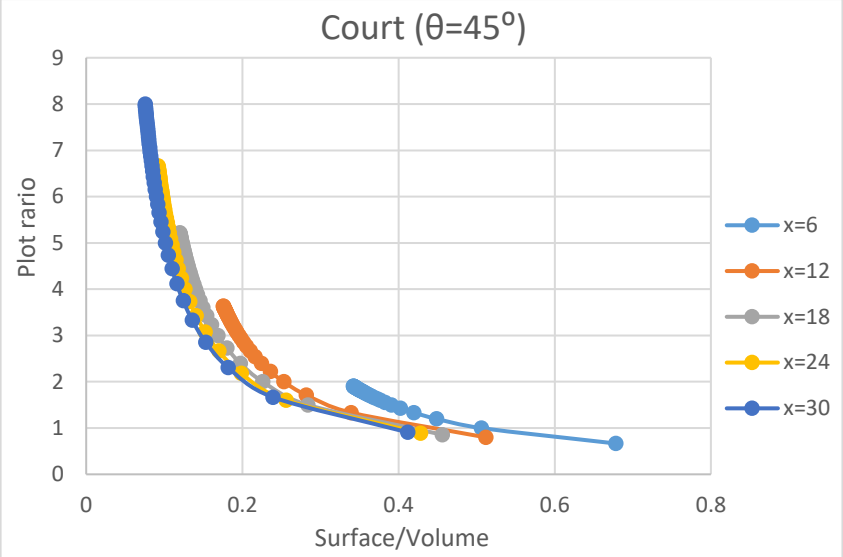

Figure 3.9: Relationship of plot ratio and surface to volume ratio in case of court form with θ=45°

As can be seen, these two indicators show a non-linear inverse trend. This is an interesting outcome that illustrates the gap in current literature. While many researchers derive conclusions based on the relationship of energy with surface to volume ratio, others develop their studies based on the relationship of energy with plot ratio—they are now shown to have opposite characteristics. Hence, the choice of density indicators is crucial. The lack of a comprehensive indicator to be used as a reliable structure for studies of energy and urban form and density is evident, which will be developed in following sections.

For urban scale studies, the choice of density indicator should possess urban characteristics. According to the definition of indicators from section 3.2, surface to volume ratio is an indicator of the compactness of buildings, meaning it is more appropriate for analyses at an individual building scale. As a result, this is not the choice of this study. Plot ratio and site coverage demonstrate urban characteristics as they consider whole site area in their definition.

3.5.2 Preliminary model and its limitations

Here, the chosen indicators and parameters are combined in a single figure of merit to depict the characteristics of any urban area with respect to land-use. Referring to Eqns (3.10), (3.11) and (3.12), the plot ratio is obtained by multiplying site coverage and the number of storeys regardless of the form of the neighbourhood (assuming all buildings have an equal number of storeys and all the storeys have the same floor area). Using this relationship, Figure 3.10 shows the relative influence of these two indicators and number of storeys. It can be seen that for any value of plot ratio having

a number of storeys, the corresponding value of site coverage can be obtained, and vice versa. Moreover, the distance between the lines showing the number of storeys decreases as *n* increases, indicating that the higher the building the lower the rate of change of plot ratio and site coverage. This aligns to that developed by Berghauser Pont and Haupt (2007) with two main differences. Firstly, their results were developed only for buildings up to 13 storeys, while the version presented here provides a more generic treatment, and secondly, their study included the open space ratio (OSR) of buildings which is not included in this study since it is in opposing correlation with site coverage and can be readily calculated through basic linear formulation.

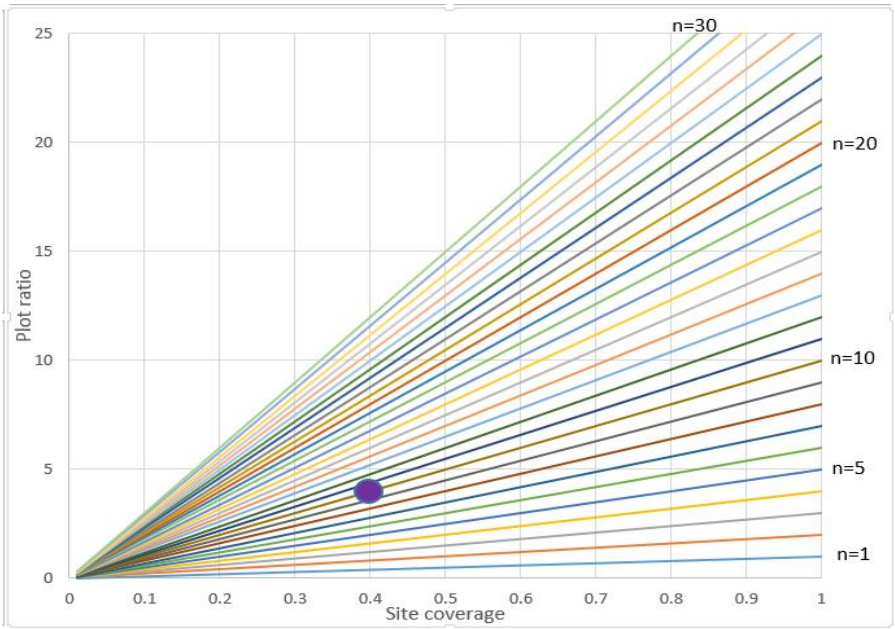

Figure 3.10: Relationship of plot ratio, site coverage and number of storeys with the example of the point corresponding to P=4, C=0.4 and n=10

From this study we seek the relationship between urban built form and density, which is not presented in Figure 3.10. Hence, there remain limitations to the usefulness of this graph which can be addressed by introducing new parameters. Having considered a particular point on the map, it is not possible to define the type of built form corresponding to that point (It can be pavilion, terrace, court or any other built form). For instance, considering the identified point on the figure corresponding to the site coverage of 0.4, number of storeys of 10 and plot ratio of 4 (Figure 3.10), this could represent an urban area with any type of built form depending on the building's cut-off angle and plan depth. Some possibilities are; pavilion with θ=65° and x=24 m, terrace with θ=45° and x=20 m, and court with θ=65° and x=9m. Hence, the design point does not identify all characteristics of the built form.

3.5.3 Emergence of the *Form Signature* tool

To give an absolute identification to all the points on the graph, the influence of plan depth (x) and cut-off angle (θ) should also be included. Therefore, combining the effect of these two geometrical parameters introduces what is now termed the *Form Signature* on the plot that distinguishes each urban built form considered in this study. Since plan depth and cut-off angle are independent variables, the range of both cannot be shown on a single diagram simultaneously. As a result, a suite of guidelines is obtained for urban planners which are an extension of what is shown in Figure 3.10. Steadman (2014b) compared cut-off angle and plan depth of different built forms using specific values as an example.

3.5.3.1 Pavilion, terrace and court

To determine the effect of plan depth, the value of cut-off angle is fixed and the analysis is undertaken for different values of plan depth (x: 6 to 60). Then, this assessment is repeated for different values of θ. The results for cut-off angle values of 25°, 45° and 65° are shown in Figure 3.11. This is done by overlaying two different datasets on one graph in an Excel spreadsheet tool (see Appendix A).

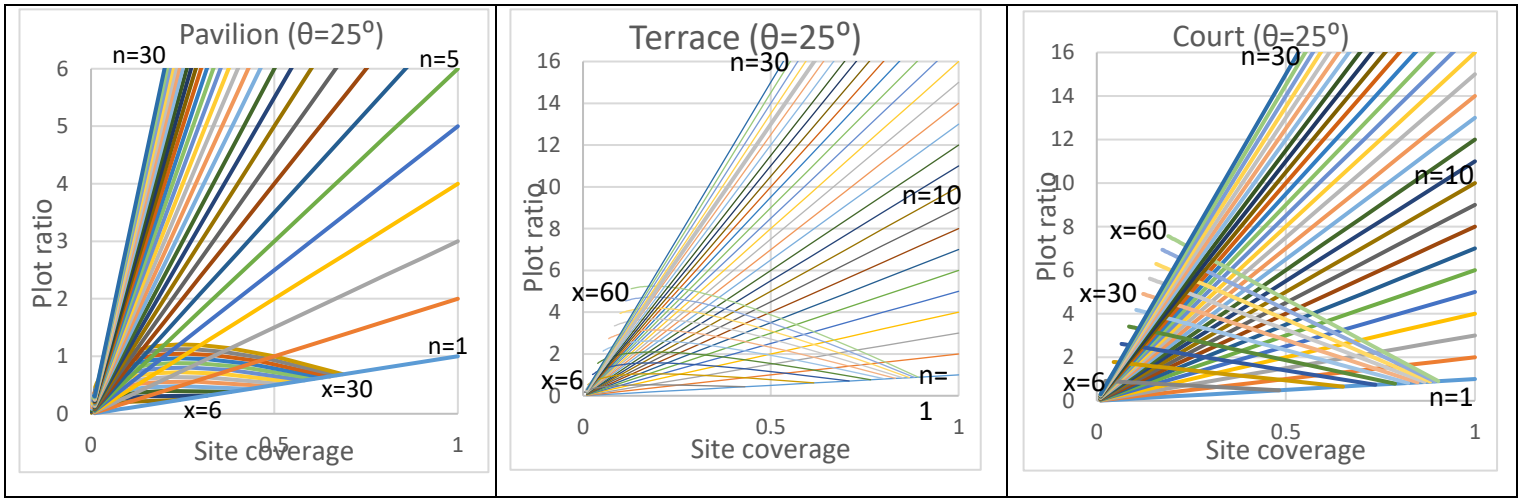

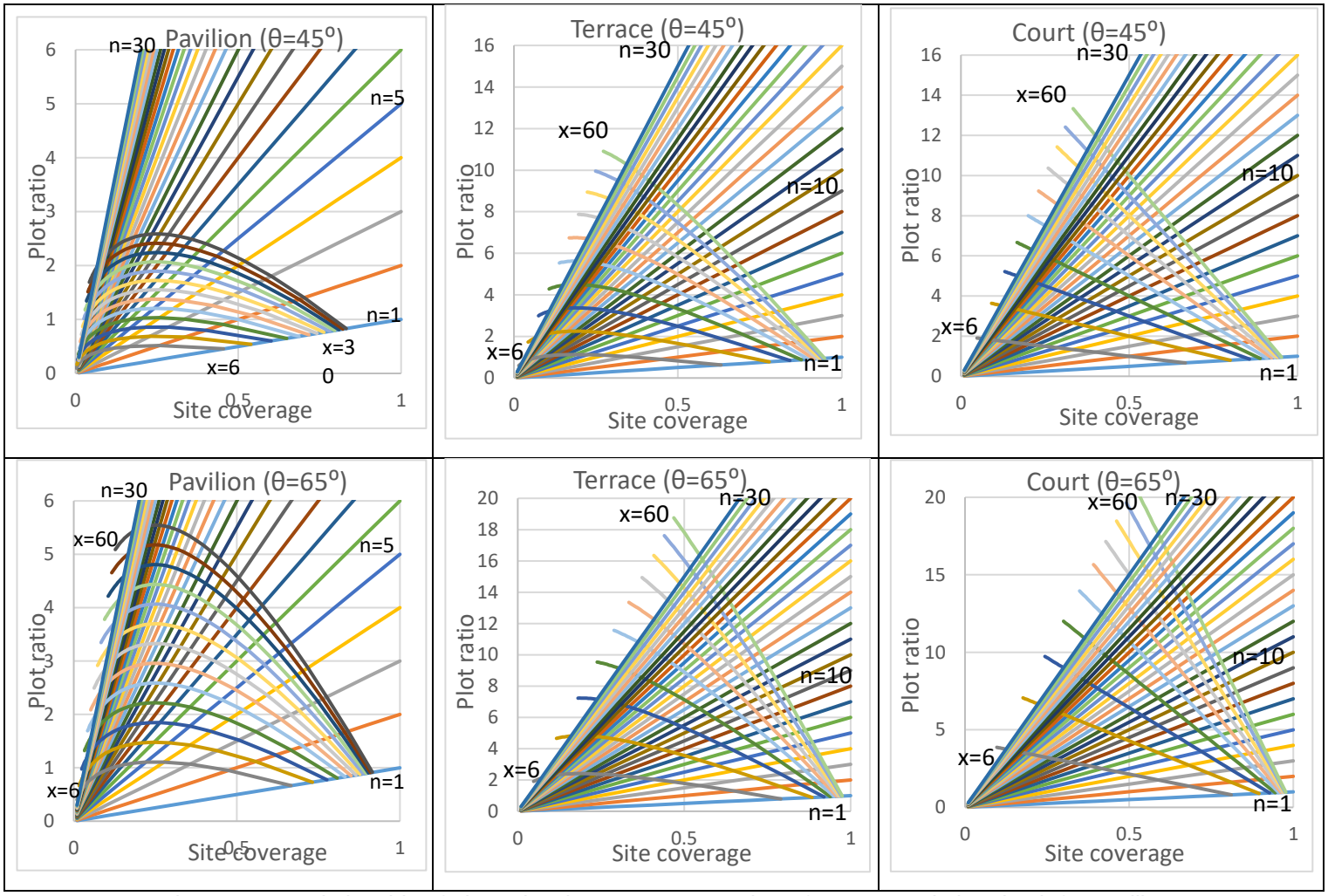

Figure 3.11: Relationship of plot ratio, site coverage, number of storeys and plan depth for pavilion (left), terrace (middle) and court (right) forms in case of cut-off angle of 25º, 45º and 65º

Using this set of characteristics, the density of any pavilion, terrace and court form neighbourhood with plan depths in the range 6m to 60m (or higher if required, via replotting) with three cut-off angles of 25°, 45° or 65°, can immediately be identified as a unique point in either of the composite diagrams. Indeed, any district with these forms can be identified with a unique point on either of those diagrams. To accommodate values not captured in the diagrams, interpolation or extrapolation can be used. The graphs specifically demonstrate the relationship of geometric variables of each build form with the density indicators. It can be concluded that:

- Increasing the cut-off angle increases both site coverage and plot ratio
- Increasing the number of floors increases plot ratio but decreases site coverage
- Increasing the plan depth increases both site coverage and plot ratio

3.5.3.2 Tunnel-court

This newly proposed built form is substantially different to more traditionally popular forms, and consequently alters the assumptions that are classically made. In tunnel-court form, although the number of storeys is assumed to be equal, the floor area of all storeys is not, since the 1st and 2nd storeys of buildings are smaller in floor area as the roads pass through them. Hence, the plot ratio is not simply the multiplication of site coverage to the number of storeys but is obtained from Eqn (3.22). Having undertaken corresponding studies for tunnel-court forms, the land-use characteristics of it are shown in Figure 3.12.

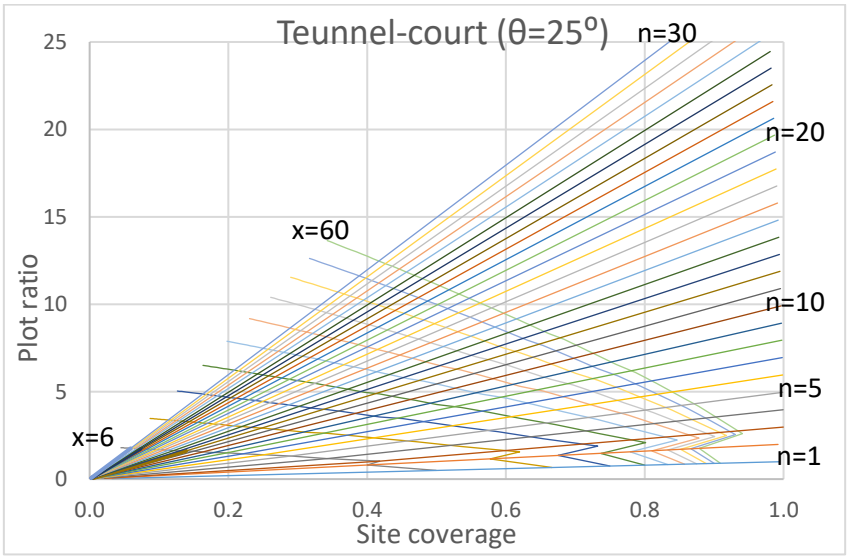

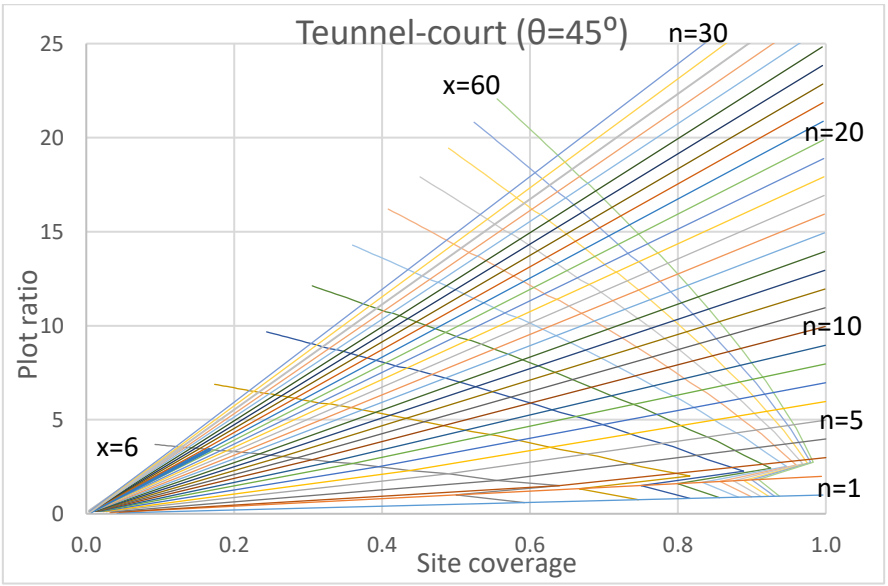

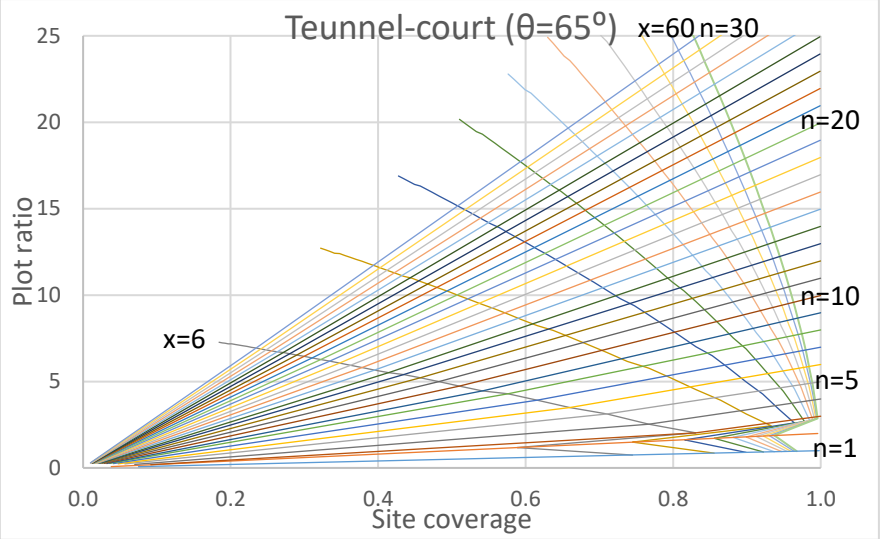

Figure 3.12: Relationship of plot ratio, site coverage, number of storeys and plan depth for tunnel-court form in case of cut-off angle of 25°, 45° and 65°.

The non-smooth features of the lines (showing the trend of *x*) at the starting point is due to the different floor area of 1st and 2nd storeys.

Figure 3.11 and Figure 3.12 again demonstrate that one indicator cannot simply define urban density because diagonal lines of plan depth show that when site coverage is high, plot ratio is low and vice versa. Therefore, particular care should be taken when using the expression 'high density'.

Presenting the results of this study is analogous to the LT method (Baker and Steemers, 2003). It proposes a set of graphs (handbook) that can be chosen according to the initial conditions. It is also available as an Excel spreadsheet tool with the potential of being enhanced to an online tool or software in the future.

3.6 Applications

The *Form Signature* tool, illustrated as a suite of graphs, fills the knowledge gap for systemically relating urban built form with urban density. It not only excludes the effect of 'interfering' factors from the analysis, but also shows the simultaneous relationship of all pertinent variables in the form-density equations. There are two main applications for this tool that are discussed in following sections.

3.6.1 Application to planning regulation for new district development

In general, the diagrams shown in Figure 3.11 and Figure 3.12 are the intersection of five key parameters that influence the density of a built area, and knowledge of one parameter a-priori enables the others to be chosen on the basis of relative compromise. Knowing four of the parameters, the remaining parameter can be readily

obtained, and the precise design of a master plan achieved. An important application of these graphical guidelines is setting thresholds for variables, specifically the density indicators. Since "*development control is an integral component of urban land use policy*" (Tang and Tang, 1999), this has been shown to be very beneficial for controlling and monitoring urban development by urban planners and policy makers. They normally restrict parameters such as plot ratio or the height of urban developments (Lai and Ho, 2001) in order to optimize contexts such as urban resilience (Sharifi, 2019), energy (Moghadam et al., 2019), population to land ratio and transportation as sustainability dimensions of the urban built environment (Deng et al., 2019). Indeed, it can visually show how changing one parameter influences others.

In the following, a number of real cases are used to demonstrate the efficacy of the presented results:

- From regulations in the city of Tokyo, the maximum plot ratio of 1 and site coverage of 0.5 is set for category II of low-rise residential zone, as restrictions (Plaza Homes, 2017). Considering pavilion form and cut-off angle of 45° to achieve acceptable daylight availability while satisfying efficient use of limited lands in the city, the admissible box for planning is shown in Figure 3.13 (left). The graph clearly shows that maximum allowable plan depth is 12m as a consequence of primary planning regulations. Hence, combining the plan depth and number of storeys inside the box, the optimum design point can be obtained.
- A guide for controlling residential development in Singapore established the maximum plot ratio of 2.8 for high density development with an equivalent number of storeys of 36 (StackedHomes, 2018). According to Figure 3.10, it needs to occupy site coverage of <0.1 to achieve this goal.
- A high-density built environment in the city of Nablus has a plot ratio of 1.29 and site coverage of 0.6 (Coccolo et al., 2016). According to Figure 3.10, the average number of storeys would be ~2.
- Tang and Tang (1999) discussed the maximum plot ratio of 6 for domestic buildings in Hong Kong. This means different combinations of site coverage and building storeys can be chosen to achieve this plot ratio restriction. For example, from a decision to commit to 10-storey buildings, the maximum

allowable site coverage will be 0.6 (based on the Figure 3.10) since the limit of 6 is already fixed for plot ratio.

- Building height limit regulation that can be found in Washington or India (Larson and Zhao, 2017).

In all the above cases, if the built form is known planners can immediately check the related set of guidelines and choose the best match of plan depth and cut-off angle for their plan from Figure 3.11 and Figure 3.12. For instance, in a hot-arid climate, the court form acquires many advantages (Javanroodi et al., 2018), and hence, the rightmost column of Figure 3.11 should be considered. Then, if policy means constructing the area with a plot ratio of 4, number of storeys of 7 and cut-off angle of 45°, looking at the related diagram, the site coverage must be 0.57 and the buildings must possess a plan depth of 27m (Figure 3.13 (right)). Alternatively, if there is a limitation on cut-off angle and plan depth, the most suitable urban built form can be chosen.

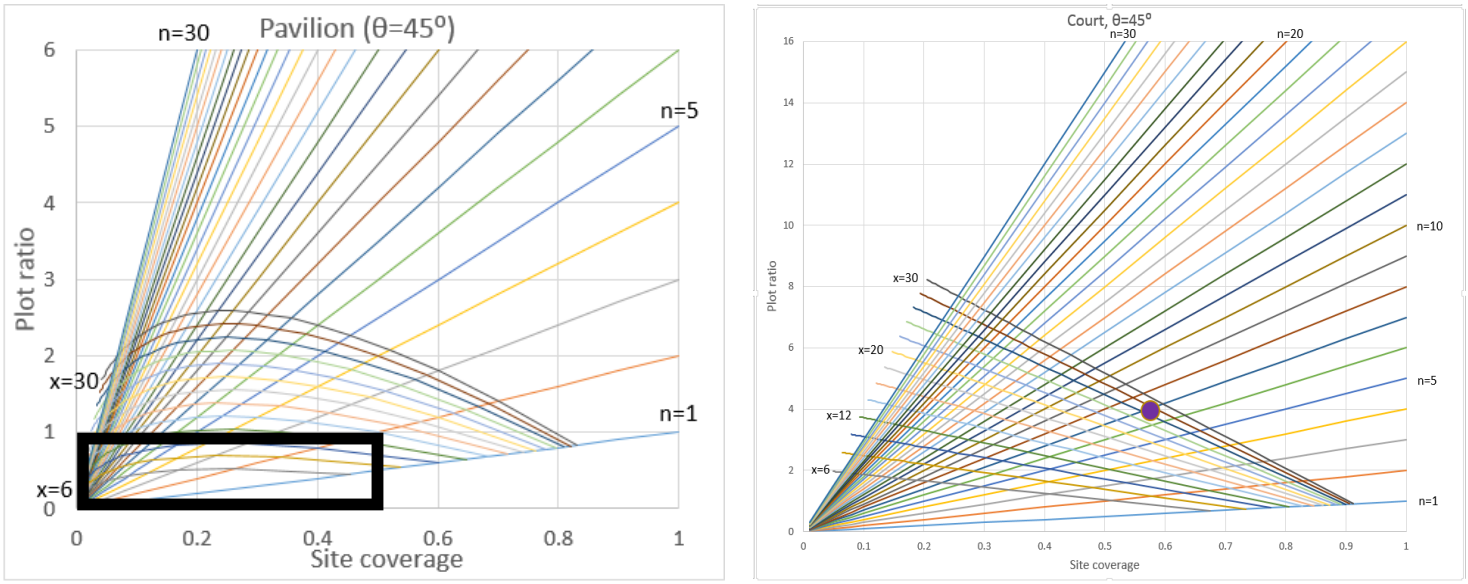

Figure 3.13: The planning restrictions in Tokyo showing the admissible box (left), Example of design point for P=4, n=7, θ=45°, C=0.57 and x=27m (right)

Therefore, the *Form Signature* can be used as a master planning tool that can shape cities in two different ways, as noted by Radlin and Hemani (2019):

"*The first is to set out a framework (or trellis) into which the city can grow as with the planted American cities or the new town extensions of many European cities. The second is the use of a masterplan to repair the fabric of the existing city, to filling gaps, impose order, improving conditions etc. as Nash did in London and Haussmann in Paris.*"

3.6.2 Application to real existed cities

3.6.2.1 Urban built form, density and climate

Built forms considered in this study currently exist in different cities around the world in different climate zones, as classified by the Koppen climate classification (Rubel and Kottek, 2010). It is important to recognize the characteristics of built forms that have emerged for different climatic conditions using the results of this study to build their respective maps which show their *Form Signature*. To this end, 32 districts from 19 cities have been selected as case studies to define their land-use characteristics using the graphical guidelines. The site coverage and plot ratio of the case studies are calculated using their plan depth and number of storeys. This information, plus the climatic condition of the cities based on the Koppen classification, is detailed in Table 3.5.

Table 3.5: List of case studies around the world including plan depth, site coverage, cut-off angle and plot ratio

Built Form	**City** (District)	***x***	***C***	***n***	***P***	**Climate**
a) Pavilion	**Auckland** (Ormiston)	13	0.26	2	0.53	Temperate (Cfb)
	Melbourne (Oakleigh East)	12	0.34	1	0.34	Temperate (Cfb)
	Barcelona (Ramble de Guipuscoa)	20	0.23	15	3.48	Temperate (Csa)
	Rome (Municipio V)	15	0.32	5	1.62	Temperate (Csa)
	Tehran (Parand)	24	0.35	6	2.1	Temperate (Csa)
	Putrajaya (Taman Pinggiran Putra)	15	0.39	1	0.39	Tropical (Af)
	Las Palmas (Calle Virgen del Pilar)	26	0.22	13	2.84	Dry (Bwh)
	Singapore (Bukit Timah)	12	0.23	2	0.46	Tropical (Af)
	Singapore (Bukit Panjang)	42	0.17	28	4.76	Tropical (Af)
	Hong Kong (Central)	40	0.26	42	10.71	Temperate (cfa)
	Boston (Winter Hill)	11	0.37	3	1.11	Continental (Dfa)
	Sao Paolo (Jardim Sao Saverio)	20	0.17	18	3	Temperate (Cfa)
b) Terrace	**London** (Hither Green)	8	0.21	2	0.42	Temperate (Cfb)
	Lincoln (Monks Road)	11	0.45	2	0.9	Temperate (Cfb)
	Prague (Solidarita)	15	0.3	2	0.6	Temperate (Cfb)
	Barcelona (La Verneda I la pau)	15	0.38	12	4.6	Temperate (Csa)

	Oslo (Sofienberg)	12	0.29	5	1.46	Continental (Dfb)
	Tehran (Parand)	14	0.4	3	1.2	Temperate (Csa)
	Putrajaya (Taman Pinggiran Putra)	18	0.57	2	1.14	Tropical (Af)
	Las Palmas (Calle Henry Dunant)	8	0.33	4	1.32	Dry (Bwh)
	Singapore (Ghim Moh Road)	16	0.22	14	3.08	Tropical (Af)
	Boston (Black Bay)	16	0.31	5	1.56	Continental (Dfa)
c) Court	**Barcelona** (Lesquerra de Leixample)	25	0.52	6	3.13	Temperate (Csa)
	Prague (Vinohrady)	17	0.42	5	2.1	Temperate (Cfb)
	Vienna (Johannesgasse)	16	0.43	5	2.13	Temperate (Cfb)
	Rome (Municipio V)	12	0.39	8	3.15	Temperate (Csa)
	Oslo (Sverdrups Gate)	15	0.48	4	1.92	Continental (Dfb)
	Casablanca (Alvalfeh)	14	0.45	6	2.57	Temperate (Csa)
	Muscat (Al Ghubrah South)	6	0.33	6	2	Temperate (Csb)
	Santiago (Villa Los Peumos)	7	0.26	3	0.78	Temperate (Csb)
d) Tunnel-court	**Casablanca** (Casbat Amin)	9	0.85	6	5.12	Temperate (Csa)
	Vienna (Hofmusikkapelle)	20	0.8	5	4.02	Temperate (Csa)

The site coverage and plot ratios of the case studies were calculated using dimensions obtained from Google Maps. Figure 3.14 shows aerial photos of selected districts from the examined cities. To this end, the lengths and widths of the buildings as well as the site areas were measured on the map to calculate density indicators. The dimensions on the Google Maps were validated by practical measurement (using laser distance meter) of two areas in Lincoln which are the buildings of the University of Lincoln along with Foster Street.

Figure 3.14: Picture of the area of the cities considered as case study a) Pavilion b) Terrace c) Court d) Tunnel-court

To demonstrate the calculation method used to obtain the value of density indicators, the detailed calculation of the Oslo court form is explained here as an exemplar case study. Figure 3.15 shows the schematic plan of Oslo case study (Sverdrups Gate) including the dimensions obtained from Google Maps.

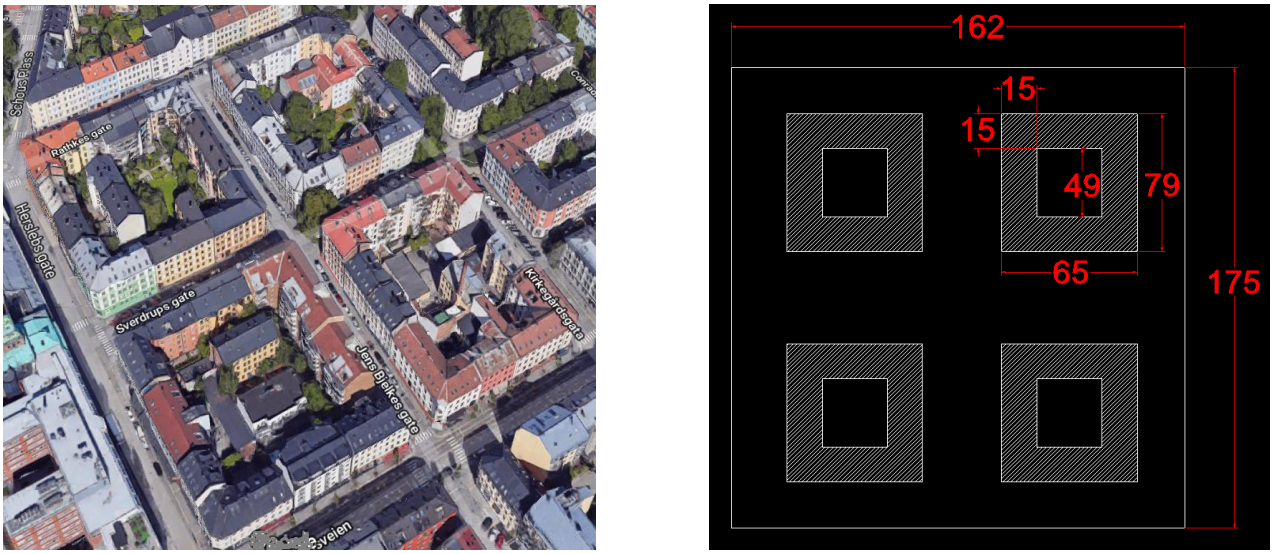

Figure 3.15: The aerial phot (left) and the schematic plan (right) of the Oslo court form case study.

Total area of the site (Z) is simply calculated as:

$Z = 162 * 175 = 28350\ m^2$

The area covered by one courtyard building is calculated as:

$A_1 = 2 * 15 * 65 + 2 * 15 * 49 = 3420\ m^2$

Having four courtyards in whole site area:

$A_{total} = 4 * 3420 = 13680$

Site coverage is calculated as A / Z:

$C = A/Z = 13680 / 28350 = 0.48$

Plot ratio is obtained from Eqn (3.12), and since these are all 4-storey buildings ($n=4$), the results is obtained as following:

$P = n * C = 4 * 0.48 = 1.92$

The same method applied for other case studies to calculate their site coverage and plot ratio.

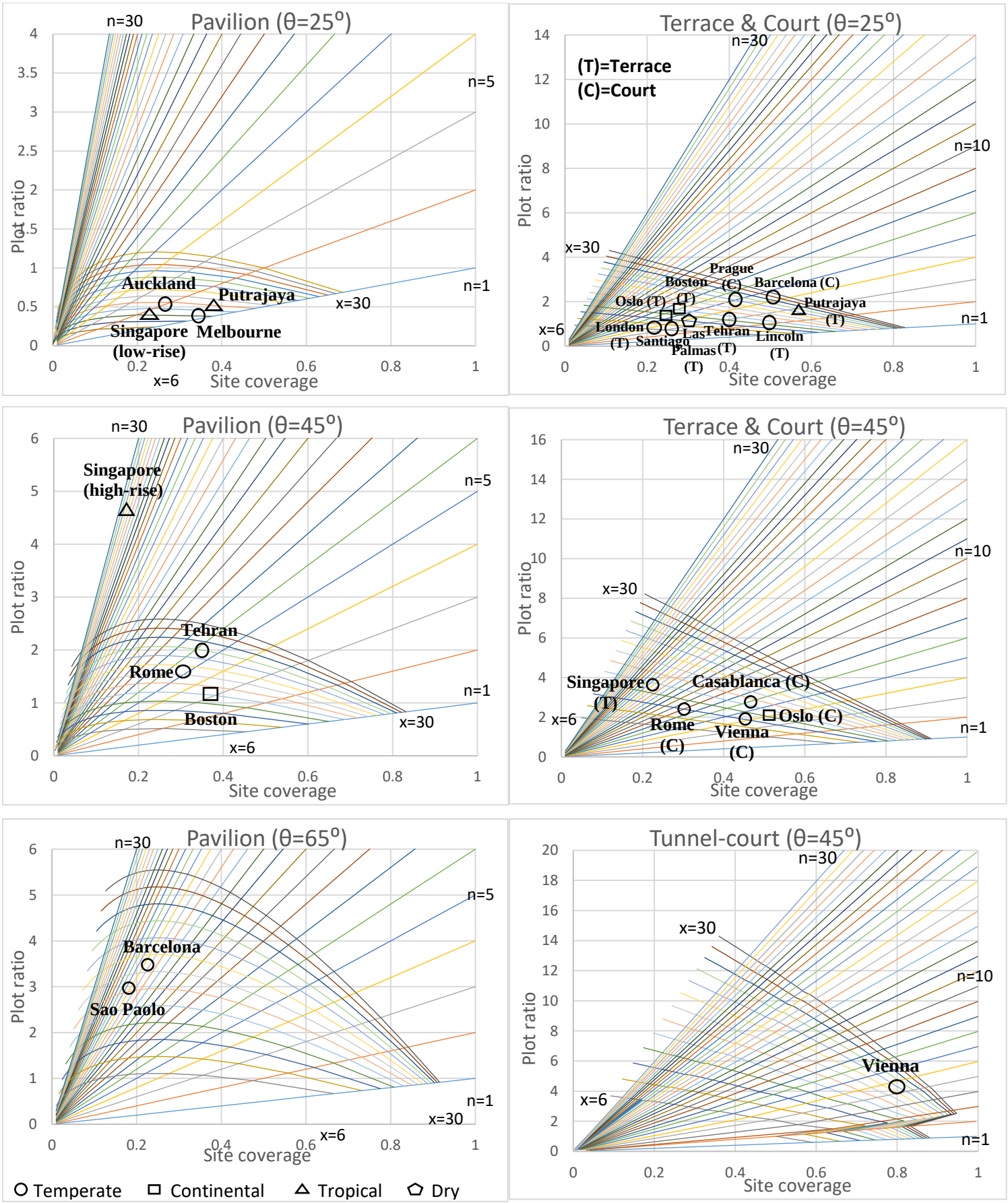

Figure 3.16: Demonstration of the case studies on the graphical guidelines as it shows their Form Signature

Figure 3.16 shows the *Form Signature* of the areas considered in the case studies. It can be seen that there is one point on the graphs which indicates the unique characteristics of the district i.e. any ambiguity resulting from consideration of different built forms is removed. The graphs relating to θ=25°, 45° and 65° are shown as exemplars, although others can be readily generated. For similar reasons, in a few cases, the cities are only approximately attributed on the graphs for illustrative purposes. Cases of Las Palmas and Hong Kong (pavilion), Prague and Barcelona (terrace) and Casablanca (tunnel-court) are not shown since their cut-off angles are around 52°,75°, 18°, 50°and 80°, respectively.

Although districts would have ideally been selected with consistent form and shape, in reality many built districts do not have same number of storeys, cut-off angle and plan depth over their entire area. In many cases, the growth of cities with deformed grids has also been observed, and a mixture of different built forms can be seen in some areas. One of the interesting functions of the presented results is defining the average cut-off angle of the cases considered since an exclusive cut-off angle can be obtained from the graphs shown in Figure 3.16 that can be considered as an identity for the district. This is a very important finding as cut-off angle has a direct relationship with daylight availability of buildings which is an influential factor for energy analysis on an urban scale. The case of a non-uniform distribution of buildings on site (density gradient not equal to one) can be justified by a change in the value of cut-off angles in the *Form Signature* tool.

By way of comparison between terrace and court forms, for instance, it can be concluded that areas with court form generally acquire a higher cut-off angle compared to terrace form. The case of tunnel court in Vienna demonstrates the highest site coverage among other case studies that is a validation for the results presented in section 3.3.2.

To establish a possible relationship between climatic condition of the cities and their form and density, the cities were classified on the graphs based on their climate. It can be seen that there is no clear relationship between climate zones and the form and density of the built areas that can be recognized, or at least it is not a substantial factor for contemporary buildings. In certain climatic zones, it is seen that climate as a factor to shape built form, is secondary to cultural aspects. For example, the court form is a very popular form in European cities. Nevertheless, in cities with similar climate and latitude in the US or Asia, they can rarely be found. There can also be overriding

reasons that a particular type of climate does/doesn't use a specific built form, such as population, available land and family wealth, which needs further analysis in the future. Furthermore, since this classification is based on the main groups of climates defined by Koppen, it is a general climate analysis and there are many subgroups that may have specific influence on form and density. This can be an area for future research.

3.6.2.2 Urban built form, density and energy

Connecting the results of this study with a heat map of the cities (an example is shown in Figure 3.17) is another important application of these guidelines. By distinguishing hot spots and finding their corresponding points on the *Form Signature* diagrams, planners can identify the worst/best form and density combinations in urban areas. This then enables future urban policies to be more precise and appropriate regarding the energy efficiency of growing urban areas.

Figure 3.17 shows the heat map of city of Lincoln in UK and its two areas with high (1) and low (2) heat intensities.

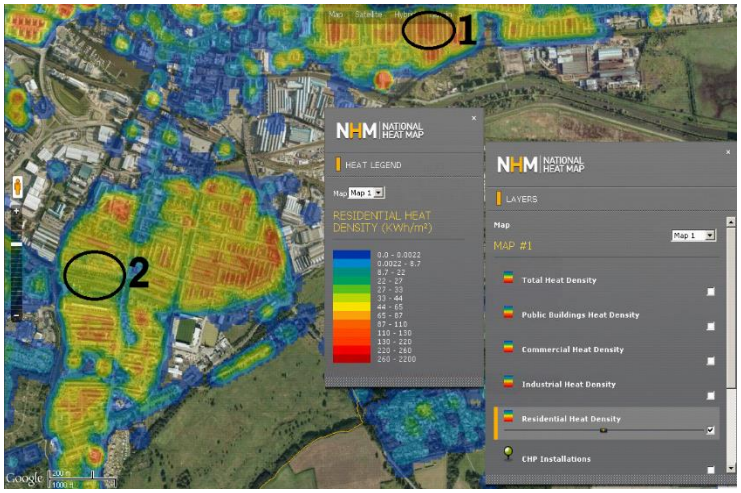

Figure 3.17: Heat map of heating energy consumption in the city of Lincoln provided by Lincoln City Council

In Figure 3.18, the corresponding points related to the areas marked on Figure 3.17 are shown on the *Form Signature* graphs. Area 1 with high heat density is shown on the left with site coverage of 0.45, plot ratio of 0.9 and cut-off angle of 25°, while area 2 with low heat intensity with lower cut-off angle (15°), site coverage (0.25) and plot ratio (0.5), representing a lower density, is shown on the right. By combining the statistical data of heat consumption over the whole city (or alternatively data from simulation) on the *Form Signature* diagrams, the relationship of form, density and energy demand of the city can be established.

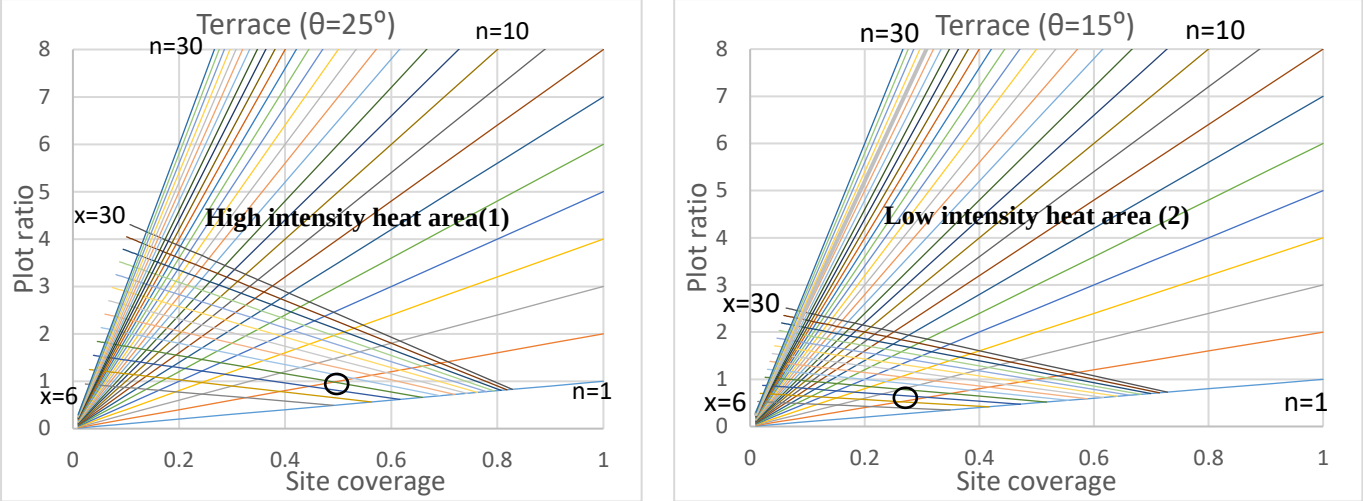

Figure 3.18: Corresponding points of Figure 3.17 on the Form Signature diagrams: high intensity heat (left), low intensity heat (right)

3.6.2.3 Urban built form, density and society

As one of the main elements of sustainability, social factors can have correlation with urban built form and density. McHarg (1969) assessed the propagation of several social issues including physical and mental diseases in the city of Philadelphia from statistical data. The outcomes were illustrated on maps of the city as shown in Figure 3.19.

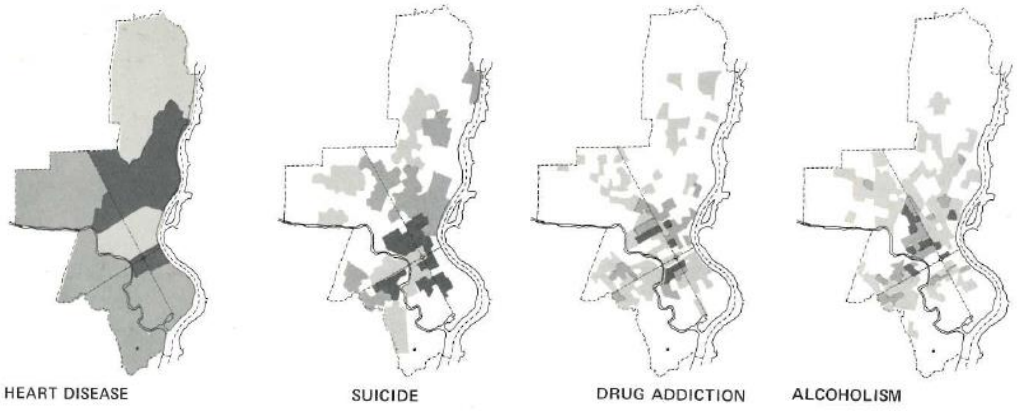

Figure 3.19: Social issues map of Philadelphia. Adopted from book of Design with Nature (McHarg, 1969)

Similarly, the crime map of the city of Lincoln published by Lincolnshire Police (2019), is shown in Figure 3.20.

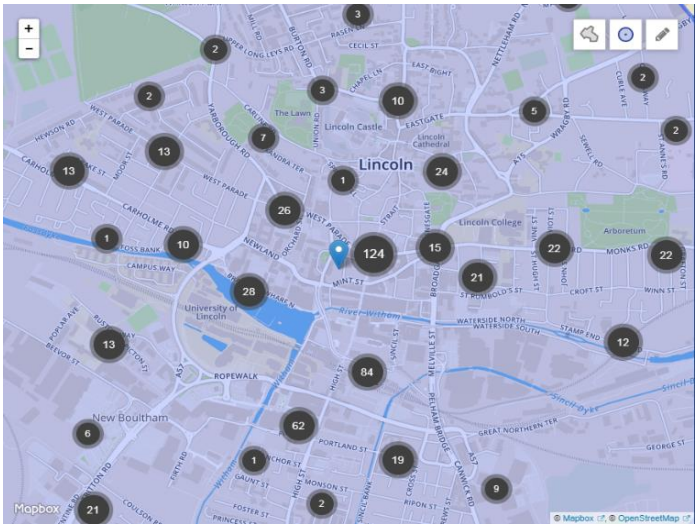

Figure 3.20: Crime map of Lincoln. Adopted from (Lincolnshire Police, 2019)

Integrating the geography of disease, suicide or crime with the *Form Signature* diagrams, the best urban built form and density to achieve a more socially sustainable city can be identified.

In addition, the *Form Signature* proposed here postulates the interconnection of urban built form and density with socio-economic variables or geometrical parameters such as passive zone floor area. This enables us to achieve more accurate plans for greater degrees of economic and energy sustainability.

However, these latter examples of the application of the *Form Signature* tool in urban planning need precise statistical analysis which is outside the scope of this study. The case studies were used to validate the model. Built form of traditional cities emerged from millennium of bottom-up decision-making processes. In other words, from morphological perspectives, traditional urban built forms emerge consistently through the application of many local interconnected design decisions that shape the overall, global, city plan, which therefore means that the overall city form is unknown. The proposed *Form Signature* is designed to accommodate both formal (orthodox) and informal (traditional) urban forms.

3.6.3 Implications for policy

In general, urban planning policies are defined based on a variety of factors including available land, property market forces, financial restrictions, social needs and efficient energy consumption patterns. Enhancement of one of these factors may result in the discouragement of others. For instance, as will be explained in Chapter 5, pavilion form buildings with greater plan depths are more energy efficient (Ahmadian

et al., 2019b). However, although it is possible to have very deep plans, it is not usually recommended as it limits the potential of passive design strategies resulting in over reliance on artificial means for environmental control of buildings such as mechanical ventilation (Evans et al., 2017) and artificial lighting (Steadman et al., 2009). This may increase energy demand of buildings while having adverse effects on user comfort, wellbeing and satisfaction. Utmost increase in plan depth of pavilion form practically results in form transformation to court form (Figure 3.21).

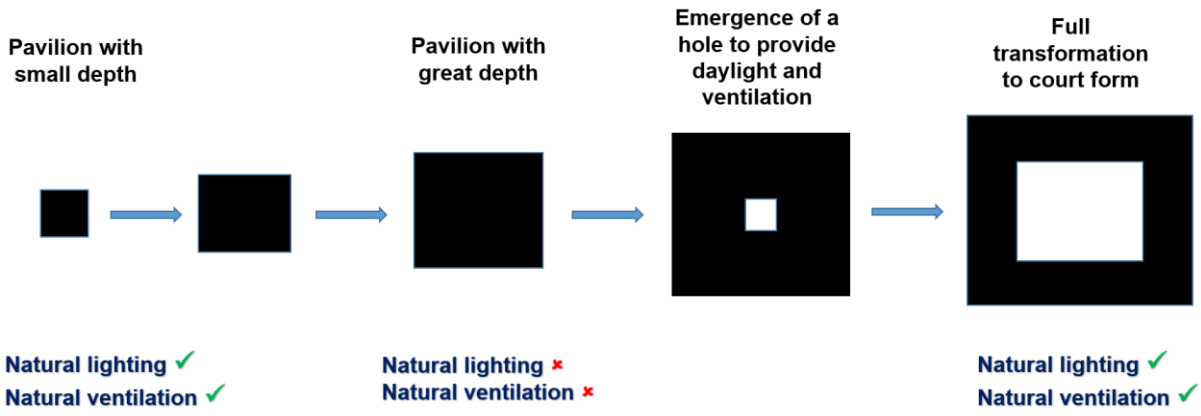

Figure 3.21: The evolutionary transformation of pavilion to court form by increasing plan depth

Court form buildings have other advantages in busy areas of a populated city such as London (e.g. beside the streets). It provides the opportunity of having windows inside the court to prevent noise and pollution (cleaning effect) to enter the building. Furthermore, for urban areas located in hot and arid climates, courtyards create better microclimate by having fountain, shadow and vegetation inside the court (Coccolo et al., 2016, Khalili and Amindeldar, 2014). Soflaei et al. (2017) showed that courtyard is a successful sustainable solution for hot-arid regions of Iran as a matter of climatic requirements as well as socio-cultural contexts.

Therefore, trade-offs between a variety of sustainability factors is a crucial task of sustainable urban planning. The development and growth of cities needs to broach the three subsets of sustainability: social, economic and environmental. The *Form Signature* tool enables planners and policy makers to achieve sustainability objectives by identifying the most suitable urban form/density permutations. By overlaying different variables of sustainability on the *Form Signature*, the diagrams propose resilient solutions for future urban developments (Figure 3.22). The common area of all analysed components on the diagram shown in Figure 3.22 demonstrates the optimum urban built form and density of the city in relation to its social, economic and

climatic condition. This tool can be used to shape urban planning policies in the future. In other words, the *Form Signature* tool enables us to transform urban morphology to urban policy.

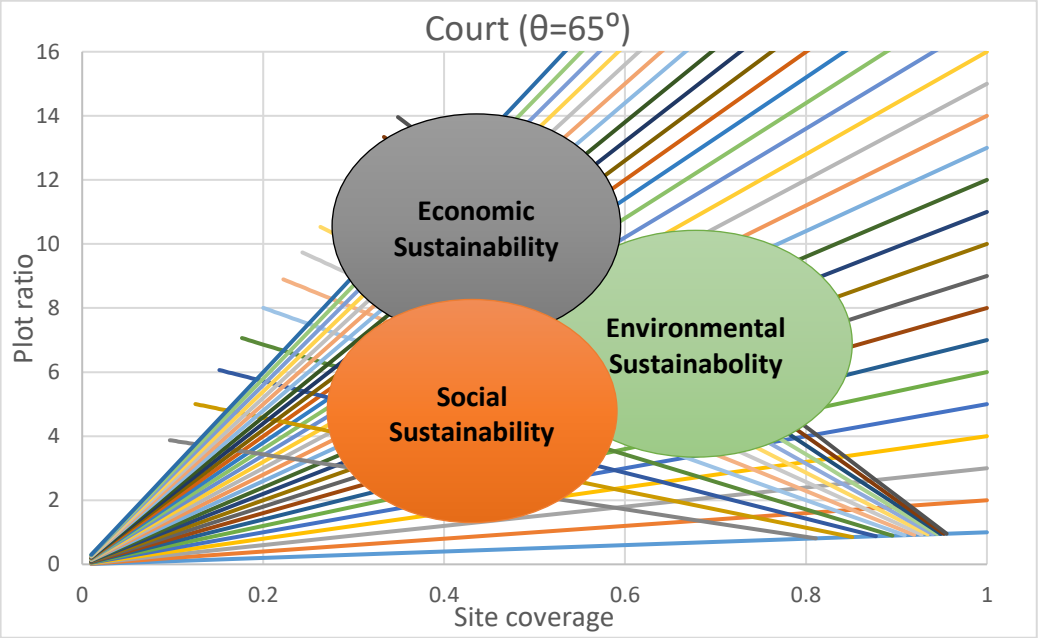

Figure 3.22: Coinciding the sustainability components on Form Signature diagrams

3.7 Conclusion

As discussed in the introduction, the world is facing the challenge of enormous urban development. The findings reported in this chapter provide rational ways of growing cities globally that enables the best possible design conditions. A set of guidelines providing a graphical means of qualitatively identifying inter-parameter sensitivity of four built forms has been presented through the introduction of *Form Signature*. The presented results facilitate identification of optimum planning conditions for sustainable development of future cities.

The guidelines recognize that there is no globally accepted definition of optimum absolute density as it is highly dependent on the consideration of different aspects that are determined by urban policies. For instance, the most appropriate urban form and density in the case of targeting lowest energy consumption is different from the case of targeting the highest economic benefits or social sustainability.

Results of case study analyses show that 1) there is no significant trend between climate and built form/density of urban areas. 2) Areas with court form have been built with higher cut-off angle compare to areas with terrace form.

In general, building higher does not directly mean higher density as it usually increases plot ratio (except in the case of pavilion/terrace that only increases up to a

specific number of storeys) and decreased site coverage. Hence, it is dependent on the desired characteristic of the built area. Also, after exceeding a certain number of storeys, for each of the built forms, no significant influence on density indicators is evident. The higher the cut-off angle, the sharper the slop of the lines showing plan depth. In this case, the *x* lines sweep larger areas of the graphs meaning that higher plot ratio and site coverage can be achieved. Furthermore, the chapter introduces a new type of urban built form, termed tunnel-court, which is able to achieve the highest density among the others considered in this analysis. For the same site coverage, tunnel-court always achieves higher plot ratio while pavilion exhibits the lowest plot ratio.

Development of the *Form Signature* concept establishes a basis for a form design tool (handbook) to inform planning decisions that optimise proposals and effectively integrate various variables. Due to its generic nature, it can be more readily utilized by practitioners, urban planners, policy makers, engineers and architects in order to develop the most appropriate built form and density in particular urban areas based on the urban planning policies of that region. Moreover, in the case of existing urban areas, these signatures provide a correlation between form and contexts. Hence, they provide a robust structure for future statistical assessments on climate, energy, economy and social issues to find their relationships with the form/density of urban areas. These are the sustainability components that need to be satisfied in order to achieve sustainable cities.

This chapter is an attempt to highlight the far-from-equilibrium structure of cities and provides a tool to decode some governing equations on urban complexity that help to understand the level of complexity for future urban studies.

Chapter 4: Selection of simulation tool and validation of the modelling approach

4.1 Introduction

Following the proposed method of study, the energy analysis part of the research uses energy simulation software and results will be related to the outcomes of Chapter 3 to answer the research question of this thesis.

The urban energy simulation software package, CitySim (Kaemco), is selected for this study because it is benefited of peculiar features that are advantageous for this study. It initially validated (in this chapter) against SAP simulation studies using data obtained for four terraced houses situated in Gainsborough (UK). By attaining the results with acceptable deviation, CitySim can be assuredly used for the rest of this analysis.

4.2 Modelling and simulation

Building energy consumption is affected by many factors such as building characteristics (e.g. building size, age, materials, insulation, glazing ratio, window type, building energy system and built form) (Elnokaly et al., 2019), urban planning (e.g. urban density affected by variables such as cut-off angle of plan), occupant density, users behaviour and climate. Many are therefore non-morphological factors (Steadman et al., 2014). For instance, the significant impact of occupant behaviour on building energy consumption has been demonstrated in several studies from different countries, such as the UK (Ben and Steemers, 2014, Sodagar and Starkey, 2016), the Netherlands (Guerra-Santin et al., 2009), South Korea (Park and Kim, 2012) and USA (Emery and Kippenhan, 2006). It was confirmed, for instance, that lifestyle and occupant age (Guerra-Santin and Itard, 2010) are determining factors when the usage of heating and ventilation systems are considered. Through use of simulation studies, selected parameters can be kept constant for all buildings to compare the influence of particular factors across all building forms. For instance, for building plans with different form and density, similar building type, occupancy profile, glazing ratio and building materials can all be considered in energy simulation software. This provides the opportunity to selectively exclude the effects of various parameters from the analysis, except urban built form and density, to facilitate an accurate comparison of site plans with different forms and densities.

4.2.1 Selection criteria for energy simulation software

Many building energy simulation packages exist that make it challenging to select the most appropriate for this research. The selection criteria for a relevant simulation tool are i) its capabilities to match the requirement of this study ii) validity and popularity of the software that has gained relevant pedigree in the research field iii) the availability of user support. There are many commercialized and well-recognized building performance simulation tools available in the market. Attia et al. (2012) compared 10 state-of-the-art building performance simulation tools such as DesignBuilder, IES-VE, eQUEST, Green Building Studio, Energy Plus and HEED by means of literature review and two online survey among architects and engineers. They considered five selection criteria for their analysis, which are 1) Usability and information management of the Interface, 2) Integration of intelligent design knowledge-base, 3) Accuracy and ability to simulate detailed and complex building components, 4) Interoperability of building modelling, and 5) Integration of tools in building design process. The packages receiving the highest percentage of agreement of suitability from both architects and engineers were DesignBuilder and IES-VE. Additionally, there are also urban energy simulation platforms that expand their level of analysis from ‘building’ scale to ‘urban’ scale. These also include consideration of urban climate which has a notable impact on the energy system (Perera et al., 2018). Through literature review and communication with experts, their suitability for this study is also investigated. Packages such as SimStadt (Nouvel et al., 2015), TEASER (Remmen et al., 2018), HUES (Holistic Urban Energy Simulation Platform), Kurke (Hukkalainen et al., 2017), Envision Scenario Planner (ESP) (Trubka and Glackin, 2016) and CitySim (Robinson et al., 2009) have been considered, and their relative merits for this study compared. The investigation showed that plenty of the mentioned tools have substantial disadvantages. For instance, EPS cannot consider the effects of shadowing from one building to another, which is an important parameter in urban energy analysis. Some features of Kurke are in Finish language and not yet been translated to English. Among those remaining, research publications predominantly use or cite CitySim and SimStadt. Simulation input is a manual process for CitySim, while it is based on CityGML geometrical database for SimStadt (Reinhart and Davila, 2016). This feature has an advantage for this research due to the high number of building plans that are necessary which can be readily drawn using AutoCAD and fed into CitySim for simulation.

After conducting an extensive investigation, and due to the nature of the underpinning research which focusses on ‘urban’ energy analysis on a scale greater than ‘building’ level, it was decided to choose an urban simulation package rather than a building simulation tool. Reinhart and Davila (2016) found that these tools show better accuracy when analysing a wider variety of buildings. Therefore, the well-known building simulation tools (such as DesignBuilder) could not be a good choice for this study, and among urban simulation tools, CitySim is recognized as the best compromise for this research which has been adopted for several previous studies investigating urban energy analysis. Le Guen et al. (2018) used CitySim for improving energy sustainability of a village in Switzerland through integration of building renovation and renewable energy. Perera et al. (2018) combined CitySim with an urban climate model (CIM) and an energy system optimization model to show the impact of urban climate on urban energy demand. Moghadam et al. (2019) adopted CitySim to develop a new visualization method for evaluation of urban heat energy planning scenarios.

It is notable that the thermal model used by CitySim is more simplified compared to ‘building’ energy simulation software (Walter and Kämpf, 2015). Instead, it readily considers influential parameters in urban energy analysis such as the shadowing effect between buildings as well as inter-reflection between external surfaces using both short and long wave radiations. CitySim considers the effect of longwave radiation by calculating the temperature of the surfaces. For instance, by changing the cut-off angle (see Chapter 5), as an important urban geometric parameter, the amount of radiative cooling to the sky is changed (Lauzet et al., 2019) which affects building energy demand. These are the peculiar features of this software that are important considerations since this study is interested in what happens outside buildings more than inside. The simplified thermal model also allows for shorter simulation execution times—a significant advantage here since the models developed in this research need to be executed thousands of times to examine the impact of different parameters on energy performance. For the purpose of this research, buildings are considered as black boxes which interact with one another and the outdoor environment, while the conditions inside the buildings are considered the same to allow for comparative study.

In conclusion, regardless of its advantageous urban simulation features, CitySim provides a suitable trade-off between input data requirements, computation time (Monteiro et al., 2017) and analysis accuracy (Walter and Kämpf, 2015).

4.2.1.1 Limitations of CitySim

Buildings are considered as black box by CitySim that neglects the internal partitions/rooms inside buildings. For multi-storey buildings, CitySim is not able to recognize the floors inside the building. It consequently cannot spread the number of occupants into their relevant floors. Hence, the total number of occupants in buildings are considered together inside the box. Moreover, the location of the appliances and radiators inside the building cannot be manipulated. These may affect the accuracy of the thermal behaviour of the internal space of the building in different zones. Nevertheless, this study is mainly concerned the trends of changes in energy patterns rather than absolute values.

CitySim cannot accurately account for the effect of daylight availability on lighting energy consumption. Therefore, lighting energy consumption is estimated per unit of floor area for the whole building.

Ideally, to accurately analyse an urban microclimate, computational fluid dynamics (CFDs) should be employed (Toparlar et al., 2017) alongside building energy simulation studies (Shirzadi et al., 2019). This facilitates the modelling of airflow around the buildings in the urban environment, which would provide a better estimation of heat loss from the building envelope. CitySim is not coupled with a CFD method in this study due to boosting the level of complexity of the analysis without getting too much out of it. According to the recommendation of the developer of CitySim, it does not make a significant change in the results of this study, while for being able to use this feature, a time-consuming training is needed.

The simplified thermal model of CitySim considers a single thermal zone per building that may affect the results specifically in taller buildings. However, this limitation was tested in this study and the results show only around 7% difference with a case that considers multiple zones per building. This difference exists for all buildings with more than one storey and is therefore not regarded as significant for the purposes of relative comparisons.

In conclusion, considering the above-mentioned limitations, CitySim still is the best compromise for the purpose of this study because of its valuable ‘urban’ energy analysis features. This study mainly tackles the condition outside the building envelope rather than the details inside the building (which can be simply considered equivalent for all buildings). Meanwhile, the study concerns the relative performance of buildings

for a comparison purpose, which mitigates the possible impact of these limitations in the holistic view of the results.

4.2.1.2 Procedure for accurate use of CitySim

The performance assessment method of using CitySim is adopted from CitySim user guide (Mutani et al., 2018).

Building models are drawn in AutoCAD where all walls, roofs, floors and grounds are drawn as ‘surfaces’ using 3DFACE. Special attention is paid to the orientation of surfaces to be recognized by CitySim. Drawings are then saved in ‘DXF’ format to be readable by CitySim.

After importing ‘DXF’ files into CitySim some building physical and occupational characteristics are defined through the interface. The rest of the characteristics are manually accomplished by changing the codes inside the ‘XML’ file (see Appendix B) from CitySim (using Notepad++) e.g. for heating and cooling periods, presence of lighting and appliances, etc.

Simulation outputs result in the generation of ‘TSV’ files, where the ‘.TH’ file is of particular interest to this study, and this is converted to a more useful Excel format. The file is composed of columns listing hourly data of heating/cooling demand, internal gains, electricity consumption and machine power, for instance.

To generate yearly/monthly accumulative figures, a MATLAB routine has been developed to aggregate the data on a monthly/yearly basis (see Appendix C).

4.2.2 Source of climate data (Meteonorm software)

Climatic data is obtained from Meteonorm; a database having measurements from 8000 weather stations, five geostationary satellites and a globally calibrated aerosol climatology. The database of ground stations is extended with data from geostationary satellites to fill gaps in areas where there are no available weather stations (Meteonorm). Furthermore, it contains algorithms to calculate extreme years as well as three IPCC Climate Change scenarios that allows projections to the year 2100.

Meteonorm can be integerated with CitySim to perform PV, solar thermal and building simulations. It has been adopted for use with CitySim in several previous studies (Coccolo et al., 2016, Moghadam et al., 2019, Mohajeri et al., 2016) and is able to provide 10 years average temperature data (2000-2009) and 20 years average radiation data (1991-2010) at any specific location on the earth. Measurements required by CitySim include air temperature, surface temperature, beam radiation,

horizontal diffuse radiation, wind speed, wind direction, relative humidity, precipitation and cloud cover fraction on hourly basis (see Appendix D). These parameters along with a horizon file of any geographical location are generated by Meteonorm ('.cli' and '.hor' files), which are readable by CitySim. Horizon data contains information about natural obstacles (e.g. mountains) around specific locations (from-180° to +180°), and allows CitySim to consider the possible impact of obstacles on the parameters such as the solar radiation received by the location (shadowing effect of the obstacles) and the wind direction and intensity, which can affect building energy consumption (Nikkho et al., 2017, Salvati et al., 2020). Huifen et al. (2014) showed that different wind angles mainly affect heating and air conditioning energy consumption, and Salvati et al. (2020) showed that reductions in wind speed can impart a significant increase in cooling energy demand. Moreover, Nikkho et al. (2017) found that wind direction and speed can lead to a 5% change in total building energy consumption (heating plus cooling).

4.2.3 Validation of the model

4.2.3.1 Use of a pilot study

CitySim has previously been validated using both monitored data and other energy simulation software: Coccolo et al. (2013) validated CitySim against EnergyPlus software using two existing buildings (a single-family dwelling and an office building). The buildings were located in EPFL campus in Ras al Kaimah (United Arab Emirates) and it was planned to transform them to achieve Minergie standard (Kriesi et al., 2011). They simulated energy consumption of the buildings using EnergyPlus software with an hourly time step. Coccolo et al. (2013) used CitySim software to simulate the energy consumption of the same buildings for comparison. The results showed 1% difference for yearly cooling demand of buildings as they existed, while the discrepancy was 19% for buildings in case of enhancing them to Minergire standard. This discrepancy was justified by the complex blinds system studied using EnergyPlus. Walter and Kämpf (2015) compared CitySim and BESTEST (Building Energy Simulation Test) comparative testing approach for calculating the annual heating and cooling energy demand as well as peak heating/cooling requirement of buildings. BESTEST is composed of a suite of simulation tools from different countries. A rectangular single room building was considered as the base case study. By changing the building characteristics (e.g. envelope inertia, number

and dimensions of windows, presence of overhang etc.), nine case studies were provided in the validation analysis. Results showed that annual and peak heating/cooling demand provided by CitySim were always between the minimum and maximum values achieved by the BESTEST tools for all case studies. In general, the results indicated less than 1% discrepancy between the two packages that demonstrates the reliability of CitySim. Moreover, they experimentally verified the tool using monitored data of the annual heating consumption of an EPFL campus building and the results showed only around 5% discrepancy.

In addition to the investigation of the above-mentioned third-party validations, the simulation model is validated for this research through use of a pilot study. In this way, not only is the reliability of the chosen modelling package further examined, but also the creditability of the modelling and its relevant assumptions used in this research are tested and verified. In this section, the results of CitySim (that works in urban scale) simulation with SAP (that works in building scale) simulation results are compared to explore the accuracy of CitySim. Because the software that works in building scale considers higher level of details for their simulation, which increases their accuracy. Similarly, Monien et al. (2017) validated an urban simulation tool, SimStadt, by comparing its results with the results obtained by building simulation software (TRNSYS) for six different buildings, and found that the deviation is less than 10% for four buildings and larger (17 and 24%) in two other cases. Coccolo et al. (2013) used the same method to validate CitySim against EnergyPlus and obtained 1-19% discrepancy. Reinhart and Davila (2016) validated urban building energy models (UBEN) against building energy models (BEM) with error range between 7% and 21% for heating energy load. Hence, if the results generated by CitySim is in a reasonable agreement with a building simulation tool, its accuracy is confirmed with good approximation.

The pilot investigation is composed of four social houses certified to the code for sustainable homes level 5 sited in Gainsborough (UK). These houses are selected firstly because of the availability of data, and secondly because, as terraced houses, they can be treated as a single building block that contains all the houses within it. This is the method that buildings are modelled in CitySim, which will be the basis of modelling in the rest of this study. Therefore, the accuracy of CitySim modelling is tested by comparison of its results with results from available data. The energy

consumption data of the houses was already available from both SAP simulation models and on-site measured data (Sodagar and Starkey, 2016).

The Standard Assessment Procedure (SAP), formulated by the Building Research Establishment (BRE), is used for the calculation of a dwelling's energy efficiency and carbon emissions in UK to demonstrate compliance under Part L of building regulations (Murphy et al., 2011). It is at the heart of government policy concerning the measurement, identification and improvement of the UK building stock, which is widely used by government departments, energy companies, local authorities and architectural practices energy audits. Furthermore, for new buildings in the UK, it is the most important calculation procedure for assessing and certifying energy performance (Kelly et al., 2012). SAP is based on a steady state method that is able to estimate energy consumption in dwellings, including space heating, water heating, lighting, electrical appliances and cooking (Crobu et al., 2013). Monthly mean internal temperatures are calculated from mean external temperature, solar and internal heat gains, heat gain utilization factor, the heating system hours of operation and its characteristics, heat losses through the fabric and the dwelling's thermal mass (Stone et al., 2014). The SAP methodology is based on a series of simple physics-based calculations (Stone et al., 2014) and empirical evidence (Murphy et al., 2011). Its reliance on simple equations creates less scope for errors to occur in calculations (Murphy et al., 2011). Some shortcomings of SAP are its simplified early stage model, its insufficient expertise to accurately interpret the SAP system that required to be demystified to enable accurate interpretation. The tool has been criticized, however, for the complexity of the procedure of assessment and it is considered time consuming for the accuracy it provides (Crobu et al., 2013). Compared with the as-built design, SAP predictions may reflect the minimum expected energy consumption since the performance of building components are more likely to be below the specifications than above them (Summerfield et al., 2011).

It should be noted that the actual measured data was not chosen for validation since the effects of occupant behaviour is known to have significant impact on the results e.g. for two mid-terrace houses under similar conditions viz. same number of occupants, similar area and volume and same geographical location, the annual energy consumption can have up to 60% difference. Other reason for this disparity could be issues with energy monitoring. Hence, this is an evidence showing that actual data is extensively affected by other parameters (Summerfield et al., 2011).

The four terraced houses are situated in Cross Street (Gainsborough, UK) with latitude of 53.401° N and longitude of -0.772° E. This is basically a building block with two mid and two end terrace houses, as shown in Figure 4.1. House numbers 1, 2 and 3 are two-storey houses with a flat roof, while house 4 is a three-storey house with slopped roof.

(a)

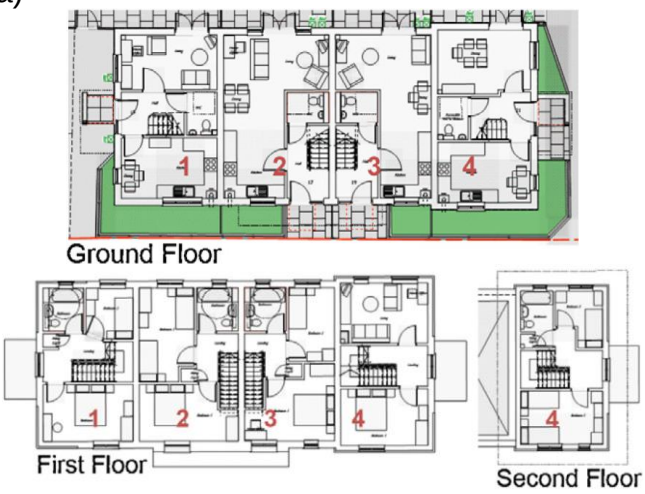

(b)

Figure 4.1: Four terrace houses in a building block (a) floor plan of houses (Adopted from Sodagar and Starkey (2016)) (b) Photo of south-east view of the block (Adopted from Senave et al. (2019))

Figure 4.2 (a) shows the block of houses without surrounding while Figure 4.2 (b) shows it among its neighbours with distances obtained from Google Maps. The presence of vegetation is not considered there it is not significant in the vicinity of the buildings.

(a)

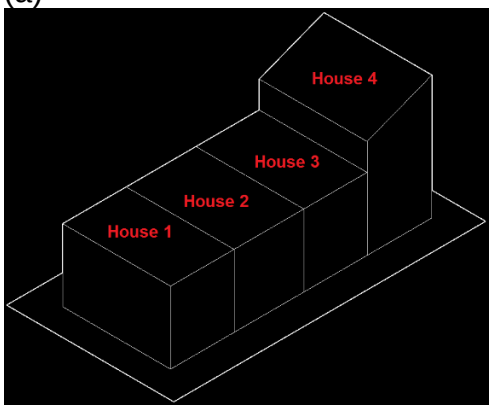

(b)

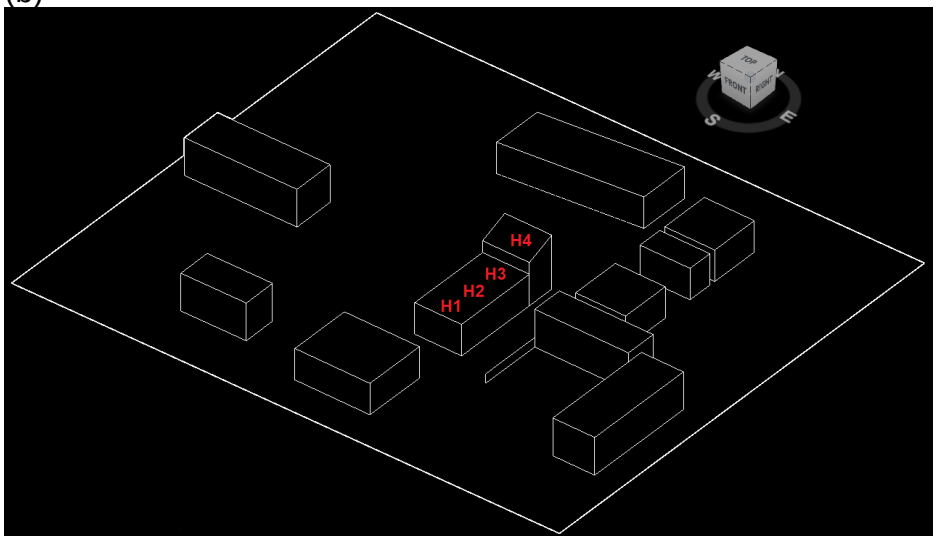

Figure 4.2: The AutoCAD model of the block (a) Only the block (b) The block neighbourhood with surrounding buildings

CitySim simulation was initially run on the model shown in Figure 4.2 (a) in order to allow for a similar implementation under the same conditions as SAP. Subsequently, CitySim simulates the model shown in Figure 4.2 (b) to demonstrate its advantages for the purpose of this study.

The physical characteristics of the houses are given in Table 4.1.

Table 4.1: Physical characteristics of houses and number of occupants

	House 1	**House 2**	**House 3**	**House 4**	**Average**
Number of floors	2	2	2	3	-
Wall U-value (W/m^2K)	0.14	0.14	0.14	0.14	0.14
Roof U-value (W/m^2K)	0.12	0.12	0.12	0.12	0.12
Floor U-value (W/m^2K)	0.12	0.12	0.12	0.12	0.12
Glazing ratio - North	0	0	0	0.1	0.1
Glazing ratio - East	0.13	0.17	0.21	0.11	0.16
Glazing ratio - South	0.12	0	0	0	0.12
Glazing ratio - West	0.21	0.27	0.21	0.19	0.22
Window U-value (W/m^2K)	1.15	1.15	1.15	1.15	1.15
Infiltration rate (ach)	0.32	0.33	0.26	0.33	0.31
Number of occupants	2	3	3	3	11 (total value)
Occupant density (m^2/per)	33.2	24.3	22.1	33.8	28.4
Sensible heat (W/person)	70	70	70	70	70
Latent heat (W/person)	45	45	45	45	45
Radiant part	0.6	0.6	0.6	0.6	0.6

Glazing ratios presented in Table 4.1 are the window to wall ratios calculated from the technical drawings of the houses.

According to *The Government's Standard Assessment Procedure for Energy Rating of Dwellings* document (SAP, 2012), the heating period of houses is considered from October to May (from day 274 of year to the day 151 of the next year). Since this assumption was made by SAP software for energy simulation of the houses, the same assumption is made in CitySim for consistency. No cooling period is considered for this pilot study. The minimum and maximum internal room temperatures (setpoint temperatures) is also taken from SAP documents, which are considered to be 20ºC and 24ºC, respectively. The minimum room temperature is 21ºC for the living room

and 18ºC elsewhere. However, since CitySim analyses the building as a single volume without considering separated rooms inside it, the average value of 20ºC is chosen.

Since the form and shape of whole buildings are of interest rather than the details inside the buildings, in this pilot study some details inside the buildings, such as location of partitions and radiators, are neglected. It should be noted that internal planning can significantly affect the energy consumption due issues such as passive solar potentials and zones coupling. However, since they are not considered in the analyses of this thesis, validation of the model with this pilot study demonstrates that ignoring these facts at an urban level is a reasonable assumption.

CitySim model considers the whole building as a united space (single volume), which means it deals with one block as big as four houses together (instead of four separated houses), with the same shape and physical features that shape overall built form, such as external walls, roofs and fenestration. In this case, for the characteristics with different values, the average value is considered (Table 4.1). For instance, the average value of infiltration rate is 0.31 ach for whole block. The number of occupants is the accumulative value for the four buildings, which is 11 people.

To have a precise evaluation of internal gains, the presence of appliances and their relevant electricity consumption are considered for houses. In the SAP predictions, regulated energy from fixed appliances such as lighting, fans and cooking, plus unregulated energy consumption from refrigeration, computer equipments and wet appliances is considered (Starkey, 2014). In CitySim, the energy consumption by fans, pumps and hot water is not considered, while lighting and appliances such as TV, PC, fridge-freezer, washing machine, oven, kettle and dishwasher are considered. It is assumed that each house has one of the mentioned appliances and the typical power required by each is obtained from CIBSE Guide F (CIBSE Guide F, 2012). These differences in assumptions for appliances may lead to discrepancies in the final results. However, since only the heating energy demand of the buildings is going to be compared, the heat generated by operating appliances is most important rather than their electricity consumption, as it affect internal gains and consequently heating energy demand of the buildings.

The climate and horizon files related to the exact geographical location of the houses were generated by Meteonorm. The model was imported to CitySim along with related climate data. The climate data is the average 10 years data at this location, which is obtained by interpolation between the main geographical points on the earth

with known data in Meteonorm. Therefore, it might not be exactly similar to the corresponding data used for SAP simulation.

The yearly space heating energy demand obtained from SAP and CitySim are shown and compared in Figure 4.3.

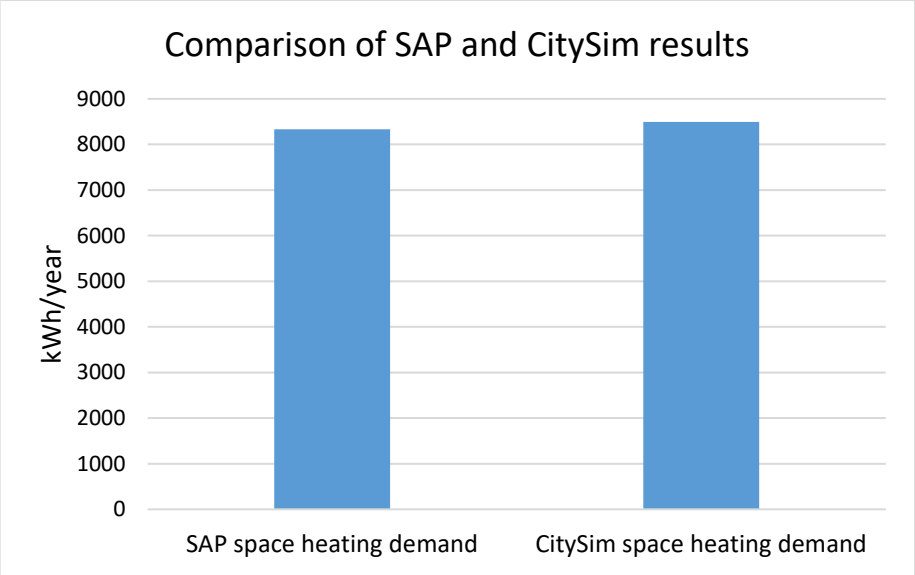

Figure 4.3: Yearly space heating energy consumption obtained by SAP and CitySim

The resulting energy consumption obtained from the CitySim model is 8494 kWh/year, which shows only a 1.9% discrepancy from the results obtained from SAP analysis (8331.13 kWh/year). Although this provides a good alignment, the differences in assumptions and performance of the simulation tools should be considered. CitySim considers the whole building as a single volume and used the average values in Table 4.1, while SAP considers each building separately including its internal belongings (e.g. number of occupants, partitions etc.) and obtained the results for each single building. They have used different weather files that influence the accuracy of predicted energy demand, because difference in outdoor temperature, wind speed and so on can certainly influence the energy demand of the building. However, the influence is more significant for calculations of cooling energy demand (Chiesa and Grosso, 2015), which is not under consideration for these buildings. Moreover, Schwartz and Raslan (2013) showed that weather files do have a considerable influence on the total predicted loads. The results of their experiments showed that even by using an identical weather file, there still is the possibility of obtaining different results for heating load calculations. These close results might be due to the similarity of input data and assumptions as well as the simplifications inherent in the algorithm structure and thermal model of both tools. *Even among the mature tools, there was*

not a common language to describe what the tools could do (Crawley et al., 2008). Using the same DWG file, different tools may calculate floor area differently (Schwartz and Raslan, 2013) that causes difference in final energy simulation results.

The collective influences of all above-mentioned parameters could have been ironed out and their aggregated impact resulted in such close alignment of results, which can be rational as Pang et al. (2016) also found when using different simulation tools. Nevertheless, it does demonstrate the reliability of CitySim and the assumptions made for this urban analysis. Due to this unexpected closeness of the results, the input data was systematically checked and after repeating the simulation the same results were obtained. Therefore, although the level of details inside the building is lower in CitySim (to perform urban analysis), it delivers results with acceptable level of certainty.

Next, the whole neighborhood of four the social houses including surrounding buildings, shown in Figure 4.2 (b), is imported into CitySim. In this way, the advantage of CitySim compare to building simulation tools is examined. The physical characteristics and occupancy profile of the houses remain as in the previous analysis. The only difference is the presence of neighbor buildings that causes shadowing effect, change the wind flow pattern around the building, and influence short and long wave irradiation being reflected between external surfaces. CitySim takes into account the influence of all these parameters. It calculates the temperature of all external surfaces that consequently determines their relevant longwave irradiation. This is a very important parameter in urban energy analysis because the geometry of street canyons, specifically in high density urban areas (Perera et al., 2018), helps trap incoming radiation and consequently stores more heat. It maintains higher surface temperatures for longer periods of time by reducing the rate of long-wave radiant cooling at night (CIBSE Guide F, 2012). This causes UHI effect.

Figure 4.4 shows the resulting (a) surface temperature (b) short-wave and (c) long-wave irradiation from external surfaces of the model simulated by CitySim for the month of February.

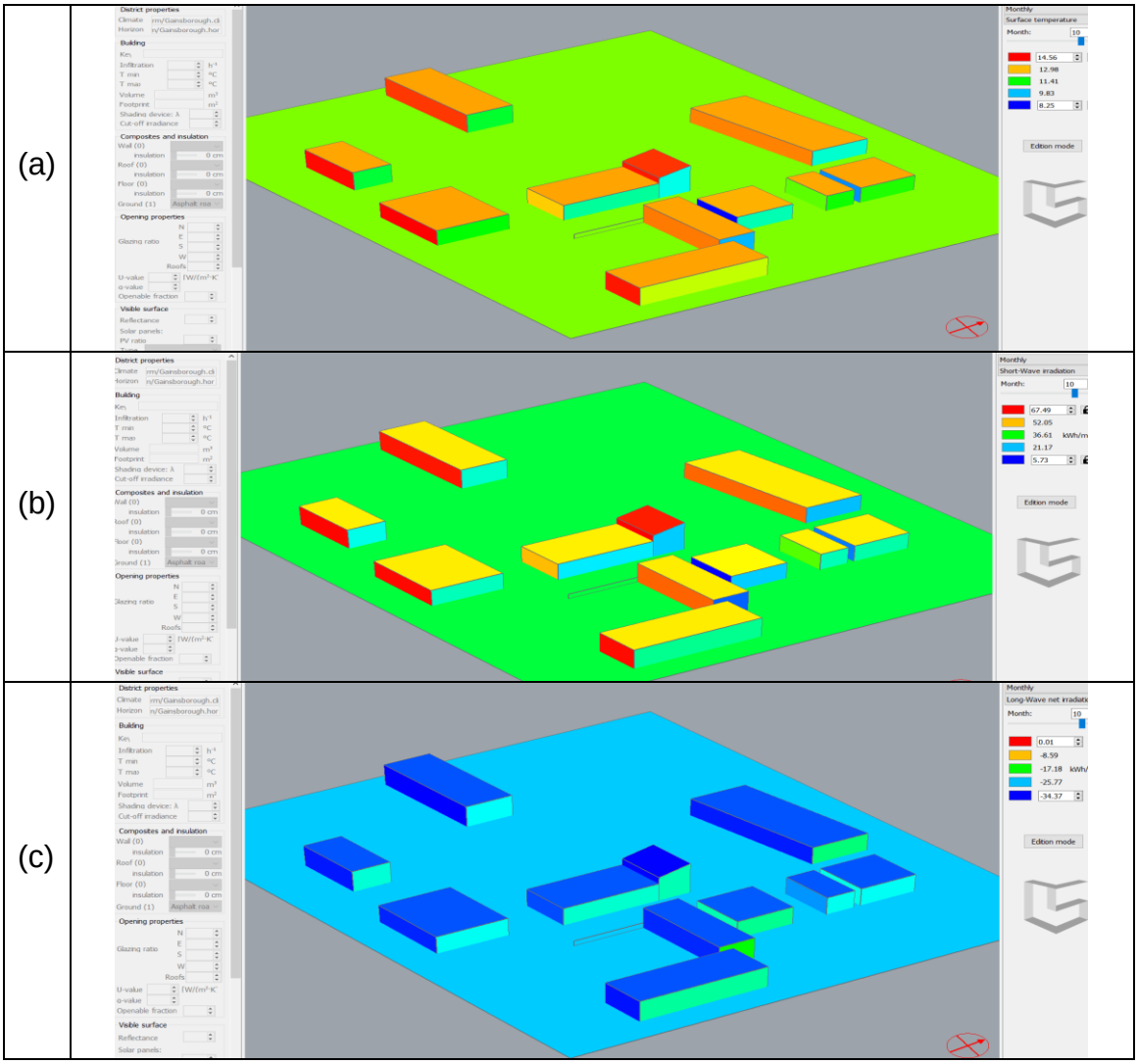

Figure 4.4: CitySim simulation results showing (a) surface temperature, (b) short-wave irradiation and (c) long-wave irradiation from external surfaces (in February).

As observed from Figure 4.4 (a), the highest surface temperature belongs to south-facing walls (without obstacles) as well as the inclined roof of house 4, shown in red. The average surface temperature during February for these hot spots is ~6.8ºC. It is clear that the other surfaces, including south-facing walls with obstacles, are cooler on average (shown by other colours). During the summer months, the hotter surfaces are the roofs rather than the south-facing walls due to the angle of the sun that is more vertical compared to the case in wintertime. For instance, the average surface temperature of hottest surfaces in July is 27ºC, which is comparable with the results obtained by Shahrestani et al. (2015). Figure 4.4 (b) shows the total short-wave irradiation received by each surface for February. It aligns with the results shown for surface temperature because the same surfaces are shown by red indicating the highest intensity of short-wave irradiation, which is around 44 kWh/m^2. This value is

more than three times higher for June due to the higher intensity of irradiance. Figure 4.4 (c) shows the average long-wave irradiation from surfaces in February. The hot spots of the plan are the same surfaces, which are shown in dark blue in this figure. This can validate the figures (a) and (b) because the surfaces with highest temperature that receive greatest short-wave irradiation are able to radiate back the greatest amount of long-ware irradiation, which totals around -23.58 kWh/m^2 for February (the value is negative because it is sent by the surfaces and not received).

The space heating energy demand is 9070.9 kWh/year, 6.7% higher than the case without considering surroundings. This is due to the shadowing effect of adjacent buildings (specifically the one situated in the southern side) causing a reduction in the internal gains and consequently increase in the heating demand (Chan, 2012, Nikoofard et al., 2011).

Figure 4.5 shows results for the second analysis with CitySim and compares the results with two previous cases.

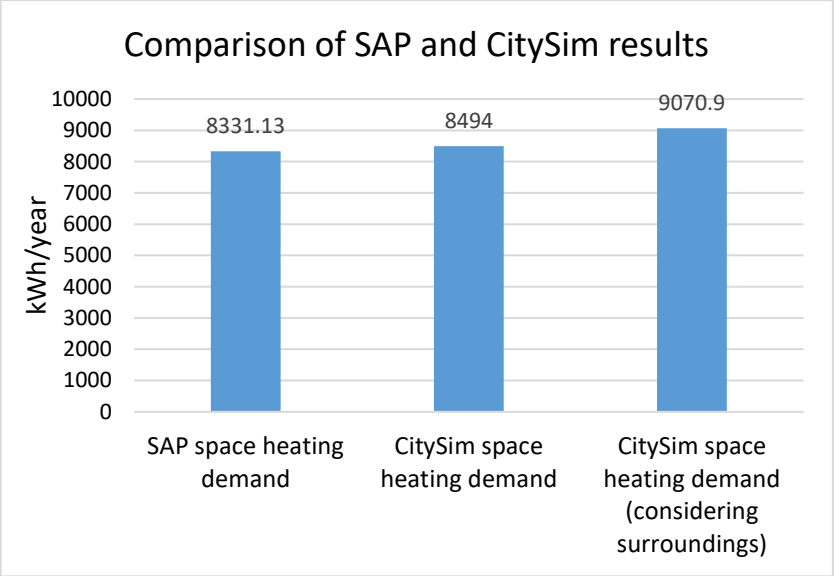

Figure 4.5: Comparison of SAP analysis results with CitySim in both cases of excluding and including surrounding buildings from and in the model

The final heating energy demand predicted by CitySim is 8.5% higher than predicted by SAP. This is a justifiable difference for validating CitySim, specifically due to the consideration of neighbor buildings that increase heating energy load (Nikoofard et al., 2011). By demonstrating the reliability of CitySim, this software is used for energy simulation in the rest of the analysis, which includes the main body of this study. To maintain the reliability of modelling, the same climate data source and the same method of preparing input drawings are adopted.

4.2.3.2 Use of benchmarking

To further increase the degree of confidence in the simulations results presented in subsequent chapters, those obtained from CitySim will also compared with a few benchmarked values taken from previous publications.

According to the Zero Carbon Hub (ZCH, 2009) report, the maximum space heating and cooling energy demand of building should be 39 kWh/m^2/year for apartments and mid terrace houses and 46 kWh/m^2/year for end of terrace, detached and semi-detached houses. Passive House Planning Package (PHPP) (Feist et al., 2007) designer's companion indicates that the maximum heat demand of a passive house building should be 15 kWh/m^2/year, while the same value is valid for cooling demand as well (Lewis, 2014).

According to the study by Ridley et al. (2013) which monitored energy performance of Camden Passive House, the total gas and electricity consumption of building was 65 kWh/m^2 per year. The building was certified to the Passive House standard, which are generally higher than what is considered for this study. Hence, it is expected to have better energy performance compared to buildings considered in this study. Ridley et al. (2013) compared the results of their study with the results obtained from other houses such as BedZed 90 kWh/m^2/year, The Long House 80 kWh/m^2/year, One Brighton 72 kWh/m^2/year and Princedale Road 63 kWh/m^2/year (Starkey, 2014).

CIBSE guide TM46 (CIBSE TM46, 2008) indicates electricity typical benchmark and fossil-thermal typical benchmark of general accommodation equal to 60 kWh/m^2 and 300 kWh/m^2, respectively. However, these numbers are somewhat dated and newly developed buildings with the latest standards are expected to show better energy performance. Moreover, fossil-thermal demand is different from building envelope energy demand and it is dependent on the efficiency of the conversion technology.

The above-mentioned values will ultimately be compared with the results obtained in section 5.2.1 to support the validity of the presented research results.

4.3 Conclusion

In this chapter the model of four terraced houses was developed and simulated in CitySim. The model considers whole building as a black box containing all four houses. This is the basis of the modelling and simulation studies using CitySim that is going to

be used in subsequent chapters. Therefore, the results of the models simulated by CitySim have been compared with readily available data of the energy analysis of the buildings from SAP. The outcome of this comparison showed only 1.9% (in case the surrounding buildings are not considered by CitySim) and 8.5% (in case the surrounding buildings are considered by CitySim) differences between the two tools, which is an acceptable tolerance. The study has shown that when neighbor buildings are considered by CitySim, energy demand increases due to the shadowing effect of adjacent buildings. This demonstrates the particular characteristics of CitySim that is able to consider the influence of the urban environment around the building. This gives a more precise estimation of building energy performance on a district/city scale. As a result, the reliability of CitySim to be adopted for the main body of this thesis has been verified.

Furthermore, benchmark figures are introduced in the previous section that show typical yearly energy demand of buildings per square meter. These numbers will be used to compare with those of presented simulations in the next chapter.

Chapter 5: Effect of urban built form and density on building energy performance

5.1 Introduction

The relationship between urban built form and density for the four presented urban built forms was established by developing the *Form Signature* in Chapter 3. In this chapter, building energy performance is added to the *Form Signature* graphs to establish the correlation of urban built form (pavilion, terrace, court and tunnel-court), density and building energy. Building energy analysis is performed on the geometrical models of the urban built forms, introduced in Chapter 3, using CitySim. The City of London, representing a temperate climate, is considered as a case study location.

To ensure a like-for-like comparison between built areas with different densities, theoretical master plans are developed for energy analysis of residential buildings. Heating, cooling and electricity energy demand of buildings can be calculated by CitySim depending on the climate, for the London case therefore, only heating and electricity energy demand is considered as explained in section 5.2.1.1. Obtaining the yearly energy demand of buildings per unit of floor area, these values are adopted to make the heat map of energy intensity on the *Form Signature* graphs. Subsequently, an energy indicator termed *Energy Equity* is introduced, representing the ratio between PV energy generation installed on the roof of the buildings, and the total building energy consumption. The values of Energy Equity are also overlaid on the *Form Signature* graphs illustrating the simultaneous correlation of building energy performance with geometric variables and density indicators. Finally, the energy performance of different built forms with similar geometric parameters (and different densities) are compared to identify the best and worst built forms in this climate. This comparison is repeated for the case of constraining density whilst changing the geometric parameters. Furthermore, the study shows that the same density for the same built form can be achieved by different combinations of geometric parameters that impact on the energy performance of buildings.

Urban planning choices have a significant effect on reducing building heating/cooling consumption (Hukkalainen et al., 2017) rather than electricity consumption. These urban planning choices affect district energy analysis that includes building energy demand, different energy supply alternatives and transportation energy. The main influential choices are land use and layout of the area

as well as the type and scale of buildings (Yeo et al., 2013). Urban and spatial planning strategies and policies need to connect urban energy efficiency actions (Zanon and Verones, 2013). With an emphasis on energy efficiency/performance, these large-scale (urban) decisions are correlated with small scale (building) decisions, which is hidden in the form and density of urban areas. Addressing this triangular correlation between urban built form, urban density and building energy is the main objective of this chapter. The chapter, therefore, addresses the identified gaps in current literature by proposing a novel urban energy planning tool for temperate climates, establishing correlations between building energy demand and PV energy generation with urban built form and density.

5.2 Case study analysis (London)

Here, geographic and climatic conditions of the metropolitan City of London are used as a case study for energy simulation. It is located in latitude of 51.5074° N and longitude of 0.1279° W, representing temperate climate in the Koppen climate classification as it resides in the subcategory of 'cfb' (Marine West Coast Climate). With a population of 9,304,016 (World Population Review, 2020b) it has a significant contribution to overall urban energy consumption, which indicate the necessity of energy optimization in it. Hence, providing guidelines for the optimization of energy with respect to its built form and density is very beneficial for future developments in this city that can conserve significant amounts of energy and prevent high levels of carbon emissions. Meanwhile, the availability of further studies on London in the literature provides the opportunity of comparing the results of this study with others. Case studies based on alternative climates are explored in Chapter 6 to examine the impact of climate on energy, form and density.

5.2.1 Building energy demand

The main part of this analysis begins by assessing the theoretical plans of buildings which are drawn according to the geometrical models developed in section 3.2. Therefore, the influence of each geometrical variable on the building energy performance can be critically observed. A site plan with an array of buildings of similar geometry is provided for input to the energy simulation (Figure 5.2, Figure 5.7, Figure 5.9 and Figure 5.11). Then, by changing the geometrical variables of the site plan (as shown in Figure 5.1) with specific intervals, new simulation trials are undertaken for all

built forms (pavilion, terrace, court and tunnel-court urban built forms) introduced in Chapter 3.

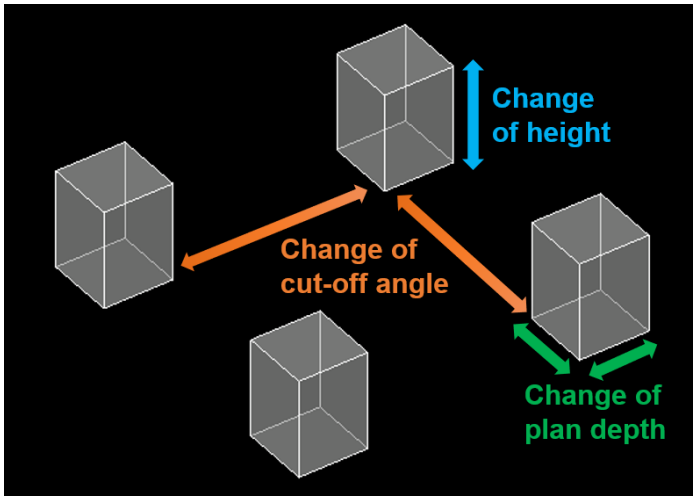

Figure 5.1: Schematic illustration of changing geometrical variables in site plan

5.2.1.1 Pavilion built form

Being inspired from geometrical models shown in Figure 3.1 (Chapter 3), an exemplar array of pavilion buildings for case of 18m plan depth, 6-storey and cut-off angle of 45º is shown in Figure 5.2. In this plan, all buildings possess exactly the same geometry, physical characteristics and occupancy profile that reflects their similar energy performance. Hence, the central building in Figure 5.2, which is marked by black circle, is the target building in this analysis. The energy performance of the remaining buildings was examined by performing simulation trials, with results indicating that due to the similarity of the buildings, the energy demand of other buildings (except the ones at the edge of the plan) are very close to that of the central building with less than 0.01% difference. The presence of the remaining buildings is due to the provision of the neighbourhood condition around the target building. However, the simulation is executed for all buildings in the plan. In this way, the performance of the building within a district is assessed that demonstrates the nature of the urban analysis considered in this study.

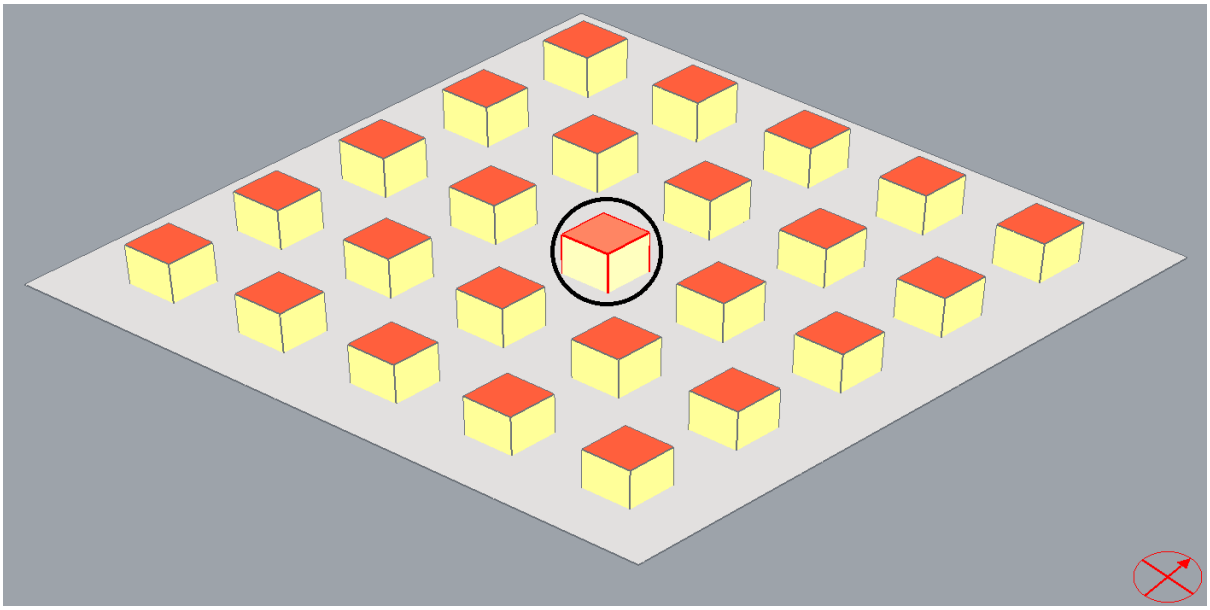

Figure 5.2: A model of pavilion-built district with series of pavilion buildings for energy simulation purpose. The target building is marked by a black circle.

The model is used with CitySim and all characteristics are defined through either the software interface or changing the underlying code. The required data has been obtained from reliable sources from the UK governmental documents and reports such as Approved Documents, CIBSE guides and SAP reports, which are referenced in the text. They are as follows:

- Internal temperature: Typical minimum (T_{min}) and maximum (T_{max}) setpoint temperature for heating and cooling periods are considered as 20ºC and 24ºC, respectively (SAP, 2012).
- Infiltration rate: The infiltration rate of all building is chosen to be 0.5 ACH according to the typical value recommended by the Building Regulations (Approved Document Part F, 2010). Reduction of the infiltration rate can have a positive impact in terms of decreasing space heating requirements (Gillott et al., 2016).
- Heating and cooling period: Heating season begins from October and lasts until the end of May according to SAP (2012). Due to the temperate climate of the UK and its mild summers, normally no cooling load is considered for residential buildings. This is not only demonstrated in the studies by other researchers (Rode et al., 2014, Steemers, 2003), but also is emphasized in the United Kingdom housing energy fact file (Palmer and Cooper, 2013). In practice, the heating season for a well-insulated building will be shorter than that for a poorly insulated building (Jung et al., 2018), which shows

the impact of building physics on building energy system design and consequently total energy consumption.

Due to the effects of climate change, it is possible that buildings in the UK will also require cooling in near future. As anecdotal evidence, the electricity consumption in Italy has been increased due to the large adoption of electric heat pumps for summer cooling (Ascione et al., 2013). This could contribute to 'built form drift' in the future—this is explored in Chapter 6.

- Envelope U-values: Following Building Regulations (Approved Document Part L1A, 2016), the current standard of U-values of walls, roofs and floors are 0.3, 0.2 and 0.25 *W/(m^2.K)*, respectively. However, according to fabric energy efficiency standard (FEES) (CIBSE guide B1, 2016), the values of 0.18, 0.13 and 0.13 *W/(m^2.K)* are considered to be good practice for walls, roofs and floors, which are much better than minimum acceptable values. A large portion of existing buildings may not have this high standard of thermal transmittance. Nevertheless, since materials and technology are continually improving, and this study is identifying the optimal options for future developments, the best practice cases are adopted in this study. It is notable that the emergence of materials with higher efficiency in future is predictable.

  A selection of materials and composites are already defined in CitySim. However, to achieve the exact U-value indicated in the Approved Document Part L1A (2016), the author determined new composite materials in CitySim code to impart the required U-values. Then, by selecting each wall, roof or floor, the desirable values were specified though the software interface.
- Windows U-value: Considered to be 1.4 *W/(m^2.K)* according to SAP (2012). Simply defined through the CitySim interface.
- Windows g-value: Considered to be 0.63 according to SAP (2012) and the Building Regulations (Approved Document Part L1A, 2016).
- Glazing ratios: The percentage of glazing for residential building is a design parameter. Hence, a range of glazing ratios can be found in buildings. Changing the glazing ratio can significantly impact building energy consumption (Eljojo, 2017, Ghisi and Tinker, 2004). Its value should be

chosen as a compromise between energy, overheating and daylight (Happold, 2018). The minimum value of glazing ratio is limited by view (CIBSE Guide F, 2012) and the maximum value is limited by energy consumption. Glazing ratio is also different based on building typology, and modern office buildings normally use highly glazed facades (DeForest et al., 2017) that is higher than normal residential buildings. Table 5.1 shows the minimum glazed area required to satisfy the view from inside for a range of plan depths.

Table 5.1: Minimum glazed areas for view (Adopted from CIBSE guide F)

Max. depth of room from outside wall / m	Minimum percentage of window-wall as seen from inside
< 8	20
$\geq 8 \leq 11$	25
$> 11 \leq 14$	30
> 14	35

An analysis is undertaken later this section to obtain the most suitable choice of glazing ratio. To this end, the minimum suitable daylight factor recommended by CIBSE guide A (2019), of 5%, is adopted. The daylight factor equation is given in the Code for Sustainable Homes technical guide (2010), as follows:

$$DF = \frac{MWuT}{A(1 - R^2)} \quad (5.1)$$

Where:

DF = the average daylight factor

W = total glazed area of windows or roof lights

A = total area of all the room surfaces (ceiling, floor, walls and windows)

R = area-weighted average reflectance of the room surfaces

M = a correction factor for dirt

T = glass transmission factor

u = angle of visible sky

To obtain the total glazed area of windows, the equation can be re-arranged for *W*. Having considered most of the variables, the equation can be simplified to Eqn (5.2).

$$W = \frac{DF(1-R^2)A}{MuT} = \frac{5(1-0.5^2)A}{1*65*0.63} = 0.0916*A \qquad (5.2)$$

In Eqn (5.2), total glazed area (*W*) is only dependent on the total area of all the room surfaces (*A*). Considering pavilion built form and changing the values of plan depth from 6 to 60m, *A,* and Consequently *W,* is obtained for each plan depth. Then, the total glazed area is divided by the total wall surface area in each case to obtain the glazing ratio of each wall. The orange line in Figure 5.3 illustrates the trendline of this analysis.

On the other hand, according to Approved Document Part L1A (2016), the total opening areas of the building (windows and doors) shall not exceed 25% of total floor area. This maximum threshold was also calculated for the pavilion building with the plan depth range given previously. The outcome of the three analyses is summarised in Figure 5.3.

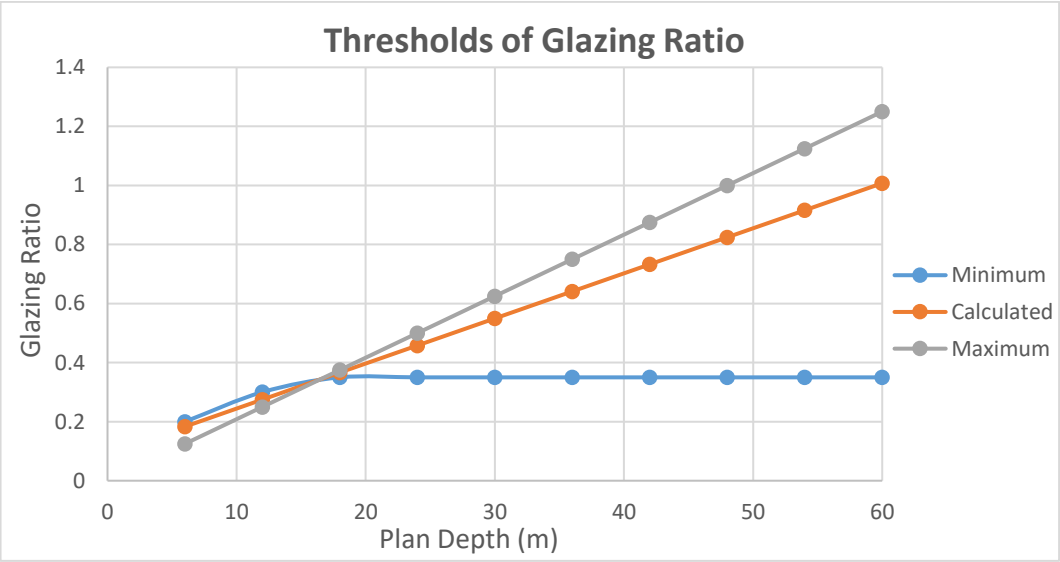

Figure 5.3: Trend of changing glazing ratio by increasing plan depth in cases of minimum, maximum and calculated values

According to Figure 5.3, the glazing ratio can be high, even close to one. It can also be seen that the maximum line (grey line) exceeds a glazing ratio of 1, which is not practically possible. This is a consequence of two factors i) this characteristic line follows the guideline regarding the maximum allowed glazing ratio, and is not sufficiently accurate for this case, and ii) the assumption considers plans with long depths (e.g. 50 or 60 m) without any partition/room, which practically not the case for residential buildings. To identify the practicality of these figures, a survey and estimation of recent building developments such as Berkeley Group (2020) was

undertaken. It showed the wide range of glazing ratios for different buildings, which demonstrates the design-oriented nature of this parameter. For instance, Happold (2018) suggested the glazing ratio of residential buildings is between 35% and 65%. Tzempelikos and Athienitis (2007) found that 30% glazing ratio for Montreal climate could ensure enough daylight for office buildings, and that increasing the ratio results in higher building heating and cooling loads.

To examine the effect of changing the glazing ratio on energy consumption, an exemplar theoretical model such as Figure 5.2 is analysed using CitySim. The model is composed of 10-storey pavilion buildings with 18m plan depth. While other input parameters are kept constant, their glazing ratio is changed from 20% to 80%. The results of yearly heating energy demand for each glazing ratio are reported per square meter, and shown in Figure 5.4.

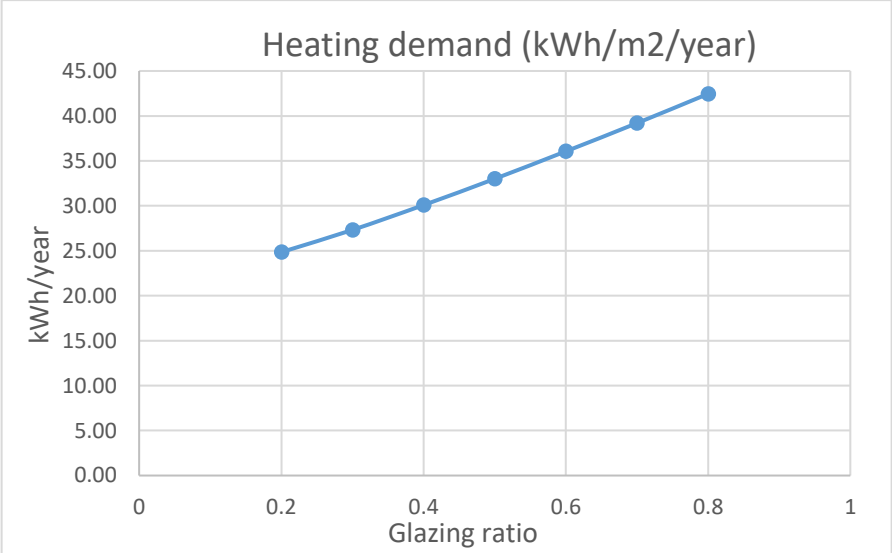

Figure 5.4: Trend of changing heating energy demand against glazing ratio for 10-storey pavilion building with 18m plan depth

It shows that higher glazing ratio means higher heating energy consumption.

The geometry and distribution of windows were considered the same for all orientations and it is acknowledged that for walls with different directions, different values of glazing ratio can be practically considered. For instance, larger south facing windows are may be better than other orientations as they can actually reduce heating loads. This is among the principles of passive solar design. However, since this is not an architectural practice

and is a comparative analysis, the same value of glazing ratio is assigned for all walls regardless of their directions. For the same reason, no shading was considered for the buildings, though the presence of shading would change internal heat gain and consequently total building energy demand. Double-glazed windows were used for this analysis, however, increasing window insulation standards (i.e. triple-glazed windows) may mitigate the sharpness of this trend line. The results shown in Figure 5.4 are compatible with the study by Feng et al. (2017) for the cold climate of a Chinese region, and Marino et al. (2017) for Italian climatic conditions. They also demonstrated that cooling energy demand shows a rising trend against increasing glazing ratio. Tereci et al. (2013) found that increased glazing ratio on the north facade increases heating energy demand, however, heating demand is unaffected by increasing the glazing ratio of the south facade. This is also confirmed in the results shown in Figure 5.4 which shows cases with the glazing ratio increasing simultaneously in all directions.

Although graphical results of Figure 5.3 shows that any glazing ratio can theoretically be chosen, Figure 5.4 shows that it is not energy efficient to increase glazing ratio without limitation. With this in mind and through a survey of recent commercial housing developments in the UK, it is concluded that 40% glazing ratio is a good practice value for this study to satisfy energy efficiency, provision of adequate daylight, and adequate viewing requirements etc. Figure 5.3 shows that 0.4 is always above the minimum required glazing ratio and supports the validity of this choice. Rode et al. (2014) also used a glazing ratio of 40% for studying the correlation of urban morphology with heating energy for four European cities including London.

- Openable area: According to CIBSE Guide F (2012) (page 5-6) and Approved Document Part F (2010), the openable area should be at least $1/20^{th}$ of floor area for rapid ventilation. Moreover, according to SAP (2012) and Approved Document Part $L1_A$ (2016), the opening areas of buildings should not exceed 25% of total floor area. As a result, the openable fraction of the walls should be at least 0.2. By further analysis and examining the openable area of existing buildings, on average the value of 0.25 provides

a good choice, and is in agreement with SAP (2012) and Approved Document Part L1A (2016) documents.

- Number of occupants: To make accurate comparisons between different models, the density of occupants in all the models was kept constant. Therefore, instead of determining number of occupants for each case, an indicator called 'floor space factor' (approved document part B) was adopted that indicates the area specified for each occupant (*m^2/person*). The value of 35 (*m^2/person*) was considered following Passive House Planning Package guidelines (Feist et al., 2007). This is also compatible with occupant density of the houses 1 and 4 of the pilot study, as shown in Table 4.1, and close to the average of all four houses which is 28.4 (*m^2/per*).
- Heat gains from occupants: The values of sensible heat, latent heat and radiant part are considered to be 70 (*W/person*), 45 (*W/person*) and 60%, respectively, which are extracted from ASHRAE Standard (2010).

Lighting and appliances are considered for all cases. They not only increase the electricity demand of building, but also increase internal heat gain of the building by turning a portion of their electricity to heat, which certainly influence the heating/cooling demand of the building.

- Lighting energy demand: To calculate the lighting energy demand and consequently the heat gain from their operation, the standard illuminance (lux) required in residential buildings is considered. Since there are different illuminance requirements for different rooms in a dwelling (Adams, 2019, Sun et al., 2011), and this study deals with whole block of buildings, an average value of 300 lux is considered for the whole building.

  Being the latest and most efficient source of lighting (Zyga, 2010), LEDs are considered in this study. To determine the amount of light provided by LEDs, luminous efficiency (lumen/W) is considered. LEDs with various luminous efficiencies are available in the market. A practical high value of efficiency using current technology is 140 lm/W, which is adopted for this study (Manfaluthy and Wilyanti, 2019), although it is recognized that technology advancements may mean higher lumens per watt variants may become available in near future (Kompulsa).

  Since each lux is equivalent to one lumen/m^2, we have:

300 lm/m^2 ÷ 140 lm/W = 2.14 W/m^2

This means for each m^2 of building floor area, 2.14 W electrical energy is required. Multiplying this value by the whole floor area of each building results in the total lighting energy consumption.

- Appliance energy demand: The typical consumption of common home appliances is considered in this study, which are chosen from CIBSE guide A (2019). For instance, a fridge-freezer with an average power of 36 W (indicating its average power between the time it is on and off); a 42-inch LED flat-screen television with a rating of 64 W; a washing machine rating of 560W; hobs with a power rating of 725W as the cooking tool. Estimation of desktop computer consumption is very difficult as there are so many different hardware configurations. Hence, after a survey of different references with a variety of power consumption ranges (DaftLogic, ElectricityUseCalculator), the value of 200 W was chosen for desktop computer consumption including its monitor and all peripherals.

Since the dimensions of the buildings (height and depth) in different site plans frequently change, it is necessary to have the consumption of above-mentioned appliances in watts per square meter. It provides the opportunity of making a fair comparison between the varieties of site plans. To this end, an assumption was made about the average floor area of UK homes. It was reported that homes built in recent decades in the UK possess around 67.8 m^2 living space (Garber, 2018) excluding hallways or staircases. A study on European housing compared the housing size of 15 European countries (Ball, 2011) and reported that new built houses in the UK are the smallest, with an average floor area close to 80 m^2 (this number is close to 140 m^2 for Denmark with the biggest dwellings). These are compatible with a BBC report indicating that the average total floor area (including hallways or staircases) of new-built UK homes is 76 m^2, and is 85 m^2 for total older plus new-built homes (Joyce, 2011). Considering 85 m^2 area as the average and specifying one of each appliance type for each household, the appliance consumption per square meter is shown in Table 5.2.

Table 5.2: Electricity consumption of appliances per household and per square meter

	For each flat (W)	Average flat size (m2)	Consumption (W/m2)
TV	64	85	0.75
PC	200		2.35
Fridge-freezer (average)	36		0.42
Washing machine	560		6.59
Hobs (cooking)	725		8.53
Microwave oven (average)	9		0.11
Kettle	220		2.59
Dishwasher	700		8.24

Above-mentioned characteristics were added to the model. The climate and horizon data of London, obtained from Meteonorm software, were fed to CitySim. The output results, which is composed of hourly data, can be aggregated to achieve monthly/yearly results. For instance, for the model shown in Figure 5.2, the monthly heating consumption of the central building is shown in Figure 5.5.

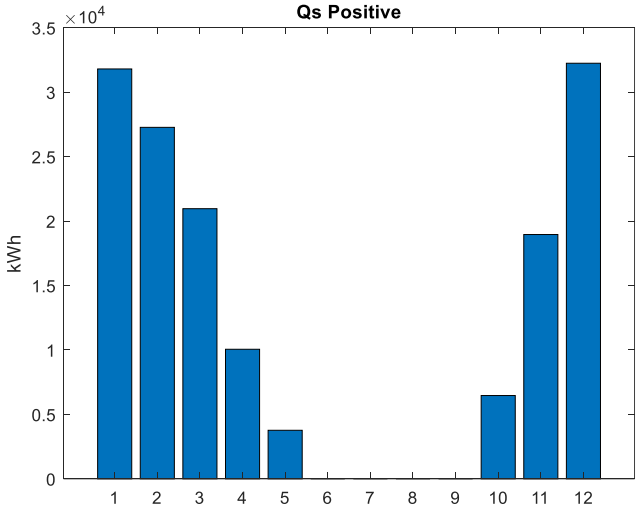

Figure 5.5: Monthly heating demand of 6-storey building with 36m plan depth and cut-off angle of 45º

The results in Figure 5.5 shows that the highest heating energy demand belongs to the three months of December, January and February which is a reasonable

outcome according to the London climate. The demand is null for four months (June-September) because the heating period considered for simulation was from October to May.

Nevertheless, following the objectives of the study to examine the influence of the urban built forms and density on energy consumption, the total annual heating and electricity energy demand of buildings per square metre of floor area is used, which is around 37 kWh/m^2/year for this exemplar case. Using units of kWh/m^2 facilitates an equitable assessment of different building plans with a range of dimensions, and also provides the opportunity to compare the results with those of previous studies (Bhiwapurkar, 2014). This number is the final value showing the intensity of energy demand in a specific point on the *Form Signature* graphs developed in Chapter 3. To determine the energy intensity of other points on the *Form Signature* graph, simulation trials are repeatedly conducted for models with:

- Number of storeys (n) from 1 to 30; Simulation trials for 1, 3, 6, 10, 20 and 30 storey buildings. These values were selected due to the fact that they have an approximate similar distance from each other on the *Form Signature* graphs (since the MATLAB code uses interpolation to generate a homogeneous heat map of energy intensity on the graphs, the results are more precise if the points chosen on the graph have constant distance from each other).
- Plan depths (x) of 6m to 60m (in 6m intervals)
- Cut-off angles of 25º, 45º and 65º in order to examine the effect of changing the distance between buildings

Hence, on the *Form Signature* graph related to each cut-off angle, the intensity of energy demand is defined by simulating the model with a particular number of storeys and plan depth. An Excel tool is developed to calculate the required parameters such as number of occupants for each model (before simulation), and process the data obtained from simulation to calculate the required values such as electricity consumption, total energy demand per m^2, PV generation and Energy Equity (see Appendix E). Aggregated results of energy for each model were overlaid on the *Form Signature* graphs as a heat map. This was accomplished using MATLAB code written with the assistance of the Math and Statistics Centre (Mash)[5] at the University of

[5] Dr Phil Ashheton

Lincoln (see Appendix F). The results not only illustrate the energy demand intensity of buildings using a colour spectrum, but also interpolates the areas between two known points on the graph. The outcome is shown in Figure 5.6, which shows the correlation of building heating/electricity energy demand with urban density in case of pavilion built form.

a)

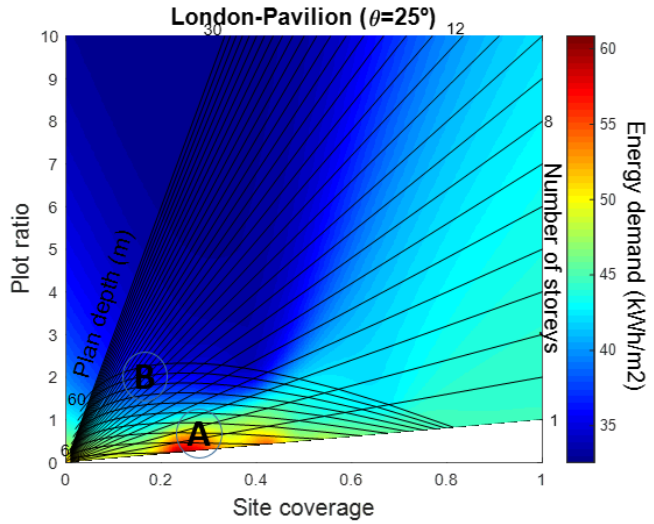

b)

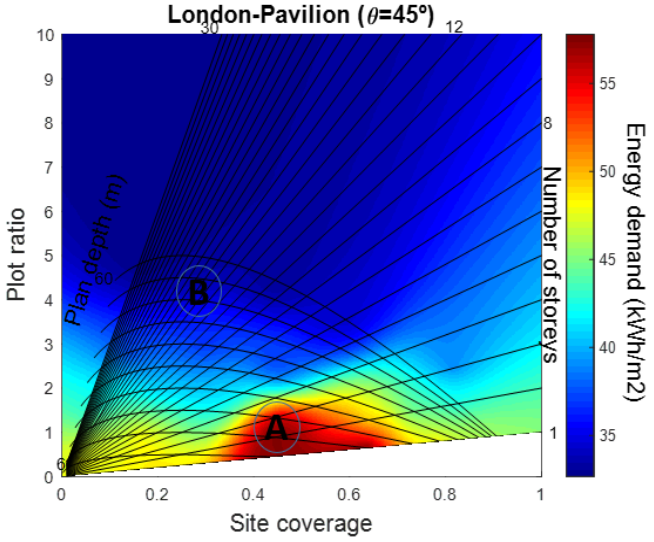

c)

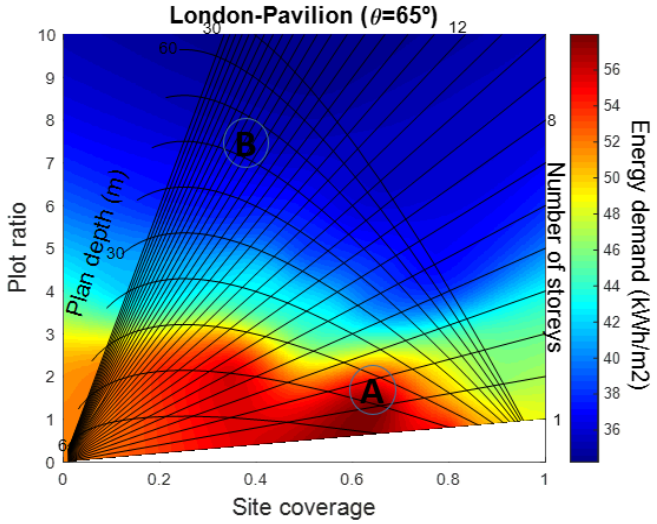

Figure 5.6: Correlation of building energy demand with urban built form and density a) pavilion θ=25° b) pavilion θ=45° c) pavilion θ=65°

In Figure 5.6, the diagonal lines stemming from the origin indicate the number of storeys (*n*), which start at 1-storey (the line with the lowest gradient) to 30-stories (the line with the highest gradient). The curved lines represent plan depth (*x*), with a range between depths of 6 to 60m. It can be seen for all cases in Figure 5.6 that urban built areas with low-rise buildings (number of storeys up to maximum four) and low plan depths (up to 24m) present worst case scenarios regarding energy consumption (e.g. point A). This region of the graph, which is shown in dark red, represent building plans with the highest energy consumption per square meter. Conversely, urban built areas with higher numbers of storeys (Monien et al., 2017, Rode et al., 2014) and plan depths (Steadman et al., 2014) demonstrate the lowest energy consumption per unit area (e.g. point B)—indicated in blue spreading towards the top of the graphs. The figures also show that designing taller buildings without increasing density incurs an energy penalty (Hamilton et al., 2017).

As an example, the energy demand of points A and B with θ=45° are compared as follows:

- Point A (2-storey building with 12 m plan depth): Energy demand = *58 kWh/m²/year*
- Point B (20-storey building with 48 m plan depth): Energy demand = *34 kWh/m²/year*

Points A and B present a region of the worst- and best-case scenarios, respectively, for this analysis. The percentage difference between them is around 52% which demonstrates the significant influence of urban density on building energy

demand. It also emphasizes the importance of energy oriented urban planning. Moreover, these results are within the range of the benchmarking values discussed in section 4.2.3.2 thereby providing a degree of validation.

The main reason behind these findings is the impact of surface to volume ratio on the heating energy demand of buildings. As discussed in Chapter 3 (section 3.4), this ratio is smaller not only for buildings with greater plan depths, but for higher buildings, though the decreasing trend of this ratio is not significant for buildings with more than 10 storeys. It demonstrates the fact that buildings with lower surface to volume ratio demand lower amount of energy per floor area (Monien et al., 2017), which shows lower energy loss from their envelope (Muhaisen and Abed, 2015, Ratti et al., 2005). However, the rate of reduction in building energy demand by increasing the plan depth is significantly sharper than its rate of change by increasing building height. This emphasizes the more significant influence of plan depth on energy demand compared with the influence of building height. This may be due to the UHI effect that is more dominant in lower floors due to the vicinity to the ground. Therefore, 'shorter and fatter' buildings, with high site coverage, are more significantly affected by the UHI effect (Javanroodi et al., 2018). It reduces heating load of the building specifically at night when the previously absorbed heat energy is being reflected. CitySim considers this effect by measuring surface temperature of all external surfaces in the built environment on an hourly basis. Moreover, in reality, lower air temperatures and higher wind speeds at higher elevations result in increased heating loads (Hamilton et al., 2017). However, this feature has not been considered here as it requires detailed CFD analysis.

The diagrams shown in Figure 5.6 can be specifically analysed as density indicators. It is observed that buildings sited in built areas with higher plot ratio are obviously more energy efficient by demanding less energy per unit floor area. This is compatible with results obtained by Leng et al. (2020) and Rode et al. (2014). Although Rode et al. considered plot ratio as density, it should be noted that this is one of several density indicators discussed in section 2.3 (Chapter 2). Hence, it cannot readily be called density without paying attention to its definition. A very important observation from these graphs is that they show that the term 'high density' is too vague to be used for urban energy analysis studies, albeit it has been adopted in many previous studies in the literature. An example of the ambiguity can be seen from the areas of the graphs that show high site coverage but low plot ratio values and vice versa. It indicates

opposing characteristics of each of the density indicators. Hence, in case of determining density by site coverage this area can be considered high density, while considering plot ratio it is low density. It proves that it certainly depends on the choice of density indicators to call an urban area ‘high density’.

Regardless of the impact of building form and shape on energy demand, they can provide opportunities for passive strategies. For instance, wind environment around buildings, which is different in higher elevations, may promote natural ventilation (Huifen et al., 2014, Salvati et al., 2020). It helps to disregard mechanical ventilation for building design that reduce energy consumption. However, in high-density cities the need for air conditioning increases due to a reduction in wind speed that diminishes the potential for natural ventilation (Pitts, 2010). Buildings with greater plan depths are not a good choice for adopting passive strategies such as natural lighting and ventilation. They also may not satisfy the social aspects of sustainability (e.g. wellbeing and comfort). As explained in Chapter 3 (see Figure 3.21), pavilion form with very long plan depth practically should be transformed to court form.

The main conclusion from these results may provide encouragement to urban planners to adopt high-rise buildings and large plan depths for new urban developments. Nonetheless, this conclusion may change by considering solar energy potential, as will be discussed in section 5.2.3.

It should be noted that the energy consumed in communal areas and by elevators has not been considered in this study. As mentioned in section 2.2.1 (Chapter 2), this energy demand is greater in taller buildings (Finch et al., 2010, Heinonen and Junnila, 2014, Myors et al., 2005). Furthermore, the energy consumed for pumping water to the top floors is higher for high-rise buildings. Therefore, the areas equivalent to taller buildings in the *Form Signature* graphs may show higher energy demand in real cases. The energy consumed for domestic hot water preparation is also excluded from this study because it is not affected by urban built form and density.

5.2.1.2 Court built form

The same method as in the previous section was used to determine the heat map of energy demand for court built form on the *Form Signature* graph. Figure 5.7 shows a site plan composed of array of buildings with court built form.

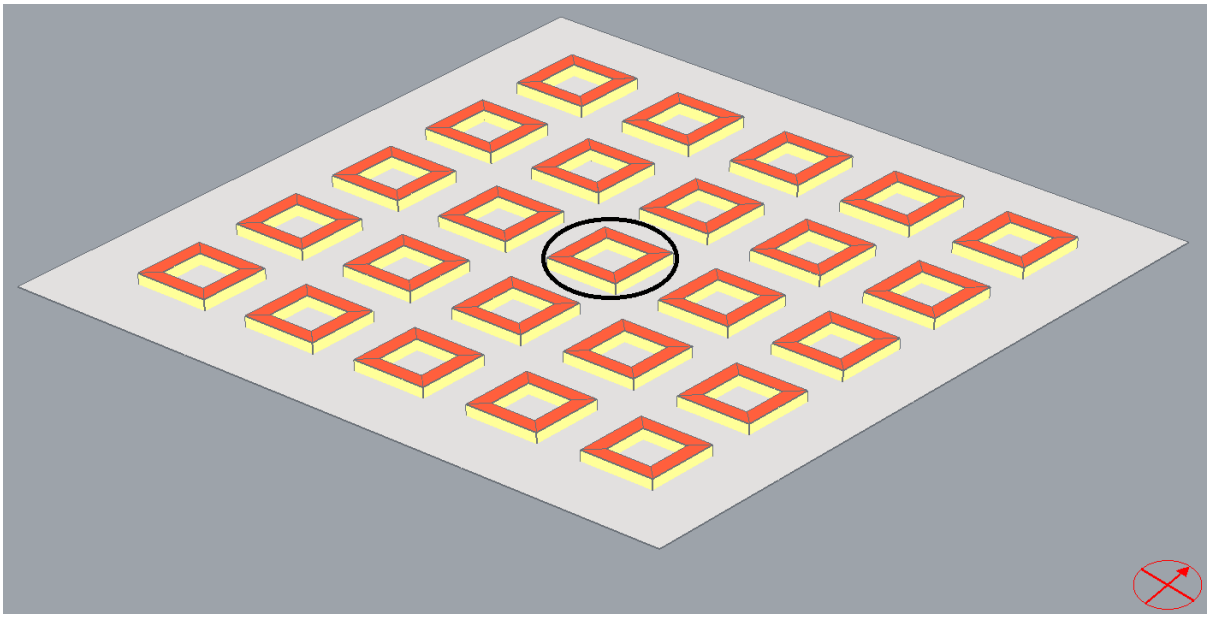

Figure 5.7: A model of court-built district with series of court buildings for energy simulation purpose. The target building is marked by a black ellipse.

As before, simulation trials were undertaken for site plans with number of storeys from 1 to 40 and plan depths from 6 to 60 m for each of the three cut-off angles. The yearly energy demands of all plans were entered into MATLAB in order to plot the heat map.

Figure 5.8 shows the heat map of energy consumption of court built form for three different cut-off angles.

a)

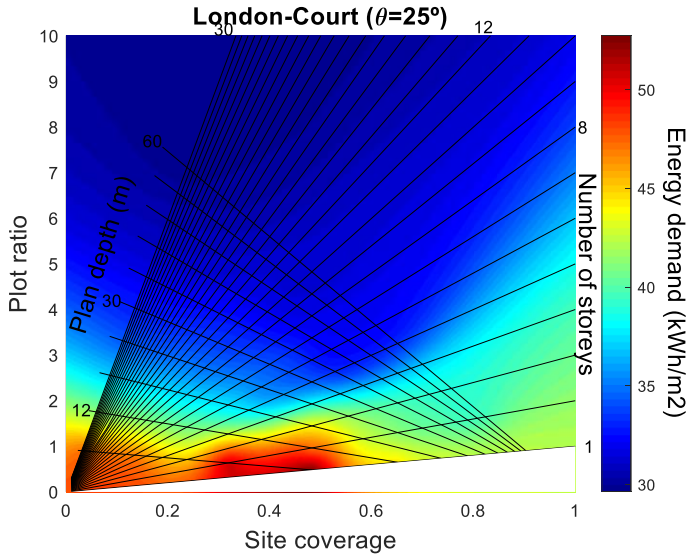

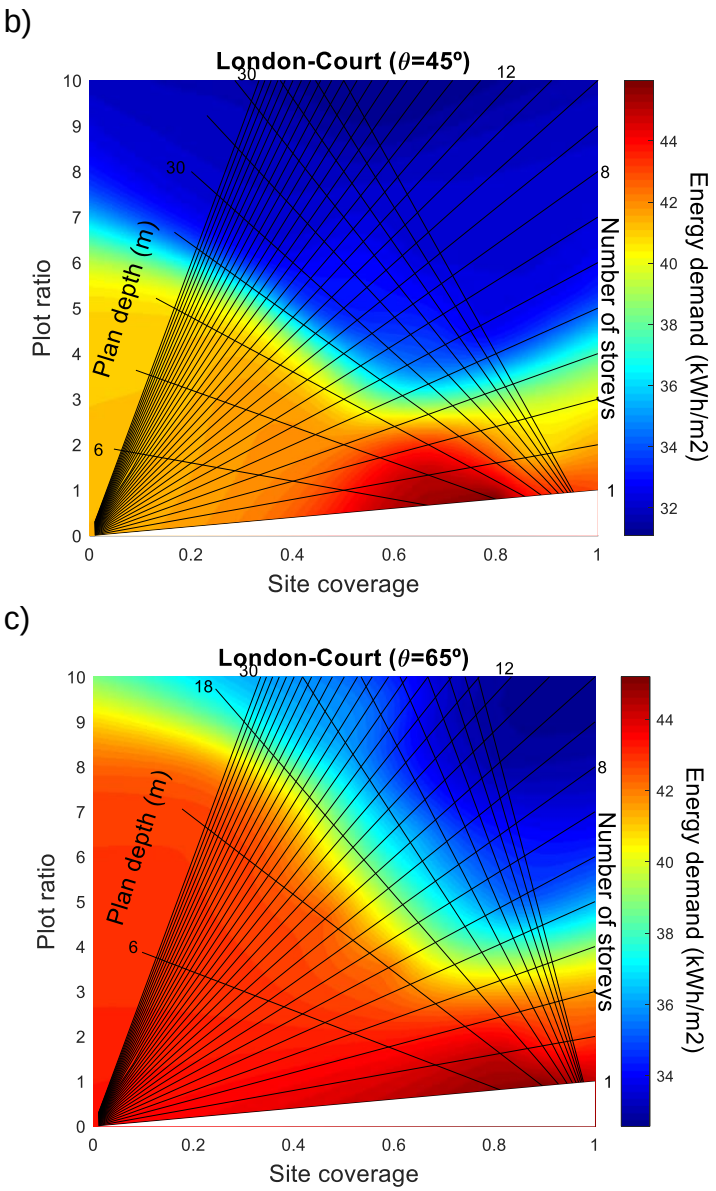

Figure 5.8: Correlation of building energy demand with urban built form and density a) court θ=25º b) court θ=45º c) court θ=65º

It can be observed that buildings with higher number of storeys and larger plan depths are more energy efficient—this is in line with previous results for the pavilion form.

5.2.1.3 Terrace built form

To identify the energy performance of terrace buildings with different densities, different configurations composed of terrace buildings are considered for simulation trials, as shown in Figure 5.9.

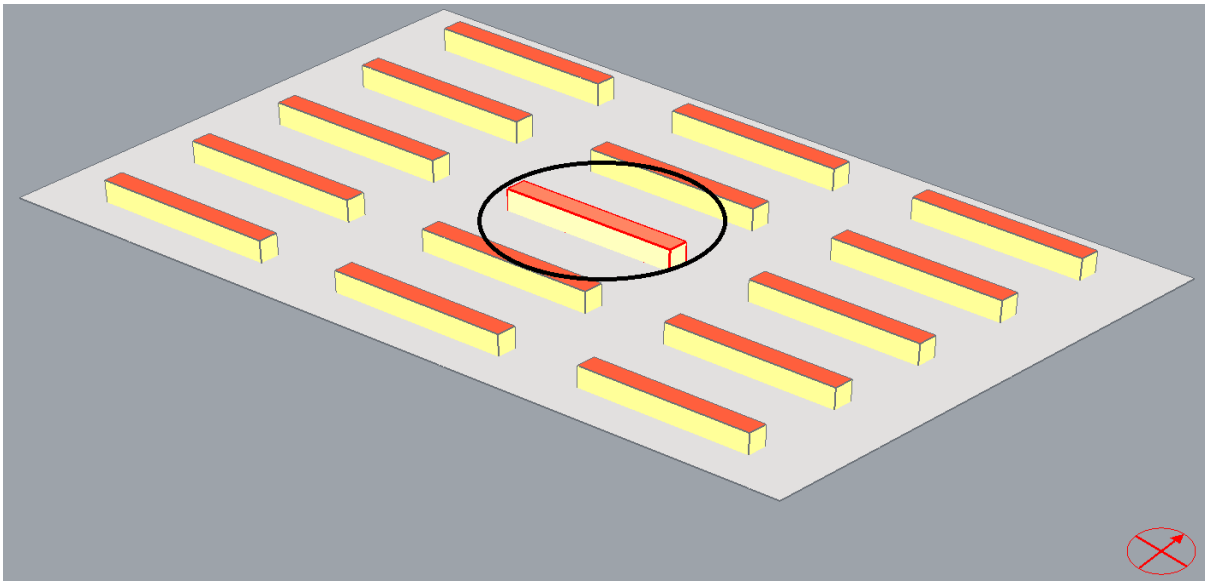

Figure 5.9: A model of terrace-built district with series of terrace buildings for energy simulation purpose. The target building is marked by a black ellipse.

Again, running simulation trials for plans with different number of storeys, plan depths and cut-off angles, the yearly energy consumption per square meter is obtained. The results are spread over the *Form Signature* graphs as a heat map, as depicted in Figure 5.10.

a)

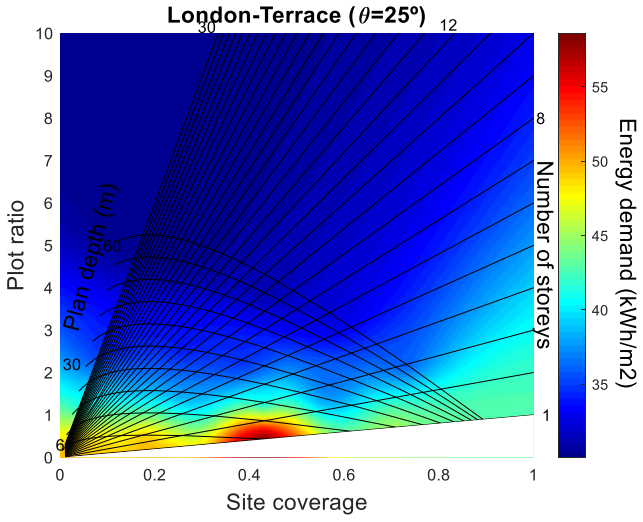

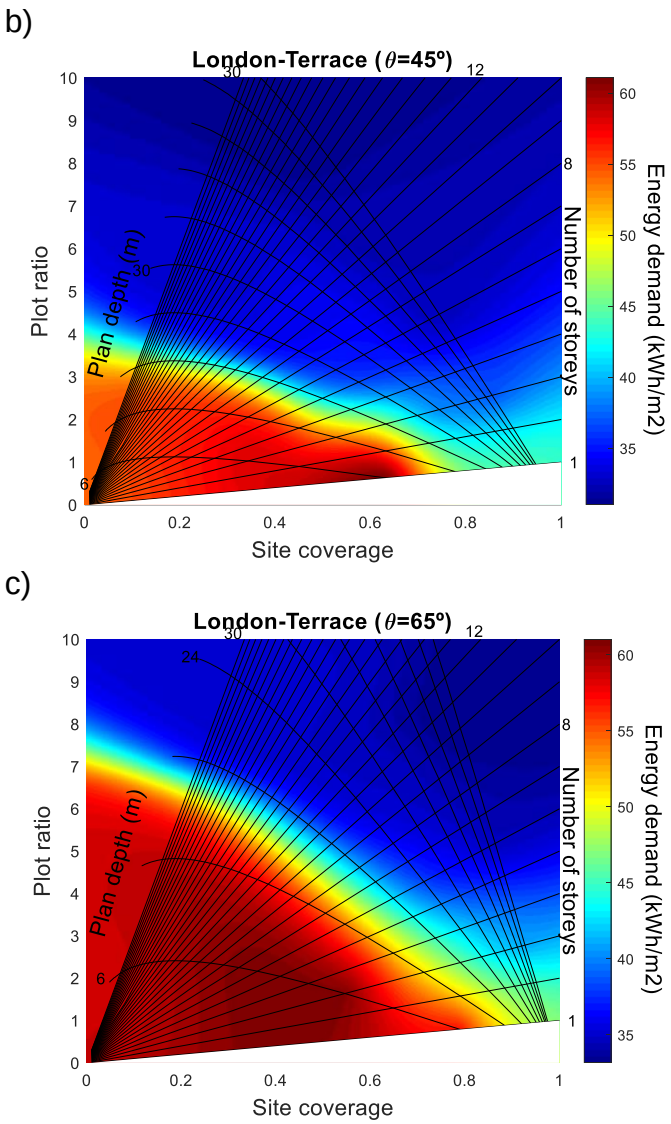

Figure 5.10: Correlation of building energy demand with urban built form and density a) terrace θ=25º b) terrace θ=45º c) terrace θ=65º

The results illustrate that the trend of intensity of building energy demand is similar to those obtained for pavilion and court forms. It means greater plan depths and number of storeys leads to lower building energy demand per square meter.

5.2.1.4 Tunnel-court built form

The peculiarity of tunnel-court form compared to other examined built forms is the difference of one and two storey building plans with the building plans with more than two storeys (see section 3.2.2 of Chapter 3). As illustrated in Figure 5.11 (a), nothing covers the road in one and two storey buildings because up to the second floor (6m height) is cut by roads. However, in buildings with more than two storeys, the roads are covered by the floors above, which creates a cruciform shape shown in Figure 5.11 (b).

(a) (b)

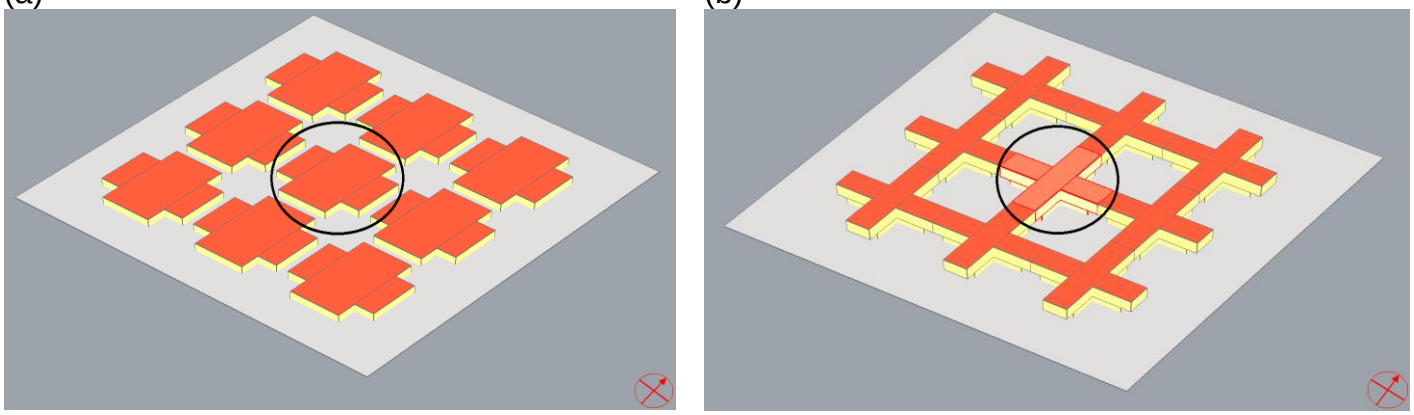

Figure 5.11: A model of tunnel-court built district with series of tunnel-court buildings for energy simulation purpose a) for 1 and 2 storey buildings b) for more than 2 storey buildings. The target building is marked by a black circle.

Models of tunnel-court form site plans with different number of storeys, plan depths and cut-off angles are prepared for 54 simulation trials to examine the impact of those variables on the energy demand of the buildings. All the other simulation assumptions are the same as for other examined built forms. The annual energy demand of the models spread over the *Form Signature* graphs as a heat map are shown in Figure 5.12.

a)

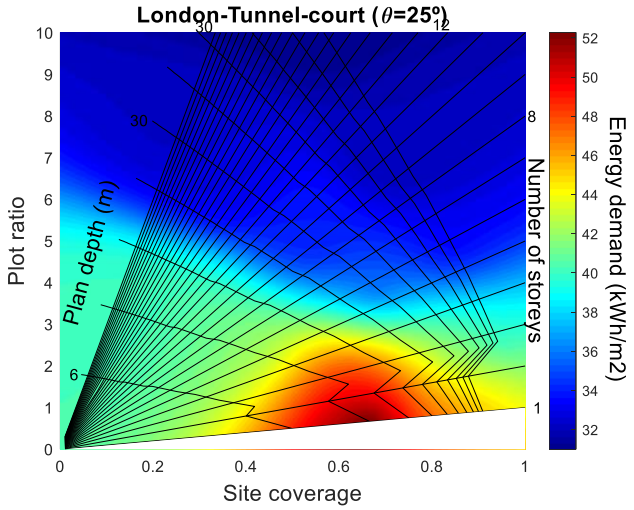

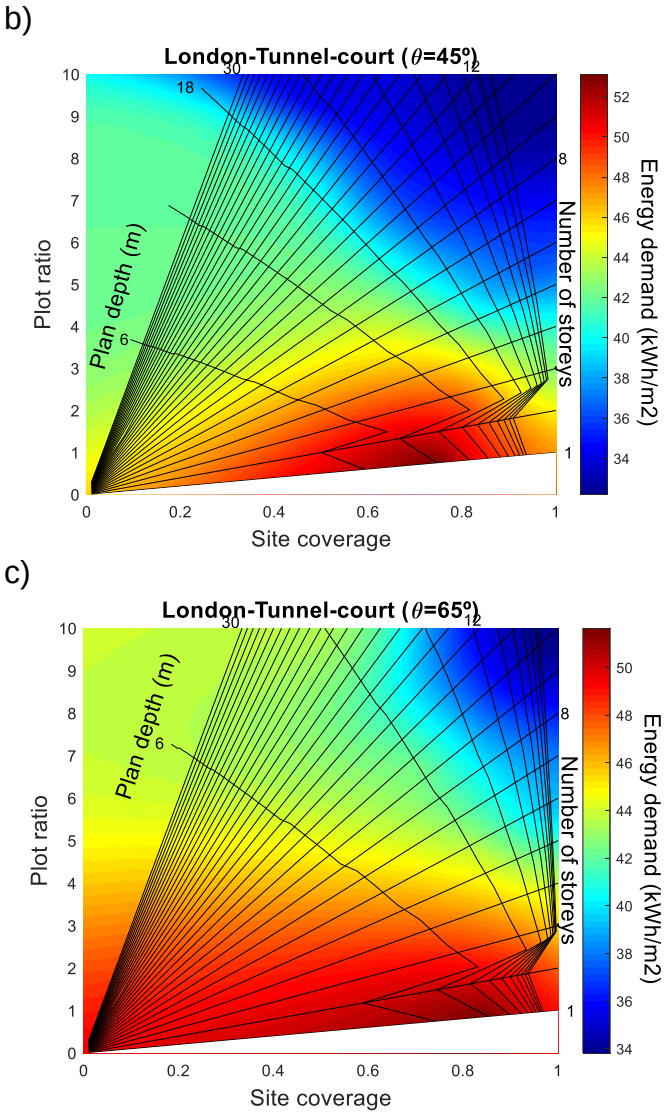

Figure 5.12: Correlation of building energy demand with urban built form and density a) tunnel-court θ=25° b) tunnel-court θ=45° c) tunnel-court θ=65°

The general trend of the intensity of energy demand on the graphs is similar to the other investigated built forms. Buildings with greater plan depths and higher number of storeys are more energy efficient.

5.2.1.5 Impact of cut-off angle on building energy demand

Thus far, building energy demand has been shown on the *Form Signature* graphs for different cut-off angles, separately. To analyse the specific influence of cut-off angle on building energy demand, in this section, building plans with similar geometry but different cut-off angles are compared. Figure 5.13 shows a plan of pavilion buildings with three different cut-off angles, but with the same plan depth and number of storeys. It demonstrates how differing cut-off angles changes distance between buildings that can affect building energy demand. This is also the case for other types of built forms.

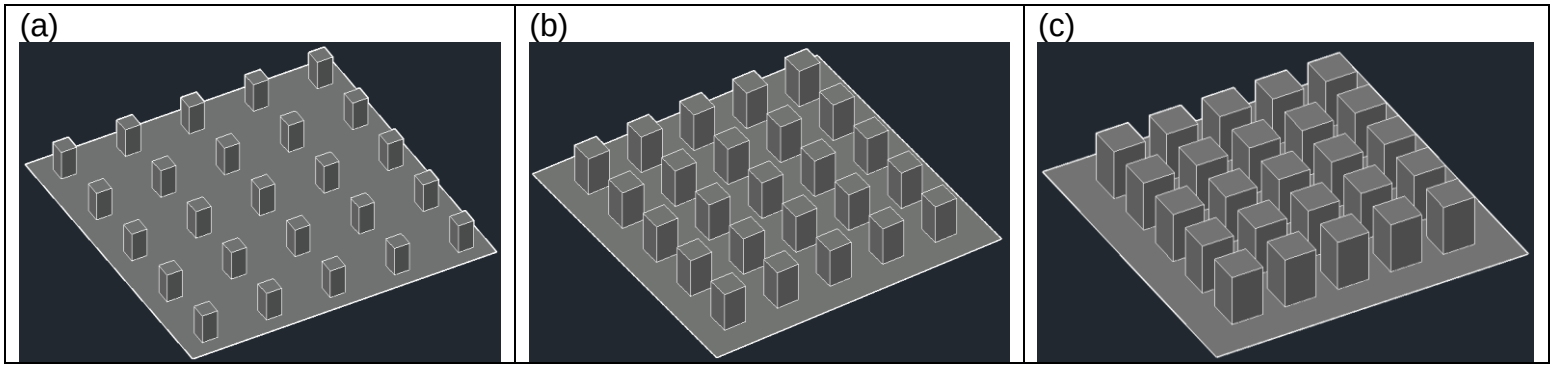

Figure 5.13: Plan of buildings with three different cut-off angles (a)25º (b)45º (c)65º

In each case simulation trials are performed with the number of floors and plan depth kept constant and the cut-off angles are changed three times from 25º to 65º. This scenario was repeated three/four times for each examined built form. The results are shown in Figure 5.14, where each bar represents yearly energy demand of specific building plan per unit of floor area that is compared with others using three different colours.

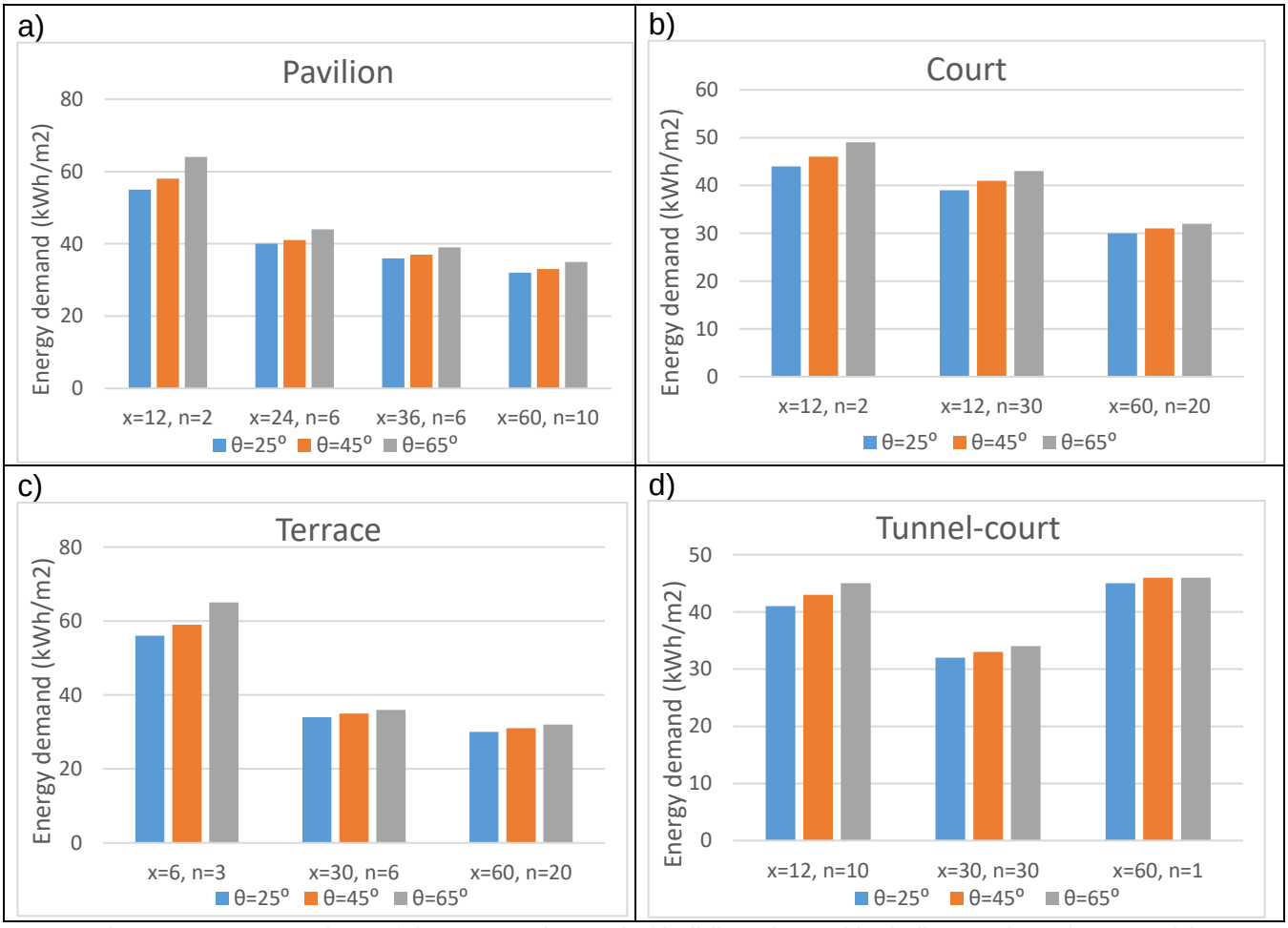

Figure 5.14: Comparison of the energy demand of building plans with similar number of storeys (n) and plan depths (x), but different cut-off angles (θ) for a) pavilion b) court c) terrace d) tunnel-court forms in London

It can be seen from the results of Figure 5.14 that in any case building plans with higher cut-off angle, which means higher density (both site coverage and plot ratio), consume more energy. This is in line with the outcome of the research by Steemers (2003). It means that, regardless of the built form, energy demand of buildings is the highest for built environment with a cut-off angle of 65º, while having cut-off angle of 25º leads to the lowest building energy demand. For instance, for pavilion buildings with plan depths of 24 m and 6 number of storeys, energy demand is equal to 40, 41 and 44 (kWh/m^2) for the θ=25º, θ=45º and θ=65º cases, respectively. Considering urban energy planning targets for London's temperate climate, this may encourage urban planners to plan new urban built areas to have lower cut-off angles by increasing the distances between buildings. Though it should be noted that the consideration of other factors of urban planning such as mobility, land use, rents/land price, outdoor thermal comfort and ecological footprint could ultimately influence the outcomes. For instance, an extremely dense built environment may cause a negative effect on the outdoor thermal comfort, while its intensity may depend on the climatic conditions. Hence, a trade-off between energy efficiency and other planning considerations may result in different planning decisions for the same location and climate. The study does, nevertheless, provide a means identifying the most effective/efficient starting point.

The main reason for this outcome is the shadowing effect of the neighbor buildings. Higher cut-off angles mean building are closer to each other, which blocks a larger portion of sunlight. This not only reduces the solar gain of buildings through glazing, but also decrease the amount of energy stored in building thermal mass. As a result, buildings need more energy to satisfy their heating energy demand (Coccolo et al., 2016). Having buildings closer to each other (i.e. higher density) could increase interreflection between external walls and trap more heat energy in the built environment that may increase the UHI effect (Li et al., 2015). It normally leads to lower heat energy demand by buildings (Li et al., 2015); however, its impact is not significant enough to overtake the opposite effect of reducing solar gain and energy stored in building thermal mass. This result is a counterexample of the theory that says high density urban developments are more energy efficient and demonstrate that densification of cities could have both positive and negative effects on total energy demand (Hui, 2001).

Those outcomes are specifically valid for the location and climatic conditions of London; however, the conclusions could be different for different climates (Resch et al., 2016). For instance, compact urban forms might be good for places with severe wind conditions as it will provide wind sheltering (Khalili and Amindeldar, 2014). The same analysis for hot and arid climate may lead to the opposite conclusions, because in that climate the buildings demand more cooling load rather than heating load (Javanroodi et al., 2018). Therefore, locating buildings closer to each other (higher cut-off angle) could protect the buildings from intensive solar radiation and decrease the cooling load (Coccolo et al., 2016). This will be investigated in Chapter 6. Even in the current analysis, if cooling demand was considered in addition to heating and electricity consumption, this conclusion might have differed. This demonstrates the impact of assumptions on the final conclusion of this and similar studies on this subject. It will be further examined in Chapter 7 when future scenarios will be considered.

Furthermore, comparison of the datasets obtained from simulation trials demonstrate that the influence of cut-off angle on the building energy demand (i.e. building heat demand in these cases) diminishes with increasing plan depth of buildings. Escalation of cut-off angle shows a slight increase in heating energy demand per unit area of buildings with big plan depths while it indicates a sharp increase in heat energy demand of small depth buildings. The impact of plan depth on the sensitivity of heating energy demand to variation of cut-off angle is more significant in the case of tunnel-court form. As it is observed from the relevant bar chart in Figure 5.14, for the case of having 60m plan depth (which is the highest value considered in this study), the impact of different cut-off angles from 65º to 45º is neutralized and the buildings indicate the same heating energy demand per square meter (i.e. 46 kWh/m^2/year).

This can be rationalized by the fact that greater depth buildings possess larger space inside their envelope to be heated, and this space (volume) is large enough to not to be easily affected by surface area around the envelope that is sensitive to external variables such as cut-off angle. Initially, it may be expected that this is the impact of surface to volume ratio, but if so, the height of buildings should have imposed the same influence on the impact of cut-off angle. Further comparative analysis depicted that building height does not show the same effect as building depth. As shown in Figure 5.14, in buildings with long plan depths (e.g. x=60 m), building energy demand does not significantly change by changing the cut-off angle, in contrast to

buildings with short plan depth (e.g. x=12 m). It shows the mitigating effect of plan depth on the sensitiveness of energy demand from cut-off angle. Although building height has a mitigation effect on changing the building's energy demand by changing cut-off angle too, its effect is not as large as that of plan depth. In other words, adding the same length to the depth of building is more mitigating compared with adding the same length to the height of building. The reason is that by increasing number of storeys the external walls area will increase rather than roof surface area which is increased by increasing plan depth. Hence, both increase surface to volume ratio but with different impacts. Increasing external walls surface area increases the sensitivity of thermal behaviour of the building to the external environment, firstly, due to increasing the glazed area that significantly effects solar gain; and secondly, the external walls are exposed to each other and are affected by inter-reflected radiation between surfaces. Both former and latter cases are affected by changing the building distances from each other as a result of different cut-off angles. Therefore, in contrast to building height, building depth significantly influences the impact of the cut-off angle on the heating energy demand of buildings.

It should be noted that changing the cut-off angle (and changing built forms) can influence important parameters such as the daylight availability of buildings (and consequently artificial lighting energy demand) and outdoor human comfort. Its impact on lighting energy demand has been neglected in this study as its contribution is negligible compared to the total energy demand of buildings—the total lighting energy demand of housing in the UK is ~3% of total housing energy (Palmer and Cooper, 2013), and the effect of daylight availability is only a small portion of this percentage. The impact of cut-off angle on outdoor human comfort is out of the scope of this study.

5.2.1.6 Heating energy demand vs. electricity demand

By examining energy demand of buildings in London's temperate climate, this chapter has investigated heating and electricity energy demand (for lighting and appliances) of buildings. Cooling energy demand calculations have been excluded because it is not widespread in residential buildings of London. The ratio of heating energy to electricity energy demand is examined for all the datasets obtained from simulation of the studied building plans with different built forms, densities and geometric variables. The results indicate that this ratio is larger, by a factor up to 2.5, for buildings with lower number of storeys and smaller plan depths. The ratio gradually

decreases when the number of storeys and plan depths increases. The minimum value is 0.65 for high-rise buildings with large plan depth (see Eqn (5.3)).

$$0.65 \leq \frac{Heating\ energy\ demand}{Electricity\ consumption} \leq 2.5 \qquad (5.3)$$

The results show that in smaller buildings with smaller floor area, heating energy demand dominates electricity energy demand. Conversely, in buildings with greater floor area (taller and wider), electricity energy demand becomes larger than the heating energy demand. This is because electricity energy is estimated based on the consumption per square meter. However, heating energy demand per unit area is reduced for larger buildings with lower surface to volume ratio (Evans et al., 2017), which indicates less energy waste from exposed surfaces (Steadman et al., 2014). It also depends on the thermal properties of the envelop (specifically U-values). For super insulated envelopes where the heat loss through the fabric is negligible the change in the ratio shown in Eqn (5.3) is lower because heating energy demand does not drastically change in these kinds of buildings. The main portion of heat loss from well-isolated buildings is due to ventilation. The relative importance of it depends on the envelope's thermal properties and the volume. Buildings with larger volumes require more ventilation and with a plan depth of more than 15m need air conditioning (Evans et al., 2017).

It can be concluded that although urban built form and density have impact on the heating energy demand of building, they do not show a significant effect on electricity energy demand (Hamilton et al., 2017). It should be noted that the conclusion regarding electricity demand is valid following the assumptions of this study. For example, heating energy is provided by gas in this study and is not connected to electricity consumption. If heating was provided by electricity (e.g. using a heat pump), the electricity consumption would definitely be affected by the chosen built form and density because they affect heating demand of building. Moreover, only normal household appliances are considered as the electricity consumers (see Table 5.2), and appliances such as fans and pumps are not considered in this study. The presence of ventilation fan in the building can increase electricity consumption in buildings with long plan depth.

5.2.2 Renewable energy potential of built environment

As discussed in Chapters 1 and 2, there are opportunities for a built environment to generate its own energy from renewable energy sources. Because *the urban fabric with its energy behavior in terms of demand and supply must be regarded as a 'whole system' in exchange with its larger environment* (Vandevyvere and Stremke, 2012). Provision of city-integrated renewable energies at the site of energy consumption could substantially contribute to the environmental, economic, and social aspects of urban sustainability (Kammen and Sunter, 2016). To maximise the renewable energy potential of an urban area, the integrated approach offered by spatial planning is required. It includes the provision of waste-to-energy plants in municipal plants as well as using lands as energy generation facilities (e.g. rooftops for solar energy) where possible (SPECIAL project). There are several renewable energy sources that can be utilized in urban areas, however, not all of them are efficient in an urban environment. At a neighbourhood scale, technologies such as combined heat and power (CHP), waste heat utilization, biomass, geothermal energy and solar heating (and cooling) are technically and economically more efficient compared with those on small scales (Jank, 2017). However, in high-density built areas a centralized approach offers better economic options (Jank, 2017). Urban energy generation technologies such as solar photovoltaics (PV), micro-wind turbines, micro-combined heat and power (μCHP) and ground-source heat pumps are so-called microgeneration systems (University of Southampton).

Wright (2008) predicts the increased utilization of ground source heat pumps and CHP fueled by biomass to support future urban energy provision. He considered them as low-carbon solutions to replace gas for space heating of buildings. Cheng et al. (2011) showed that medium to low density housing increases the chance of harvesting renewable energy sources. Ghosh et al. (2006) emphasised the advantage of low-density housing for boosting the potential of biomass and solar heating energy generation. Whilst using CHPs requires a concentration of activities (Echenique et al., 2012), adaptation of ground source heat pumps needs low-density urban development (Echenique et al., 2012, Hargreaves et al., 2017). However, if adaptation of ground source heat pumps is considered in conjunction with city developments, it has potential for high-density cities as well (Pitts, 2010). Another option for high-density urban areas is producing energy from waste by using anaerobic digestion technology (Pitts, 2010).

Several types of vertical axis wind turbines can be used in the built environment (Casini, 2016). These small wind turbines perform better toward the outskirts of a city (Drew et al., 2013). Increasing the building height is considered the best solution to exploit the increase of both wind speed and wind exposed facade for integrating wind turbine with buildings (ELMokadem et al., 2016). In general, there is a limited wind potential in urban areas (Cheng et al., 2011), specifically in dense cities because of the disruption to wind flow caused by nearby buildings and the consequent poor performance (Pitts, 2010). Meanwhile, their integration with buildings requires a strengthening of building structures to tolerate extra load of the rotating blades and consequently increased cost of structure (Galsworthy, 2015). Finally, due to noise and safety issues, they may raise objections from residents (Pitts, 2010).

Solar energy has been the most popular type of renewable energy source analysed by researchers in this field of study. It is the most widespread decarbonized generation technology due to declining capital costs, modularity and easy maintenance (Parra et al., 2016). There is a strong correlation between solar capacity of cities and indices of urban morphology (Zhu et al., 2020). Hachem et al. (2011) discovered that some configurations of a certain building shape are more efficient for using solar electricity generation. Sarralde et al. (2015) found that the solar irradiation of roofs and facades could grow by around 9% and 45%, respectively. It was concluded by several authors that increasing density has negative impact on solar energy potential (Byrd et al., 2013, Chatzipoulka et al., 2016, Margalit, 2016, Mohajeri et al., 2016), however, Cheng et al. (2006) proved that depending on the choice of density indicator, higher values of site coverage and plot ratio may have a different effect on solar energy potential. One of the main difficulties of using PVs in urban areas is a lack of availability of suitable mounting surfaces of sufficient size and orientation to get good amounts of harvested energy and avoid over-shading by other buildings (Pitts, 2010). Therefore, in this study the potential of PV energy generation on buildings with different forms and densities is now investigated.

5.2.3 Solar energy potential in London case study

To consider the potential of PV energy generation in urban built areas (i.e. PVs are mounted on building roofs), additional simulation trials are conducted assuming that 90% of all building roofs are covered by PV panels. The panels could be installed in south-face (in northern hemisphere) or east-west directions, where the former case

is the optimum orientation (George and Anto, 2012) and the latter case improves profile matching with consumption (Arora et al., 2016). The optimum tilt angle depends on the latitude and can be determined for each month to get the maximum irradiation (George and Anto, 2012). There are variety of calculation methods for fixed tilt installation. Some suggest different formulas for different latitudes (Landau, 2017), and others suggests constant formulas for all latitudes (REUK). For instance, the latter suggests that PV panels should be mounted at an angle of 10 to 15 degrees plus the site's latitude. Considering latitude of 51 degrees for London, solar panels should be mounted at the angle of approximately 34 degrees (Jacobson and Jadhav, 2018). However, since all the buildings have flat roof, installation of PVs with the desirable angle causes complexity in providing building models for CitySim. Moreover, at the time of this analysis, there was not any available guideline/information regarding this feature of CitySim. Therefore, horizontal installation of panels on the flat roof of buildings is considered for this study, though in practice it causes an issue with the self-cleaning feature of the panels. It should be noted that changing the angle of PVs does not make any relative difference in the comparative results of this study. Façade PVs might not always be economically justifiable because of their rather low efficiency due to the shadowing effect of the adjacent buildings and the angle of the sun. Hence, they are not considered in this study.

The PV model chosen for this study is a solar panel with 250W power called *1SolTech 1-STH-250*, which is embedded in CitySim. It is a Monocrystalline Silicon type with 1,652mm length and 990mm width with peak efficiency of 15.29% (SolarDesignTool). The efficiency of this model is very close to the latest models of current technology (Charles, 2019, Mitsubishi).

It should be noted that in order to utilize the highest portion of electricity generated by PVs, batteries are needed to store the generated energy (or alternatively the electricity can be traded with the grid through net metering) since the PV energy generation profile does not match with the consumption pattern of residential buildings (Pitts, 2010). This study does not seek to match supply and demand profiles. Instead it focusses on the annual energy performance of buildings and the potential of solar energy generation. Hence no battery storage facility is considered. In case of considering batteries, the dissipated percentage of the PV generation (depending on the batteries efficiency) is subtracted from the annual building energy generation.

Furthermore, batteries are currently expensive, though the technology is under development and their price and efficiency is being enhanced.

5.2.3.1 Energy Equity indicator

An energy indicator, termed 'Energy Equity', is introduced in this study that is an indication of building energy self-sufficiency. It is defined as the ratio of energy generated by building-mounted PVs with respect to total building energy demand, as shown in Eqn (5.4):

$$E_{equity} = \frac{E_{generation}}{E_{consumption}} \tag{5.4}$$

Energy equity values greater than one means the building achieves an energy surplus, while a value of unity indicates that the building is energy self-sufficient. Simulation trials of this chapter consider annual heating and electricity energy consumption plus PV energy generation, and are repeated for different site plans and building geometries. The value of Energy Equity is used as a relative metric and can be superimposed on the *Form Signature* graphs for each built form.

5.2.3.2 Solar energy potential on the *Form Signature* graphs: Urban built form, density and Energy Equity

Results for pavilion, court, terrace and tunnel-court forms are shown in Figure 5.15 representing the intensity of energy equity on the *Form Signature* graphs.

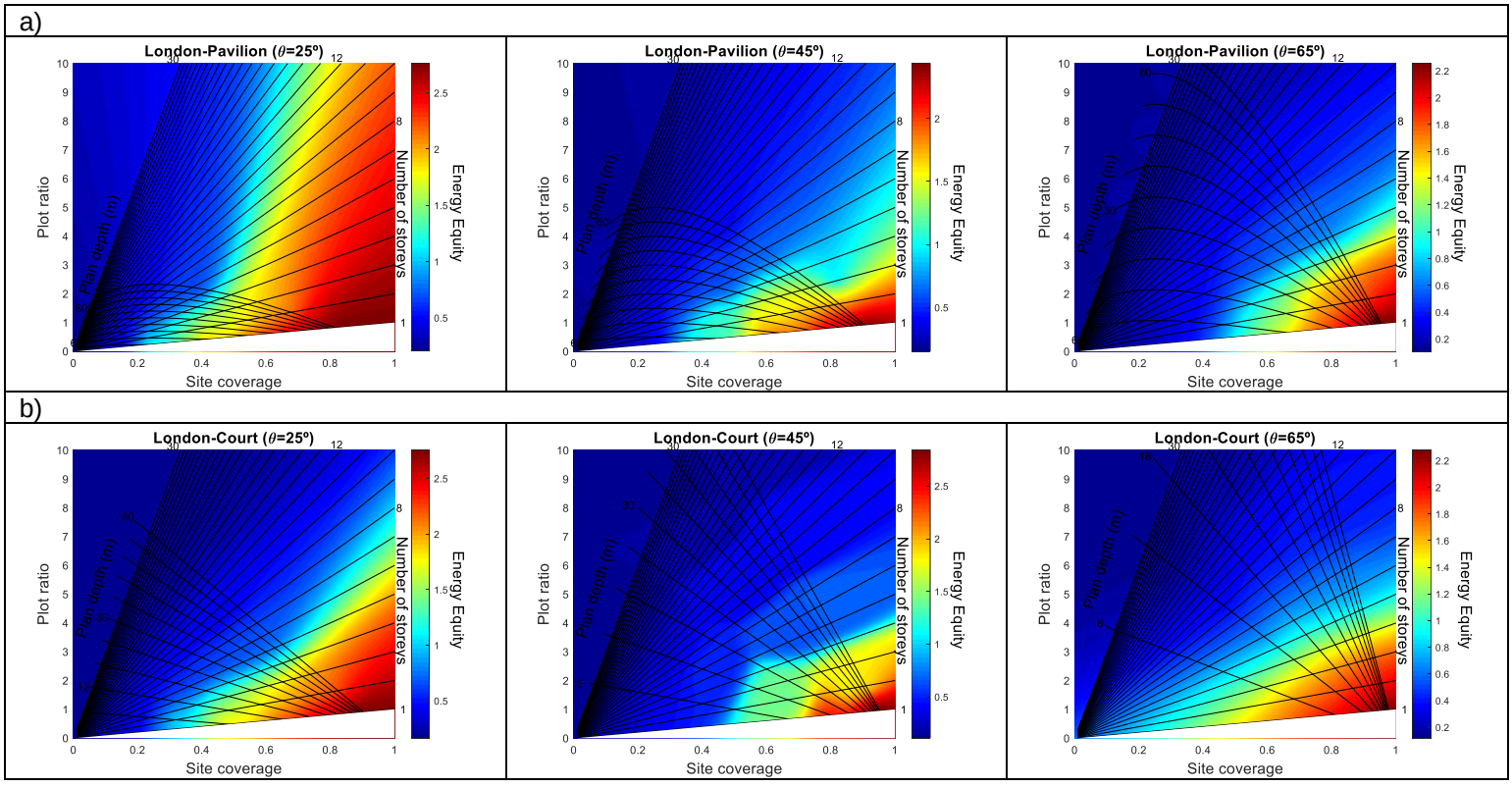

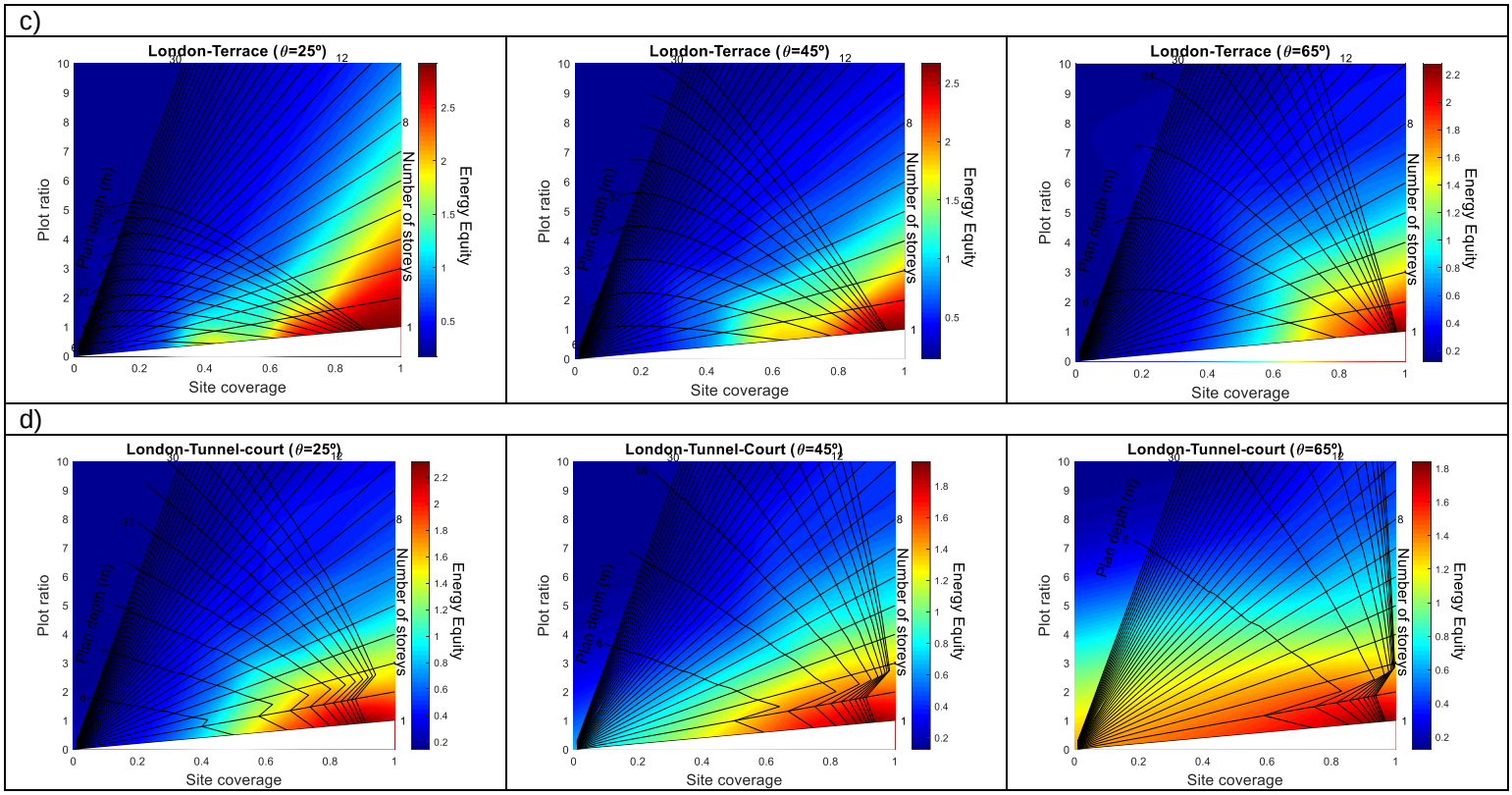

Figure 5.15: Correlation of energy equity indicator, considering the impact of PV generation, with urban built form and density a) pavilion b) court c) terrace d) tunnel-court

From Figure 5.15, it can be concluded that built areas with greater plan depths and lower number of storeys possess greater potential for solar energy harvesting. The red and orange areas of the graph represent the urban area that can potentially achieve greater solar energy generation compared to its energy consumption. It corresponds to low values of plot ratio (Cheng et al., 2006, Mohajeri et al., 2016) but high values of site coverage (Cheng et al., 2006). Therefore, it cannot be simply concluded that this is a high- or low-density area as each indicator tells different story, though the studies such as Waibel et al. (2016) and Makido et al. (2012) simply refer to energy performance of high/low density areas by relying solely on one chosen indicator. Other studies just referred to low density buildings (Ghosh et al., 2006) or medium to low density housing (Cheng et al., 2011) as the areas with higher potential of solar heating. In contrast to the results of Figure 5.6, high-rise buildings are not of interest as they show lower energy performance when PV energy generation is considered. This suggests that consideration of geometry and density of the built environment will be different for future urban developments if utilization of renewable energy potential, specifically solar energy potential (Sarralde et al., 2015), is a priority. It should be noted that if façade PVs are considered in addition to roof mounted PVs,

by increasing compactness in a neighbourhood, the potential of PV generation on facades is significantly reduced (Mohajeri et al., 2016). Whilst lower site coverage would allow better solar access to façade PVs (Cheng et al., 2006), average building height has a greater impact (Sarralde et al., 2015). Finally, layout and orientation are very influential on façade PVs compared to roof PVs (Hachem et al., 2011), though this study is not interested in the layout/orientation and only examined form and density.

An interesting application of these graphs is the ability to determine the appropriate urban density that buildings can energetically be self-sufficient (this is indicated in bright blue which represents an Energy Equity value of one). In red areas where the Energy Equity is greater than one, the building generates more energy than it demands and can be exported to the national grid (McKenna et al., 2018) or be stored to be used for purposes such as charging electric vehicles (Byrd, 2017) or provision of electricity in times of energy deficit (e.g. peak time). Having identical densities, it is more difficult to achieve building energy self-sufficiency in court form in comparison to pavilion form (see

Table 5.4).

5.2.3.3 Impact of cut-off angle on solar energy generation

The amount of PV energy harvested can be affected by the cut-off angle due to the shadowing effect of buildings on the roof of adjacent building. This is the case when there are buildings with different heights in a district. In this study, all the buildings have the same height, which means that there is no shadowing of one building on another to affect the rooftop PV generation. However, particularly in court and tunnel-court built forms, the dimension of the buildings is changed by changing cut-off angle that influence the amount of PV generation. As shown in Figure 3.1 (Chapter 3), the variable distance of *L* is a factor present in the geometry of each block in court and tunnel-court built forms, while it only marks the distance between blocks in cases of pavilion and terraced forms. Therefore, by changing the cut-off angle the dimensions of each block of court/tunnel-court is adjusted accordingly. This means that the roof area of the block would changes, and this affects the amount of PV energy harvested. This aspect is now discussed further below:

- Pavilion and terraced built forms: no change. Example: Total PV energy generation of 10-storey pavilion building with 24 m plan depth is around 74600 kWh/year regardless of the magnitude of cut-off angle.
- Court and tunnel-court built forms: Change is applied. Example: Total PV energy generation of 10-storey court building with 12 m plan depth is 469600, 260680 and 160800 kWh/year for cut-off angles of 25º, 45º and 65º, respectively.

In conclusion, increasing cut-off angle of court and tunnel-court buildings reduces the amount of PV energy generation due to shortening of the available roof surface area, while it does not have any impact for pavilion and terrace built forms.

5.2.4 Comparison of energy performance of different built forms

The *Form Signature* graphs have established relationships of energy with density for each urban built form separately. However, one of the objectives of this study is to provide a comparison of relative energy performance of the different urban built forms. To this end, building plans of different built forms but with similar cut-off angles, plan depths and number of storeys, are compared. The results are shown in Figure 5.16 which combine the results of the numerical study in Chapter 3 (data from geometrical modelling of built forms) and the simulation results of this chapter (data from energy analysis of sections 5.2.1 and 5.2.3).

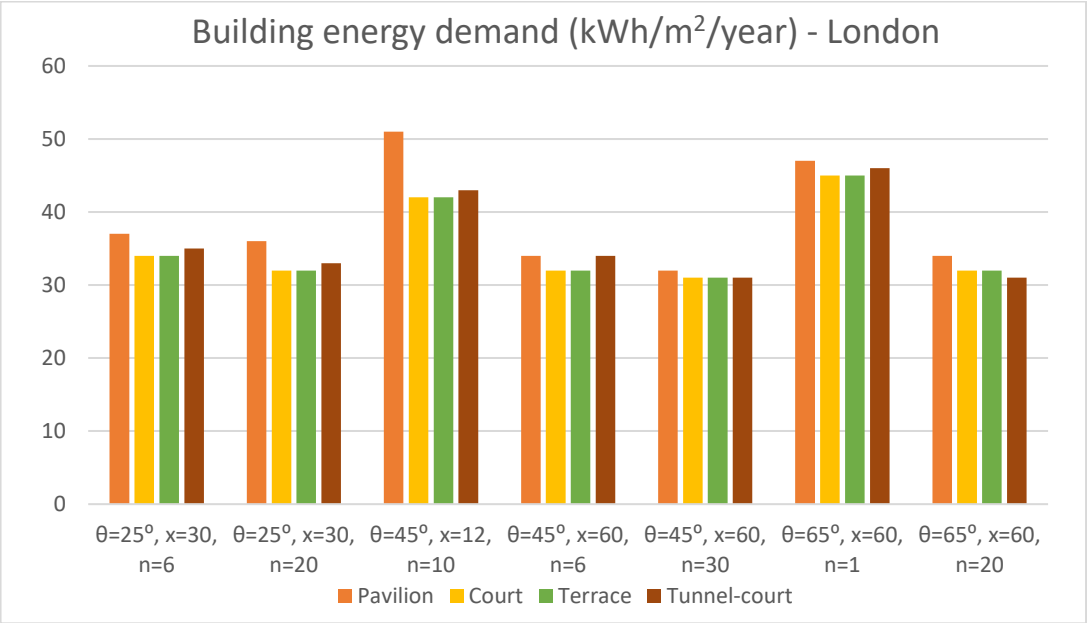

Figure 5.16: Comparison of energy demand of the built forms with the same cut-off angles, plan depths and number of storeys in London

It can be seen from the bar chart that in all cases pavilion built form demonstrates the highest energy demand per square metre of floor area, while court and terraced built forms are the most energy efficient built forms with approximately same order of magnitude. Tunnel-court form is in the middle by indicating lower energy demand compared pavilion and slightly higher demand compared to terraced and court forms. For instance, a pavilion built district composed of 20 storey buildings with cut-off angle of 25º and plan depth of 30 m demands 36 kWh/m^2 of energy per year, while both terraced and court built forms require only 32 kWh/m^2 of energy per year. The equivalent energy demand of tunnel-court form buildings is 33 kWh/m^2. This means that terraced and court built forms are almost 12% more energy efficient than pavilion built form, while they are only 3% more energy efficient than tunnel-court form.

A possible justification for 3% and 12% increase of energy demand in tunnel-court and pavilion built forms, respectively, is the higher surface to volume ratio compared with terraced and court built forms. This indicator represents the amount of external surfaces exposed to outdoor environment. The higher this ratio, the more energy is wasted through building envelope. This aligns with the results shown in Figure 3.8 (Chapter 3) which compares the trend of changing surface to volume ratio against geometrical variables of different urban built forms. In Figure 3.8, pavilion built form shows the highest surface to volume ratio while terraced and court forms, being very close to each other, have much lower surface to volume ratio than pavilion. This is reflected in Figure 5.16 by demonstrating higher energy demand of pavilion buildings compared with terrace and court buildings. This alignment between the results obtained here and the mathematical modeling results of Chapter 3 shows the validity of the obtained results and confirms the appropriateness of the methodology selected for the research.

Although the difference between energy demand of pavilion and terrace/court built forms is only 4 kWh/m^2 in above-mentioned example, it will create a large difference in the total building energy consumption of London when multiplied across the total built area of the city. According to the data published by the government (MAYOR OF LONDON, 2015), total housing floor area in London is 35,925,205 m^2. Multiplying this number to 4 kWh/m^2 of annual energy demand difference between the two built forms, there would be 143,700,820 kWh of energy saving per year. It emphasises the importance of the choice of built form that should be considered in energy efficient urban planning for metropolitan cities.

It should be noted that, as the envelope becomes more energy efficient, as insulation materials improve, the surface/volume ratio becomes less important (Ahmadian et al., 2019a). Also, a lower quality of building envelope, which is practically the case in the majority of existed buildings, result in larger differences in the bars shown in Figure 5.16 due to higher energy losses from the envelope, and reflects the greater influence of built form on energy demand of low standard buildings.

Although surface to volume ratio of terraced and court differ slightly, their energy demand per square meter is equal. There are a number of reasons for this. First, their surface to volume ratios are very close. Second, the inequity of their forms alters parameters such as shadowing effect, wind direction and radiative interreflection between surfaces. For instance, in contrast to terraced built form, court form has more walls that are exposed to each other. As shown in Figure 5.17, this may increase radiative interreflection between surfaces that increases the surface temperature of external walls by capturing more energy from the sun in the built environment. Furthermore, it may cause more shadowing effect specifically from east-west direction. Generally, the accumulative effect of the mentioned factors resulted in the similar energy efficiency of those two forms as shown in Figure 5.16.

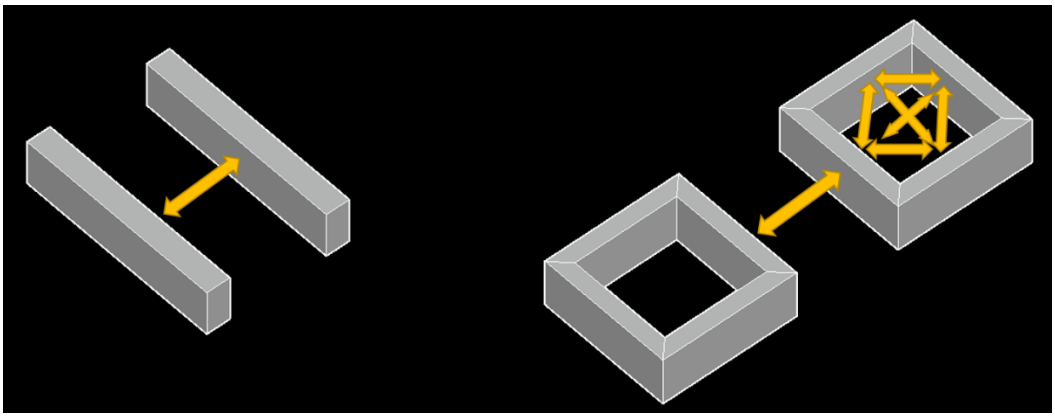

Figure 5.17: Comparison of shadowing effect and inter-reflection between external surfaces in terrace and court built forms

The outcome is different when considering building solar energy harvesting in addition to energy demand. Using Energy Equity data for the same cases originally considered in Figure 5.16, are compared and shown in Figure 5.18. The results from the selected cases indicate better performance of tunnel-court form compared with the others, while pavilion proves itself as the worst performer, having the lowest Energy Equity value. Court and terrace forms are in the middle, though their Energy Equity value is closer to tunnel-court form, proving their acceptable energy performance.

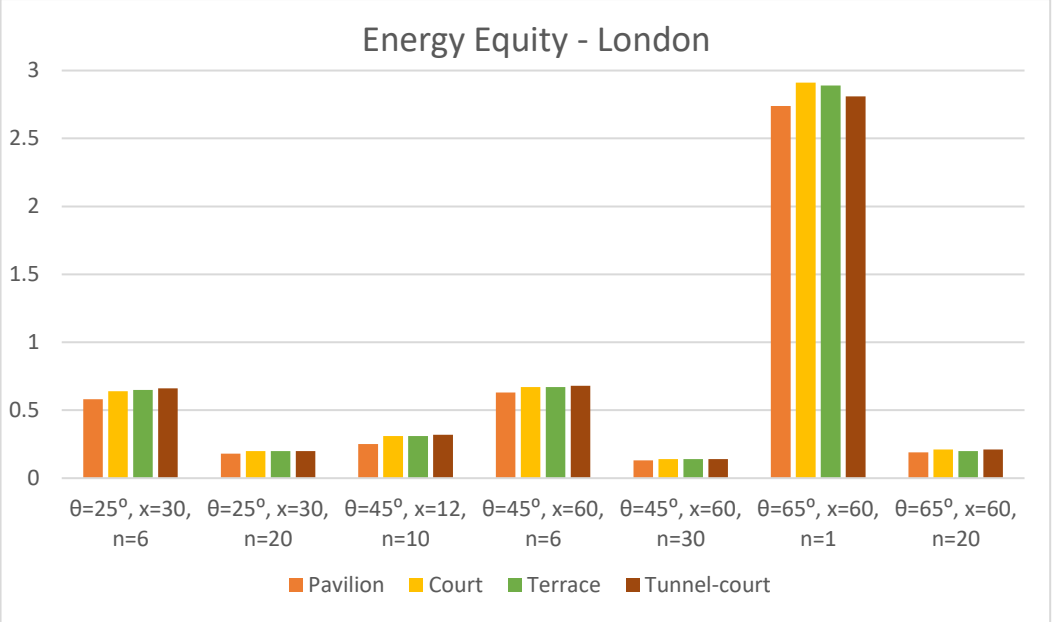

Figure 5.18: Comparison of Energy Equity of the built forms with the same cut-off angles, plan depths and number of storeys in London

Low values of Energy Equity are a result of the small roof area of buildings compared to their total energy demand. It corresponds to the indicator called *area of roof to floor area ratio* (see Chapter 2, section 2.3) that represents the proportion of roof area to the plot ratio of building (Byrd et al., 2013), and according to the results of Figure 5.18, this is the lowest for pavilion built form. In contrast, it has relatively high for tunnel-court form as a result of its large effective roof area as it covers some parts of the roads (see Figure 3.1, Chapter 3) which creates a tunnel for transportation.

In an exceptional case of Figure 5.18 (θ=25º, x=60 and n=1), tunnel-court form shows an unexpected low value of Energy Equity since all buildings are 1-storey in this case. As discussed in section 3.2.2, tunnel-court form buildings with less than three storeys do not have the road covered by buildings. This means there is exceptionally low roof area available to be covered by PV panels. It reduces total PV energy generation that consequently leads to a lower value of Energy Equity.

It should be noted that the amount of PV energy harvested in all cases were calculated assuming that all building had flat roofs and had a horizontal installation of PV panels. Solar energy generation may therefore differ in practice as a result of individual PV installation practice (i.e. east-west direction) or having inclined roofs. However, since this study is considering relative merits, the comparative outcomes should not be affected.

Thus far, the comparisons made in this section have been based on the geometrical parameters of urban built forms (i.e. cut-off angle, plan depth and number of storeys) and equality has been considered throughout. However, it is notable that the equality of those parameters does not mean that they possess the same urban density in the built environment. Hence, the values for their site coverage and plot ratio are normally different. For instance, in the first case shown in Figure 5.16 and Figure 5.18, the density (site coverage and plot ratio) of different built forms is given in Table 5.3.

Table 5.3: Comparison of density and energy performance of different built forms

θ=25⁰, x=30, n=6	**Pavilion**	**Court**	**Terrace**	**Tunnel-court**
Site coverage	0.191	0.437	0.383	0.683
Plot ratio	1.147	2.624	2.296	3.845
Energy demand ($kWh/m^2/year$)	37	34	34	35
Energy Equity	0.58	0.64	0.65	0.66

It can be seen that all built forms have the same cut-off angle, plan depth and number of storeys but site coverages and plot ratios are different. Pavilion has the lowest density, highest energy demand and lowest Energy Equity, while tunnel-court has the highest density but with medium energy demand and highest Energy Equity. Court and terraced forms have medium density, lowest energy demand and medium Energy Equity. The last two cases depict approximately similar energy performance, however, the density of court built form is higher than terraced form. This comparison suggests that, for London climatic conditions, urban areas with court built form can reach higher density compared with terraced built form with similar energy performance. Therefore, if the urban policy is aiming for highest density, court built form should be chosen rather than terraced built form to be more energy efficient (regardless of other factors being influenced by built form).

For a fixed density, built forms can be compared with each other from another viewpoint. In this scenario they all have similar densities, however, their geometrical characteristics are different. For instance, considering the density of; site coverage $\simeq$ 0.45 and plot ratio $\simeq 4.5$, the geometrical variables of the built forms plus their energy performance indicators are summarized in Table 5.4.

Table 5.4: Comparison of the energy performance of different built forms with similar density

Site coverage ≃ 0.45 ***Plot ratio ≃ 4.5***	**Pavilion**	**Court**	**Terrace**	**Tunnel-court**
Cut-off angle	θ=45º	θ=45º	θ=45º	θ=45º
Plan depth (m)	x=60	x=24	x=30	x=12
Number of storeys	n=10	n=10	n=10	n=10
Energy demand (kWh/m^2/year)	33	35	34	43
Energy Equity	0.39	0.37	0.38	0.32

Table 5.4 shows that with a constant urban density, pavilion has the best energy performance among the studied built forms. It not only has the lowest energy demand, but also the highest Energy Equity that shows its energy sustainability. Tunnel-court form shows the worst energy performance compared with the others of the same density. Terrace and Court built forms are ranked second and third, respectively. The main reason behind this is the greater plan depth of the pavilion built form (x=60m) with respect to the other cases in

Table 5.4. As discussed in section 5.2.1.1, buildings with greater plan depths has lower energy demand and higher Energy Equity.

It is notable that all the cases depicted in

Table 5.4 have cut-off angles of 45º and the only geometrical variable that changes their density is plan depth. However, the same density with the same built form can be achieved by changing the cut-off angle as well. In this case, if cut-off angle increases, plan depth must be decrease (and vice versa) to preserve density. Therefore, the same built form with the same density may have different energy performance depending on the geometry of the urban built area. Exemplar scenarios are shown in Table 5.5 for two court-built areas with similar densities.

Table 5.5: Exemplar scenarios for court built forms with similar densities but different geometrical variables and energy performance

	Site coverage	**Plot ratio**	**Cut-off angle**	**Plan depth** (m)	**Number of storeys**	**Energy demand** (kWh/m^2/year)	**Energy Equity**
Court 1	≃ 0.45	≃ 4.5	θ=45º	x=24	n=10	35	0.37
Court 2	≃ 0.45	≃ 4.5	θ=65º	x=12	n=10	44	0.29

It can be seen that although they both have the same density their energy performance is significantly different. The energy demand of the first case is 23% less than the second, while its Energy Equity is 24% higher than the second case. This is a considerable difference which shows the importance of geometry for achieving target densities. As discussed in section 5.2.1.5, a higher cut-off angle for a London climate leads to higher energy demands. The second case in Table 5.5 has a higher cut-off angle and smaller plan depth where both result in higher energy demand and lower Energy Equity. Therefore, a built form with the same density may acquire very different energy performance that must be taken into consideration for urban planning and policy making purposes.

In conclusion, urban energy planning can be set according to two different policies, as shown in Figure 5.19. Keeping the geometrical variable constant, tunnel-court built form is the most energetically sustainable built form for London because its ratio of renewable energy generation to total energy demand is the highest. For constant density scenario, pavilion built form is the most energetically sustainable for London because it not only conserves more energy in its envelope but also has a higher potential of renewable energy generation. In this scenario, opposite to that shown previously, the tunnel-court built form shows the worst energy performance.

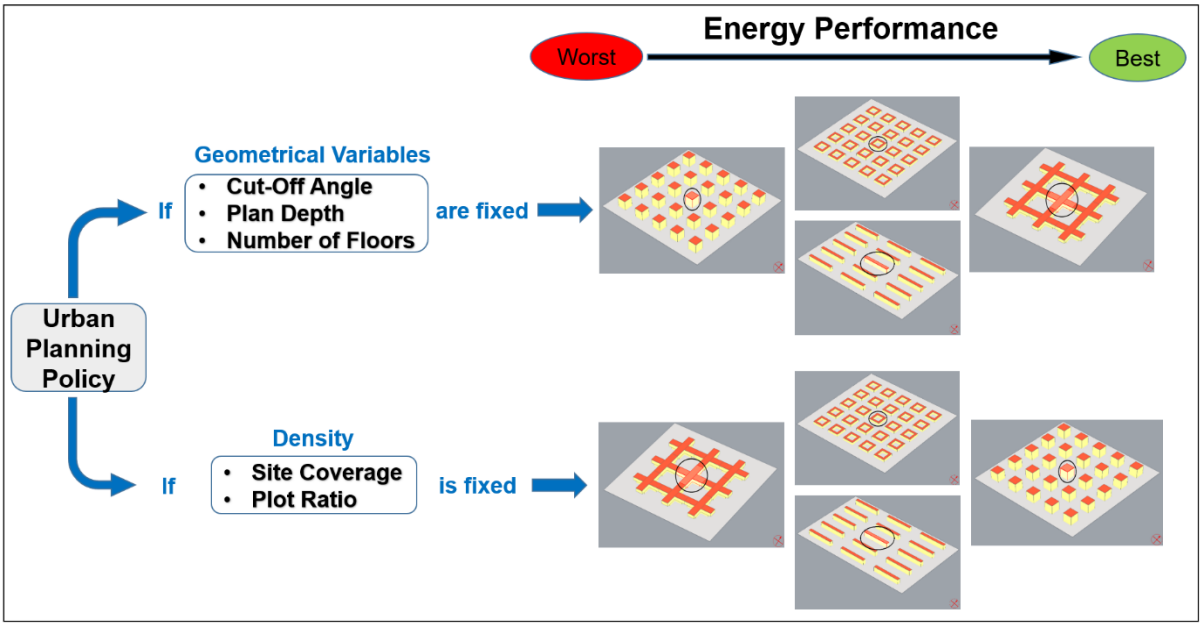

Figure 5.19: Ranking the energy performance of urban built forms according to two different urban planning policies for London climate

Therefore, the 'appropriate' or 'inappropriate' urban built forms for London climatic conditions depend on the policy targets.

The findings of this chapter provide urban planning guidelines and demonstrate the simultaneous correlation of urban geometrical variables and the two most popular density indicators. It provides the opportunity for urban planners to decide on the most energy-efficient built form and density following urban planning policies. If policy fixes one, two or all the geometrical variables, by looking at the *Form Signature* graphs and changing density in the permitted areas of the chosen graph (according to the policy), the most energy-efficient site plan with specific density can be selected. While if the policy fixes the density of the site plan, the most appropriate built form can be selected by changing geometrical variables.

5.3 Discussion and conclusion

This chapter proposes a novel urban energy planning tool to provide recommendations of the most appropriate energy-efficient built form and density for temperate climatic conditions. This is achieved by demonstrating the simultaneous correlation between building energy demand and PV energy generation with urban built form and density. Adaptation of the two popular urban density indicators shows the comprehensiveness of the analysis and fills a gap in the knowledge for making a comparison between results of similar studies.

The results of this chapter demonstrate that the high energy intensity areas of the relevant *Form Signature* graph for each cut-off angle are approximately similar. It shows the significant effect of plan depth and number of storeys on the trend of building energy performance. In all cases, buildings with lower number of storeys and plan depths provide worst-case scenarios regarding energy demand. These areas are indicated by a dark red colour on the *Form Signature* graphs that are normally equivalent to low plot ratios and medium to high site coverages. In contrast, buildings with greater plan depths and greater number of storeys are best-case scenarios for minimum energy demand—these areas indicated in dark blue on the graphs correspond to greater plot ratios, while the magnitude of their site coverage varies depending on the cut-off angle.

Cut-off angle impacts on the energy performance of urban built areas due to changing the factors such as shadowing and radiative interreflection between buildings in the form of both short and long wave radiation (CIBSE Guide F, 2012). The outcome of this study indicates that, lowering cut-off angle and having buildings further apart from each other reduces the heating consumption as compared with

cases with higher cut-off angles regardless of the built form. Lower cut-off angle means lower density as a matter of both site coverage and plot ratio. Hence, this is a counterintuitive example of the idea that denser built areas are more energy efficient than disperse areas. Nevertheless, this is true for built areas with temperate climatic condition (e.g. London) and cannot be generalised for other climates (this will be examined in Chapter 6). Another outcome relevant to the choice of cut-off angle is that the heating energy demand of buildings with larger plan depths is less sensitive to cut-off angle variations, while it is more sensitive to cut-off angle variations for small depth buildings. This is due to the larger space of the deep buildings that make their energy demand less influenced by the external environment.

The magnitude of heating energy demand compared to electricity demand for lighting and appliances is shown to be smaller in taller and wider buildings with higher surface to volume ratio. These results demonstrate the significant effect that urban built form and density have on heating energy demand and the negligible effect it has on electricity energy demand (assuming gas heating).

Conversely, if PV panels are considered to be installed on building roofs, as the most conventional renewable energy source being utilized in the built environment, the outcome differs. With the introduction of the concept of Energy Equity, it is shown that buildings with a lower number of storeys and greater plan depths have better energy performance due to their higher potential for solar energy harvesting. The red areas on the *Form Signature* graphs represent built environment with highest solar energy generation that provide a surplus of energy. In this case, the building harvests more energy than it demands, which can then be exported to the national grid or be stored to be used for purposes such as charging electric vehicles, heating domestic hot water or provision of electricity for the time of energy shortage (e.g. peak times). This area of the graphs corresponds to high site coverage and low plot ratio. Hence, the urban planning advice for increasing solar energy generation (and its ratio to energy consumption) in urban areas is ‘shorter and fatter’ buildings rather than ‘taller and narrower’. This is a logical outcome because greater plan depths provide bigger surface area on the building roof for installation of PV panels. Moreover, lower number of storeys means lower plot ratio and a smaller number of occupants that reduce energy consumption per building. Therefore, shorter and fatter buildings can easier facilitate achieving building energy self-sufficiency by making a balance between energy demand and supply of the building using the Energy Equity indicator.

A comparison of the relative energy performance of built forms with similar geometrical variables (Keeping the geometrical variables constant), indicates that terrace and court forms have the lowest energy demand followed by tunnel-court form, while highest energy demand is incurred by the pavilion form. On the other hands, when solar energy generation is considered in addition to building energy demand, tunnel-court form is the most energetically sustainable built form by virtue of having the highest value of Energy Equity. It is followed by terrace and court forms, while pavilion form shows the worst total energy performance.

Comparing built forms with similar density (keeping the density constant), pavilion is the most efficient and sustainable built form for London climatic conditions since it not only conserves more energy in its envelope, but also has higher potential of renewable energy generation. It is followed by terraced and court forms, while, in contrast to the previous scenario, tunnel-court form shows the worst energy performance by having not only the highest energy demand, but also the lowest Energy Equity. Furthermore, having the same density for any specific urban built form does not mean they necessarily have similar energy performance. It is possible to have two sites with the same built form and density, while their energy performances are different. This is because with different combinations of the geometrical variables the same value of density can be achieved. Therefore, it is highly recommended that to make a true comparison between the energy performance of different urban built forms, their urban density and geometrical variables must be analysed simultaneously.

As a result, when considering building energy performance, the ‘best’ and ‘worst’ urban built form for London climatic conditions can be either pavilion or tunnel-court built form, depending on urban planning policies.

This study has also shown that it is critical to use the terms ‘high density’ or ‘low density’ appropriately because it depends on the choice of density indicator. The use of *Form Signature* graphs shows the simultaneous change of two density indicators and demonstrate that in some areas corresponding to high values of site coverage have low values of plot ratio and vice versa. For instance, as discussed previously, areas of the graphs with high site coverage and low plot ratio represent built-up area with high solar energy potential. They can neither be called high density nor low density. It may be called high density as a matter of site coverage and low density as a matter of plot ratio. However, in general they should not be considered as either high or low density unless greater qualification is given. Therefore, before using those

terms, the choice of density indicator should be clearly interpreted to not only avoid confusion, but also facilitate decent comparison between different studies.

Chapter 6: Impact of climate on building energy performance and its correlation with urban built form and density

6.1 Introduction: The importance of design with climate

Another important element to be considered to precisely answer the research question of this thesis is climate, which is related to the geographical location of a city. It impacts on the magnitude and type of building energy demand and the potential of renewable energy generation, specifically solar energy in this case. It consequently influences the relationship of energy with urban form and density (Tsirigoti and Tsikaloudaki, 2018). For instance, the positive effect of the variation of a particular parameter such as density or sky view factor in one climate can act negatively for other climatic conditions (Morganti et al., 2012). Therefore, there is no one-size-fits-all answer to this research question. This makes it important to design buildings according to climatic conditions during initial first stages of the design process (Heidari, 2010). In fact, climatic variables must be known in order to predict the thermal behaviour of the building envelope (Oral and Yilmaz, 2003).

It was realized in the 1970s that common practices for building designs were not effective without including the specific effects of climate. However, in contemporary designs and with the use of mechanical equipment (e.g. air conditioning system) to providing satisfactory thermal conditions, even less attention has been paid to climatic conditions. Built forms are therefore often very similar in every corner of the world regardless of climate showing that human is losing the skills to design with climate. More recently, with more focus on sustainability (which was the consequence of Climate Change), we have begun to seriously consider climate conditions for achieving sustainable building/urban designs. Dursun and Yavas (2015) emphasized that to have a sustainable urban development, a climate-sensitive urban design guideline is urgently needed for their case study in cold climates. Their findings show that the urban built environment should be consistent with climatic conditions. Muhaisen (2006) suggested general rules and guidelines for efficient design of courtyards in four different climatic regions. Kocagil and Oral (2015) showed that building form and settlement texture are influential parameters for heating and cooling loads of buildings in a hot-dry climate zone in order to provide optimum conditions. Khalili and Amindeldar (2014) identified that traditional courtyards have emerged in

the hot-arid regions of Iran to reduce the detrimental aspects of the climate. This built form provides better microclimatic conditions for occupants and is considered as a low energy consumption building form. Strømann-Andersen and Sattrup (2011) described that in northern European cities with high latitudes and associated low solar inclinations, urban density is of particular concern since urban geometry affects solar access much more here than in other urban centers around the world. Wong et al. (2011) assessed the effect of the air temperature variation in urban conditions on the building energy consumption in the tropical climate of Singapore and emphasized that outdoor air temperature can determine the energy savings of buildings. It is well established in the Subtropical Design Handbook (Kennedy, 2010) that the region's climate-derived character is advantageous to develop low-energy urban forms and innovative low-energy buildings. It specifically suggests an open and permeable built environment for the subtropical region in Australia.

Therefore, climate not only influences building energy demand but also determines suitable built forms and density of urban areas. Although previous studies have investigated the impact of climate on building energy demand and the suitability of urban forms independently, few have considered the impact of climate on the correlation of energy with urban built form and density. In this chapter, three case studies from different climate zones are considered in addition to the London case study (see Chapter 5) to identify the impact of climate on this correlation. For each case, the correlation of building energy performance with urban geometric parameters and two density indicators are empirically investigated based on the *Form Signature* graphs (developed in Chapter 3, section 3.5.3), while the specific impact of cut-off angle is examined separately. Then, the energy performance of the four selected built forms; pavilion, terrace, court and tunnel-court (as examined in Chapter 5) are compared in each of the climatic zones. At the end of the chapter, the data from all case studies are aggregated to provide a comparison of the energy performance of the four built forms in the different climates. This analysis also demonstrates the practicality of the tool proposed in Chapter 3 to be adopted for different climates.

6.2 Case study selection and analysis

To investigate the impact of climate on building energy demand and the potential for solar energy harvesting, other case studies from different climatic conditions are

selected using the Köppen climate classification system (also known as the Köppen–Geiger) (Peel et al., 2007). It divides the earth into five main zones as follows:

- Group A: Tropical (mega thermal) climates
- Group B: Dry (arid and semiarid) climates
- Group C: Temperate (mesothermal) climates
- Group D: Continental/cold (microthermal) climates
- Group E: Polar and alpine (montane) climates

Each zone is sub-divided into several subcategories that are classified by two or three letters as an abbreviation, where each of them indicates a specific criterion (Peel et al., 2007). Each case study region is selected to represent one of the main climate zones. London (Cfb: Temperate-Without dry season-Warm summer) has already been selected from group C. Three other large metropolitan cities with great populations and large energy consumptions are selected based on their diverse climatic conditions. In this case Singapore (Af: Tropical-Rainforest) represents group A, Phoenix (Bwh: Arid-Desert-Hot) represents group B and Helsinki (Dfb: Continental-Without dry season-Warm summer) represents group D. This study does not find any necessity to analyse a city from polar and alpine climate (group E) due to two reasons. Firstly, there are no large metropolitan urban areas in these parts of the earth to be investigated. Secondly, the outcome would be identical to continental cold climate (i.e. Helsinki case study) with similar (but sharper) trends. Therefore, this climate category is disregarded in this study. Notably, all selected cities include both high and low-density districts as well as inner-city and suburbia.

Similar to the analysis undertaken for the London case study in Chapter 5, the simulation method is adopted for energy analysis of the other cities in this chapter. The same number of site plans of buildings for each built form (pavilion, terrace, court and tunnel-court) are obtained by changing the geometrical variables, which then fed into CitySim to develop energy simulation models (as described previously in Chapter 5).

In practice, the physical characteristics of a building envelope are influenced by the climatic conditions. Parameters such as building material, glazing ratio and walls/windows U-values may differ in different climates. However, in this study, in order to be consistent in all case studies and to focus the study on the impact of climate on the built form, density and building energy demand, these parameters are kept

constant for all climatic zones. Additional input data such as infiltration rate, occupant density and room setpoint temperature are also kept self-consistent. In this case therefore, values chosen for above-mentioned parameters are the same as what was previously considered for the London case study (see section 5.2.1.1 of Chapter 5). The only input data for the simulation that is variable for different case studies is the heating/cooling period considered for energy simulations. This factor is the direct offspring of the climate that must be varied for different climates. Climate can significantly change the balance between heating and cooling demand of urban blocks (Tsirigoti and Tsikaloudaki, 2018). The method for identifying this factor is separately explained for each case study. Climate files of each of the three selected locations is derived from Meteonorm (which contains nine different climatic parameters as explained in section 4.2.2 of Chapter 4).

6.2.1 Tropical hot and humid climate (Singapore)

Here, the geographic and climatic conditions of the metropolitan City of Singapore are used as the case study. Singapore is an equatorial city with a hot, humid and rainy climate, located in the latitude of 1.3521° N and longitude of 103.8198° W, with a population of 5,875,857 people (World Population Review, 2020d).

Energy consumption of buildings contribute about a third of Singapore's total electricity production (Chua and Chou, 2010). The Building and Construction Authority of Singapore encourage 80% of the residential built area to use passive design strategies (GM RB, 2016). However, the energy performance of a building is measured according to the efficiency of active mechanical and electrical systems (GM RB, 2016).

In Singapore, the average temperature during the day and the night is almost constant throughout the year. Therefore, buildings require only cooling related energy consumption all year round, with no heating energy needed (Chua and Chou, 2010). In tropical climates, heat gain and cooling loads are critical elements of a building's energy performance (Ng et al., 2013). The indoor operative temperature should be maintained within 24 ºC and 26 ºC (SS 553, 2009). To be consistent with London case studies, the maximum setpoint temperature is considered 24 ºC for the Singapore case studies. For CitySim simulations only cooling periods are implemented for the whole year, while the heating period is eliminated. The annual cooling energy consumption in Singapore is defined as the annual electrical energy consumption of the air-conditioning system (Chua and Chou, 2010). Cooling energy is considered to be

supplied by a heat pump in the simulations for this case study. Therefore, it increases the total electricity consumption of buildings, though it is independently calculated from the electricity consumption of home appliances.

6.2.1.1 *Form Signature* graphs for Singapore

Simulations trials are undertaken for different site plans by changing the number of storeys, plan depth and cut-off angle, as explained in section 5.2.1 of Chapter 5 and schematically shown in Figure 5.2, Figure 5.7, Figure 5.9 and Figure 5.11. It includes 216 simulation trials and the resulting values, which are the yearly energy demand per m^2, are used to develop the relevant heat maps on the *Form Signature* graphs, as shown in Figure 6.1.

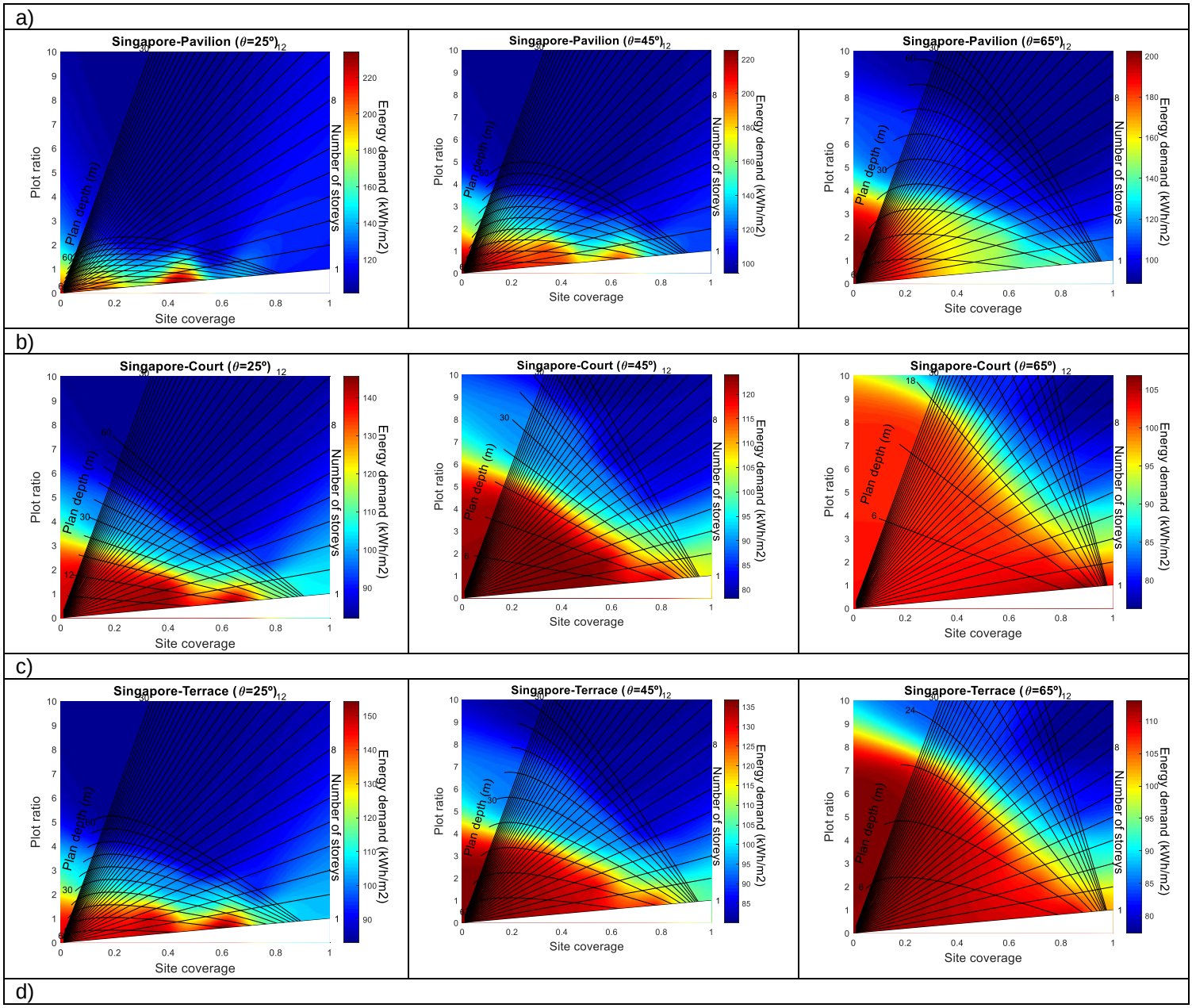

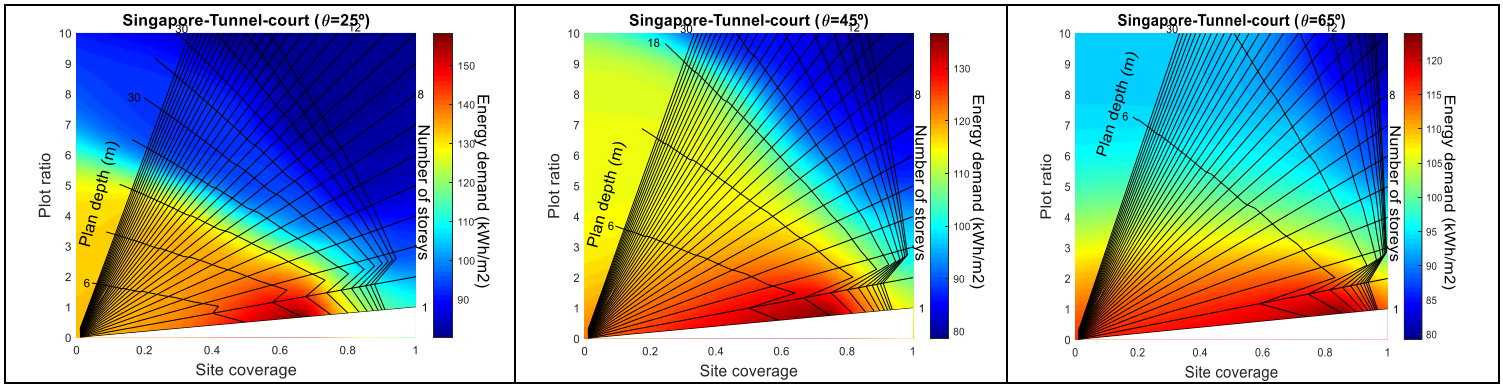

Figure 6.1: Correlation of building energy demand with urban built form and density for Singapore case study a) pavilion b) court c) terrace d) tunnel-court built forms

The graphs shown in Figure 6.1 show the magnitude of building energy demand with respect to the change in density and geometric parameters of each urban built form. The highest energy demand, shown in dark red, belongs to the buildings with a lower number of storeys and smaller plan depth for court/tunnel-court forms (e.g. one-storey building with 12m depth), while it corresponds to higher number of storeys and smaller plan depths for pavilion/terrace forms. This is equivalent to low values of plot ratio, while the magnitude of site coverage varies depending on the cut-off angle. Building energy demand gradually decreases by increasing the number of storeys and plan depth. This reduction continues to reach its minimum value for court and tunnel-court forms. However, in pavilion and terrace forms increasing number of storeys causes a slight increase in energy demand in high-rise buildings with more than 20 storeys. Therefore, increasing site coverage is beneficial in all cases as a matter of energy efficiency, while the plot ratio should be increased with some caution. Specifically, increasing plot ratio is always efficient for court and tunnel-court forms, but should only be increased in conjunction with site coverage for pavilion and terrace forms.

The results emphasize the importance of urban density and geometrical parameters on building energy demand in this climate. For instance, the highest energy demand of a terrace building (with θ=45º) in this analysis is around 160 kWh/m^2/year, while it is only 80 kWh/m^2/year for the most efficient building with 30 storeys and plan depth of 60m. It shows 100% change in energy demand of buildings with the same form but different density, number of storeys and plan depth. This variance could be greater if the cut-off angle is also changed (addressed in section 6.2.1.2). The numbers attained in this analysis are in the range of the values presented by similar studies. Shabunko et al. (2018) obtained values ranging from approximately

69 to 47.8 kWh/m^2 for the benchmarking of residential buildings in Brunei Darussalam, which has a similar climate with Singapore. Lam et al. (2001) obtained numbers between 179 and 187 kWh/m^2 for office buildings in Singapore, which normally demands higher energy than residential buildings due to the consumption of office equipment, pumps and vent fans that are not considered in this study.

Simulations trials considering the addition of roof-mounted PV energy harvesting allows values of *Energy Equity* to be calculated and used to show the correlation of building solar energy potential with urban built form and density—see Figure 6.2.

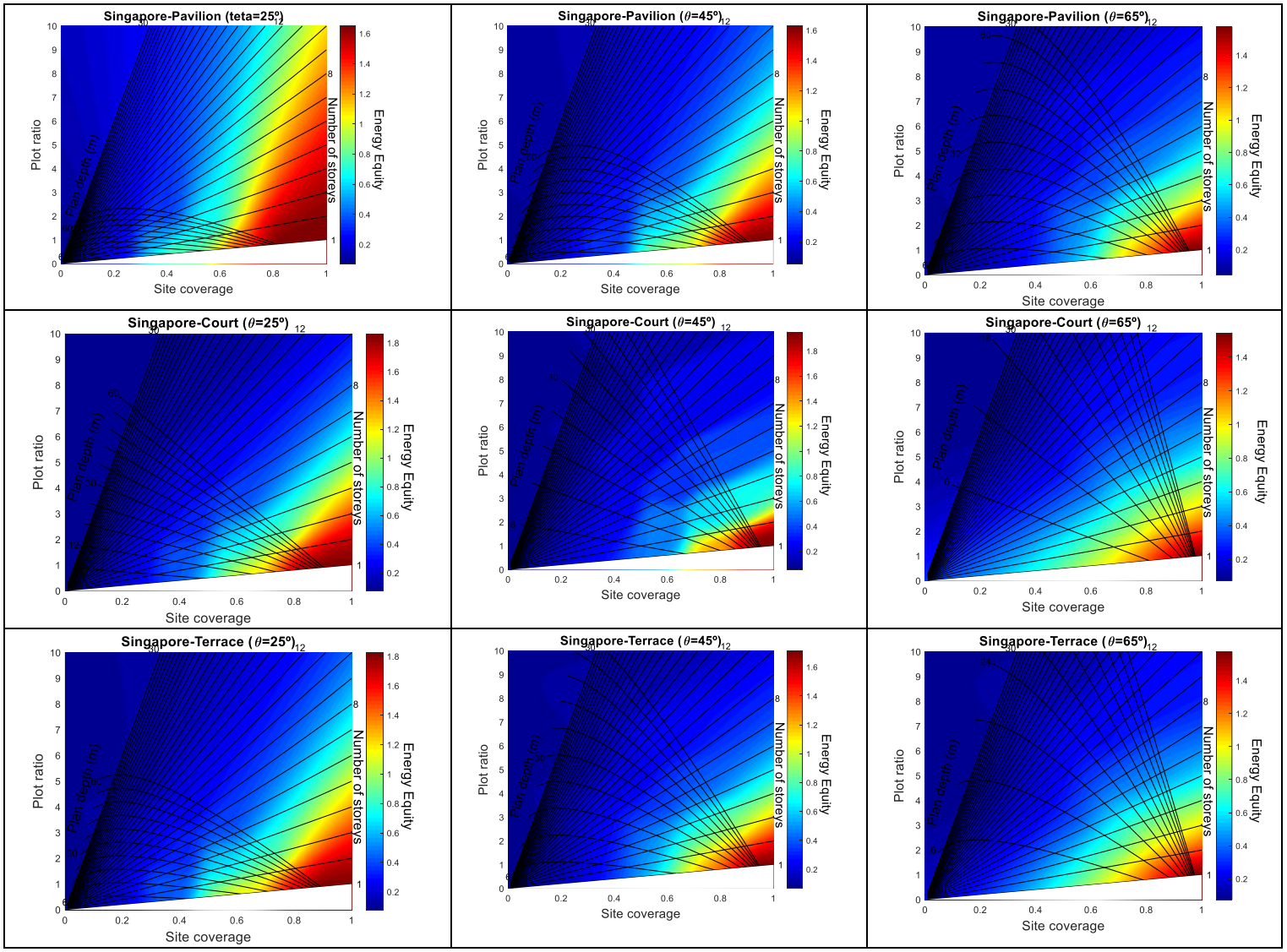

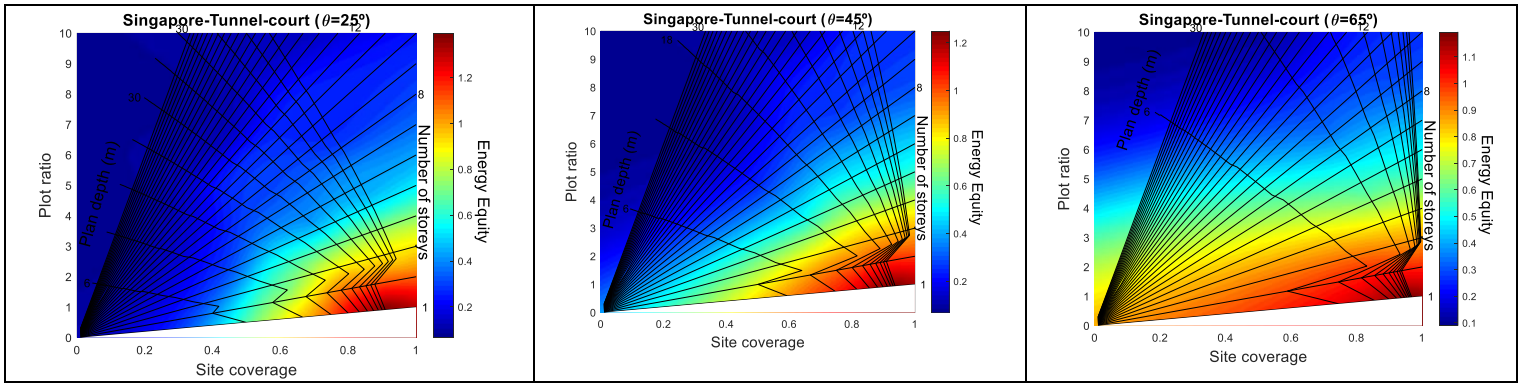

Figure 6.2: Correlation of Energy Equity indicator with urban built form and density for different built forms for Singapore case study

From Figure 6.2, for all built forms, it can be seen that buildings with a lower number of storeys and greater plan depths acquire a higher potential for PV generation. The reason is larger roof areas and lower energy demand per m^2 which allows the Energy Equity ratio to attain values greater than one (the dark red color in the plots). This is equivalent to having high values of site coverage and low values of plot ratio. In a comparison of case studies, the intensity of sunshine in Singapore is undoubtedly much higher than London. Therefore, it is assumed that buildings in Singapore should more readily reach a state of self-sufficiency than in London. However, this may not be the case as the amount of energy demand in Singapore is higher due to the large amount of cooling load expected in buildings. This will be extensively discussed in section 6.3.

6.2.1.2 Impact of cut-off angle in the Singapore climate

To investigate the impact of cut-off angle on building energy demand, building plans composed of similar buildings but different cut-off angles are compared and the results for different built forms collected, and summarised in Figure 6.3.

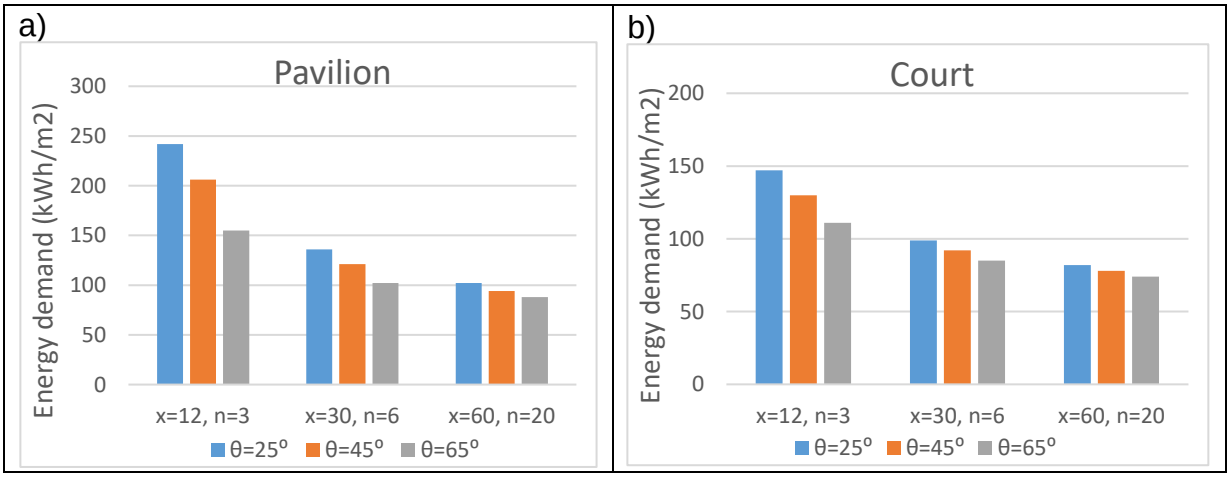

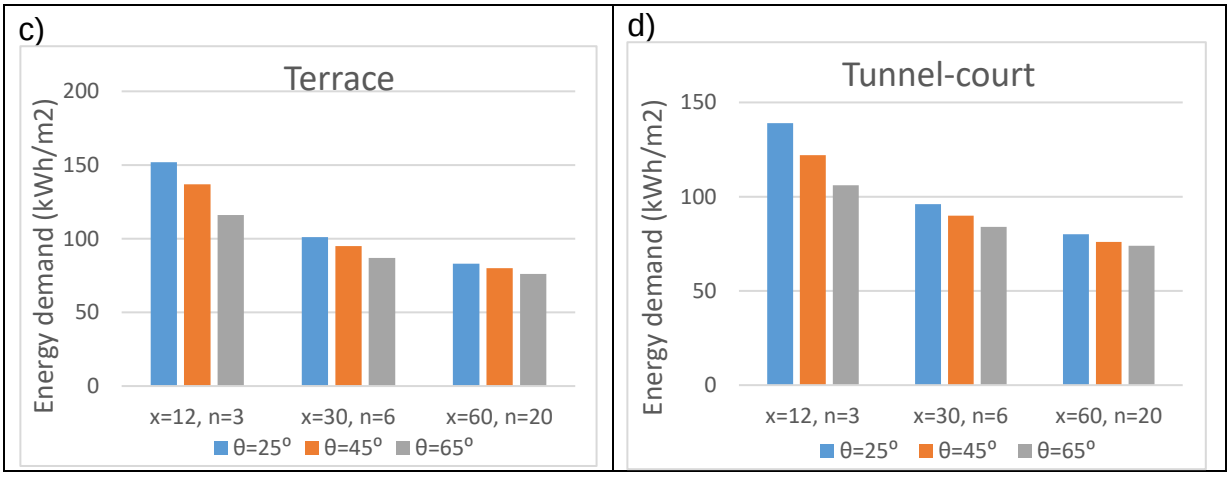

Figure 6.3: Impact of cut-off angle on building energy demand for different built forms in Singapore

The results show that, regardless of the built form and other geometric parameters, increasing cut-off angle reduces building energy demand for the Singapore climate. Changing the cut-off angle from 25º to 65º can diminish building energy demand from approximately 8% to 56% depending on the plan depth. This reduction is more significant in buildings with small plan depth (e.g. x=12m) and minor in buildings with deep plans (e.g. x=60m).

Increasing cut-off angle means reducing the distances between buildings that resulted in increasing both density indicators, site coverage and plot ratio. Therefore, higher density reduces building energy demand in the Singapore case. This result is exactly the opposite to the conclusions obtained from a similar analysis for London detailed in Chapter 5 (section 5.2.1.5); emphasizing that the impact of urban density on building energy demand definitely depends on the climate and geographical location.

The reason behind the results of this comparison is that the energy demand in London is due to heating while it is cooling in Singapore. By increasing the cut-off angle the buildings become closer and therefore they become more shielded from solar irradiation. The shadowing effect of adjacent buildings reduces solar heat gain that consequently decreases the cooling energy requirement of a building (Chan, 2012, Nikoofard et al., 2011, Numan et al., 1999). This is also emphasized by Wong et al. (2011) discussing that increasing surrounding buildings heights reduces the cooling load in this climate. It can also change the micro-climatic condition around the buildings that slightly cools down the temperature around the building envelope, which causes lower heat transfer from the walls.

6.2.1.3 Energy performance of different built forms in Singapore

To analyse the energy performance of buildings with different built forms but similar geometrical parameters, the data obtained from energy simulation trials are compared and shown in Figure 6.4.

a)

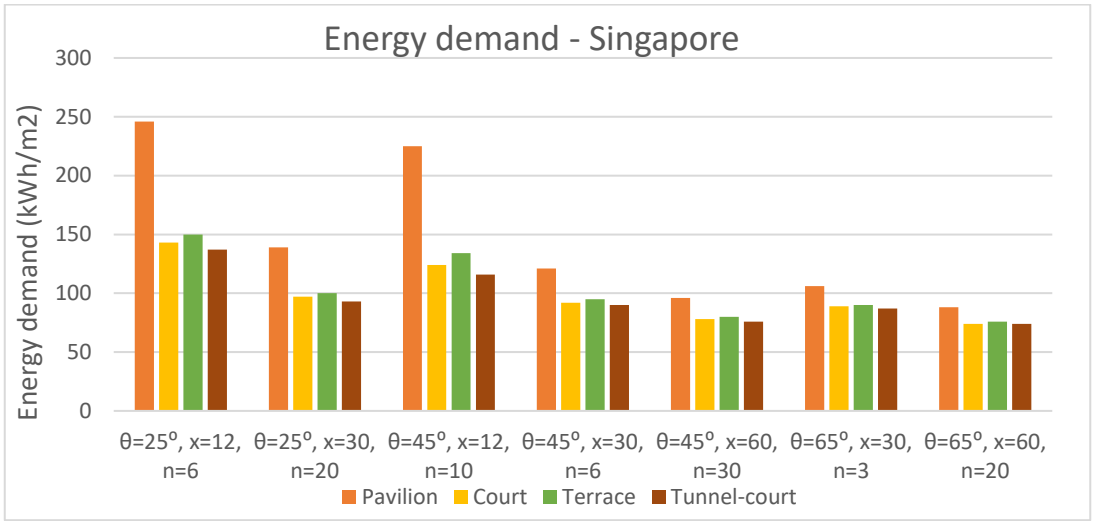

b)

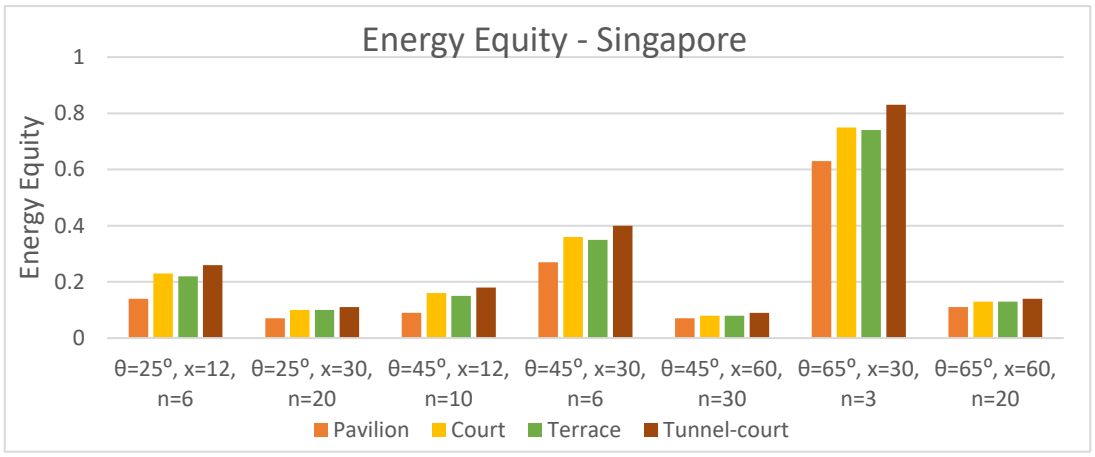

Figure 6.4: Comparison of building energy performance of the studied built forms with the same cut-off angles, plan depths and number of storeys in Singapore a) energy demand b) Energy Equity

Two separated diagrams are presented in Figure 6.4 showing (a) energy demand and (b) Energy Equity for the different built forms. It can be observed from Figure 6.4 (a) that the energy demand of pavilion form is the highest while tunnel-court form shows the lowest energy demand. Court and terrace forms are in the middle with court form being the lower of the two. This difference in their energy demand is because i) they have different surface to volume ratios, as shown in Chapter 3 (section 3.4), that results in a different amount of envelope energy loss, and ii) the different built forms (shapes) create incurred different degrees of shadowing effects on the external walls and protect the building from intense sunlight, which is valid for court and tunnel-court

forms that have lower cooling loads. Finally, although their geometric variables are similar, their urban densities are different (see Table 6.1).

Figure 6.4 (b) shows that tunnel-court form possesses the highest Energy Equity, while pavilion shows the lowest value. Again, court and terrace forms are placed in the middle. These results demonstrate that tunnel-court form has the highest potential for PV harvesting with respect to its energy demand, and is therefore the most sustainable built form (when keeping geometric variables constant) for Singapore's climate, and can readily attain energy self-sufficiency.

It should be noted that having similar geometries does not necessarily mean that they all deliver the same urban density. Table 6.1 shows the contrasting values of site coverage and plot ratio for the studied built forms with similar geometrical variables.

Table 6.1: Comparison of density and energy performance of different built forms with similar geometric parameters

θ=45⁰, x=60, n=10	**Pavilion**	**Court**	**Terrace**	**Tunnel-court**
Site coverage	0.444	0.667	0.632	0.889
Plot ratio	4.444	6.667	6.32	8.593
Energy demand (kWh/m^2/year)	94	80	81	78
Energy Equity	0.21	0.25	0.25	0.27

This is just an exemplar case from the data obtained in the analysis, which is valid for all the other cases. It can be seen that pavilion form acquires the lowest density, while tunnel-court form acquired the highest density. This shows the advantageous characteristic of tunnel-court form that is able to deliver the highest density (in both density indicators considered here). This is one of the reasons that it has the lowest energy demand, which is 78 kWh/m^2/year in this example. Hence, it demonstrates that higher urban density is more energy efficient in Singapore's climate, though other factors such as the built form itself are influential too.

This comparison emphasizes that the similarity of geometrical parameters shall not be confused with the similarity of urban density. In the case of keeping density constant but with the geometric parameters of the built forms varied, an opposite ranking of built forms can be observed when considering energy performance—this has been extensively discussed in section 5.2.4 of Chapter 5 (See Table 5.5).

6.2.2 Hot and arid climate (Phoenix)

Here, the geographic and climatic conditions of the metropolitan City of Phoenix as the capital of the state of Arizona in the USA is used as the case study. This is representative of a hot and arid climate. It is located in the latitude of 33.4484° N and longitude of 112.0740° W, with a population of 1,703,080 people (World Population Review, 2020c).

Phoenix has a long, hot summer and short, mild winter that means the main portion of total building energy demand comes from cooling loads. It is one of the sunniest cities in the world with approximately 300 days of sunshine per year and the intensity of sunshine is very high due to its desert location. It makes this city a suitable candidate for the study in this thesis since the potential of PV energy harvesting in cities is being considered.

Looking at historical climate data for Phoenix (U.S. Climate Data, 2021) and following information provided by authors of previous studies on this city (Guhathakurta and Williams, 2015, Sailor et al., 2012), the typical building cooling period is considered to be from April to October and the heating period from November to March. The high percentage of the total cooling load is consumed in May-September, while there is smaller demand in the shoulder months of April and October. Also, the main heating load is demanded between December and February, while relatively small heating loads are demanded between November and March. In this study, all the above-mentioned periods (including shoulder months) are considered for the building energy simulation trials for two reasons i) due to the desert location of the city, there is normally a substantial change in temperature between daytime and nighttime (although this fluctuation is slightly mitigated as a result of the Urban Heat Island effect). This diurnal variation imposes energy demand in either day or night-time of the shoulder months. The thermal behavior of the hot-dry climate is very distinctive due to wide daily and seasonal fluctuations (Kocagil and Oral, 2015). ii) it is then better to compare with the Singapore case study which has a full 12 months of energy analysis. Phoenix and Singapore both have a hot climate, however, they possess considerably different climatic conditions that create distinctly different human feeling and building energy requirements. Therefore, to reach the human comfort zone, different strategies should be adopted. Singapore requires 12 months of cooling while Phoenix requires seven months of cooling and five months of heating. Hence,

although 12 months of energy simulation is considered for both, their comparison is expected to deliver different results (section 6.3).

6.2.2.1 Form Signature graphs for Phoenix

Similar to the previous case studies, simulations trials are undertaken for a variety of site plans (but using climate and horizon files of Phoenix) and the results are overlaid as a heat map on the Form Signature graphs, as shown in Figure 6.5.

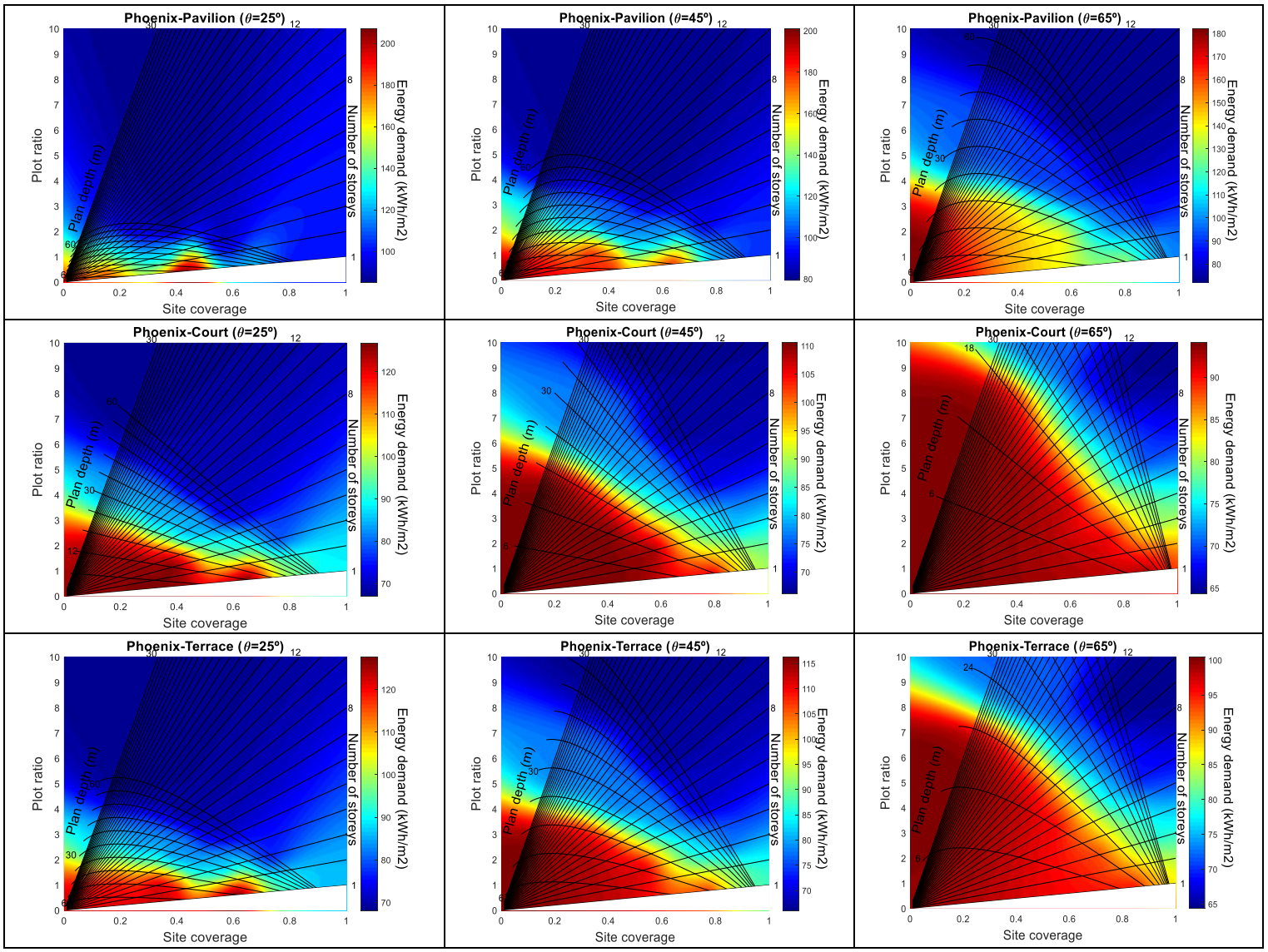

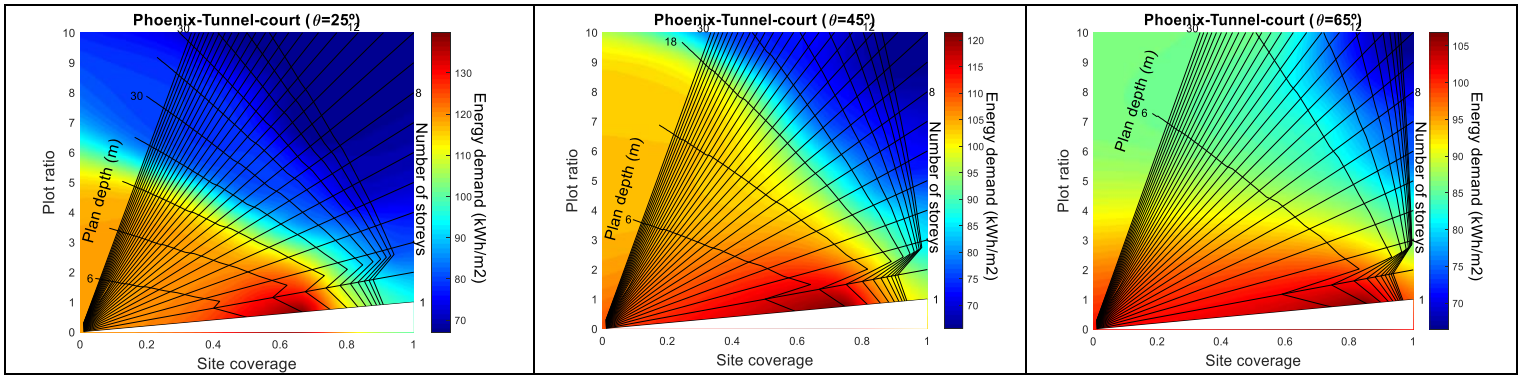

Figure 6.5: Correlation of building energy demand with urban built form and density for different built forms for Phoenix case study

It can be seen from Figure 6.5 that the trend of changing building energy demand on the *Form Signature* graphs of Phoenix is similar to the Singapore case (Figure 6.1). The reason is that the energy demand of buildings in Phoenix is cooling dominated. Accordingly the cooling energy demand of a building in Phoenix is at least seven times higher than its heating demand (see section 6.2.2.4). Therefore, the same arguments (as Singapore case) governing the correlation of building energy demand with density indicators and geometric variables also apply here (see descriptions of section 6.2.1.1). Javanroodi et al. (2018) also concluded that higher site coverage results in a reduction of building cooling load in hot-arid climates.

Nonetheless, the absolute values of building energy demand are different from Singapore case study. For instance, the highest energy demand of a terrace building (with θ=45º) for Phoenix is around 130 kWh/m^2/year, while the lowest energy demand is only 66 kWh/m^2/year for the most efficient building with 30 storeys and 60m plan depth. Although this is ~100% difference in energy demand of buildings with the same built form but different density, number of storeys and plan depth, the absolute values are, on average, 18% lower than values obtained for the Singapore case. This will extensively be discussed in section 6.3.

By considering roof-mounted PV energy generation for simulations, the values of Energy Equity are calculated and used to show the correlation of building solar energy potential with urban built form and density, as shown in Figure 6.6.

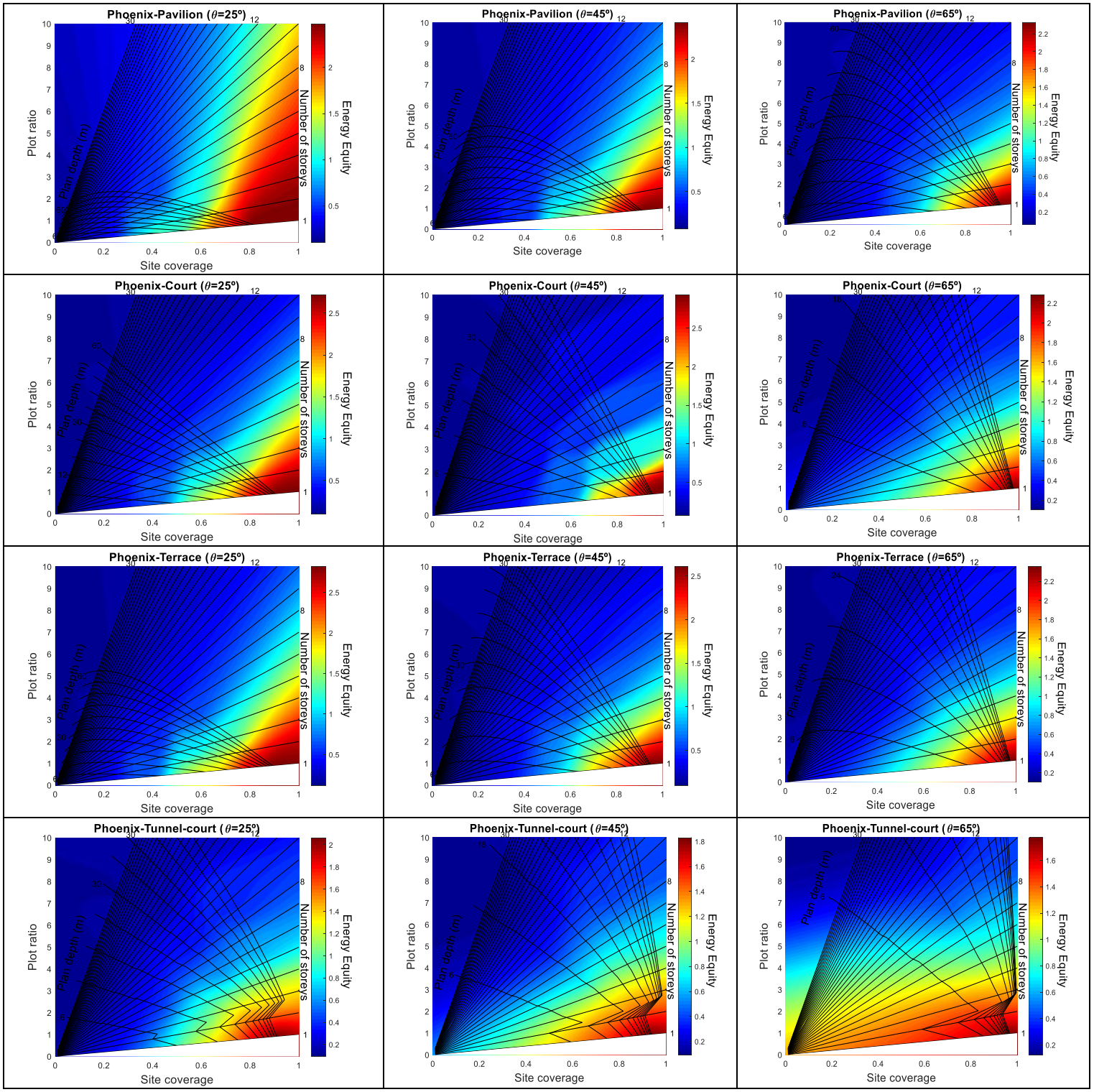

Figure 6.6: Correlation of Energy Equity indicator with urban built form and density for different built forms for Phoenix case study

Figure 6.6 show that similar to London and Singapore, buildings with lower number of storeys and greater plan depths acquire greater potential for PV generation that corresponds to high values of site coverage and low values of plot ratio. Comparing Phoenix and Singapore, both with hot climates, the former achieves significantly higher values of Energy Equity due to the fact that i) the solar energy generation is

greater in Phoenix due to its longer and more intense sunlight during the year, and ii) the yearly energy demand of Phoenix is smaller because buildings require lower cooling load. A full summary comparison of the case studies will be made in section 6.3.

6.2.2.2 Impact of cut-off angle in Phoenix climate

The influence of cut-off angle on building energy demand for different built forms in Phoenix are analysed and compared for several cases in Figure 6.7.

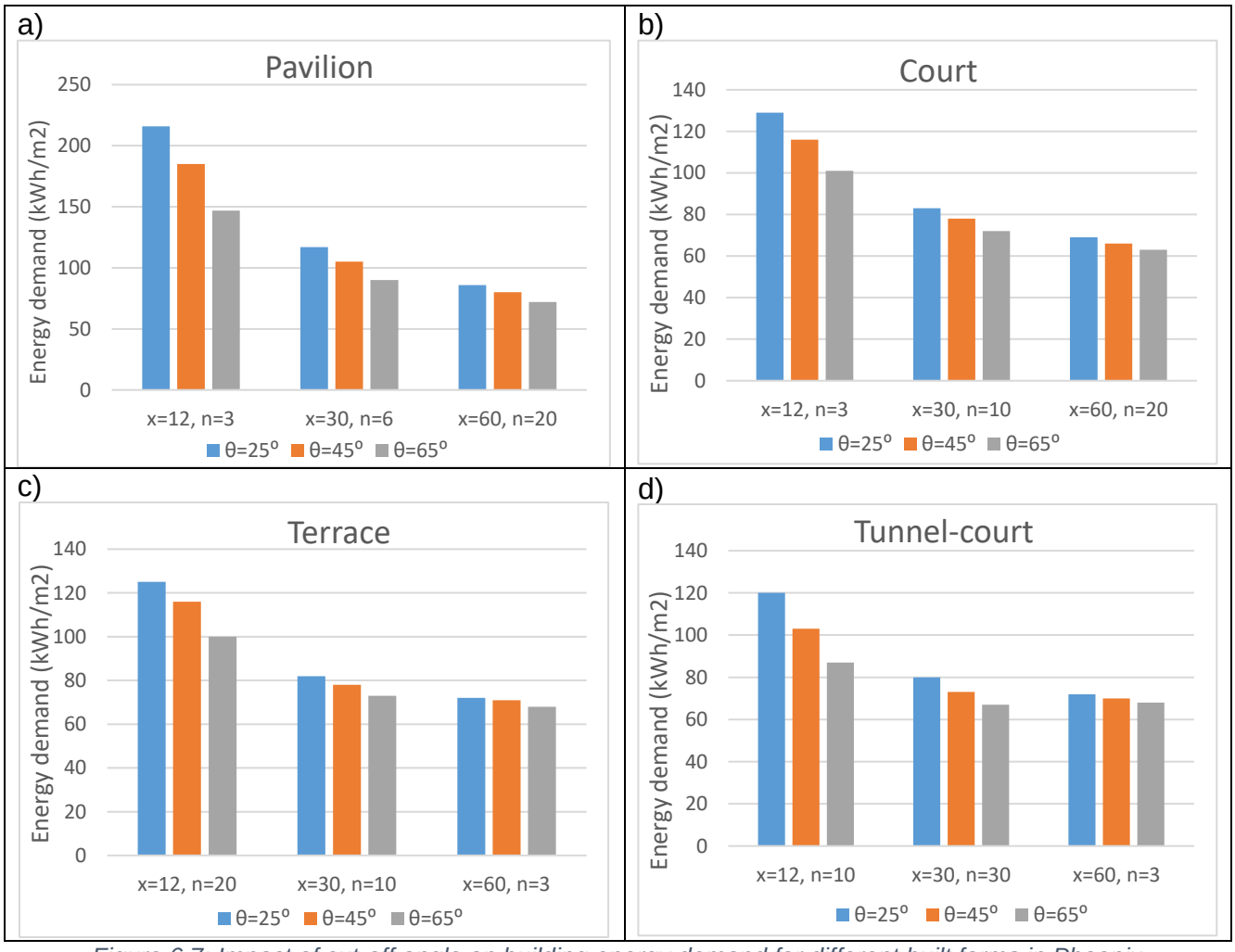

Figure 6.7: Impact of cut-off angle on building energy demand for different built forms in Phoenix

Figure 6.7 shows that increasing the cut-off angle in Phoenix climatic conditions leads to a reduction in building energy demand. It means that higher urban density is advantageous for hot-arid climates. It reflects the fact that a lower distance between buildings protects them from intense solar radiation that results in lower cooling energy demand in this climate. Similarly, Coccolo et al. (2013) discovered that stand-alone buildings in hot-arid climate of United Arab Emirates need 5% more cooling energy. This is also in line with the urban planning recommendation for the city of Cairo (with

hot-arid climate) that use an indicator called *building height/lane width* ratio (La rédaction, 2019). Higher values of this ratio are recommended for this climate, which is equivalent to higher values of cut-off angle in this study.

This outcome is also similar to that for Singapore (see Figure 6.3) but opposite to the results from London case study analysis (see Chapter 5, section 5.2.1.5). This is because the buildings in Phoenix are cooling-dominated similar to Singapore and unlike London that require heating load. However, the trend of this reduction is not as pronounced as for Singapore due to the fact that the buildings in Phoenix demand heating load in wintertime, while cooling is required for buildings in Singapore all year round. This heating load is the element that mitigate the sharpness of this trend. The data obtained in this study shows that by increasing cut-off angle, heating load increases while cooling load decreases. Changing cut-off angle from 25º to 65º can reduce building energy demand between approximately 6% and 47% (depending on the plan depth) comparing to Singapore that is between 8% and 56%. This shows the mitigating effects of the heating load presented in the Phoenix case study. This reduction is still more significant in buildings with small plan depth compared with buildings with deep plans.

6.2.2.3 Energy performance of different built forms in Phoenix

To compare different built forms with similar geometrical parameters, their building energy performance data are classified, and the several cases are presented in Figure 6.8.

a)

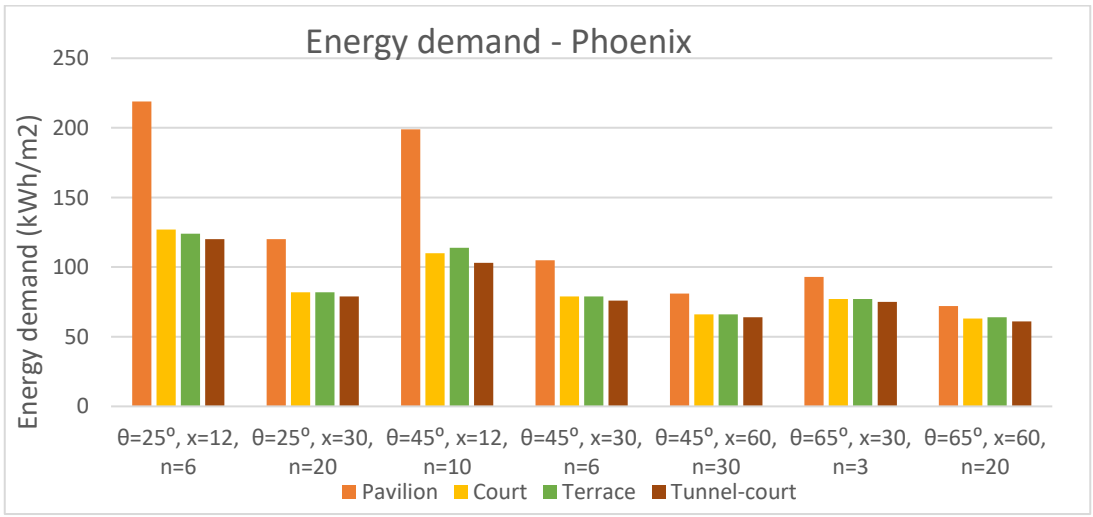

b)

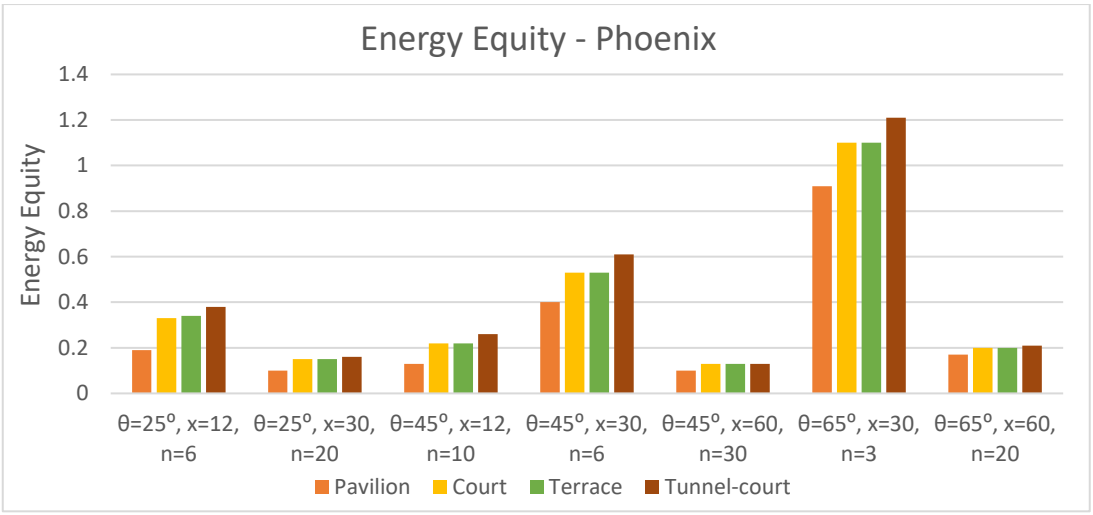

Figure 6.8: Comparison of building energy performance of the studied built forms with the same cut-off angles, plan depths and number of storeys in Phoenix a) energy demand b) Energy Equity

From Figure 6.8 it is observed that the comparative performance of the studied built forms is similar to the Singapore case study (see Figure 6.4). Among the selected built forms, tunnel-court form not only has the lowest energy demand, but also obtains the highest Energy Equity values. It explicitly demonstrates that when keeping geometrical variables constant, this is the most energy efficient built form for Phoenix. In contrast, pavilion shows the weakest performance. Court and terrace built forms are in the middle with very similar performance. This is similar to the London case, while in Singapore court form performs better than terrace form. The reason behind this ranking of built forms is fully explained in section 6.2.1.3.

Suitable energy performance of court form has been shown by Soflaei et al. (2017) who confirmed that courtyard houses in hot-arid climate regions of Iran provide a successful sustainable design compatible with climate requirements as well as socio-cultural aspects. Traditional courtyards can provide a more compact urban fabric along with passive cooling and heating strategies that reduce cooling and heating load of buildings in this climate. Heidari (2010) also considered courtyards as the best building form in the desert climate. The only built form in Figure 6.8 that affords better energy performance than the court form is the tunnel-court form. The reason is the similarity in the shape of these two built forms where both contain an inner yard, and their difference is the connectivity of tunnel-court form with respect to court. This appears to provide better building performance, however, since this type of built form is newly introduced in this study, there are no traditional examples to show its energy performance. Inspired by this study, this built form can be considered for future urban

developments as an energy efficient and environmentally sustainable alternative to more traditional solutions.

The analysis and conclusions for section 6.2.1.3 (see Table 6.1) regarding distinguishing between constant density and constant geometric variables are also valid for this case study.

6.2.2.4 Cooling vs. heating energy demand

Since Phoenix is the only case study that includes both heating and cooling energy simulations, the impact of the ratio of these two loads is now investigated. The analysis has indicated that cooling loads are considerably greater than heating loads, which is a tangible result due to the climatic conditions of Phoenix. In general, however, both cooling and heating loads can be reduced by increasing the number of storeys and plan depth. This has an exception in pavilion and terrace forms where the cooling load, after a sharp decrease up to 10 storeys, begins to slightly increase for buildings with a higher number of storeys. However, this is only noticeable with small plan depths and low cut-off angle. Furthermore, by increasing the cut-off angle, heating and cooling loads increases and decreases, respectively.

To make further investigation, the ratio between the two types of loads is analysed using Eqn (6.1):

$$6.5 \leq \frac{Cooling\ energy\ demand}{Heating\ energy\ demand} \leq 22.5 \qquad (6.1)$$

It can be seen that the minimum (6.5) and maximum (22.5) values are considerably different from each other and the range is more than a factor of three. It highlights the significant influence of built form and density on this ratio. The highest values belong to pavilion form with small plan depth and low cut-off angle, while the lowest values belong to tunnel-court form with small plan depth and high cut-off angle. The ratio decreases with increasing cut-off angle due to the impact of cut-off angle on cooling and heating demand (see section 6.2.2.2). The impact of plan depth on this ratio depends on the cut-off angle with greater plan depths resulting in higher values when the cut-off angle is small, while this correlation is the opposite when the cut-off angle is big.

6.2.3 Continental cold climate (Helsinki)

Here, the geographic and climatic conditions of the metropolitan City of Helsinki are used as the case study, which is a member of the cold climate category. It is the

capital city of Finland, located in the latitude of 60.1699° N and longitude of 24.9384° W, with a population of 1,304,851 people (World Population Review, 2020a).

To define the heating and cooling seasons in Helsinki, previous studies and organizational documents are investigated. Kalamees et al. (2012) modified EN ISO 15927-4:2005 method and proposed to divide a year into three periods as winter/heating period (November, December, January, February), summer/cooling period (May, June, July, August) and spring–autumn/intermediate period (March, April, September, October). Jylhä et al. (2015) also divided a year into three seasons for building energy analysis, although they classified the months with some differences from the study by Kalamees et al. (2012). Their seasons include the major heating season (November, December, January, February, March), the cooling season (May, June, July, August) and the intermediate season (April, September, October). Meanwhile, the Finnish Energy association (Finish Energy) defines the heating season from the first day of October to the last day of April, while the rest of the months are simply called non-heating season. A document published by Scottish government (Shearer and Anderson, 2008) defined the heating season of Nordic countries from September to May for non-domestic buildings, while the graphical results by Jung et al. (2018) show that the main heating load of energy-efficient buildings is demanded from October to April (with small heating demand in September and May), while the main cooling load is demanded in June, July and August. However, office buildings were considered in their study and not residential buildings. In the report provided for the ENTRANZE Project (Zangheri et al., 2014) which investigates heating and cooling energy demand and loads for different building types in different countries of the EU, the data related to the domestic sector of Helsinki shows the main heating load is demanded between October and April (with small demand in September and May), while it shows a small amount of cooling demand only in August. Acknowledging the above studies and to be consistent with London case study, only the heating period is considered for simulation trials of Helsinki, which is considered to be the period between October and May.

The dominant heat source for apartment blocks in Finland is district heating (Vainio et al., 2017). For the purpose of this study, gas is used for preparation of heat for homes. It should be noted that utilization of a district heating network (DHN) can be more energy efficient and sustainable than the adoption of individual gas boilers per residence since DHN normally uses the waste heat of a CHP plant (Ahmadian and

Schmidt, 2020). However, to be consistent with the previous case studies, gas boilers are considered here for Helsinki as well.

6.2.3.1 Form Signature graphs for Helsinki

Using the climate and horizon data of Helsinki, simulation trials are performed for a variety of site plans to obtain yearly energy demand of buildings per unit of area. The results are shown as a heat map on the *Form Signature* graphs in Figure 6.9.

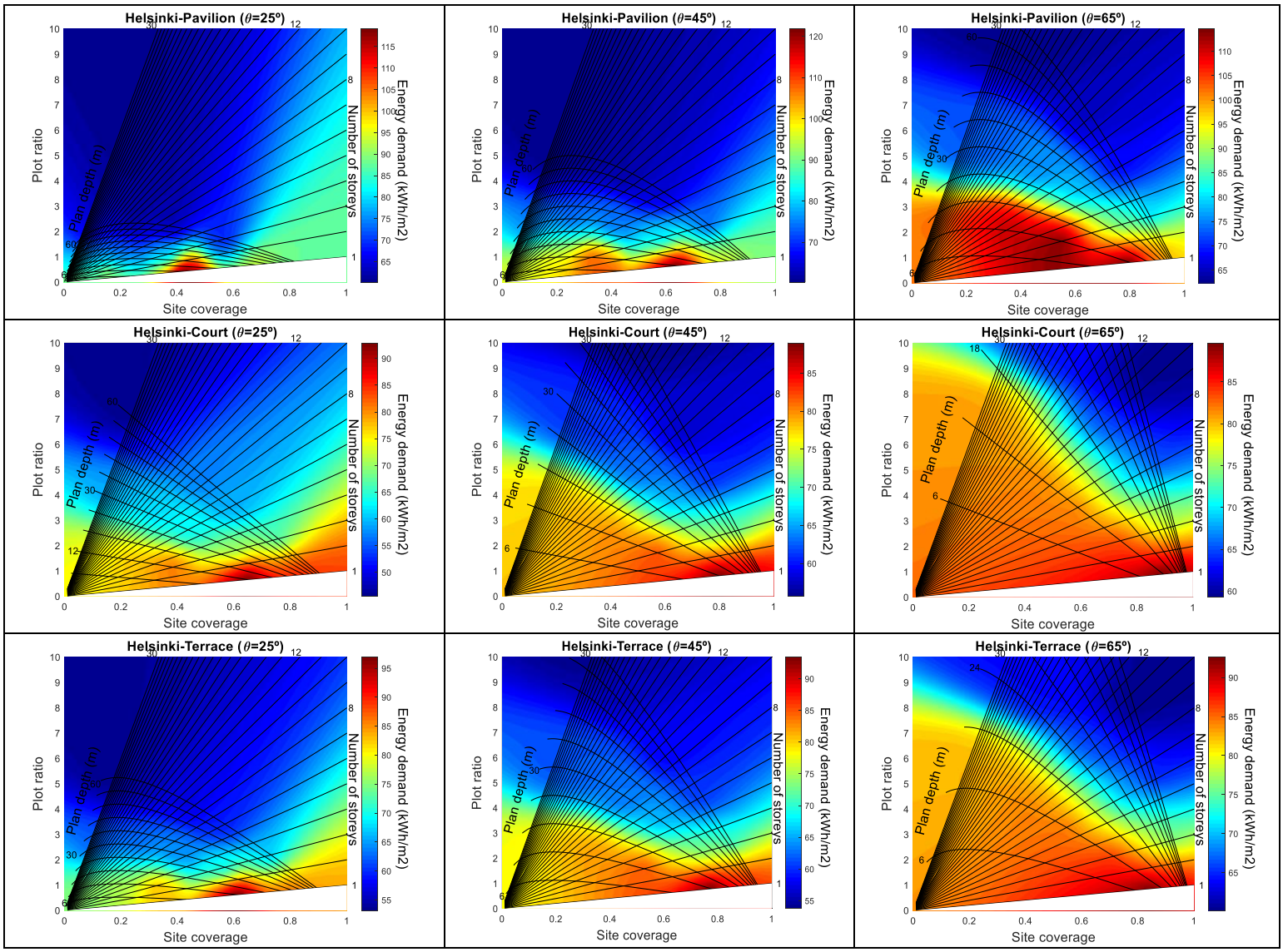

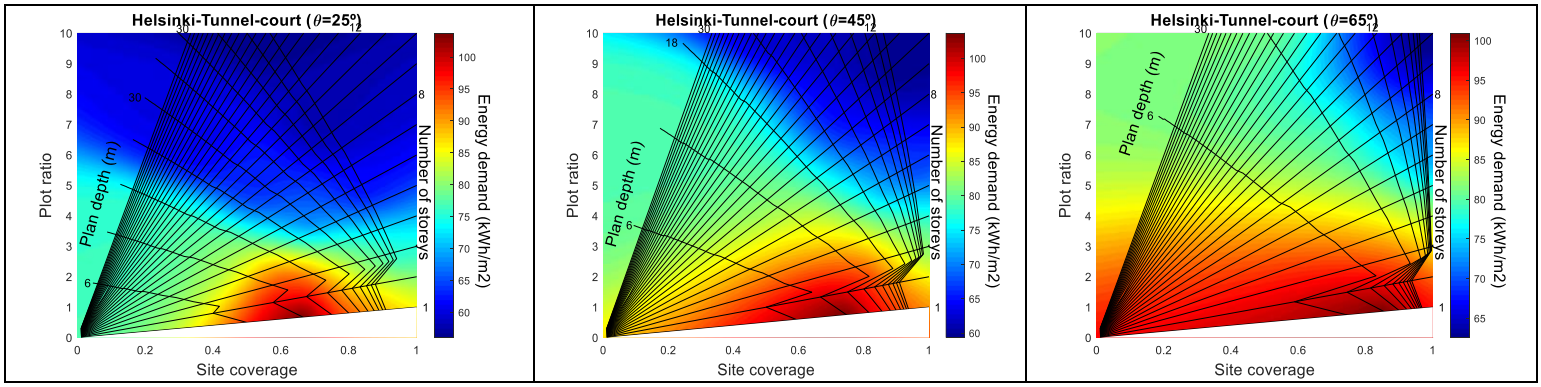

Figure 6.9: Correlation of building energy demand with urban built form and density for different built forms for Helsinki case study

From Figure 6.9 the characteristics of the building energy demand on the *Form Signature* graphs of Helsinki is similar to that of London. Buildings with a lower number of storeys and smaller plan depths have higher energy demand. Buildings with a high energy efficiency (depicted by dark blue areas on the graphs) with higher numbers of storeys and greater plan depths is equivalent to greater plot ratios. Multi storey buildings are considered as a good solution for the cold climate regions (Dursun and Yavas, 2015). The reason for this similarity is that only pure heating loads are demanded from buildings in both Helsinki and London. The only difference is the absolute values of building energy demand which are significantly greater for Helsinki compared with London. This is due to the fact that the cold weather in Helsinki is more intense and imposes a bigger heating load for the buildings. For instance, the building energy demand of a 6-storey court building (with θ=45º and x=12m) for Helsinki is 81 kWh/m^2/year, while it is only 42 kWh/m^2/year for London.

As a matter of validation of the results obtained from this analysis, Hukkalainen et al. (2017) found that the summation of heating and electricity consumption of an apartment building in Finland is around 66 kWh/m^2/year, and was around 102 kWh/m^2/year in the study by Jylhä et al. (2015).

Considering roof-mounted PV energy harvesting, values of Energy Equity are again obtained through simulation trials. The resulting values are used to show the correlation of building solar energy potential with urban built form and density on the *Form Signature* graphs, as shown in Figure 6.10.

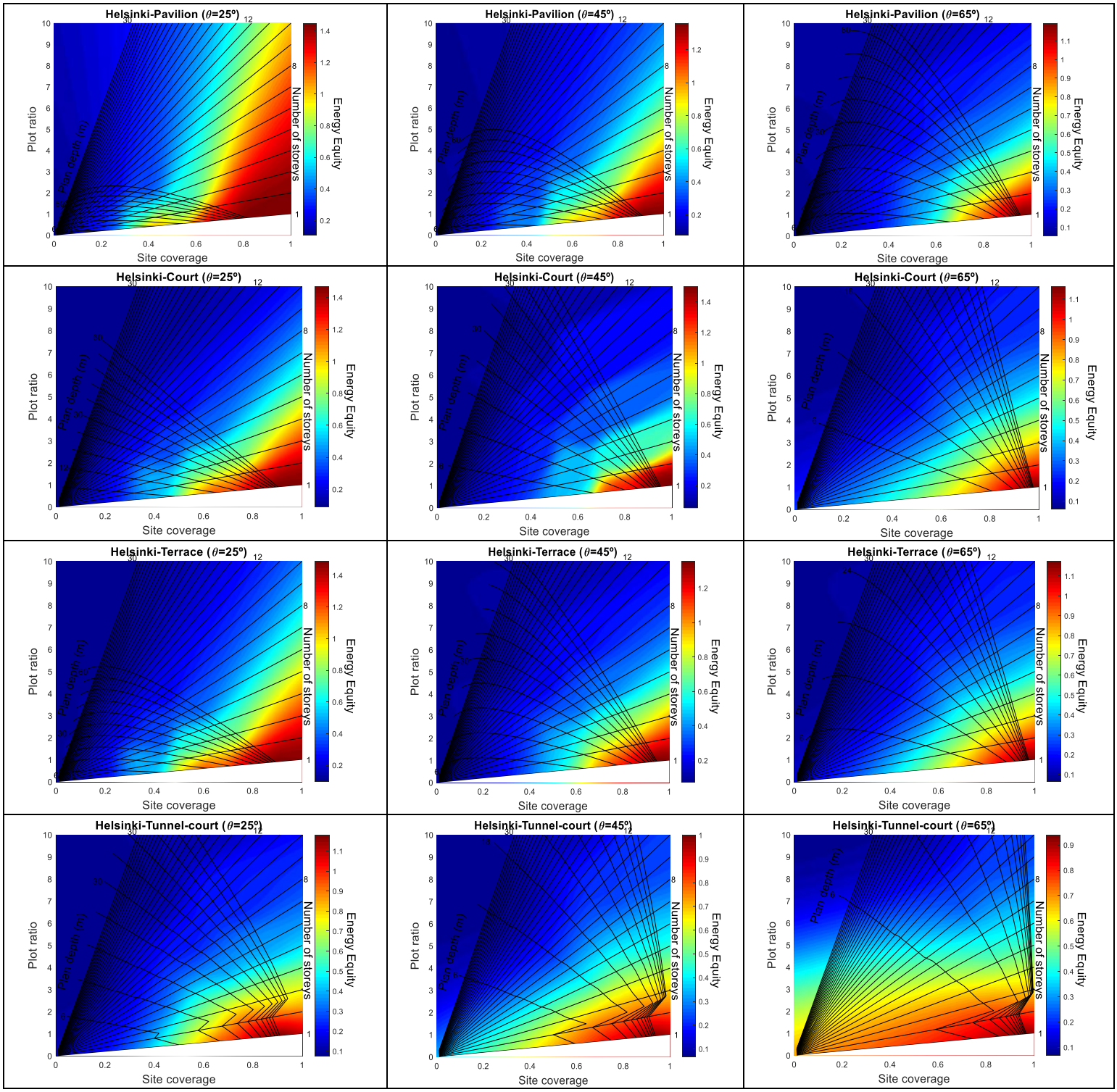

Figure 6.10: Correlation of Energy Equity indicator with urban built form and density for different built forms for Helsinki case study

Figure 6.10 shows that the characteristics of Energy Equity on the *Form Signature* graphs is similar to the previous case studies. Buildings with a lower number of storeys and greater plan depths acquire higher potential of PV generation with respect to their energy demand. This corresponds to high values of site coverage and low values of

plot ratio. However, the absolute values of their Energy Equity differ from each other, and this will be discussed in detail in section 6.3.

6.2.3.2 Impact of cut-off angle in Helsinki climate

Similar to the previous case studies, the impact of cut-off angle on building energy demand in Helsinki is investigated. The comparison of cases for the four studied urban built forms is shown in Figure 6.11.

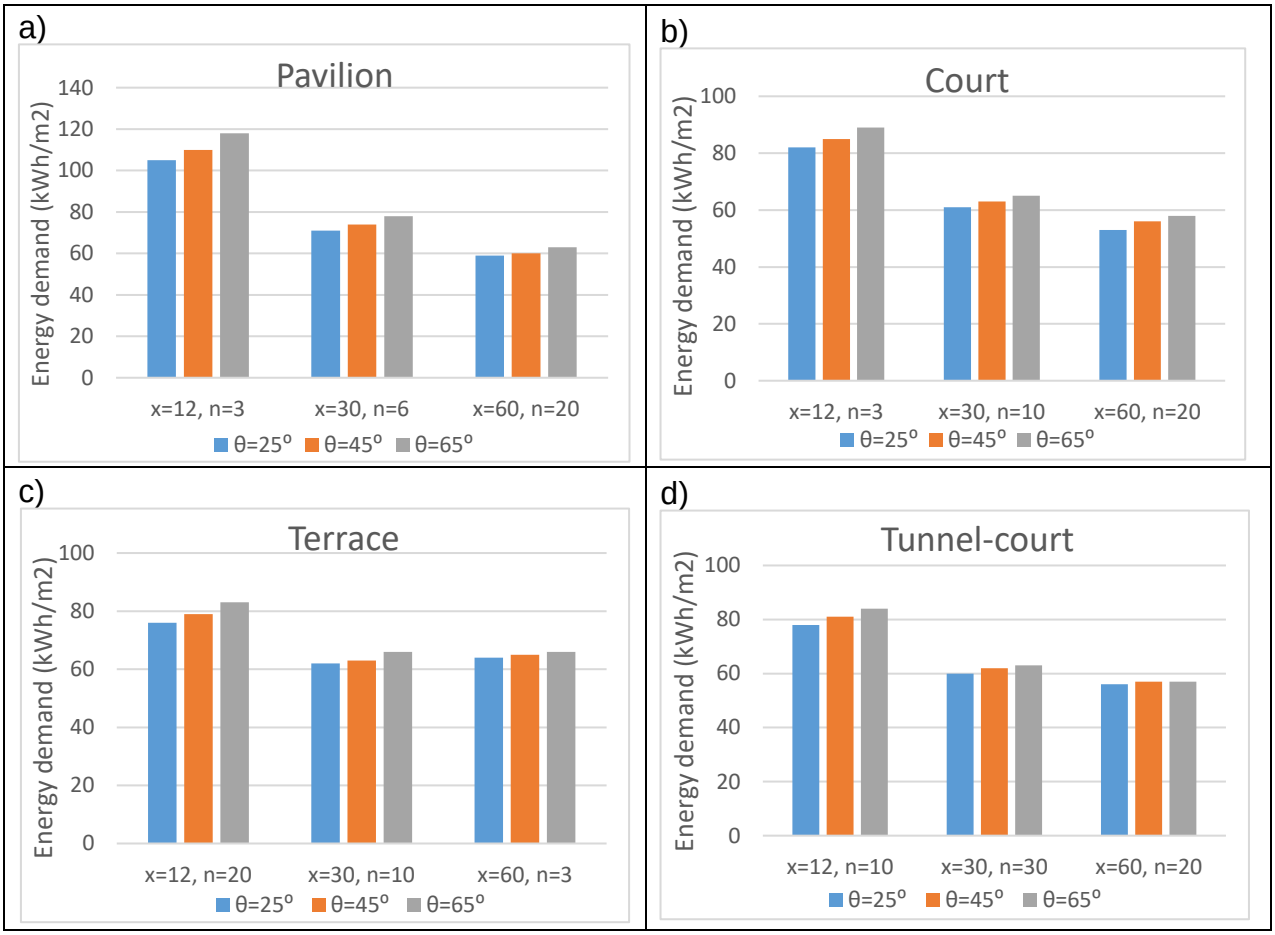

Figure 6.11: Impact of cut-off angle on building energy demand for different built forms in Helsinki

It can be seen from Figure 6.11, that greater cut-off angle results in higher building energy demand in Helsinki climatic conditions, meaning that a higher urban density is not advantageous for continental/cold climates. Since buildings in Helsinki require a significant amount of heating energy, having buildings close to each other prohibit them from useful solar gain in wintertime, resulting in a higher heating energy demand. This is compatible with the conclusion made by Strømann-Andersen and Sattrup (2011) in their study on the city of Copenhagen that is situated close to Helsinki with a similar climate.

Varying the cut-off angle from 25º to 65º can increase building energy demand between approximately 2% and 12%, depending on the plan depth. This demonstrates that the change in Helsinki building energy demand by altering cut-off angle is significantly smaller than the change it imposes to the Singapore or Phoenix building energy demand.

It should be noted that by increasing demand for summer cooling due to climate change, dense urban contexts may be more efficient in the future for the cities with this climate too (Morganti et al., 2012). This will be investigated in Chapter 7.

6.2.3.3 Energy performance of different built forms in Helsinki

Energy performance of the selected built forms with similar geometrical parameters are compared to identify the most suitable built form for Helsinki. Values for several cases are presented in the bar chart shown in Figure 6.12.

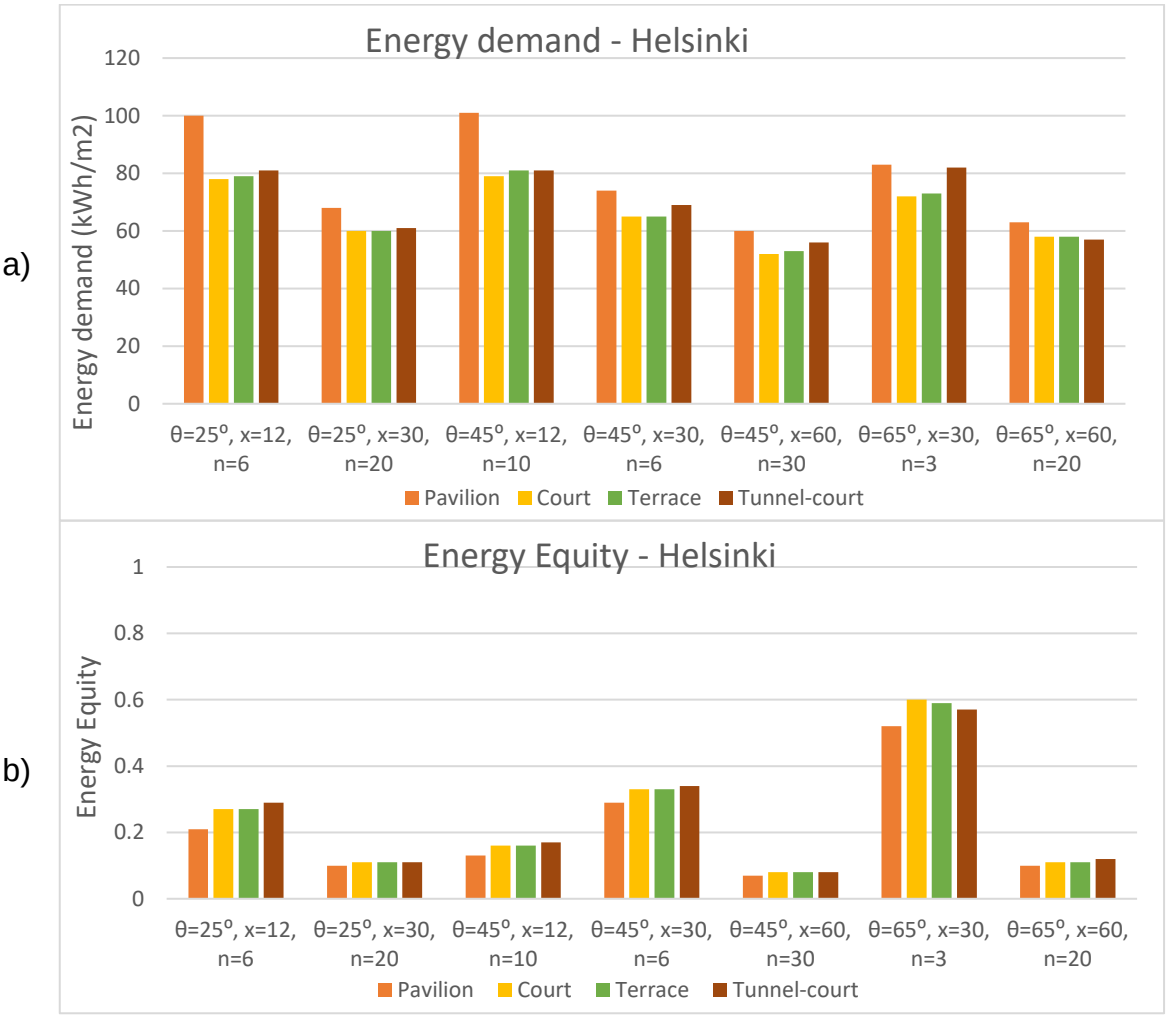

Figure 6.12: Comparison of building energy performance of the studied built forms with the same cut-off angles, plan depths and number of storeys in Helsinki a) energy demand b) Energy Equity

Figure 6.12 shows that pavilion form has the highest energy demand and lowest Energy Equity which makes it the worst choice for the Helsinki climate. Tunnel-court form has a medium energy demand, while it possesses the highest Energy Equity, which shows its considerably high potential of PV energy generation. Terrace and court forms are identical as a matter of Energy Equity and ranked in the middle. However, they show the lowest energy demand (terrace has slightly higher demand than court form) compared to the other built forms. Being compatible with these results, Dursun and Yavas (2015) found that the court form is beneficial in cold climate as it would provide the opportunity to trap warm air in courtyards between buildings. It also acquires other advantages such as protecting outdoor spaces against winds, maximising solar access and minimising shading in winter whilst being open to breezes in summer (St Clair, 2010). The study by Muhaisen (2006), which evaluated the performance of court form in four cities (Rome, Kuala Lumpur, Cairo and Stockholm) with similar climates to the four case studies of this thesis, showed the advantages of courtyard buildings for these four climates and emphasised that this consideration should be noted at design stage. This is in line with the outcomes from the case study analysis of this thesis as the court form (along with the newly introduced tunnel-court form) showed the best energy performance for all case studies.

The same analysis and conclusions derived in section 6.2.1.3 (see Table 6.1) regarding distinction between constant density and constant geometric variables are valid for this case study as well.

6.3 Comparison of different climates

Thus far, the correlation of building energy performance with urban built form and density has been investigated for each climate separately. Here, the results obtained from all case studies are aggregated to make a comparison between the energy performance of the studied built forms in the different climates. The resulting values from the four case studies are compared in the 3-dimensional diagram of Figure 6.13.

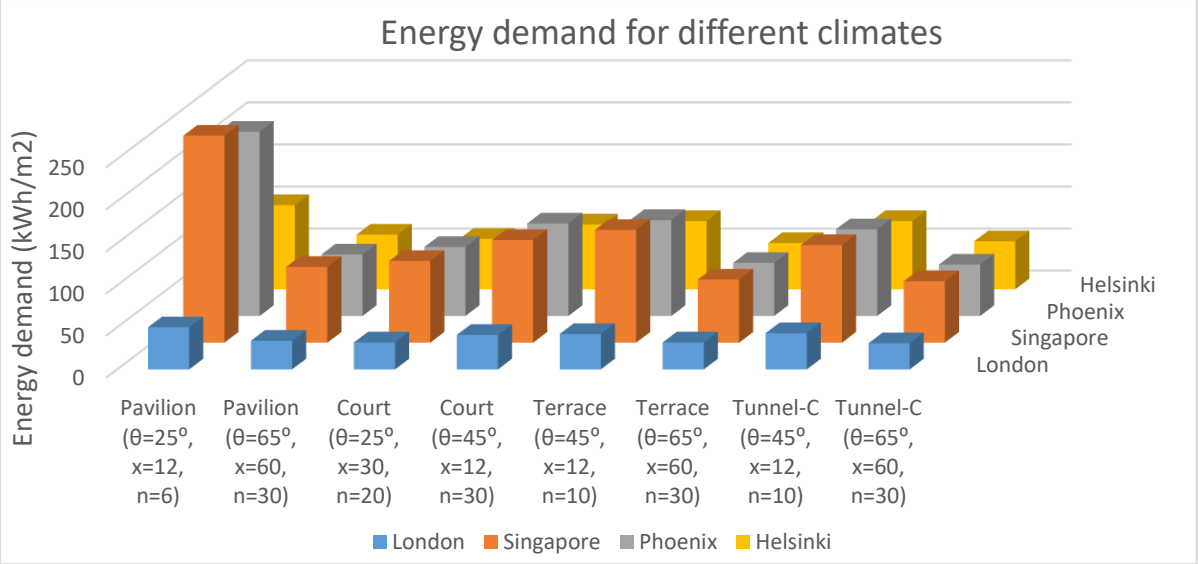

Figure 6.13: Comparison of the energy demand of the built forms with similar geometric parameters in different climates

In Figure 6.13, the columns related to each case study are identified by a different color. There are eight cases with similar built form, n, x and θ, for the different case studies (distributed along the Y-axis with different colors). The cases have been chosen among more than 200 available datasets, where the general trend of all of them are similar to the chosen cases. In each case, built form, cut-off angle, plan depth and number of storeys are kept constant, which means the density is constant too as a result of the similarity of all parameters considered. Therefore, the only variable in each case is climate. It can be observed that the lowest energy demand belongs to London, having a significant difference compared to the others. The next lowest energy demand is associated with Helsinki and is followed by Phoenix. Finally, the highest energy demand belongs to Singapore.

The low energy demand of London is due to its temperate climate which necessitates less heating energy to reach the thermal comfort temperature of occupants. Due to the cold climate of Helsinki, the outside temperature has larger divergence from the inside setpoint room temperature. Phoenix and Singapore mainly require cooling demand that itself requires more energy compared with heating demands. Moreover, according to the assumptions of this study, they demand energy 12 months of a year, while it is only eight months for London and Helsinki. Therefore, these two case studies show higher energy demand. Notably, the weather in Phoenix is harsher and hotter in the summer period which requires higher cooling demand to the buildings, but nevertheless requires less total energy than Singapore which requires cooling all year round (Phoenix buildings require heating for five months of a

year that reduces the total yearly energy demand of buildings compared with Singapore).

To investigate the scale of these differences, the case of terrace form with θ=45º, x=12m and n=10 is analysed here. The resulting energy demand of buildings in London, Helsinki, Phoenix and Singapore are 42, 81, 114 and 134 kWh/m^2/year, respectively. This shows that yearly building energy demand in Helsinki, Phoenix and Singapore are 93%, 171% and 190% higher than in London. This highlights the significant impact of climate on building energy demand.

Among the cases shown in Figure 6.13, the first case that is composed of Pavilion form with θ=25º, x=12m and n=6 shows a relatively abnormal high energy demand for the Phoenix and Singapore case studies. In this specific instance, the energy demands for these two case studies are unexpectedly much higher than London and Helsinki, and their percentage differences are not following the above-mentioned trend. In fact, the energy demand for Phoenix and Singapore are 338% and 392% higher than London, respectively, while they have only a 12% difference between each other. This substantial difference is due to a combination of three features, i) it is a pavilion, ii) it has a small plan depth, and iii) it has a low cut-off angle. The pavilion built form consists of smaller internal space compared with other built forms, therefore, its envelope energy efficiency is more vulnerable to outside weather conditions. In addition, it has a small plan depth that makes it even more sensitive to the changes happening outside the building, and finally (and more importantly), the low cut-off angle increases the cooling load of the building in hot climates (i.e. Phoenix and Singapore). As previously demonstrated in Figure 6.3 and Figure 6.7, in hot climates that require significant cooling loads, the increasing cut-off angle would decrease cooling demand of buildings. Therefore, in plans with a low cut-off angle the difference between energy demand in hot climates and the cities such as London and Helsinki (that require heating load) are very significant. As shown in Figure 6.14, by increasing the cut-off angle, heating load increases (opposite to cooling load) and the difference significantly reduces in the building plans with high cut-off angles (e.g. θ=65º).

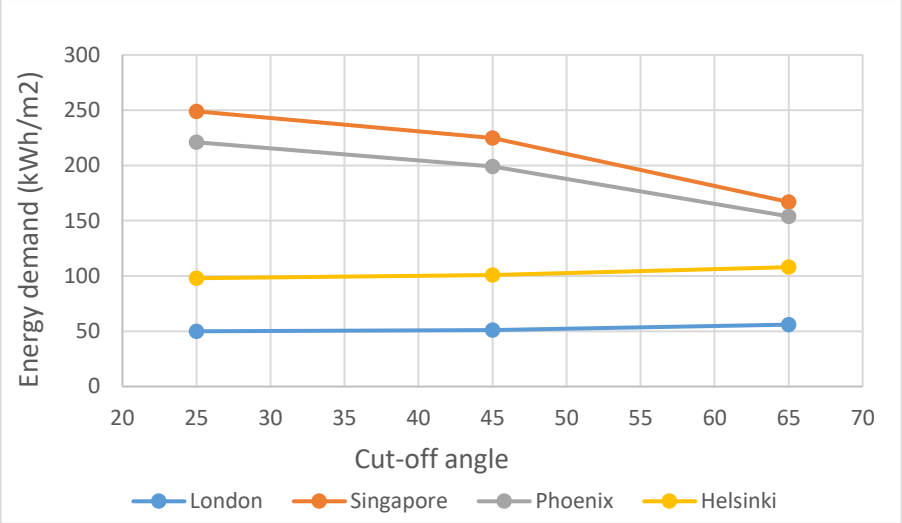

Figure 6.14: Trend of changes in the energy demand of different case studies by increasing cut-off angle

A similar analysis is now performed by considering PV energy generation in addition to building energy demand for the different climates. Similar cases to Figure 6.13 are compared using their Energy Equity values, as shown in Figure 6.15.

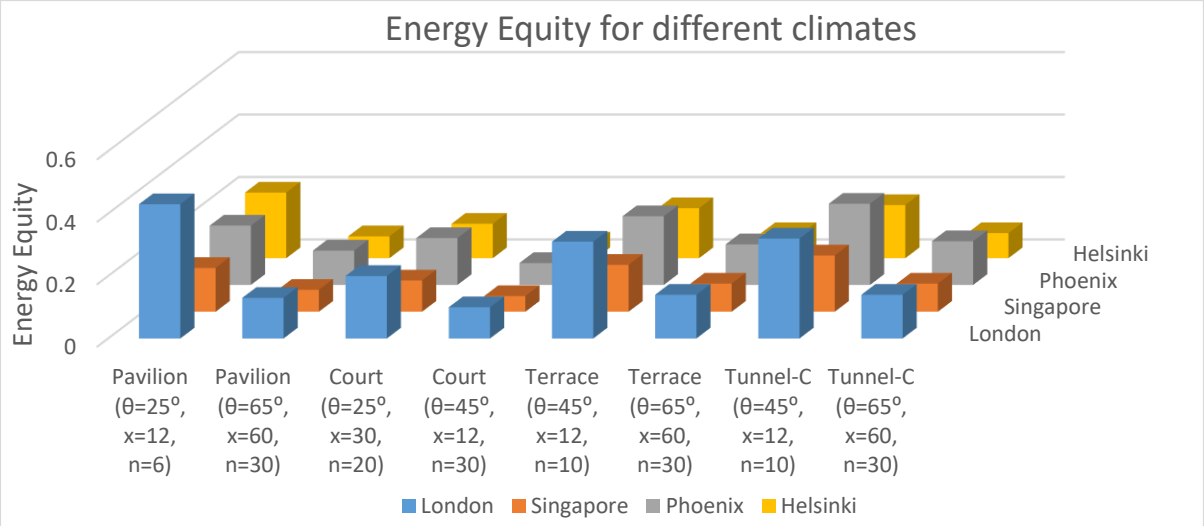

Figure 6.15: Comparison of the Energy Equity of the built forms with similar geometric parameters in different climates

Having similar geometry, density and built form in each case, Figure 6.15 shows only the impact of climate on the Energy Equity indicator. It can be seen that the Energy Equity of London is evidently higher than the others in all cases except with θ=65º, where the domination of the London case study, with respect to Phoenix, is not very significant (the reason will be discussed in the last paragraph of this section). Phoenix is ranked second in this comparison, achieving evidently higher values than Singapore and Helsinki except in the first case. As explained when considering the

results of Figure 6.14, in that exceptional case, the cooling load in Phoenix and Singapore is very high which creates a substantial reduction in their Energy Equity. In this case, Helsinki, despite its low solar potential, acquires a higher value of Energy Equity than those. By way of a holistic comparison of the lowest-ranked case studies, Helsinki and Singapore, it is seen that Helsinki has greater Energy Equity than Singapore in site plans with low cut-off angle, while it is opposite in cases with large cut-off angles. This is connected to their energy demand (the denominator of the Energy Equity equation). It is shown in Figure 6.14 that increasing cut-off angle increase energy demand of Helsinki (and decrease Singapore's) that reduced its Energy Equity value (and magnifies Singapore's). Therefore, although the amount of solar radiation in Singapore is substantially greater than Helsinki, their Energy Equity values are relatively similar. This affirms the advantage of introducing the Energy Equity indicator in this study, otherwise, it could be simply assumed that solar energy potential of these case studies is ranked from 1 to 4 as Phoenix, Singapore, London and Helsinki following their climatic conditions and geographical location. According to the results of the simulation trials of PV energy generation, London PV generation is 1% more than Helsinki, Singapore is 54% more than London and Phoenix is 26% more than Singapore. This means that there is a 95% difference between the best and worst cases. Therefore, although there is a 55% difference between PV generation potential of Helsinki and Singapore, their Energy Equity values remain similar.

As discussed above, for the cases with θ=65º, the Energy Equity of London is very close to that of Phoenix (and in the last case they are almost equal). The reason again is that in plans with high cut-off angle, building energy demand in London is increased while in Phoenix it is decreased (see Figure 6.14), which causes an opposite impact on the Energy Equity. Moreover, the reason that in the last case their Energy Equity is equal is that this is a tunnel-court form with θ=65º. For the Tunnel-court form the roof surface area available for PV installation is greater than in other built forms, and in Phoenix, the intensity of solar radiation is greater than the other studied cities, specially London. These two features combined considerably increase the Energy Equity of Phoenix which results in equality of its value with London's.

6.4 Conclusion

Following the identification of the relationship of building energy performance with urban built form and density in the previous chapter, the impact of climatic conditions

on this relationship is investigated in this chapter. Many studies in the literature indicate the significance of climatic factors on building energy performance. However, the impact of climate on the relationship of building energy and urban form requires further investigation.

In addition to the London case study considered in the previous chapter, three other case studies have been chosen from contrasting climates. Considering the Koppen climate classification system, the cities of Singapore, Phoenix and Helsinki are selected where each of them representing a different climate zone. Simulation trials are adopted for this analysis using CitySim. The climate data of each case study is obtained from Meteonorm software. The resulting data are compared in different stages and the outcomes are explained as follows:

The trend of change of energy demand and Energy Equity on the *Form Signature* graphs are almost similar for all case studies, though the absolute values of the mentioned parameters are different in each case. Taller and wider buildings (which is equivalent to having a higher plot ratio) require lower energy demand than buildings with a lower number of storeys and smaller plan depths. This has a small exception in pavilion and terrace forms in Singapore and Phoenix where there is a slight increase in the cooling load of high-rise buildings. As a matter of Energy Equity, in all case studies, it is always more beneficial to have a lower number of storeys and greater plan depths, which corresponds to higher site coverage and lower plot ratio.

By increasing the cut-off angle, which increases both site coverage and plot ratio, the energy demand of buildings in London and Helsinki rise while it reduces building energy demand in Singapore and Phoenix. The reason is that energy demand in London and Helsinki is heating-dominated while in Singapore and Phoenix is cooling-dominated. The findings show that closely packed buildings provide shade for their neighbours, resulting in cooler environments that increase the heating load while decreases cooling load. The impact of cut-off angle on the building energy demand of cooling-dominated buildings is significantly higher than on heating-dominated buildings.

When comparing built forms with similar geometric variables, pavilion form acquires highest energy demand in all case studies. Tunnel-court form shows the lowest energy demand in Singapore and Phoenix, while the terrace and court forms show the lowest energy demand in Helsinki and London. Meanwhile, tunnel-court form achieves the highest value of Energy Equity in all case studies, where the lowest value

belongs to pavilion. These results could be opposite if the density is fixed instead of geometric variables. The magnitude of difference between Energy Equity of tunnel-court and pavilion forms is significantly higher for cooling-dominated buildings. The results show that the tunnel-court form performs between 7% and 32% higher than pavilion form in London and Helsinki, while it performs between 27% and 67% higher than pavilion form in Singapore and Phoenix. It demonstrates the higher importance of choice of built form in hotter climates.

Finally, and most importantly, the direct comparison of the studied built forms in the chosen case studies shows that yearly building energy demand is a minimum in London while it is maximum in Singapore. Helsinki and Phoenix are in the middle, though Phoenix shows higher energy demand than Helsinki. Building Energy Equity is the highest for London that is followed by Phoenix because of their higher potential for solar energy generation with respect to their building energy demand. The value of this indicator is low for Singapore and Helsinki with approximately similar values. When the cut-off angle of the building plan is low, Helsinki acquires higher Energy Equity while Singapore shows higher values in case of having a greater cut-off angle. Hence, buildings in London can achieve energy self-sufficiency easier than in the other case studies.

Chapter 7: Future Cities

7.1 Introduction

Here, consideration is given to the impact of global warming and the penetration of EVs to the market, and how they will influence decision making for future urban developments. The average temperature of the earth has been increasing since the mid-20th century due to greenhouse gas emissions into the atmosphere. This anthropogenic climate change has been caused by human activities, particularly the burning of fossil fuels. This interrupts the balance of natural global cycles leading to uncharacteristic climate events (as discussed in Chapter 1, section 1.1). It obliges humans to urgently take serious action, and an important aspect of this is the planning of future cities. Sustainable energy use in urban areas is feasible through the integration of improved building energy performance, urban geometry and climate change at the planning and design stages (Mangan and Oral, 2020). Changes in mean weather patterns and extreme weather events have direct and indirect impact on energy systems from both a risk and market perspective (Berger and Worlitschek, 2019). Moreover, consideration of the developing technologies is very crucial as this can influence the optimal shape of future cities (see Chapter 2).

In this chapter, the future climate predicted by Intergovernmental Panel on Climate Change (IPCC) is used for new simulation trials of the City of London. The penetration of private EVs and the scenario of charging them from roof-mounted PV panels is considered which adds more load to energy consumption of buildings. The results are compared with the previous results from the London case study (Chapter 5) to investigate the differences of current and future optimum urban built forms and density.

The primary contribution of the chapter is identification of the most efficient urban built forms along with their recommended geometrical parameters for the future London temperate climate. It determines the combined effect of climate change, technological developments, and government policies on the future of cities and relates them to urban built form and density indicators.

7.2 Future scenarios

At the Paris Agreement in 2015, a durable framework was provided to avoid the threatening consequences of climate change by limiting global warming to below 2°C over pre-industrial levels, and preferably keeping it below 1.5°C. It was followed by the IPCC report entitled *Global Warming of 1.5°C* (Masson-Delmotte et al., 2018)

emphasizing that it is still possible to keep the temperature rise below 1.5°C but only through rapid transitions in energy, land, urban infrastructure and industrial systems. The aim of the Paris Agreement is to create a continuous cycle that sustains pressure on countries to raise their ambitions over time. To this end, UK set a legally binding target of net zero emissions by 2050 making it the first major economy to pass net zero emissions laws (UK government, 2019). The main areas for carbon emission reduction are power, buildings and transport, by using renewable and clean energy sources, increasing the EPC standard of all homes, and ending the sale of petrol and diesel cars by 2030 (WWF UK). Here then, the future climatic conditions of London in 2050 along with proposed transportation strategy is investigated to identify their impact on building energy performance and its relationship with urban built form and density. The average UK surface air temperature has increased by ~1ºC since the mid-1980s, which has caused frequent warmer summers compared with the 1971–2000 average (Rodrigues et al., 2013). There has been little attention to the cooling of dwellings in the UK for historical reasons. However, as the temperature rises, there will be a rise in the rate of synthetic cooling requirements during summer periods (Rodrigues et al., 2013). Hence, adaptation of air-conditioning for cooling purpose is being increasingly demanded (Kolokotroni et al., 2012). This is one of the key differences between the current and future scenarios for building energy optimization in the temperate climate of the UK that is investigated by comparing the results of this analysis with the results obtained in Chapter 5. Nevertheless, natural ventilation still has a positive impact and a good design using natural ventilation together with the potential of adaptive comfort can reduce the need for synthetic cooling. To this end, the importance of transforming the physical form of buildings and cities to be consistent with the changing climate is of increasingly significant (see Chapter 6). The results of this chapter give recommendations for the most energy efficient built forms to be adopted for future climatic conditions. It is notable that over-reliance on air-conditioning may result in more compact built form as it displaces cooling by natural cross-ventilation.

It should be noted that many assumptions can be taken into consideration that influence the predictive patterns of the future. The energy mix that is used in cities will be different and variable types of fuels could be used. For instance, there might be no gas heating in 2050, and PV panels with greater generation capacity might be developed, more efficient building materials might be available to reduce heat loss,

and even home appliances with higher energy efficiency might be accessible for occupants that reduce building electricity consumption.

This study acknowledges all the possible upcoming technological developments; however, it focuses on the impact of climate change and the utilization of EVs. In addition, in it assumed that home appliances and lighting energy consumption will be 22% more efficient (Bansal et al., 2011, Borg and Kelly, 2011). Other characteristics remain similar to those used in Chapter 5 to be consistent with the present scenario of the London case study. Comparative analysis determines the difference between the percentages of heating, cooling and electricity requirements in the present and in the future.

7.2.1 Global Warming

IPCC issued a special report proposing six different emission scenarios for future climate change (Nakicenovic and Swart, 2000). These are classified into four storyline families, namely A1, A2, B1 and B2. A1 family is composed of three scenarios (A1F1, A1B and A1T) characterizing alternative developments of energy technologies, while other families have only one scenario each. The scenarios are alternative images of how the future might be which is the product of a complex dynamic system determined by driving forces such as demographic and socio-economic development as well as technological changes. Figure 7.1 shows the predicted trend of changing carbon dioxide emissions by 2100.

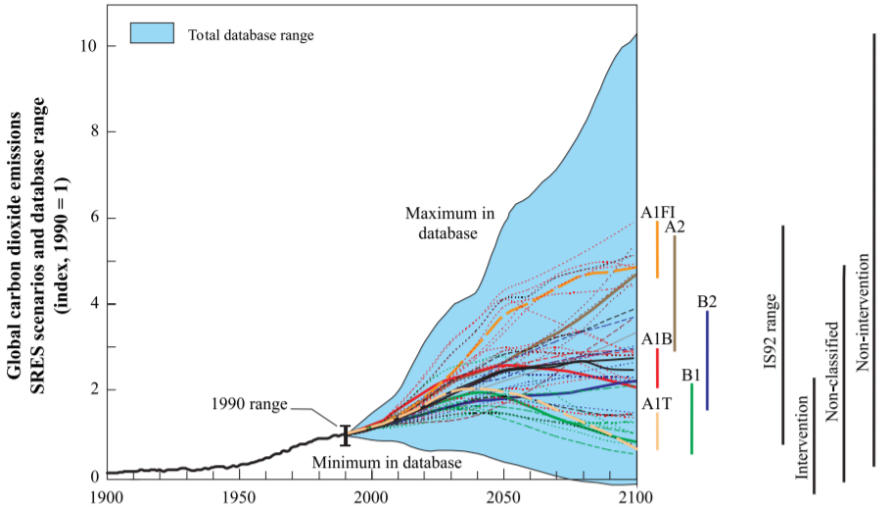

Figure 7.1: Prediction of carbon dioxide emissions in different IPCC scenarios (Adopted from Nakicenovic and Swart (2000))

From Figure 7.1, it is observed that scenario A1F1 has the highest emissions, followed by A2. This study considers one of the two worse-case scenarios (A2 and A1F1) to emphasize the possible consequences of ignoring climate change, and, since Meteonorm software is able to generate predicted future climate data for CitySim for A2 (but not A1F1), A2 is specifically chosen for the study. Notably, Jylhä et al. (2015) also show that A2 causes more significant change in future building energy demand compared with B1 and A1B scenarios (albeit for Finland). The underlying trends in scenario A2 is self-reliance and preservation of local identities, continuously increasing global population, regionally oriented economic development and per capita economic growth, where technological changes are more fragmented and slower than in other storylines.

7.2.2 Penetration of EVs into the transportation network

As discussed in Chapter 2, planning and policymaking for urban areas should be undertaken by considering ongoing/future means of transportation (e.g. EVs) rather than current technologies (i.e. ICEVs), since it is expected that ICEVs will be largely phased out in many parts of the world. To achieve the 2050 zero carbon target in the UK, the transportation system, as a major pollution contributor (accounting for 26% of the UK's greenhouse gas emissions (Gabbatiss, 2018)), needs to be urgently decarbonized. This will be done by replacing ICEVs with EVs. Currently only 0.08% of the total 32 million cars on the roads are EVs (EST, 2020)). This percentage is accelerating following several service and financial incentives such as tax reductions for EVs, offering free parking spaces to EVs and allowing them to use the bus lanes, and Plug In Grants towards the cost of installing a charge point at home (EST, 2020). The latter aspect is a key basis for the analysis presented in what follows.

The energy use (and carbon production) of EVs is very dependent on how they are charged. If EVs are charged by PVs mounted on residential roofs, then the energy is comparatively emission and cost free. Furthermore, smart grids and micro-grids allow for energy to be generated away from home so that a vehicle need not be at the point of generation in order to benefit. The future use of virtual power plants (VPPs) will also make it possible to utilize energy stored throughout an urban area to be directed towards electrically powered public transport (Nikonowicz and Milewski, 2012). This disruptive technology combined with smart grids and 'blockchain' energy supply (Mengelkamp et al., 2018, Pieroni et al., 2018) may suggest that dispersed

cities of lower density will be more energy efficient for both buildings and transport. Therefore, it is argued that policy on urban form should be based on the technologies of the future rather than the past. For example, with new disruptive technologies, households will not only consume electricity but are also likely to generate it. With the use of VPPs, the urban population will become 'prosumers' (both providers & consumers) and will have a stake in power plants that could be controlled by the local communities themselves or local councils. This will challenge the current structure of the grid network providers and their business models.

In the scenario considered for this analysis, it is assumed that all household EVs will be charged by their private plug-ins which are supplied by roof-mounted PVs. Therefore, the electricity consumed by EVs is added to the total energy demand of the buildings. To this end, the analysis procedure shown in Figure 7.2 is adopted.

Figure 7.2: The schematic of the method used for calculation of EVs energy consumption

In the geometric building models developed for this study the number of the occupants is based on the constant occupant density determined in section 5.2.1.1 (Chapter 5). Therefore, for calculating the total number of the electric cars used in the building models, it is essential to calculate the number of the cars per person/occupant.

The first step is to find the percentage contribution of EVs in the market in 2050. According to the forecast published by The Faraday Institution (2019), the uptake of EVs in the UK will increase up to 95% by 2040—see Figure 7.3.

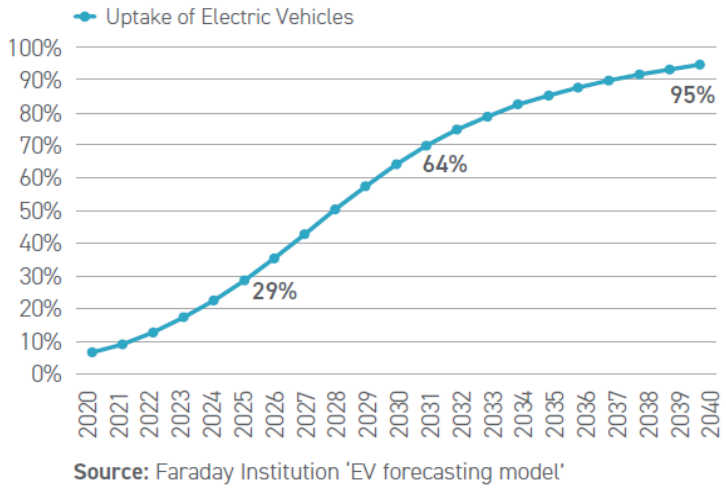

Figure 7.3: Trend of uptake of EVs into the UK market from 2020 to 2040

From Figure 7.3, it can be concluded that this value can reach 100% by 2050. This is supported by the Department for Transport (2018) writing that they plan for almost every car and van to be zero emission by 2050. The next step is to identify the average number of cars per person to be able to estimate number of the cars possessed by the occupants in the building models. According to data provided by the Department for Transport, 39% of London households own a car, 16% own more than one car and 45% have no car (Barrett et al., 2020). The percentages are very similar to the report published by Transport for London (2012), and is equivalent to an average of 0.3 cars per adult. However, to obtain an updated value for 2020, a brief analysis is undertaken. Statistica (2019) categorized the number of households in the UK based on the number of persons per household, amounting to the average number of persons per household being 2.36 for the UK. Although this is for whole of the UK, it is very close to the number announced in the Mayor of London (2011) website, which is 2.47 for 2011. This study therefore selects 2.4 as a value in between the two, considering that there has been a decreasing trend since 2011. Since this study needs to estimate the number of cars per person (occupant) for simulation trials, the following method of calculation is used:

Considering 16% of the households own two cars (Barrett et al., 2020), this value is accounted twice (i.e. 32%) as the households with one car. By adding this percentage to the percentage of the households with one car (39%, as mentioned in the previous paragraph), the value of 71% is obtained. Therefore, the portion of people who own car is obtained as follows (Eqn (7.1)):

$$0.71\left(\frac{car}{household}\right) * \frac{1}{2.4}\left(\frac{household}{person}\right) = 0.3\left(\frac{car}{person}\right) \qquad 7.1)$$

As a result, the value of 0.3 car per person is used for energy modelling. Multiplying this by the number of the occupants in each building model allows the total number of the EVs for each building plan to be obtained.

Next, the average distance travelled by each car in London is estimated. According to the data published by the UK Government (2020), the annual mileage of private cars is 7200 including business mileage, commuting mileage and other private mileage. By multiplying this number to the electricity consumption of an EV per mile, its annual electricity consumption is obtained. The Electric Vehicle Database (2021) publish a list of EV models along with their energy consumption. The average consumption of all the available cars listed is 0.307 *kWh/mi*, with the lowest

consumption belonging to the Tesla Model 3 Standard Range Plus with 0.235 *kWh/mi*. In this study, the most energy efficient car is considered since we are considering the future, and since technology is continuously being developed, this is considered as reasonable. Finally, assuming a power transfer efficiency of 90% for battery charging with the associated power electronic converters, the electricity demand from EVs is multiplied by 1.1 to obtain the yearly electricity consumption of EVs from PVs.

It should be noted that most of the above-mentioned values might differ in future following the possible changes in the factors such as government policy, technology development, and occupant lifestyle (e.g. more online shopping) that is by itself affected by family economic condition and demography of London. For instance, number of persons per household, the willing of people for having their own car (e.g. this might change by the planned development of public transportation), the average distance travelled by car, penetration of new autonomous vehicles into the market and the efficiency of EVs (and also PVs) might change in 30 years' time from now.

7.2.3 Simulation trials and results

Building Energy Performance simulation is a key tool to predict the energy performance of buildings based on future climatic scenarios (Al Qadi et al., 2017). Building models similar to those used in Chapter 5 (section 5.2.1) are used with CitySim. However, the simulation models have plenty of differences with Chapter 5. The predicted future climate option (i.e. IPCC A4 for 2050) is selected in Meteonorm to generate a future climate file instead of using the current climate file of London. Also, it is assumed that the occupants own EVs, which are charged by the energy harvested from building-integrated PVs. The electricity consumption of the EVs is therefore added to the building's energy consumption. Finally, in addition to heating and electricity demand, cooling loads are also considered in anticipation that buildings will require cooling as a result of global warming (Kolokotroni et al., 2012, Rodrigues et al., 2013). Kolokotroni et al. (2012) showed that this requirement will be more significant in urban areas such as London due to intensification of the UHI effect (which is also readily incorporated into CitySim). Therefore, here, photovoltaic system is used to cover EVs, home electricity, space heating and cooling demand of the buildings (Roselli and Sasso, 2016).

The heating season in the UK will be considered shorter due to global warming (Collins et al., 2010, Gupta and Gregg, 2012) along with improvements in insulation

materials. Therefore, months with a low heating demand (see Figure 5.5 of Chapter 5) are eliminated from the heating period, leaving November to March as the heating period. The cooling season is chosen to be between June and August, corresponding to the hottest months of a year according to the climate data and as used by other studies (Amoako-Attah and Bahadori-Jahromi, 2013).

After executing 216 simulation trials for building plans with the considered built forms, densities and geometric variables, the results of annual energy demand for different built forms are shown as heat maps on the *Form Signature* graphs shown in Figure 7.4.

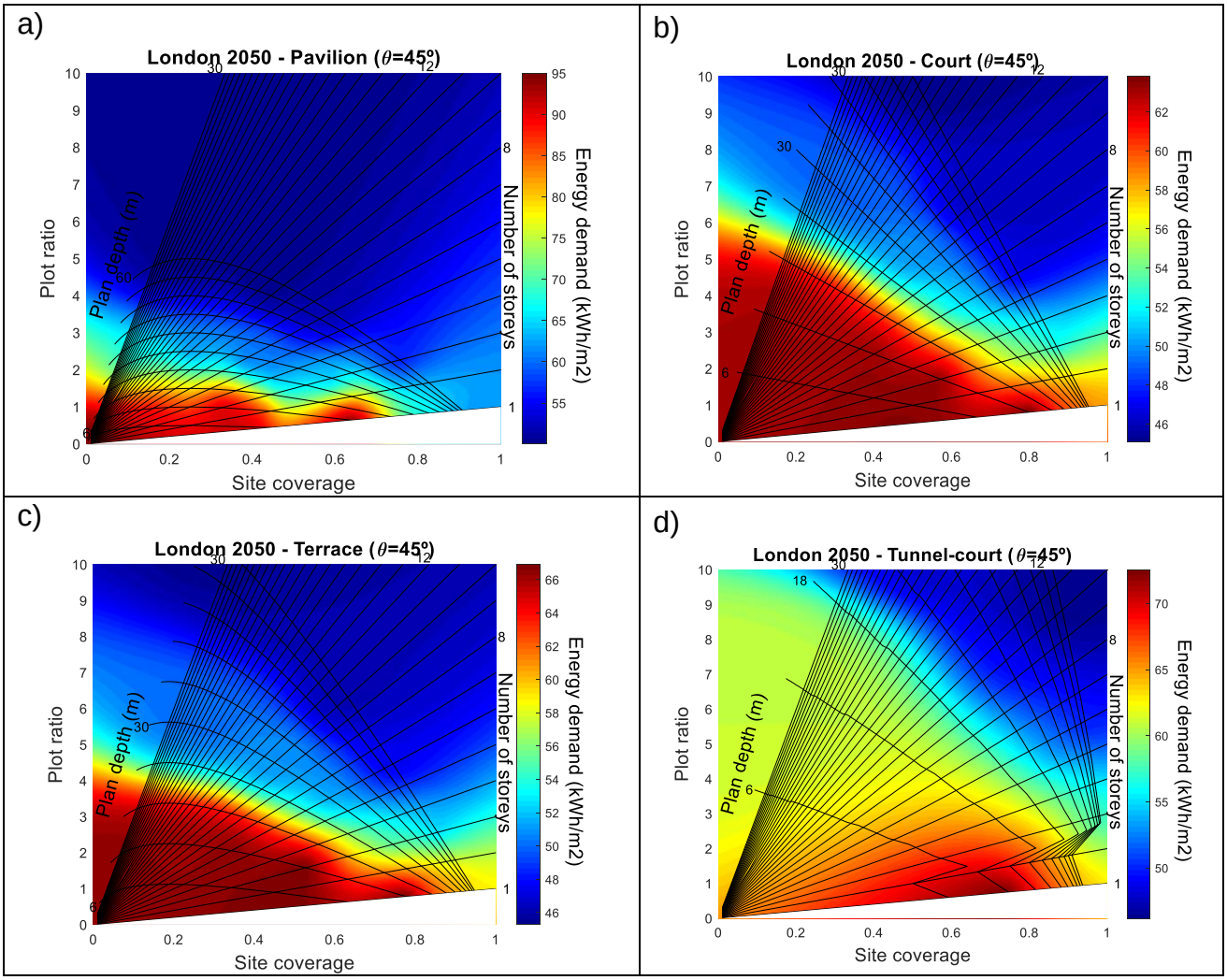

Figure 7.4: Correlation of building energy demand (including EV consumption) with urban built form and density for different built forms for London case study in 2050

In Figure 7.4, only the *Form Signature* graphs of the built forms with θ=45º are shown (as the average cut-off angle considered for this study). Results for θ=25º and θ=65º are not considered to avoid repetition since the trends are very similar. Comparing the results with those in Chapter 5 (Figure 5.6, Figure 5.8, Figure 5.10 and

Figure 5.12), it can be seen that the trend of change from high intensity to low intensity energy spots on the graphs are similar, however, the magnitude of the energy demand values in Figure 7.4 are greater than those in Chapter 5. The reasons behind this will be explained in section 7.3.

In general, Figure 7.4 shows that following the predicted climate of 2050 and usage of EVs, buildings with more storeys and greater plan depths (i.e. higher values of both site coverage and plot ratio) will have lower energy demand per unit area. There is only one exception in the pavilion built form when plan depth is small (e.g. x=12m), where increasing number of storeys from 6 to 30 leads to an increase in the energy demand caused by increasing cooling load during the summer. The reason is that pavilion form has significantly higher surface to volume ratio compared with the other built forms (see Figure 3.8). Therefore, when the building is high, the external walls of the building has a large surface area exposed to the outside environment which has twofold impact on increasing the cooling load. Firstly, the building has a greater glazing area leading to high solar gain during the day, which consequently requires increased cooling. Secondly, there will be more heat gain through the envelope that also increase the cooling load in the hot season. These points are particularly influential for pavilion buildings with small plan depth because the space inside the building is narrow and significantly vulnerable to the outdoor conditions.

The simulations also considered PV energy generation from building roofs. The resulting values of Energy Equity are shown in Figure 7.5.

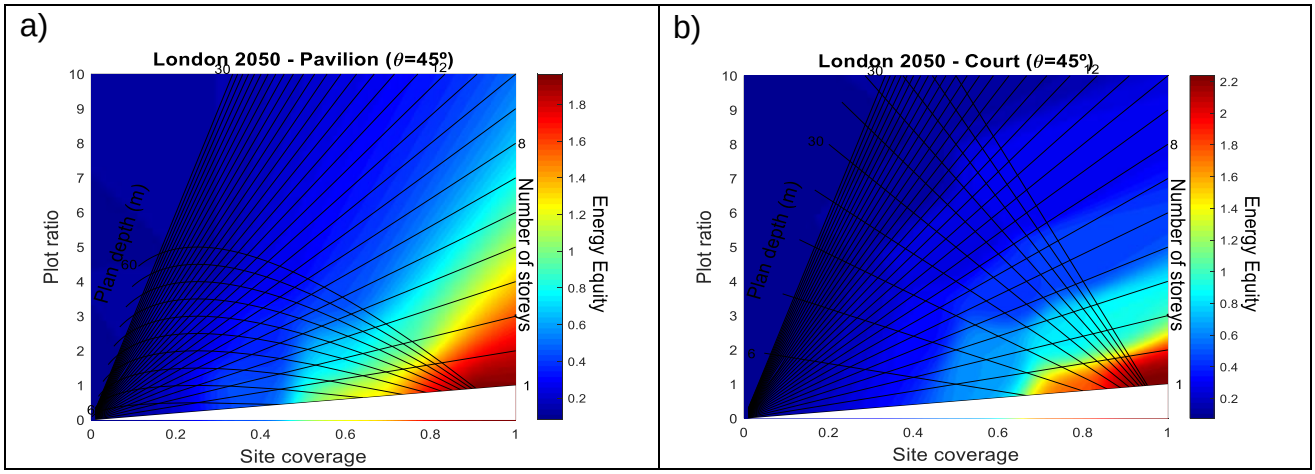

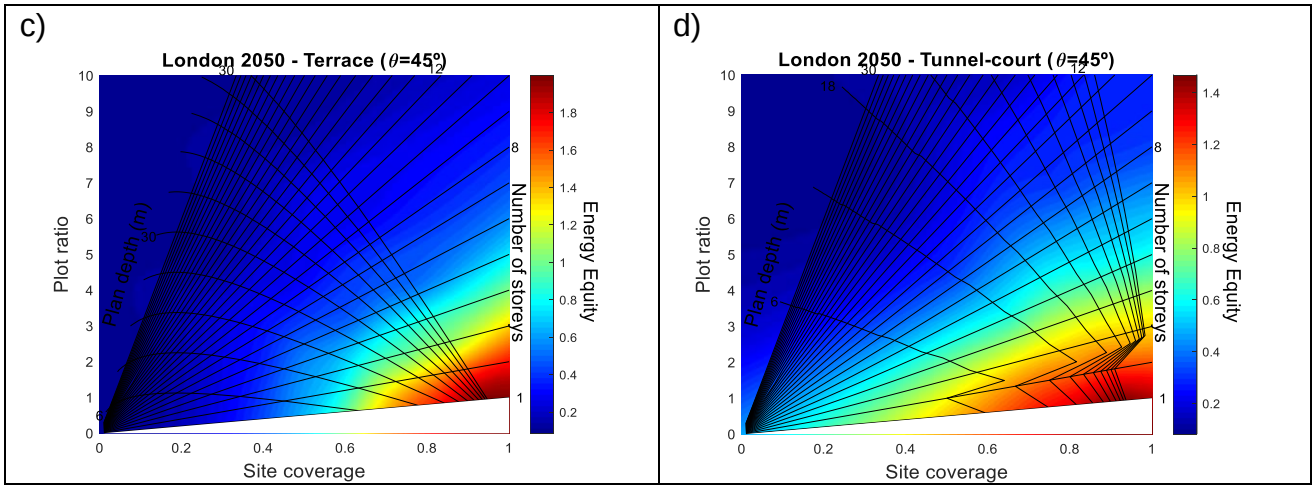

Figure 7.5: Correlation of Energy Equity indicator with urban built form and density for different built forms for London case study in 2050

The results indicated in Figure 7.5 demonstrate that buildings with greater plan depths and lower number of storeys will be still favourable in 2050 because of their greater potential for harvesting solar energy. Therefore, higher values of site coverage and lower values of plot ratio will be desirable. This conclusion is similar to the current situation of London (see Figure 5.15), however, the magnitude of Energy Equity will be smaller in 2050 for three reasons, i) buildings will require cooling energy due to global warming, ii) the use of EVs and their charging from building-mounted PVs, iii) the predicted climate scenario generated by Meteonorm (IPCC AR4 A2) indicates that PV energy generation in 2050 will be slightly lower than at present. The data obtained from the simulations in this study shows 0.6% reduction in annual PV energy generation from present to 2050 climatic conditions. This has resulted from disregarding the future development in PV technology that will certainly increase the PV energy efficiency. Otherwise, the annual PV energy generation in 2050 would be higher than the current scenario. Each of these act to reduce the Energy Equity of the buildings considered in Figure 7.5 compared with Figure 5.15. Overall, the results show that in this future scenario only one-storey buildings (regardless of their built form) are able to generate enough PV energy to supply the total energy demand of the building (i.e. obtaining Energy Equity>1).

To investigate the self-sufficiency of the buildings for generating enough electricity for charging EVs, the PV/EV ratio is defined as in Eqn (7.2) that excluded other types of energy demands except EV consumption.

$$0.27 \leq \frac{PV\ generation}{EV\ consumption} \leq 8.12 \qquad 7.2)$$

This ratio is equal to 8.12 for one-storey buildings and 0.27 for 30-storey building, regardless of the built form. The results show that the buildings with up to eight storeys are able to provide enough electricity for the total annual EV consumption of the occupants. While buildings with more than eight storeys possess a PV/EV ratio of lower than one.

To identify the impact of cut-off angle on building energy demand in 2050 and predict the optimum cut-off angle, the energy demand of plans of buildings with different cut-off angles are compared in Figure 7.6.

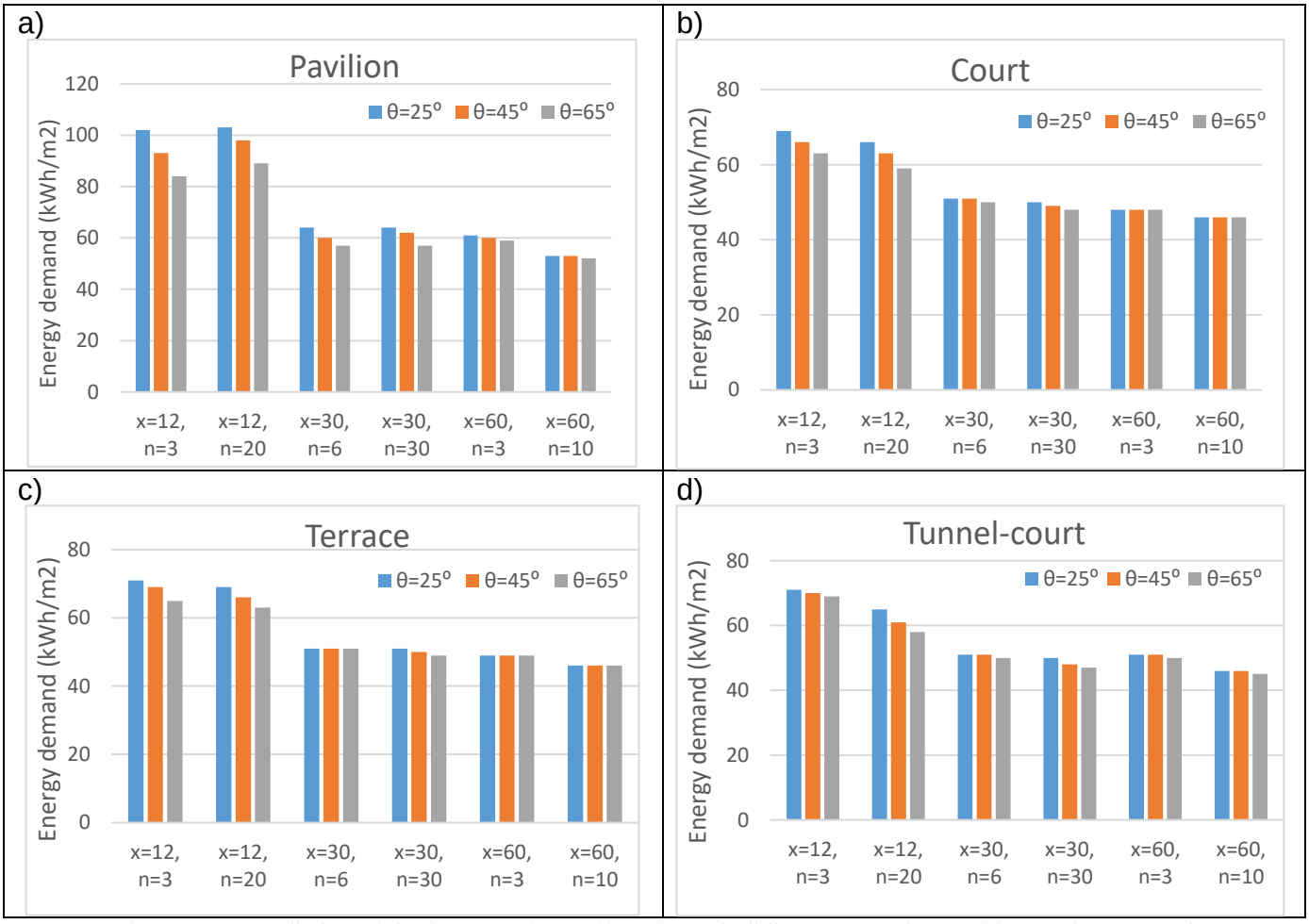

Figure 7.6: Prediction of the impact of cut-off angle on building energy demand in London 2050 a) Pavilion, b) Court, c) Terrace and d) Tunnel-court built form

As can be observed from Figure 7.6 that increasing the cut-off angle will mainly cause a reduction in building energy demand for buildings with small plan depth, while it does not make a significant impact in buildings with great plan depth. Therefore, the significant decreasing trend of building energy demand versus increasing cut-off angle in buildings with x=12m gradually diminishes to no change in buildings with x=60m. Only pavilion and tunnel-court built forms keep the decreasing trend of the building

energy demand for buildings with great depths, which still show ~2% decrease in building energy demand when the cut-off angle is varied between 25º to 65º.

By comparison with the results obtained from London case study in Chapter 5 (see Figure 5.14) which showed an increase in building energy demand with increasing cut-off angle, these now show the opposite trend. The reason behind this is the presence of cooling load for the future scenarios. As discussed in section 6.2.1.2 (Chapter 6), increasing cut-off angle would decrease the cooling load by blocking a larger portion of the solar energy received by the buildings. Although building energy demand is composed of heating, cooling, electricity and EV consumption (see Figure 7.8), only heating and cooling loads are affected by changing cut-off angle. The effect of increasing cut-off angle on the heating demand is opposite to its impact on the cooling demand (see Figure 6.14 of Chapter 6). It can be concluded from Figure 7.6 that in small depth buildings, the decrease in cooling load is more significant than the increase in heating load (which can be due to the ease of cross ventilation). Therefore, building energy performance acts as a cooling dominated system, though the absolute amount of heating energy demand is larger than the cooling energy demand as its heating to cooling ratio is normally higher than one (see Eqn 7.3). It shows an important point demonstrating that building cooling load is more sensitive than its heating load with respect to external changes such as varying the cut-off angle. In buildings with greater plan depths, the increase in heating demand and decrease in cooling demand almost neutralise each other and the total building energy demand does not show a significant variation against increasing cut-off angle.

The ratio of heating over cooling energy demand is an indicator that shows whether the building energy system is either heating or cooling dominated, and is directly dependent on the climatic conditions of the site location. It can be used for prediction of the building energy performance in different locations and a variety of site plans with different geometry and density. The maximum and minimum threshold of this ratio for the case of London in 2050 is shown in Eqn (7.3).

$$0.65 \leq \frac{Heating\ energy\ demand}{Cooling\ energy\ demand} \leq 9.65 \qquad 7.3)$$

This ratio of normally greater than one, reaching the values close to 10 at its maximum, except when considering a few cases of the pavilion form with very small plan depth (i.e. 12m) where the ratio is lower than one. This demonstrates that the

amount of heating load is significantly bigger than cooling load in a majority of the building plans in this case study and the buildings are heating dominated. However, as discussed earlier, cooling load is more sensitive to the outside environmental and play a key role in the response of building energy demand to the cut-off angle change (see Figure 7.6).

The ratio is larger for court and tunnel-court forms compared with pavilion and terrace forms. It also increases by increasing the plan depth, decreasing the number of storeys and increasing the cut-off angle. It means that having deep buildings with lower number of storeys ('shorter and fatter' buildings) along with a small distance between the buildings would result in a higher portion of heating demand with respect to cooling demand, and vice versa. Indeed, the combined effect of these three geometrical variables along with altering the built form can cause up to a 15 times change in the heating to cooling ratio of a building.

To analyse the energy performance of buildings with different built forms but similar geometrical parameters, the data obtained from energy simulation are compared and shown in Figure 7.7.

a)

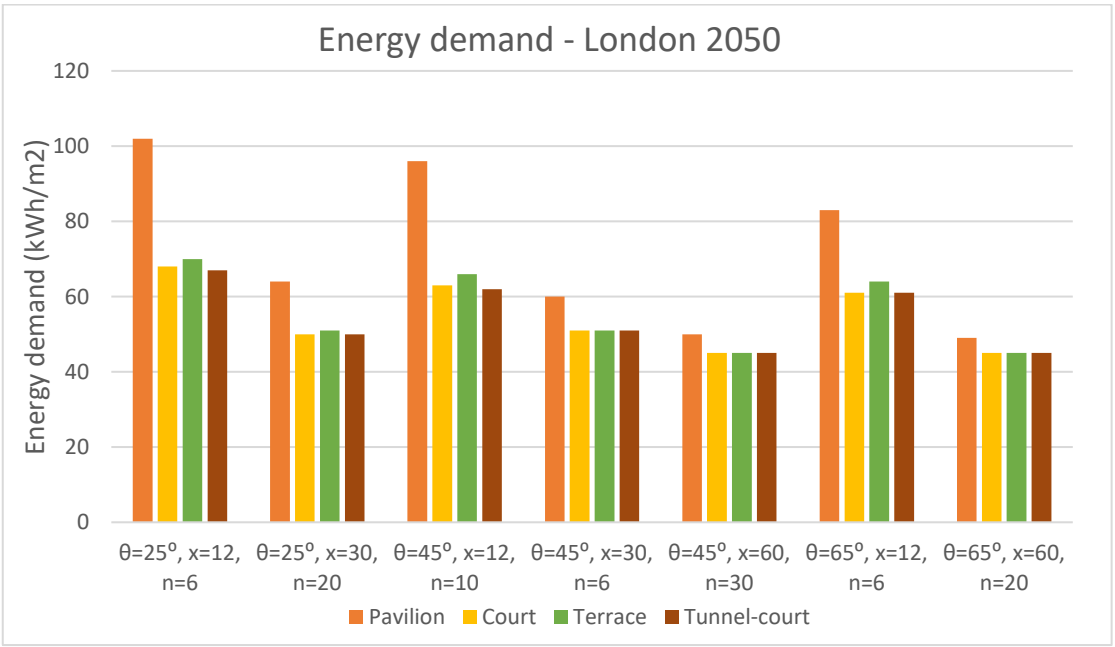

b)

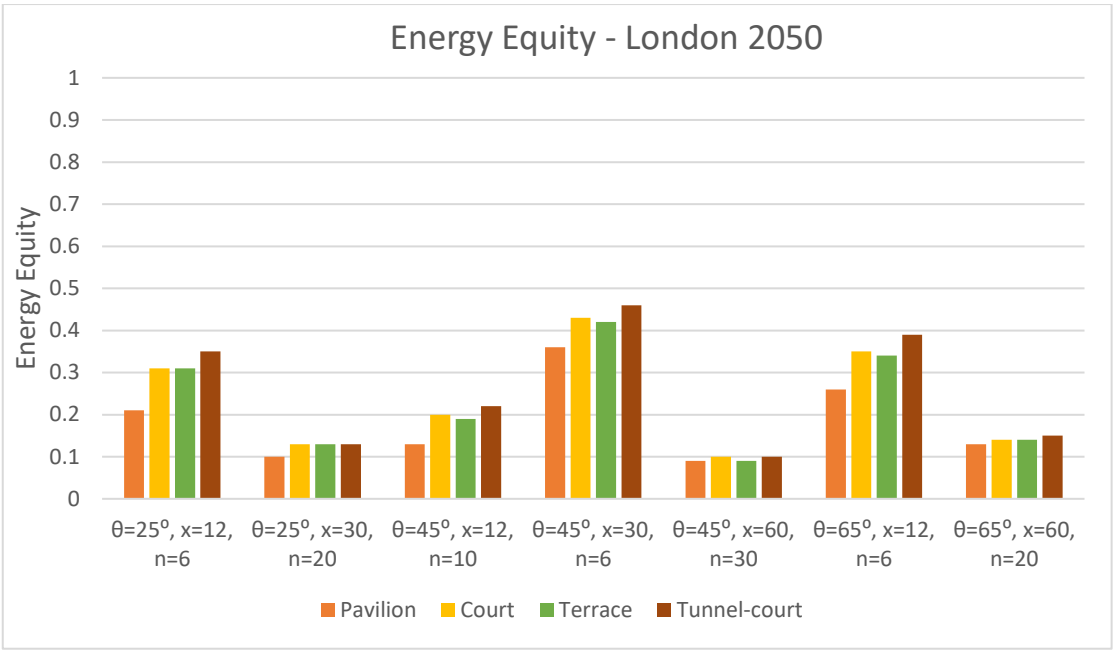

Figure 7.7: Comparison of the predicted building energy performance of the studied built forms with the same cut-off angles, plan depths and number of storeys in London 2050: a) energy demand b) Energy Equity

From Figure 7.7, it is observed that tunnel-court built form not only has the lowest energy demand, but also gains the highest value of Energy Equity among the other built forms. In contrast, pavilion form shows the poorest performance. The performance of terrace and court forms are worse than tunnel-court form but better than pavilion. The outcome of this comparative analysis is similar to the results obtained in Chapter 5 for current climatic conditions in London, but with a few important differences. Tunnel-court form showed higher energy demand than court and terrace forms in Chapter 5 (see Figure 5.16), while in this analysis it shows the lowest energy demand. Moreover, court and terrace forms had identical energy demand in Chapter 5 (Figure 5.16), while here, being very close to tunnel-court form, court form shows lower energy demand than terrace form. These two differences show that court and tunnel-court forms which both have an internal courtyard perform better when cooling energy load is considered in addition to heating. It suggests that these two built forms are energetically more advantageous for the future urban developments of London to cope with the changing climate. Meanwhile, the domination of the Energy Equity of the tunnel-court form compared to the other built forms will be more significant in 2050 (Figure 7.7) with respect to the current climate of London (Figure 5.18).

As shown in Chapter 5 (Table 5.3), having similar geometric variables does not mean that all the compared built forms have the same density. In fact, tunnel-court form acquires the highest density and pavilion gains the lowest density (see Figure

3.5). Hence, in the case of keeping density constant, the built forms would have different geometric variables and their ranking as a matter of energy performance may most probably change (see

Table 5.4).

7.3 Discussion and comparison

The resulting values obtained from the analysis of the future scenarios should be compared with the results obtained using the current climate of London in Chapter 5 to discover the differences between building energy performance in different built forms and densities now and in 2050. Therefore, building energy demand of eight sample cases are compared in the stacked bar chart shown in Figure 7.8.

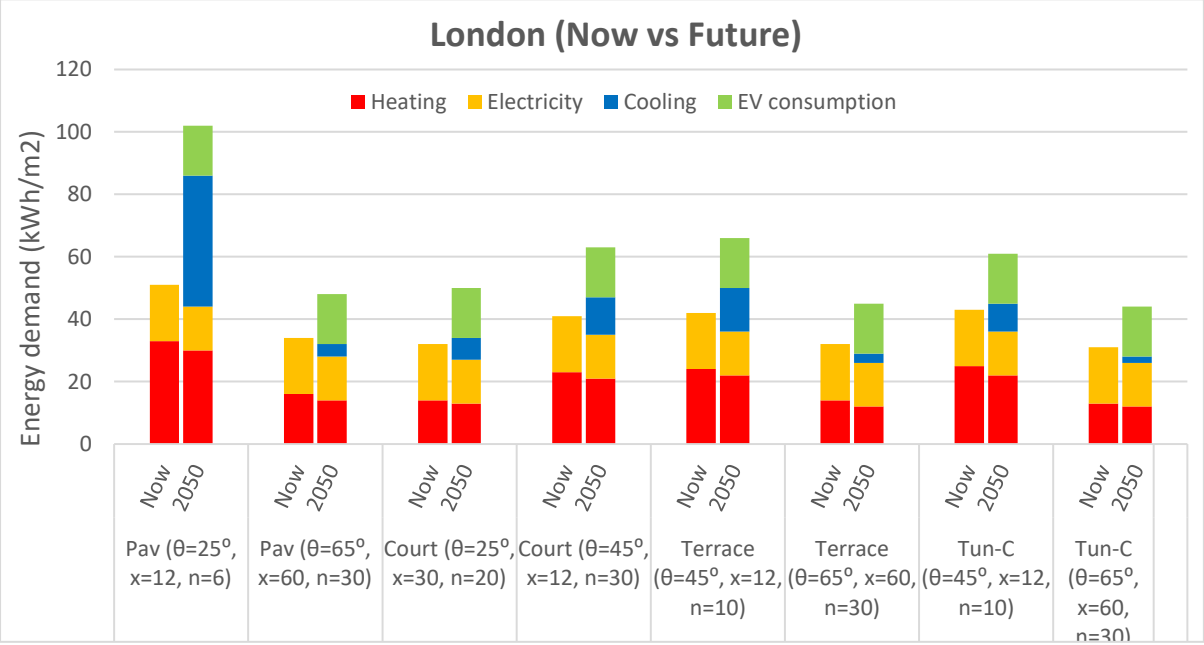

Figure 7.8: comparison between the current and future (2050) building energy consumption in London

From Figure 7.8, it can be seen that in all cases the total building energy demand in 2050 is significantly higher than now due to a number of reasons: an additional EV charging load has been added to the building load (shown in green). This is equal to 16 *kWh/m²/year* for all cases since it is calculated according to the number of the occupants (as explained in section 7.2.2) and since the occupant density is the same for all the cases, the value of EV consumption per m^2 is equal for all the cases; there is an additional cooling load (shown in blue) that was disregarded for the current scenario. On the other hand, the two other types of energy consumption are slightly reduced in 2050. i) The heating load (shown in red) is lower in the future scenario (between 8% and 15%) compared with the current scenario. ii) The electricity

consumption (shown in orange) is 18 *kWh/m²/year* for current and 14 *kWh/m²/year* for future scenarios due to consideration of technology advancement in home appliances energy efficiency (as mention in section 7.2).

On average, total building energy demand in 2050 is 48% higher than the current scenario due to the above-mentioned reasons. An exceptional case where future building energy demand is much higher than the current scenario (it is 100% higher) is the first case shown in the left side of Figure 7.8 (pavilion, θ=45º, x=12 and n=6). The reason is the large amount of cooling demand (i.e. 42 *kWh/m²/year*) that is significantly higher (3-21x) than the cooling demand in the other cases. Indeed, as a pavilion with small plan depth, its cooling load is higher than its heating load, which is one of the rare cases with a heating to cooling ratio of less than one (as explained in section 7.2.3).

Several studies in the literature confirmed that the overall building energy consumption will be higher in the future (Jylhä et al., 2015, Mangan and Oral, 2020, Wan et al., 2011). However, the percentage increase in previous studies is not as high as that obtained in this study. The reason is that in this study, the building is considered as 'prosumers' and generates PV electricity to supply energy for building energy demand including EV consumption. Therefore, EV energy demand is added to the overall energy consumption of the buildings in the future scenario. Furthermore, in this study, cooling load was not considered for current scenario, therefore, it gave more weight to the total energy demand of future scenario.

Other studies normally predicted lower heating demand and higher cooling demand for the future (Berger and Worlitschek, 2019, Jylhä et al., 2015, Kolokotroni et al., 2012, Mangan and Oral, 2020). Berger and Worlitschek (2019) predicted a 40% decrease of heating degree days and 1300% increase of cooling degree days for Switzerland. Mangan and Oral (2020) predicted that heating energy consumption in Istanbul will increase by 14% in 2030 and decrease by 39% and 53% in 2060 and 2090, respectively. Wan et al. (2011) also predicted a decreasing trend of building heating load for the variety of climatic conditions in China. The study by Kolokotroni et al. (2012) took London as the case study and predicted a reduction in heating demand in 2050 due to higher external temperatures, though they considered office buildings and not residential buildings.

It should be noted that different studies have used different climate data sources that can cause divergence in the simulation results due to the predictive nature of the

climate data for future. For instance, the weather file used by Wan et al. (2011) includes information about dry-bulb temperature, wet-bulb temperature, global solar radiation, wind speed and wind direction. However, the weather file used for this study contains additional information regarding cloud cover fraction, precipitation, surface temperature and diffused horizontal radiation. These parameters can change the predicted climatic conditions and add more precision to the energy analysis results. Moreover, Kolokotroni et al. (2012) used UKCIP02 weather files that were available at the time of their study and they mentioned that the resulting weather files for 2050s may overestimate the impact of climate change. Having considered the weather file generated by Meteonorm for this thesis, it shows that during the heating season the hourly air temperature in 2050 is not necessarily always higher than the weather file generated for the current climate case. It can be seen that for some days (and nights) in the future, the weather shows higher temperatures and in others it is opposite. There are also more fluctuations between the temperature of daytime and nighttime in 2050. Moreover, as mentioned in section 7.2.3, the simulations result of this study confirmed that, considering the similar PV panel models, the amount of PV energy generation in 2050 is 0.6% lower than the current situation (which had a lowering effect on the Energy Equity). This can be due to consideration of nebulosity in the Meteonorm weather file which will be an important parameter to be considered for the future as more extreme weather is expected.

Eyre and Baruah (2015) presented new scenarios for residential energy use in the UK to 2050 by considering the factors such as population and some systemically different approaches for delivering residential heat energy, and concluded that the future of UK residential space heating is very uncertain. The current building form and urban density of the neighborhoods can lead to an increase in the energy demand (Perera et al., 2021). It should be also mentioned that reducing cooling demand is more important than reducing heating demand in terms of environmental impact, even in a heating dominated climate since providing cooling energy contributes to greater greenhouse gas emissions (Kolokotroni et al., 2012). Therefore, to produce less emissions in the future of London built environment, deep plan court and tunnel-court buildings with lower number of storeys and great cut-off angle are recommended.

7.4 Conclusion

The climate is changing across the globe due to the global warming phenomenon that, together with technological developments, will impact on city energy consumption including building and transportation energy demand. This chapter considers a London case study to analyse the future scenario of changing climate and the penetration of EVs into the transportation network by 2050 (following the UK government commitments). In this chapter, the IPCC AR4 A2 scenario for climate change is chosen and the relevant weather file is obtained from Meteonorm software. It is adopted by CitySim for energy simulation of the same building plans as used in Chapter 5. Moreover, the number of EVs per occupants is calculated to estimate their yearly energy consumption. It is assumed that they are charged by building-mounted PVs, hence, their energy demand is added to the overall energy demand of the buildings.

The results indicate that, in 2050, buildings with greater plan depth and lower number of storeys (being equivalent to high site coverage and low plot ratio) acquire higher values of Energy Equity that increase the possibility of building energy self-sufficiency. Although this trend is similar to the current scenario, the magnitude of Energy Equity is considerably lower in the future scenario because of i) an extra cooling load, ii) added EV's to the building load. Unlike the current climate of London, increasing cut-off angle mainly leads to a reduction in energy demand (with no effect on the buildings with great plan depth) that shows the impact of having cooling load in the building energy demand. It is also concluded that the building cooling load is more sensitive against the external environment changes such as varying the cut-off angle compared with the building heating load.

Having similar geometry, the tunnel-court form indicates the highest Energy Equity and the lowest energy demand, while the pavilion form shows the poorest performance. Generally, court and tunnel-court forms show better energy performance in future climate scenarios compared with their performance in the current climate. Therefore, it can be suggested that for the future urban developments of London, these two built forms are energetically more advantageous to cope with the changing climate.

Finally, results of simulation trials indicate that the total building energy demand in 2050 is 48% higher, on average, than in the current climate, as a result of additional cooling load and EV energy consumption to the building energy demand. This increase

is much higher for the buildings with low heating to cooling ratio, which is the product of some specific combination of built form, density and geometrical parameters. For instance, it happens for the buildings with small plan depth, low cut-off angle and high number of storeys, where their effect is magnified in pavilion and terrace forms. Hence, the results from this chapter recommend that these configurations should be avoided for upcoming urban development of London to avoid excessive building cooling demand in the future that has the higher contribution in environmental pollution compared with heating demand.

Chapter 8: Conclusions, recommendations, and future works

8.1 Introduction

The primary conclusions from this thesis are now outlined, along with recommendations and proposed future work. This study has established the relationships between urban built form and density with energy flows in cities through analysis of relative building energy demand and the potential impact of PV energy harvesting. This necessarily requires consideration of climatic conditions, which are therefore included in the analyses. A combination of empirical and quantitative research methods is adopted including the development of geometrical models of the chosen built forms as well as energy simulation trials. The main findings are outlined next.

8.2 Main findings

A critical literature review (primarily Chapters 1 and 2) shows that there remains a debate on the relative merits of compact cities versus urban sprawl development, particularly with regard to energy consumption and renewable energy generation. Moreover, it is notable that an acceptable common definition of urban density has yet to be addressed appropriately. Previous studies have used a variety of density indicators that make it difficult to directly compare results. Furthermore, the influence of the urban built form, which affects building energy demand, has not previously been considered in combination with urban density and their impact on the future adoption of PVs for energy harvesting. This thesis argued that not only more than one density indicators are required to effectively address the definition of urban density, but also their interrelationship with urban built form is an important consideration. It also argued that the form and density of future urban areas should be determined by consideration of developing and future technologies (e.g. PVs and EVs).

8.2.1 Conclusions

The mentioned arguments identified the objectives of the thesis as the main milestones of this study leading to the following conclusions.

8.2.1.1 Relationship of urban built form with density

To meet the first objective of this thesis, the relationship between urban built form and density was established by developing geometric models of four urban built forms

and analysing them with respect to two density indicators (Chapter 3). This resulted in the development of the *Form Signature* framework as one of the main contributions of this thesis. It determines the simultaneous correlation between urban built form, density and geometrical variables of the site plan. The *Form Signature* provides a structure for connecting different urban sustainability elements (i.e. environmental, economic and social factors) with urban built form and density. From the *Form Signature* graphs it is proven that having taller buildings does not necessarily lead to higher density—and can increase one density indicator, while decreasing the other. Therefore, careful consideration is necessary when using the phrase 'high-density' as subsequent outcomes are shown to be highly dependent on the choice of density indicator. A key contribution has been the introduction of the tunnel-court built form and its relative merits in terms of land-use and energy performance when compared with other popular built forms.

8.2.1.2 Relationship of energy with urban built form and density

Following the statements of objectives 2 and 3 of the thesis (Chapter 1), the correlation of building energy performance with urban built form and density was analysed in Chapter 5. To this end, the energy performance (energy demand plus PV generation) of more than 200 site plans with different geometries were simulated using the CitySim urban energy simulation tool and the results overlaid on the *Form Signature* graphs. This was done for the temperate climate of London. Furthermore, as a contribution of this study, an energy indicator termed Energy Equity is introduced which considers the ratio of building energy demand and PV energy harvesting.

The main conclusions are:

- The geometrical variables of the built forms have a significant effect on building energy performance. By increasing number of storeys and plan depth (i.e. low plot ratios and medium to high site coverages), energy demand is reduced, while increasing cut-off angle (equivalent to increasing both density indicators) results in an increase of energy demand. Nevertheless, the Energy Equity of buildings with a lower number of storeys and greater plan depths, are higher (i.e. high values of site coverage and low values of plot ratio), that means those buildings can reach energy self-sufficiency or even provide an energy surplus. It highlights the fact that

consideration of developing technologies (i.e. renewables) will change the geometry and density of the optimum urban developments.

- When comparing the built forms, if geometrical variables are similar, tunnel-court form showed the best energy performance and pavilion form showed the worst. Nevertheless, having similar geometrical variables does not mean they have the same density. Hence, if the density is to be similar, pavilion form is the best case and tunnel-court form is the worst. This highlights the important of urban policies on recognition of the best built form and density in urban areas.
- A very important conclusion from this study is that it is possible to have site plans with similar built forms and densities but with different energy performance since the same value of density can be achieved by different combinations of geometrical variables. Hence, it is critical to simultaneously consider urban density and geometrical variables of the site plans to make a true comparisons of energy performances. This is an inherent feature of the developed *Form Signature* graphs.

Hence, a primary contribution is the proposal of a novel urban energy planning tool (based on the *Form Signature*) to help urban planners and policymakers to determine the most appropriate energy-efficient built form and density for temperate climatic conditions which is extended to other climates in Chapter 6.

8.2.1.3 Impact of climate on determining the most appropriate built form and density

Climate is an important factor that impacts building energy demand and generation. It also can make an influence on the emergence of the specific built form and density in cities. Therefore, to address objective 4 in this thesis, the effect of climate on the relationship of energy with urban built form and density is investigated using four case studies relating to four different climatic environments (Chapter 6). The outcomes of the study are:

- The trend of change of energy demand and Energy Equity on the *Form Signature* graphs are similar for all case studies. Moreover, building energy demand can be reduced by increasing cut-off angle in Singapore (between 8% and 56%) and Phoenix (between 6% and 47%) type climates (where buildings mainly demand cooling load), although it rises in London

(between 2.5% and 16.5%) and Helsinki (between 2% and 12%) where buildings mainly demand heating load. It indicates the more significant impact of cut-off angle on building energy demand in hotter climates.

- Annual building energy demand is the lowest in London, followed by Helsinki and Phoenix, respectively, and Singapore shows the highest energy demand. However, when PV generation is additionally considered, London achieves the highest value of Energy Equity, followed by Phoenix (up to 20% lower than London), while Singapore (up to 48% lower than London) and Helsinki (up to 51% lower than London) have the lowest Energy Equity.

The results highlight that varying urban density and geometry has a different impact on the building energy performance depending on the associated climate. Therefore, urban planning guidelines should be adjusted according to the climatic conditions.

8.2.1.4 Consideration of the future scenarios

Considering the changing climate and penetration EVs into the transportation system, buildings will require higher energy in 30 years' time for London's temperate climate. The results of this study (Chapter 7) shows that court and tunnel-court forms will be more energetically sustainable solutions. Meanwhile, buildings with lower number of storeys, greater plan depth and cut-off angle are more energy efficient for future climatic conditions and technological developments in London.

8.2.2 Contributions to urban planning and policy making

This study contributes to the understanding of the intercorrelation of important parameters that create the physical shape of cities, which led to the emergence of the *Form Signature* tool. This, together with building energy analysis, has provided guidelines for urban energy planning. Recommendations for policymakers, urban planners, practitioners and other professionals when developing future urban areas as a result of the work carried out in this thesis, are as follows:

1. Although many studies and governmental documents simply use density or other parameters such as building height for directing urban developments, it has been shown that at least two urban density indicators and all three influential geometrical variables (plan depth, cut-off angle and number of storeys) must be considered, and the *Form Signature* graphs allow this in a concise graphical

format. These allow a true comparison between the energy performance of different urban built forms with different densities and determine an optimum design point.

2. Existed urban areas may not be efficient or have enough capacity to digest the future changes. It is very important to consider developing and future technologies (e.g. renewable energy technologies), the emergence of more efficient isolating materials, penetration of EVs in the market and changing climatic conditions when considering future urban developments. This study recommends court and tunnel-court built forms with shorter and wider buildings and lower distance from each other for the future of London. Furthermore, the presence of predictive models for farer future is also beneficial such as the models that consider 'flying cars' as the main mean of urban transportation in the future.
3. In this study, tunnel-court built form is introduced and demonstrated the best energy performance among the other built forms when geometric variables are kept similar. However, whilst yet to be widely adopted, the results in this study show it can have substantial implications for building energy usage (up to 22% and 63% lower energy demand compared with pavilion in heating dominated and cooling dominated buildings, respectively), where it can provide an energy efficient and environmentally sustainable built form subject to economic viability of its construction, efficiency of its embodied energy consumption and occupant satisfaction of its livability.
4. The higher significance of the difference between Energy Equity of tunnel-court and pavilion forms in cooling-dominated buildings (between 27% and 67%) compared with heating-dominated buildings (between 7% and 32%) emphasises the higher importance of choice of built form in hotter climates.

8.3 Future work

Despite the multi-variable analysis adopted in this research, the study has potential to be extended in a number of ways. Here, several prospective research directions are proposed:

1. The urban energy planning tool presented in this study (the *Form Signature* plus energy analysis results) can be developed into a digital/on-line tool. All the required data is available and the known parameters can be inputted into the

tool (e.g. climate, recommended density or maximum allowed building height) and the remaining unknown parameters (e.g. the most suitable built form or estimation of building energy demand) exported from the tool.

2. Considering the United Nations sustainable development goals (United Nations, 2015), this study contributes to five of the 17 goals including *Affordable and Clean Energy*, *Sustainable Cities and Communities*, *Climate Action* and *Life on Land*. The remaining goals can be subject of the future studies. The *Form Signature* graphs have a substantial potential to be linked to the main components of sustainability; environmental, economic and social (e.g. user satisfaction including comfort, health etc.). The tool can be further developed by overlaying results of city scale economic and social analysis on the graphs. For instance, the correlation of human pathology or certain types of crime with built form and density can be analysed in specific cities. At the time of writing this thesis, we are in the midst of a global COVID-19 pandemic and the results could be used for a study of the occurrence of COVID-19 infections and its correlation with built form/density. The outcome may promote the use of lower density urban developments since 'social distancing' may be more achievable. A question to pose here is that could this suggest 'good' and 'bad' built form and densities? Therefore, discovering the above-mentioned correlations assists planners and policymakers for more sustainable building design and urban planning. Furthermore, to discover the possible relationship of climate with urban parameters, the limited number of case studies considered in Chapter 3 can be extended to a greater number from around the world, followed by conducting a statistical analysis.
3. Only PV energy harvesting has been considered for this study. The possibility of using other types of renewable energies such as roof-mounted micro wind turbines, geothermal heat pump and biomass can be examined by adaptation of the presented methods. This would identify which types of renewable technologies are most efficient in urban areas (with different built forms and densities) subject to different climates.
4. More work can be undertaken to enhance the underpinning modelling sections. For instance, consideration of multi-zone thermal analysis along with an adaptation of a CFD analysis tool will lead to more precise results. Meanwhile, calculation of energy usage by domestic hot water or type of equipment like an

elevator (specifically for taller buildings) will add more load to the energy demand of the buildings, though it may not cause a significant difference in an overall trend of the comparative analyses.

5. Finally, this study focused on the operational energy of buildings, however, the effect of embodied energy of buildings is also important to be considered (using a life cycle assessment) when determining the sustainability of buildings. This may be more relevant in taller buildings with more material and additional equipment.

References

2010. Code for Sustainable Homes

Technical Guide. Department for Communities and Local Government.

ABERGEL, T., DULAC, J., HAMILTON, I., JORDAN, M. & PRADEEP, A. 2019. Global Status Report for Buildings and Construction: Towards a zero-emissions, efficient and resilient buildings and construction sector. International Energy Agency, Global Alliance for Buildings and Construction, UN environment programme.

ADAMS, C. 2019. *Ergonomic Lighting Levels by Room for Residential Spaces* [Online]. Available: https://www.thoughtco.com/lighting-levels-by-room-1206643 [Accessed 2020].

AHMADIAN, E., BYRD, H., SODAGAR, B., MATTHEWMAN, S., KENNEY, C. & MILLS, G. 2019a. Energy and the form of cities: the counterintuitive impact of disruptive technologies. *Architectural Science Review,* 62**,** 145-151.

AHMADIAN, E. & SCHMIDT, R.-R. 2020. Exergy analysis of district energy systems and comparison of their exergetic, energetic and environmental performance. *International Journal of Exergy,* 32**,** 103-129.

AHMADIAN, E., SODAGAR, B., BINGHAM, C., ELNOKALY, A. & MILLS, G. 2021. Effect of urban built form and density on building energy performance in temperate climates. *Energy and Buildings***,** 110762.

AHMADIAN, E., SODAGAR, B., MILLS, G. & BINGHAM, C. Correlation of urban built form, density and energy performance. Journal of Physics: Conference Series, 2019b. IOP Publishing, 012005.

AHMADIAN, E., SODAGAR, B., MILLS, G., BYRD, H., BINGHAM, C. & ZOLOTAS, A. 2019c. Sustainable cities: The relationships between urban built forms and density indicators. *Cities,* 95.

AHVENNIEMI, H., HUOVILA, A., PINTO-SEPPÄ, I. & AIRAKSINEN, M. 2017. What are the differences between sustainable and smart cities? *Cities,* 60**,** 234-245.

AL QADI, S. B., ELNOKALY, A. & SODAGAR, B. Predicting the energy performance of buildings under present and future climate scenarios: lessons learnt. 2017. Conference Paper· May 2017 Conference: FIRST INTERNATIONAL CONFERENCE ON ….

ALBINO, V., BERARDI, U. & DANGELICO, R. M. 2015. Smart cities: Definitions, dimensions, performance, and initiatives. *Journal of Urban Technology,* 22**,** 3-21.

AMOAKO-ATTAH, J. & BAHADORI-JAHROMI, A. 2013. Impact of future climate change on UK building performance. *Advances in environmental research,* 2**,** 203-227.

APPAVOU, F., BROWN, A., EPP, B., LEIDREITER, A., LINS, C., MURDOCK, H., MUSOLINO, E., PETRICHENKO, K., FARRELL, T. & KRADER, T. 2017. Renewables 2017 global status report. *Renewable Energy Policy Network for the 21st Century. Paris: REN21.*

APPROVED DOCUMENT PART F 2010. The Building Regulations Part F, Ventilation. *Crown Copyright, London*.

APPROVED DOCUMENT PART L1A 2016. The Building Regulations Part L1A, Conservation of fuel and power. *Publ. by NBS, UK*.

ARBABI, H. & MAYFIELD, M. 2016. Urban and Rural—Population and Energy Consumption Dynamics in Local Authorities within England and Wales. *Buildings,* 6**,** 34.

ARORA, K., DIU, S. & ROPER, J. 2016. Solar PV on commercial buildings
A guide for owners and developers. *In:* CENTRE, B. N. S. (ed.).
ARUNDEL, R. & RONALD, R. 2017. The role of urban form in sustainability of community: The case of Amsterdam. *Environment and Planning B: Urban Analytics and City Science,* 44**,** 33-53.
ASCIONE, F., DE MASI, R. F., DE ROSSI, F., FISTOLA, R., SASSO, M. & VANOLI, G. P. 2013. Analysis and diagnosis of the energy performance of buildings and districts: Methodology, validation and development of Urban Energy Maps. *Cities,* 35**,** 270-283.
ASHRAE STANDARD 2010. Standard 62.1-2010 (2010). ventilation for acceptable indoor air quality, atlanta, ga. American Society of Heating, Refrigerating and Air-Conditioning Engineers, Inc.
ATTIA, S., HENSEN, J. L., BELTRÁN, L. & DE HERDE, A. 2012. Selection criteria for building performance simulation tools: contrasting architects' and engineers' needs. *Journal of Building Performance Simulation,* 5**,** 155-169.
BAKER, N. & STEEMERS, K. 2003. *Energy and environment in architecture: a technical design guide*, Taylor & Francis.
BALL, M. 2011. RICS European housing review 2003. Royal Institution of Chartered Surveyors United Kingdom.
BANISTER, D., WATSON, S. & WOOD, C. 1997. Sustainable cities: transport, energy, and urban form. *Environment and Planning B: planning and design,* 24**,** 125-143.
BANSAL, P., VINEYARD, E. & ABDELAZIZ, O. 2011. Advances in household appliances-A review. *Applied Thermal Engineering,* 31**,** 3748-3760.
BARRETT, S., WILLS, J. & WASHINGTON-IHIEME, M. 2020. *Reclaim the kerb: The future of parking and kerbside management* [Online]. Center for London. Available: https://www.centreforlondon.org/reader/parking-kerbside-mangement/chapter-1/#car-ownership-in-london-has-changed-little-over-time [Accessed January 2021].
BATTY, M. 2013. *The new science of cities*, MIT press.
BATTY, M. 2017. Cities in disequilibrium. *Non-Equilibrium social science and policy.* Springer, Cham.
BEN, H. & STEEMERS, K. 2014. Energy retrofit and occupant behaviour in protected housing: A case study of the Brunswick Centre in London. *Energy and Buildings,* 80**,** 120-130.
BERGER, M. & WORLITSCHEK, J. 2019. The link between climate and thermal energy demand on national level: A case study on Switzerland. *Energy and Buildings,* 202**,** 109372.
BERGHAUSER PONT, M. & HAUPT, P. 2007. The Spacemate: density and the typomorphology of the urban fabric. *Urbanism laboratory for cities and regions: progress of research issues in urbanism.*
BERKELEY GROUP. 2020. Available: https://www.berkeleygroup.co.uk/ [Accessed 2020].
BHIWAPURKAR, P. Determinants of Urban Energy Use: Density and Urban Form. ARCC Conference Repository, 2014.
BOCCALATTE, A., FOSSA, M., GAILLARD, L. & MENEZO, C. 2020. Microclimate and urban morphology effects on building energy demand in different European cities. *Energy and Buildings,* 224**,** 110129.

BORG, S. P. & KELLY, N. 2011. The effect of appliance energy efficiency improvements on domestic electric loads in European households. *Energy and Buildings,* 43**,** 2240-2250.
BOUKARTA, S. & BEREZOWSKA, E. 2017. Exploring the Energy Implication of Urban Density in Residential Buildings. *Journal of Applied Engineering Sciences,* 7**,** 7-14.
BREHENY, M. 1995. The compact city and transport energy consumption. *Transactions of the institute of British Geographers,* 20**,** 81-101.
BURRELL, E. 2015. *What is the Heat Loss Form Factor?* [Online]. Available: https://elrondburrell.com/blog/passivhaus-heatloss-formfactor/ [Accessed 2021].
BYRD, H. 2012. The case for policy changes in New Zealand housing standards due to cooling and climate change. *Journal of Environmental Policy & Planning,* 14**,** 360-370.
BYRD, H. 2017. The Power of Subarbia. *In:* BERGER, A., KOTKIN, J. & GUZMAN, C. B. (eds.) *Infinite Suburbia.* New York: Princeton Architectural Pres.
BYRD, H., HO, A., SHARP, B. & KUMAR-NAIR, N. 2013. Measuring the solar potential of a city and its implications for energy policy. *Energy policy,* 61**,** 944-952.
BYRD, H. & MATTHEWMAN, S. 2014. Exergy and the city: the technology and sociology of power (failure). *Journal of Urban Technology,* 21**,** 85-102.
CAO, X., DAI, X. & LIU, J. 2016. Building energy-consumption status worldwide and the state-of-the-art technologies for zero-energy buildings during the past decade. *Energy and buildings,* 128**,** 198-213.
CASINI, M. 2016. Small vertical axis wind turbines for energy efficiency of buildings. *Journal of Clean Energy Technologies,* 4**,** 56-65.
CHAN, A. 2012. Effect of adjacent shading on the thermal performance of residential buildings in a subtropical region. *Applied energy,* 92**,** 516-522.
CHARLES, E. 2019. *Solar Panel Specifications: Reading a Solar Panel Datasheet* [Online]. Available: https://blog.spiritenergy.co.uk/contractor/solar-panel-specifications [Accessed 2019].
CHATTERJEE, S. & KAR, A. K. Smart Cities in developing economies: A literature review and policy insights. 2015 International Conference on Advances in Computing, Communications and Informatics (ICACCI), 2015. IEEE, 2335-2340.
CHATZIPOULKA, C., COMPAGNON, R. & NIKOLOPOULOU, M. 2016. Urban geometry and solar availability on façades and ground of real urban forms: using London as a case study. *Solar Energy,* 138**,** 53-66.
CHEN, H., JIA, B. & LAU, S. 2008. Sustainable urban form for Chinese compact cities: Challenges of a rapid urbanized economy. *Habitat international,* 32**,** 28-40.
CHEN, Y.-J., MATSUOKA, R. H. & LIANG, T.-M. 2018. Urban form, building characteristics, and residential electricity consumption: A case study in Tainan City. *Environment and Planning B: Urban Analytics and City Science,* 45**,** 933-952.
CHENG, V. 2009. Understanding density and high density. *Designing High-Density Cities.* Routledge.
CHENG, V., DESHMUKH, S., HARGREAVES, A., STEEMERS, K. & LEACH, M. A study of urban form and the integration of energy supply technologies. World Renewable Energy Congress-Sweden; 8-13 May; 2011; Linköping; Sweden, 2011. Linköping University Electronic Press, 3356-3363.

CHENG, V., STEEMERS, K., MONTAVON, M. & COMPAGNON, R. Urban form, density and solar potential. PLEA 2006, 2006.
CHIESA, G. & GROSSO, M. 2015. The influence of different hourly typical meteorological years on dynamic simulation of buildings. *Energy Procedia,* 78**,** 2560-2565.
CHUA, K. & CHOU, S. 2010. Energy performance of residential buildings in Singapore. *Energy,* 35**,** 667-678.
CHURCHMAN, A. 1999. Disentangling the concept of density. *Journal of Planning Literature,* 13**,** 389-411.
CIBSE GUIDE A 2019. Environmental design. The Chartered Institution of Building Services Engineers.
CIBSE GUIDE B1 2016. Heating. The Chartered Institution of Building Services Engineers.
CIBSE GUIDE F 2012. Energy Efficiency in Buildings: CIBSE Guide F. Chartered Institution of Building Services Engineers.
CIBSE TM46 2008. Energy benchmarks. The Chartered Institution of Building Services Engineers.
CLEVENGER, C. M. & HAYMAKER, J. The impact of the building occupant on energy modeling simulations. Joint International Conference on Computing and Decision Making in Civil and Building Engineering, Montreal, Canada, 2006. Citeseer, 1-10.
COCCOLO, S., KÄMPF, J. H. & SCARTEZZINI, J.-L. Design in the desert. A Bioclimatic project with urban energy modelling. Proceedings of building simulation, 2013.
COCCOLO, S., MONNA, S., KAEMPF, J. H., MAUREE, D. & SCARTEZZINI, J.-L. 2016. Energy demand and urban microclimate of old and new residential districts in a hot arid climate. *36th International Conference on Passive and Low Energy Architecture.* Los Angeles.
COLLINS, L., NATARAJAN, S. & LEVERMORE, G. 2010. Climate change and future energy consumption in UK housing stock. *Building Services Engineering Research and Technology,* 31**,** 75-90.
CRAWLEY, D. B., HAND, J. W., KUMMERT, M. & GRIFFITH, B. T. 2008. Contrasting the capabilities of building energy performance simulation programs. *Building and environment,* 43**,** 661-673.
CRESWELL, J. W. & TASHAKKORI, A. 2007. Differing perspectives on mixed methods research. Sage Publications Sage CA: Los Angeles, CA.
CROBU, E., LANNON, S. C., RHODES, M. & ZAPATA-LANCASTER, M. 2013. Simple simulation sensitivity tool.
DAFTLOGIC. *List of the Power Consumption of Typical Household Appliances* [Online]. Available: https://www.daftlogic.com/information-appliance-power-consumption.htm [Accessed 2020].
DCLG 2006. Planning policy statement 3: Housing. Department for Communities and Local Government London.
DEBBAGE, N. & SHEPHERD, J. M. 2015. The urban heat island effect and city contiguity. *Computers, Environment and Urban Systems,* 54**,** 181-194.
DEFOREST, N., SHEHABI, A., SELKOWITZ, S. & MILLIRON, D. J. 2017. A comparative energy analysis of three electrochromic glazing technologies in commercial and residential buildings. *Applied energy,* 192**,** 95-109.
DELMASTRO, C., MUTANI, G., SCHRANZ, L. & VICENTINI, G. 2015. The role of urban form and socio-economic variables for estimating the building energy

savings potential at the urban scale. *International Journal of Heat and Technology,* 33**,** 91-100.
DENG, W., PENG, Z. & TANG, Y.-T. 2019. A quick assessment method to evaluate sustainability of urban built environment: Case studies of four large-sized Chinese cities. *Cities,* 89**,** 57-69.
DEPARTMENT FOR TRANSPORT 2018. The Road to Zero: Next Steps Towards Cleaner Road Transport and Delivering our Industrial Strategy. Department of Transport.
DIELEMAN, F. & WEGENER, M. 2004. Compact city and urban sprawl. *Built Environment,* 30**,** 308-323.
DOHERTY, M., NAKANISHI, H., BAI, X. & MEYERS, J. 2009. Relationships between form, morphology, density and energy in urban environments. *GEA Background Paper,* 28.
DREW, D., BARLOW, J. & COCKERILL, T. 2013. Estimating the potential yield of small wind turbines in urban areas: A case study for Greater London, UK. *Journal of Wind Engineering and Industrial Aerodynamics,* 115**,** 104-111.
DU, P., WOOD, A., DITCHMAN, N. & STEPHENS, B. 2017. Life Satisfaction of Downtown High-Rise vs. Suburban Low-Rise Living: A Chicago Case Study. *Sustainability,* 9**,** 1052.
DURSUN, D. & YAVAS, M. 2015. Climate-sensitive urban design in cold climate zone: the City of Erzurum, Turkey. *International Review for Spatial Planning and Sustainable Development,* 3**,** 17-38.
EASTON, M. 2017. How much of your area is built on? : BBC NEWS.
ECHENIQUE, M. H., HARGREAVES, A. J., MITCHELL, G. & NAMDEO, A. 2012. Growing cities sustainably: does urban form really matter? *Journal of the American Planning Association,* 78**,** 121-137.
ELECTRIC VEHICLE DATABASE. 2021. *Energy consumption of electric vehicles* [Online]. Electric Vehicle Database. Available: https://ev-database.uk/cheatsheet/energy-consumption-electric-car [Accessed January 2021].
ELECTRICITYUSECALCULATOR. *Electricity usage of a Desktop Computer* [Online]. Available: http://energyusecalculator.com/electricity_computer.htm [Accessed 2020].
ELJOJO, A. K. 2017. Effect of windows size, position and orientation on the amount of energy needed for winter heating and summer cooling. *Journal of Engineering Research and Technology,* 1**,** 1-8.
ELMOKADEM, A. A., MEGAHED, N. A. & NOAMAN, D. S. 2016. Systematic framework for the efficient integration of wind technologies into buildings. *Frontiers of Architectural Research,* 5**,** 1-14.
ELNOKALY, A., AYOUB, M. & ELSERAGY, A. 2019. Parametric investigation of traditional vaulted roofs in hot-arid climates. *Renewable Energy,* 138**,** 250-262.
EMERY, A. & KIPPENHAN, C. 2006. A long term study of residential home heating consumption and the effect of occupant behavior on homes in the Pacific Northwest constructed according to improved thermal standards. *Energy,* 31**,** 677-693.
EMMANUEL, R. & STEEMERS, K. 2018. Connecting the realms of urban form, density and microclimate. *Building Research & Information,* 48**,** 804-808.
EST. 2020. *On the path to net zero: Transport* [Online]. Energy Saving Trust. Available: https://energysavingtrust.org.uk/path-net-zero-transport/ [Accessed January 2021].

EVANS, S., LIDDIARD, R. & STEADMAN, P. 2017. 3DStock: A new kind of three-dimensional model of the building stock of England and Wales, for use in energy analysis. *Environment and Planning B: Urban Analytics and City Science,* 44**,** 227-255.
EWING, R. & RONG, F. 2008. The impact of urban form on US residential energy use. *Housing policy debate,* 19**,** 1-30.
EYRE, N. & BARUAH, P. 2015. Uncertainties in future energy demand in UK residential heating. *Energy Policy,* 87**,** 641-653.
FARRELL, T. 2014. The Farrell review of Architecture+ the Built Environment, our Future in Place. *London. http://www.farrellreview.co.uk/downloads/TheFarrellreview.pdf.*
FEIST, W., PFLUGER, R., KAUFMANN, B., SCHNIEDERS, J. & KAH, O. 2007. Passive house planning package 2007. *Specifications for Quality Approved Passive Houses, Technical Information PHI-2007/1 (E), Darmstadt, Passivhaus Institut (December 2007)*.
FENG, G., CHI, D., XU, X., DOU, B., SUN, Y. & FU, Y. 2017. Study on the influence of window-wall ratio on the energy consumption of nearly zero energy buildings. *Procedia Engineering,* 205**,** 730-737.
FERRARA, M., PRUNOTTO, F., ROLFO, A. & FABRIZIO, E. 2019. Energy Demand and Supply Simultaneous Optimization to Design a Nearly Zero-Energy House. *Applied Sciences,* 9**,** 2261.
FINCH, G., BURNETT, E. & KNOWLES, W. Energy consumption in mid and high rise residential buildings in British Columbia. Building Enclosure Science & Technology (BEST2) Conference, 2010.
FINISH ENERGY. Available: https://energia.fi/en [Accessed August 2020].
GABBATISS, J. 2018. *Transport becomes most polluting UK sector as greenhouse gas emissions drop overall* [Online]. INDEPENDENT. Available: https://www.independent.co.uk/climate-change/news/air-pollution-uk-transport-most-polluting-sector-greenhouse-gas-emissions-drop-carbon-dioxide-climate-change-a8196866.html [Accessed February 2021].
GALSWORTHY, J. 2015. Ask a CTBUH Expert: Jon Galsworthy: Wind Turbines on Tall Buildings. *CTBUH Journal***,** 53-53.
GARBER, S. 2018. *Shrinking homes: the average British house 20% smaller than in 1970s* [Online]. Available: www.which.co.uk/news/2018/04/shrinking-homes-the-average-british-house-20-smaller-than-in-1970s/ [Accessed 2020].
GEORGE, A. & ANTO, R. Analytical and experimental analysis of optimal tilt angle of solar photovoltaic systems. 2012 International Conference on Green Technologies (ICGT), 2012. IEEE, 234-239.
GHISI, E. & TINKER, J. A. Window sizes required for the energy efficiency of a building against window sizes required for view. Proceedings of the CIB World Building Congress, Toronto, Canada, 2004.
GHOSH, S., VALE, R. & VALE, B. 2006. Domestic energy sustainability of different urban residential patterns: a New Zealand approach. *International Journal of Sustainable Development,* 9**,** 16-37.
GILLOTT, M., LOVEDAY, D. L., WHITE, J., WOOD, C., CHMUTINA, K. & VADODARIA, K. 2016. Improving the airtightness in an existing UK dwelling: The challenges, the measures and their effectiveness. *Building and Environment,* 95**,** 227-239.
GLAECONOMICS 2005. More residents, more jobs? The relationship between population, employment and accessibility in London. London: GLA Economics.

GM RB 2016. Green Mark for Residential Buildings. Technical Guide and Requirements. *In:* AUTHORITY, B. A. C. (ed.). Singapore.
GODOY-SHIMIZU, D., STEADMAN, P., HAMILTON, I., DONN, M., EVANS, S., MORENO, G. & SHAYESTEH, H. 2018. Energy use and height in office buildings. *Building Research & Information,* 46**,** 845-863.
GOMEZ-IBANEZ, J. A. 1991. A global view of automobile dependence. *American Planning Association. Journal of the American Planning Association,* 57**,** 376-378.
GORDON, I. R., MACE, A. & WHITEHEAD, C. 2016. Defining, measuring and implementing density standards in London: London plan density research project 1. *2016 Density review.* LSE London.
GORDON, P., RICHARDSON, H. W. & JUN, M.-J. 1991. The commuting paradox evidence from the top twenty. *Journal of the American Planning Association,* 57**,** 416-420.
GREENBERG, B. L. 1991. *Guidelines for the reurbanisation of Metropolitan Toronto*.
GROßE, J., FERTNER, C. & GROTH, N. B. 2016. Urban structure, energy and planning: findings from three cities in Sweden, Finland and Estonia. *Urban Planning,* 1**,** 24-40.
GUERRA-SANTIN, O. & ITARD, L. 2010. Occupants' behaviour: determinants and effects on residential heating consumption. *Building Research & Information,* 38**,** 318-338.
GUERRA-SANTIN, O., ITARD, L. & VISSCHER, H. 2009. The effect of occupancy and building characteristics on energy use for space and water heating in Dutch residential stock. *Energy and buildings,* 41**,** 1223-1232.
GUHATHAKURTA, S. & WILLIAMS, E. 2015. Impact of urban form on energy use in central city and suburban neighborhoods: lessons from the phoenix metropolitan region. *Energy Procedia,* 75**,** 2928-2933.
GÜNERALP, B., ZHOU, Y., ÜRGE-VORSATZ, D., GUPTA, M., YU, S., PATEL, P. L., FRAGKIAS, M., LI, X. & SETO, K. C. 2017. Global scenarios of urban density and its impacts on building energy use through 2050. *Proceedings of the National Academy of Sciences***,** 201606035.
GUPTA, R. & GREGG, M. 2012. Using UK climate change projections to adapt existing English homes for a warming climate. *Building and Environment,* 55**,** 20-42.
HACHEM, C., ATHIENITIS, A. & FAZIO, P. 2011. Investigation of solar potential of housing units in different neighborhood designs. *Energy and Buildings,* 43**,** 2262-2273.
HAMILTON, I., EVANS, S., STEADMAN, P., GODOY-SHIMIZU, D., DONN, M., SHAYESTEH, H. & MORENO, G. 2017. All the way to the top! The energy implications of building tall cities. *CISBAT 2017.* Switzerland.
HAPPOLD, B. 2018. Energy, Overheating and Daylight in Tall Buildings Study. OPDC.
HARGREAVES, A., CHENG, V., DESHMUKH, S., LEACH, M. & STEEMERS, K. 2017. Forecasting how residential urban form affects the regional carbon savings and costs of retrofitting and decentralized energy supply. *Applied Energy,* 186**,** 549-561.
HASSAN, A. M. & LEE, H. 2015. The paradox of the sustainable city: definitions and examples. *Environment, development and sustainability,* 17**,** 1267-1285.
HEIDARI, S. 2010. A deep courtyard as the best building form for desert climatean introduction to effects of air movement (Case study: Yazd). *Desert,* 15**,** 19-26.

HEINONEN, J. & JUNNILA, S. 2014. Residential energy consumption patterns and the overall housing energy requirements of urban and rural households in Finland. *Energy and buildings,* 76**,** 295-303.
HILDON, A. & BYRD, H. 1984. The Better Insulated House Programme.
HILLIER, B. 2007. *Space is the machine: a configurational theory of architecture*, Space Syntax.
HING-WANG, F. 2007. 2006 Population By-census: Summary Results. Hing Kong Census and Statistics Department.
HO, A. 2012. *Energy Efficient Suburbia-Transforming the Perceived Oxymoron: A Case Study of the Impact of Smart Energy Technologies on Urban Form in Auckland, New Zealand.* University of Auckland.
HOLISTIC URBAN ENERGY SIMULATION PLATFORM. *Welcome to the HUES Platform* [Online]. Available: https://hues-platform.github.io/index.html [Accessed 2020].
HOUGHTON, J. 2009. *Global warming: the complete briefing*, Cambridge university press.
HUANG, Y., MUSY, M., HÉGRON, G., CHEN, H. & LI, B. 2008. 663: Towards urban design guidelines from urban morphology description and climate adaptability.
HUI, S. C. 2001. Low energy building design in high density urban cities. *Renewable energy,* 24**,** 627-640.
HUIFEN, Z., FUHUA, Y. & QIAN, Z. 2014. Research on the impact of wind angles on the residential building energy consumption. *Mathematical Problems in Engineering,* 2014.
HUKKALAINEN, M., VIRTANEN, M., PAIHO, S. & AIRAKSINEN, M. 2017. Energy planning of low carbon urban areas-Examples from Finland. *Sustainable Cities and Society,* 35**,** 715-728.
IEA 2009. *Cities, Towns and Renewable Energy,* Paris, OECD Publishing.
JABAREEN, Y. R. 2006. Sustainable urban forms: Their typologies, models, and concepts. *Journal of planning education and research,* 26**,** 38-52.
JACOBS, J. 1961. *The death and life of great American cities,* New York, Random House.
JACOBSON, M. Z. & JADHAV, V. 2018. World estimates of PV optimal tilt angles and ratios of sunlight incident upon tilted and tracked PV panels relative to horizontal panels. *Solar Energy,* 169**,** 55-66.
JANK, R. 2017. Annex 51: Case studies and guidelines for energy efficient communities. *Energy and Buildings,* 154**,** 529-537.
JAVANROODI, K., MAHDAVINEJAD, M. & NIK, V. M. 2018. Impacts of urban morphology on reducing cooling load and increasing ventilation potential in hot-arid climate. *Applied Energy,* 231**,** 714-746.
JAVANROODI, K. & NIK, V. M. 2019. Impacts of Microclimate Conditions on the Energy Performance of Buildings in Urban Areas. *Buildings,* 9**,** 189.
JENKS, M., JENKS, M. & DEMPSEY, N. 2005. *Future forms and design for sustainable cities*, Routledge.
JOINER, D. 2010. Sustainable Urban Behaviour. *New Zealand Sustainable Building Conference SB10.* Wellington, New Zealand: Department of Building and Housing.
JONES, S. R., GILLOTT, M., BOUKHANOUF, R., WALKER, G., TUNZI, M., TETLOW, D., RODRIGUES, L. & SUMNER, M. 2019. A system design for distributed energy generation in low-temperature district heating (LTDH) networks. *Future Cities and Environment,* 5.

JOYCE, J. 2011. *'Shoebox homes' become the UK norm* [Online]. Available: www.bbc.co.uk/news/uk-14916580 [Accessed 2020].
JUNG, N., PAIHO, S., SHEMEIKKA, J., LAHDELMA, R. & AIRAKSINEN, M. 2018. Energy performance analysis of an office building in three climate zones. *Energy and Buildings,* 158**,** 1023-1035.
JYLHÄ, K., JOKISALO, J., RUOSTEENOJA, K., PILLI-SIHVOLA, K., KALAMEES, T., SEITOLA, T., MÄKELÄ, H. M., HYVÖNEN, R., LAAPAS, M. & DREBS, A. 2015. Energy demand for the heating and cooling of residential houses in Finland in a changing climate. *Energy and Buildings,* 99**,** 104-116.
KAEMCO. *CitySim Pro* [Online]. Kaemco. Available: www.kaemco.ch/download.php [Accessed 2018].
KALAMEES, T., JYLHÄ, K., TIETÄVÄINEN, H., JOKISALO, J., ILOMETS, S., HYVÖNEN, R. & SAKU, S. 2012. Development of weighting factors for climate variables for selecting the energy reference year according to the EN ISO 15927-4 standard. *Energy and Buildings,* 47**,** 53-60.
KALUA, A. 2020. Urban Residential Building Energy Consumption by End-Use in Malawi. *Buildings,* 10**,** 31.
KAMMEN, D. M. & SUNTER, D. A. 2016. City-integrated renewable energy for urban sustainability. *Science,* 352**,** 922-928.
KAZAS, G., FABRIZIO, E. & PERINO, M. 2017. Energy demand profile generation with detailed time resolution at an urban district scale: A reference building approach and case study. *Applied Energy,* 193**,** 243-262.
KELLY, S., CRAWFORD-BROWN, D. & POLLITT, M. G. 2012. Building performance evaluation and certification in the UK: Is SAP fit for purpose? *Renewable and Sustainable Energy Reviews,* 16**,** 6861-6878.
KENNEDY, R. 2010. Subtropical Design in South East Queensland: A Handbook for Planners, Developers and Decision-Makers.
KHALILI, M. & AMINDELDAR, S. 2014. Traditional solutions in low energy buildings of hot-arid regions of Iran. *Sustainable Cities and Society,* 13**,** 171-181.
KOCAGIL, I. E. & ORAL, G. K. 2015. The effect of building form and settlement texture on energy efficiency for hot dry climate zone in turkey. *Energy Procedia,* 78**,** 1835-1840.
KOLOKOTRONI, M., REN, X., DAVIES, M. & MAVROGIANNI, A. 2012. London's urban heat island: Impact on current and future energy consumption in office buildings. *Energy and buildings,* 47**,** 302-311.
KOMPULSA. *LED Power Consumption: How Much Energy Do LEDs Consume?* [Online]. Available: https://www.kompulsa.com/led-power-consumption-how-much-energy-do-leds-consume/ [Accessed 2020].
KOSTOFF, R. N., BOYLAN, R. & SIMONS, G. R. 2004. Disruptive technology roadmaps. *Technological Forecasting and Social Change,* 71**,** 141-159.
KRIESI, R., AABID, F., ROULET, C.-A., VIGLIOTTI, F. & SCARTEZZINI, J.-L. 2011. Towards a Minergie Standard for tropical climates. EPFL.
LA RÉDACTION. 2019. *Urban planning in cities with hot and dry climates: the case of Cairo* [Online]. Available: https://www.construction21.org/articles/h/urban-planning-in-cities-with-hot-and-dry-climates-the-case-of-cairo.html [Accessed 2020].
LAI, L. W. & HO, W. K. 2001. A probit analysis of development control: a Hong Kong case study of residential zones. *Urban Studies,* 38**,** 2425-2437.
LAM, K. P., WONG, N. H. & CHANDRA, S. The use of multiple building performance simulation tools during the design process-a case study in Singapore. Seventh

International IBPSA Conference, edited by Lamberts R, Negrao C, Hensen J, 2001. 815-822.
LANDAU, C. R. 2017. *Optimum Tilt of Solar Panels* [Online]. Available: http://www.solarpaneltilt.com/ [Accessed 2020].
LARSON, W. & ZHAO, W. 2017. Telework: Urban form, energy consumption, and greenhouse gas implications. *Economic Inquiry,* 55**,** 714-735.
LAUZET, N., RODLER, A., MUSY, M., AZAM, M.-H., GUERNOUTI, S., MAUREE, D. & COLINART, T. 2019. How building energy models take the local climate into account in an urban context–A review. *Renewable and Sustainable Energy Reviews,* 116**,** 109390.
LE GUEN, M., MOSCA, L., PERERA, A. T. D., COCCOLO, S., MOHAJERI, N. & SCARTEZZINI, J.-L. 2018. Improving the energy sustainability of a Swiss village through building renovation and renewable energy integration. *Energy and Buildings,* 158**,** 906-923.
LEE, G. & JEONG, Y. 2017. Impact of Urban and Building Form and Microclimate on the Energy Consumption of Buildings-Based on Statistical Analysis. *Journal of Asian Architecture and Building Engineering,* 16**,** 565-572.
LEFÈVRE, B. 2009. Urban Transport Energy Consumption: Determinants and Strategies for its Reduction.. An analysis of the literature. *SAPI EN. S. Surveys and Perspectives Integrating Environment and Society*.
LEKWOT, V., UCHENNA, E. & ALFRED, J. 2012. Climate change and poverty: Assessing impacts in Nigeria. *Journal of Environmental Management and Safety,* 3**,** 13-27.
LENG, H., MA, Y., WONG, N. H. & MING, T. 2020. Urban morphology and building heating energy consumption: Evidence from Harbin, a severe cold region city. *Energy and Buildings***,** 110143.
LEWIS, S. 2014. *PHPP Illustrated. A Designer's Companion to the Passive House Planning Package*, Riba publishing.
LI, Q., QUAN, S. J., AUGENBROE, G., YANG, P. P.-J. & BROWN, J. Building energy modelling at urban scale: integration of reduced order energy model with geographical information. Building Simulation, 2015.
LIN, J., LI, N., MA, G. & ZHOU, J. The Impact of Eco-Feedback on Energy Consumption Behavior: A Cross-Cultural Study. ISARC. Proceedings of the International Symposium on Automation and Robotics in Construction, 2016. IAARC Publications, 1.
LINCOLNSHIRE POLICE. 2019. *Crime map of Lincoln* [Online]. Available: https://www.police.uk/lincolnshire/NC14/crime/+nys7wA/ [Accessed 10 April 2019].
LOMAS, K. J. 2010. Carbon reduction in existing buildings: a transdisciplinary approach. *Building Research & Information,* 38**,** 1-11.
LONGLEY, P. A. & MESEV, V. 2002. Measurement of density gradients and space-filling in urban systems. *Papers in regional science,* 81**,** 1-28.
MAKIDO, Y., DHAKAL, S. & YAMAGATA, Y. 2012. Relationship between urban form and CO 2 emissions: evidence from fifty Japanese cities. *Urban Climate,* 2**,** 55-67.
MANDAL, A. & BYRD, H. 2017. Density, Energy and Metabolism of a proposed smart city. *Journal of Contemporary Urban Affairs,* 1**,** 57-68.
MANFALUTHY, M. & WILYANTI, S. LED efficacy as key indicator to evaluate bulb lighting. AIP Conference Proceedings, 2019. AIP Publishing LLC, 050003.

MANGAN, S. D. & ORAL, G. K. 2020. Impacts of future weather data on the energy performance of buildings in the context of urban geometry. *Cogent Engineering,* 7**,** 1714112.
MANN, M. E. 2009. Do global warming and climate change represent a serious threat to our welfare and environment? *Social Philosophy & Policy,* 26**,** 193.
MARCH, L. 1972. Elementary models of built forms. *In:* MARTIN, L. & MARCH, L. (eds.) *Urban Space and Structures.* Cambridge University Press.
MARGALIT, H. 2016. *Energy, Cities and Sustainability: An Historical Approach*, Routledge.
MARINO, C., NUCARA, A. & PIETRAFESA, M. 2017. Does window-to-wall ratio have a significant effect on the energy consumption of buildings? A parametric analysis in Italian climate conditions. *Journal of Building Engineering,* 13**,** 169-183.
MARTIN, L. & MARCH, L. 1972. *Urban space and structures*, Cambridge University Press.
MASSON-DELMOTTE, V., ZHAI, P., PÖRTNER, H.-O., ROBERTS, D., SKEA, J., SHUKLA, P. R., PIRANI, A., MOUFOUMA-OKIA, W., PÉAN, C. & PIDCOCK, R. 2018. Global Warming of 1.5°C. *An IPCC Special Report on the impacts of global warming of 1.5°C,* 1.
MATSUMOTO, T., SANCHEZ-SERRA, D. & OSTRY, A. 2012. *Compact city policies: a comparative assessment*, OECD.
MAUREE, D., COCCOLO, S., KAEMPF, J. & SCARTEZZINI, J.-L. 2017. Multi-scale modelling to evaluate building energy consumption at the neighbourhood scale. *PloS one,* 12**,** e0183437.
MAYOR OF LONDON. 2011. *Context and Strategy* [Online]. Available: https://www.london.gov.uk/what-we-do/planning/london-plan/current-london-plan/london-plan-chapter-one-context-and-strategy-5#:~:text=However%2C%20the%20Census%20that%20year,projected%20scale%20of%20household%20growth. [Accessed January 2021].
MAYOR OF LONDON. 2015. *LONDON DATASTORE: Average Floor Area* [Online]. Available: https://data.london.gov.uk/average-floor-area-by-borough/ [Accessed February 2021].
MCHARG 1969. *Design with nature*, American Museum of Natural History New York.
MCKENNA, E., PLESS, J. & DARBY, S. J. 2018. Solar photovoltaic self-consumption in the UK residential sector: New estimates from a smart grid demonstration project. *Energy Policy,* 118**,** 482-491.
MENGELKAMP, E., NOTHEISEN, B., BEER, C., DAUER, D. & WEINHARDT, C. 2018. A blockchain-based smart grid: towards sustainable local energy markets. *Computer Science-Research and Development,* 33**,** 207-214.
METEONORM. *Meteonorm Software* [Online]. Meteotest. Available: https://meteonorm.com/en/ [Accessed 2019].
MINISTRY FOR THE ENVIRONMENT. 2018. *Our land 2018* [Online]. Available: https://www.mfe.govt.nz/publications/environmental-reporting/our-land-2018 [Accessed June 2018].
MITSUBISHI Photovoltaic Modules. *In:* ELECTRIC, M. (ed.).
MOGHADAM, S. T., COCCOLO, S., MUTANI, G., LOMBARDI, P., SCARTEZZINI, J.-L. & MAUREE, D. 2019. A new clustering and visualization method to evaluate urban heat energy planning scenarios. *Cities,* 88**,** 19-36.

MOHAJERI, N., UPADHYAY, G., GUDMUNDSSON, A., ASSOULINE, D., KÄMPF, J. & SCARTEZZINI, J.-L. 2016. Effects of urban compactness on solar energy potential. *Renewable Energy,* 93**,** 469-482.

MONIEN, D., STRZALKA, A., KOUKOFIKIS, A., COORS, V. & EICKER, U. 2017. Comparison of building modelling assumptions and methods for urban scale heat demand forecasting. *Future Cities and Environment,* 3**,** 1-13.

MONTEIRO, C. S., PINA, A., CEREZO, C., REINHART, C. & FERRÃO, P. 2017. The use of multi-detail building archetypes in urban energy modelling. *Energy Procedia,* 111**,** 817-825.

MORGANTI, M., COCH ROURA, H. & CECERE, C. 2012. The effects of urban obstructions in Mediterranean climates: built form typology, density and energy. *ACE: architecture, city and environment,* 7**,** 13-26.

MUHAISEN, A. S. 2006. Shading simulation of the courtyard form in different climatic regions. *Building and Environment,* 41**,** 1731-1741.

MUHAISEN, A. S. & ABED, H. M. 2015. Investigation of the Thermal Performance of Building Form in the Mediterranean Climate of the Gaza Strip. *IUG Journal of Natural Studies,* 21.

MURPHY, G. B., KUMMERT, M., ANDERSON, B. & COUNSELL, J. 2011. A comparison of the UK Standard Assessment Procedure and detailed simulation of solar energy systems for dwellings. *Journal of Building Performance Simulation,* 4**,** 75-90.

MURRAY, P., MARQUANT, J., NIFFELER, M., MAVROMATIDIS, G. & OREHOUNIG, K. 2020. Optimal transformation strategies for buildings, neighbourhoods and districts to reach CO2 emission reduction targets. *Energy and Buildings,* 207**,** 109569.

MUTANI, G., COCCOLO, S., KAEMPF, J. & BILARDO, M. 2018. CitySim Pro Urban energy modelling. *In:* TORINO, D. O. E. O. P. D., THE SOLAR ENERGY AND BUILDING PHYSICS LABORATORY (LESO-PB, E. & FRIBOURG, T. H. É. D. I. E. D. A. D. (eds.).

MUTANI, G., DELMASTRO, C., GARGIULO, M. & CORGNATI, S. P. 2016. Characterization of building thermal energy consumption at the urban scale. *Energy Procedia,* 101**,** 384-391.

MYORS, P., O'LEARY, R. & HELSTROOM, R. 2005. Multi Unit Residential Buildings Energy & Peak Demand Study.

NAKICENOVIC, N. & SWART, R. 2000. Emissions scenarios. Special report of the Intergovernmental panel on climate change. Cambridge University Press, Cambridge.

NEWMAN, P. & JENNINGS, I. 2012. *Cities as sustainable ecosystems: principles and practices*, Island Press.

NEWMAN, P. G. & KENWORTHY, J. R. 1989a. *Cities and automobile dependence: An international sourcebook,* Aldershot and Brookfield.

NEWMAN, P. W. & KENWORTHY, J. R. 1989b. Gasoline consumption and cities: a comparison of US cities with a global survey. *Journal of the american planning association,* 55**,** 24-37.

NG, P. K., MITHRARATNE, N. & KUA, H. W. 2013. Energy analysis of semi-transparent BIPV in Singapore buildings. *Energy and buildings,* 66**,** 274-281.

NICHOLS, B. G. & KOCKELMAN, K. M. 2015. Urban form and life-cycle energy consumption: Case studies at the city scale. *Journal of Transport and Land Use,* 8**,** 115-128.

NICK R. 2014. *Why Demographia's data is irrelevant and misleading* [Online]. Greater Auckland. Available: https://www.greaterauckland.org.nz/2014/10/28/why-demographia-is-fundamentally-wrong/ [Accessed 2018].
NIKKHO, S. K., HEIDARINEJAD, M., LIU, J. & SREBRIC, J. 2017. Quantifying the impact of urban wind sheltering on the building energy consumption. *Applied Thermal Engineering,* 116**,** 850-865.
NIKONOWICZ, L. B. & MILEWSKI, J. 2012. Virtual Power Plants-general review: structure, application and optimization. *Journal of Power Technologies,* 92**,** 135.
NIKOOFARD, S., UGURSAL, V. I. & BEAUSOLEIL-MORRISON, I. 2011. Effect of external shading on household energy requirement for heating and cooling in Canada. *Energy and buildings,* 43**,** 1627-1635.
NOUVEL, R., BRASSEL, K.-H., BRUSE, M., DUMINIL, E., COORS, V., EICKER, U. & ROBINSON, D. SimStadt, a new workflow-driven urban energy simulation platform for CityGML city models. Proceedings of International Conference CISBAT 2015 Future Buildings and Districts Sustainability from Nano to Urban Scale, 2015. LESO-PB, EPFL, 889-894.
NUMAN, M., ALMAZIAD, F. & AL-KHAJA, W. 1999. Architectural and urban design potentials for residential building energy saving in the Gulf region. *Applied energy,* 64**,** 401-410.
OKE, T. & EAST, C. 1971. The urban boundary layer in Montreal. *Boundary-Layer Meteorology,* 1**,** 411-437.
ORAL, G. K. & YILMAZ, Z. 2003. Building form for cold climatic zones related to building envelope from heating energy conservation point of view. *Energy and Buildings,* 35**,** 383-388.
OSORIO, B. M., MCCULLEN, N., WALKER, I. & COLEY, D. 2016. Understanding the relationship between energy consumption and urban form. *Athens Journal of Sciences*.
PALMER, J. & COOPER, I. 2013. United Kingdom housing energy fact file. Department of Energy and Climate Change London.
PANG, X., NOUIDUI, T. S., WETTER, M., FULLER, D., LIAO, A. & HAVES, P. 2016. Building energy simulation in real time through an open standard interface. *Energy and Buildings,* 117**,** 282-289.
PARK, J. & KIM, H. 2012. A field study of occupant behavior and energy consumption in apartments with mechanical ventilation. *Energy and buildings,* 50**,** 19-25.
PARRA, D., WALKER, G. S. & GILLOTT, M. 2016. Are batteries the optimum PV-coupled energy storage for dwellings? Techno-economic comparison with hot water tanks in the UK. *Energy and Buildings,* 116**,** 614-621.
PEEL, M. C., FINLAYSON, B. L. & MCMAHON, T. A. 2007. Updated world map of the Köppen-Geiger climate classification.
PEPONIS, J., ALLEN, D., FRENCH, S., SCOPPA, M. & BROWN, J. Street connectivity and urban density. 6th International Space Syntax Symposium Istanbul: ITU Faculty of Architecture, 2007. Citeseer.
PERERA, A., COCCOLO, S. & SCARTEZZINI, J.-L. 2019. The influence of urban form on the grid integration of renewable energy technologies and distributed energy systems. *Scientific reports,* 9**,** 1-14.
PERERA, A., COCCOLO, S., SCARTEZZINI, J.-L. & MAUREE, D. 2018. Quantifying the impact of urban climate by extending the boundaries of urban energy system modeling. *Applied Energy,* 222**,** 847-860.

PERERA, A., JAVANROODI, K. & NIK, V. M. 2021. Climate resilient interconnected infrastructure: Co-optimization of energy systems and urban morphology. *Applied Energy,* 285**,** 116430.
PHILIPP, R., PABLO, V. & RICKY, B. 2011. Cities and energy: urban morphology and heat energy demand. LSE Cities.
PIERONI, A., SCARPATO, N., DI NUNZIO, L., FALLUCCHI, F. & RASO, M. 2018. Smarter City: Smart Energy Grid based on Blockchain Technology. *International Journal on Advanced Science, Engineering and Information Technology,* 8**,** 298-306.
PITTS, A. 2010. Energy in high-density cities. *Designing high-density cities for social and environmental sustainability***,** 263-271.
PLAZA HOMES. 2017. *Floor-Area Ratio (FAR) and Building Coverage Ratio (BCR) in Japan* [Online]. Tokyo: Tokyo Real Estate News and Information. Available: https://www.realestate-tokyo.com/news/floor-area-ratio-and-building-coverage-ratio/ [Accessed 28/10 2018].
RADLIN, D. & HEMANI, S. 2019. Climax City: Masterplanning and the Complexity of Urban Growth.
RAFIEE, A., DIAS, E. & KOOMEN, E. 2019. Analysing the impact of spatial context on the heat consumption of individual households. *Renewable and Sustainable Energy Reviews,* 112**,** 461-470.
RAPOPORT, A. 1975. Toward a redefinition of density. *Environment and Behavior,* 7**,** 133-158.
RATTI, C., BAKER, N. & STEEMERS, K. 2005. Energy consumption and urban texture. *Energy and buildings,* 37**,** 762-776.
RATTI, C. & CLAUDEL, M. 2016. *The city of tomorrow: Sensors, networks, hackers, and the future of urban life*, Yale University Press.
RATTI, C., RAYDAN, D. & STEEMERS, K. 2003. Building form and environmental performance: archetypes, analysis and an arid climate. *Energy and buildings,* 35**,** 49-59.
REINHART, C. F. & DAVILA, C. C. 2016. Urban building energy modeling–A review of a nascent field. *Building and Environment,* 97**,** 196-202.
REMMEN, P., LAUSTER, M., MANS, M., FUCHS, M., OSTERHAGE, T. & MÜLLER, D. 2018. TEASER: an open tool for urban energy modelling of building stocks. *Journal of Building Performance Simulation,* 11**,** 84-98.
RESCH, E., BOHNE, R. A., KVAMSDAL, T. & LOHNE, J. 2016. Impact of urban density and building height on energy use in cities. *Energy Procedia,* 96**,** 800-814.
REUK. *Solar Panel Mounting Angle* [Online]. REUK: The Renewable Energy Website. Available: www.reuk.co.uk/wordpress/solar/solar-panel-mounting-angle/ [Accessed 2020].
RICKABY, P. A. 1987. An approach to the assessment of the energy efficiency of urban built form. *In:* HAWKES, D., OWERS, J., RICKABY, P. & STEADMAN, P. (eds.) *Energy and Urban Built Form.* Butterworth-Heinemann.
RICKWOOD, P., GLAZEBROOK, G. & SEARLE, G. 2008. Urban structure and energy—a review. *Urban policy and research,* 26**,** 57-81.
RIDLEY, I., CLARKE, A., BERE, J., ALTAMIRANO, H., LEWIS, S., DURDEV, M. & FARR, A. 2013. The monitored performance of the first new London dwelling certified to the Passive House standard. *Energy and Buildings,* 63**,** 67-78.
ROBINSON, D., HALDI, F., LEROUX, P., PEREZ, D., RASHEED, A. & WILKE, U. CitySim: Comprehensive micro-simulation of resource flows for sustainable

urban planning. Proceedings of the Eleventh International IBPSA Conference, 2009. 1083-1090.
RODE, P., KEIM, C., ROBAZZA, G., VIEJO, P. & SCHOFIELD, J. 2014. Cities and energy: urban morphology and residential heat-energy demand. *Environment and Planning B: Planning and Design,* 41**,** 138-162.
RODRIGUES, L. T., GILLOTT, M. & TETLOW, D. 2013. Summer overheating potential in a low-energy steel frame house in future climate scenarios. *Sustainable Cities and Society,* 7**,** 1-15.
ROGERS, R. 1997. *Cities for a small planet,* London, Faber and Faber Limited.
ROSELLI, C. & SASSO, M. 2016. Integration between electric vehicle charging and PV system to increase self-consumption of an office application. *Energy Conversion and Management,* 130**,** 130-140.
RUBEL, F. & KOTTEK, M. 2010. Observed and projected climate shifts 1901–2100 depicted by world maps of the Köppen-Geiger climate classification. *Meteorologische Zeitschrift,* 19**,** 135-141.
SAILOR, D. J., ELLEY, T. B. & GIBSON, M. 2012. Exploring the building energy impacts of green roof design decisions–a modeling study of buildings in four distinct climates. *Journal of Building Physics,* 35**,** 372-391.
SALVATI, A., PALME, M., CHIESA, G. & KOLOKOTRONI, M. 2020. Built form, urban climate and building energy modelling: case-studies in Rome and Antofagasta. *Journal of Building Performance Simulation,* 13**,** 209-225.
SAP 2012. The government's standard assessment procedure for energy rating of dwellings. *Building Research Establishment, Watford, UK.*
SARRALDE, J. J., QUINN, D. J., WIESMANN, D. & STEEMERS, K. 2015. Solar energy and urban morphology: Scenarios for increasing the renewable energy potential of neighbourhoods in London. *Renewable Energy,* 73**,** 10-17.
SAWIN, J. L., SVERRISSON, F., SEYBOTH, K., ADIB, R., MURDOCK, H. E., LINS, C., EDWARDS, I., HULLIN, M., NGUYEN, L. H. & PRILLIANTO, S. S. 2013. Renewables 2017 Global Status Report. REN21.
SCHWARTZ, Y. & RASLAN, R. 2013. Variations in results of building energy simulation tools, and their impact on BREEAM and LEED ratings: A case study. *Energy and Buildings,* 62**,** 350-359.
SCHWARZ, N. 2010. Urban form revisited—Selecting indicators for characterising European cities. *Landscape and urban planning,* 96**,** 29-47.
SENAVE, M., REYNDERS, G., SODAGAR, B., VERBEKE, S. & SAELENS, D. 2019. Mapping the pitfalls in the characterisation of the heat loss coefficient from on-board monitoring data using ARX models. *Energy and Buildings,* 197**,** 214-228.
SHABUNKO, V., LIM, C. & MATHEW, S. 2018. EnergyPlus models for the benchmarking of residential buildings in Brunei Darussalam. *Energy and Buildings,* 169**,** 507-516.
SHAHRESTANI, M., YAO, R., LUO, Z., TURKBEYLER, E. & DAVIES, H. 2015. A field study of urban microclimates in London. *Renewable Energy,* 73**,** 3-9.
SHARIFI, A. 2019. Resilient urban forms: A macro-scale analysis. *Cities,* 85**,** 1-14.
SHEARER, D. & ANDERSON, B. 2008. International comparison of energy standards in building regulations for non-domestic buildings: Denmark, Finland, Norway, Scotland, and Sweden. *Report for BRE Scotland*.
SHIRZADI, M., NAGHASHZADEGAN, M. & MIRZAEI, P. A. 2019. Developing a framework for improvement of building thermal performance modeling under urban microclimate interactions. *Sustainable Cities and Society,* 44**,** 27-39.

SILVA, M., OLIVEIRA, V. & LEAL, V. 2017. Urban Form and Energy Demand: A Review of Energy-relevant Urban Attributes. *Journal of Planning Literature*, 0885412217706900.
SODAGAR, B. & STARKEY, D. 2016. The monitored performance of four social houses certified to the Code for Sustainable Homes Level 5. *Energy and Buildings,* 110, 245-256.
SOFLAEI, F., SHOKOUHIAN, M. & ZHU, W. 2017. Socio-environmental sustainability in traditional courtyard houses of Iran and China. *Renewable and Sustainable Energy Reviews,* 69, 1147-1169.
SOLARDESIGNTOOL 1SolTech 1-STH-250 (250W) Solar Panel.
SPECIAL PROJECT Spatial Planning & Energy
A guide for planners. European Council of Town Planners (ECTP-CEU) and Town and Country Planning Association (TCPA).
SS 553 2009. SINGAPORE STANDARD: Code of Practice for Air-Conditioning and Mechanical Ventilation in Buildings. Singapore: SPRING Singapore.
ST CLAIR, P. 2010. Guidelines For Climate Responsive Design In Cold Climates With Particular Reference To Beijing, China.
STACKEDHOMES. 2018. *Plot Ratio – Why you need to know (and how to calculate it)* [Online]. StackedHomes. Available: https://stackedhomes.com/blog/plot-ratio-need-know-calculate/ [Accessed 28/10 2018].
STARKEY, D. 2014. *Post Occupancy Evaluation: A Critical Investigation into Zero Carbon Housing projects with Reference to the UK.* MSc. Sustainable Architectural Design, University of Lincoln.
STATISTICA. 2019. *Number of households in the United Kingdom (UK) in 2019, by size (in 1,000)* [Online]. Statistica. Available: https://www.statista.com/statistics/281627/households-in-the-united-kingdom-uk-by-size/ [Accessed January 2021].
STEADMAN, P. 2014a. *Building types and built forms*, Troubador Publishing Ltd.
STEADMAN, P. 2014b. Density and built form: integrating 'Spacemate'with the work of Martin and March. *Environment and Planning B: Planning and Design,* 41, 341-358.
STEADMAN, P. & BROWN, F. 1987. Estimating the exposed surface area of the domestic stock. *In:* HAWKES, D., OWERS, J., RICKABY, P. & STEADMAN, P. (eds.) *Energy and urban built form.* Butterworth-Heinemann.
STEADMAN, P., EVANS, S. & BATTY, M. 2009. Wall area, volume and plan depth in the building stock. *Building Research & Information,* 37, 455-467.
STEADMAN, P., HAMILTON, I. & EVANS, S. 2014. Energy and urban built form: an empirical and statistical approach. *Building Research & Information,* 42, 17-31.
STEADMAN, P., HAMILTON, I., GODOY-SHIMIZU, D., SHAYESTEH, H. & EVANS, S. 2017. *High-Rise Buildings: Energy and Density* [Online]. UCL Energy Institute Home. Available: https://www.ucl.ac.uk/bartlett/energy/news/2017/jun/ucl-energy-high-rise-buildings-energy-and-density-research-project-results [Accessed January 2018].
STEEMERS, K. 2003. Energy and the city: density, buildings and transport. *Energy and buildings,* 35, 3-14.
STEPHENSON, J., BARTON, B., CARRINGTON, G., GNOTH, D., LAWSON, R. & THORSNES, P. 2010. Energy cultures: A framework for understanding energy behaviours. *Energy policy,* 38, 6120-6129.

STEWART, D. J. 1999. Changing Cairo: the political economy of urban form. *International Journal of Urban and Regional Research,* 23**,** 103-127.
STONE, A., SHIPWORTH, D., BIDDULPH, P. & ORESZCZYN, T. 2014. Key factors determining the energy rating of existing English houses. *Building Research & Information,* 42**,** 725-738.
STONE JR, B. & RODGERS, M. O. 2001. Urban form and thermal efficiency: how the design of cities influences the urban heat island effect. *Journal of the American Planning Association,* 67**,** 186-198.
STRØMANN-ANDERSEN, J. & SATTRUP, P. A. 2011. The urban canyon and building energy use: Urban density versus daylight and passive solar gains. *Energy and Buildings,* 43.
SUGAHARA, M. & BERMONT, L. 2016. Energy and Resilient Cities. *OECD Regional Development Working Papers*.
SUMMERFIELD, A., RASLAN, R., LOWE, R. & ORESZCZYN, T. How useful are building energy models for policy? A UK perspective. 2011. IBPSA.
SUN, W.-S., TSUEI, C.-H. & HUANG, Y.-H. 2011. Simulating the illuminance and efficiency of the LEDs used in general household lighting. *Physics Procedia,* 19**,** 244-248.
TANG, B.-S. & TANG, R. M. 1999. Development control, planning incentive and urban redevelopment: evaluation of a two-tier plot ratio system in Hong Kong. *Land use policy,* 16**,** 33-43.
TERECI, A., OZKAN, S. T. E. & EICKER, U. 2013. Energy benchmarking for residential buildings. *Energy and Buildings,* 60**,** 92-99.
THE FARADAY INSTITUTION 2019. The Road to Electrification – from the Internal Combustion Engine to the Battery Electric Vehicle. The Faraday Institution.
TOPARLAR, Y., BLOCKEN, B., MAIHEU, B. & VAN HEIJST, G. 2017. A review on the CFD analysis of urban microclimate. *Renewable and Sustainable Energy Reviews,* 80**,** 1613-1640.
TRANSPORT FOR LONDON 2012. Roads Task Force – Technical Note 12
How many cars are there in London and who owns them? : Transport for London.
TRUBKA, R. & GLACKIN, S. 2016. Modelling housing typologies for urban redevelopment scenario planning. *Computers, Environment and Urban Systems,* 57**,** 199-211.
TSAI, Y.-H. 2005. Quantifying urban form: compactness versus' sprawl'. *Urban studies,* 42**,** 141-161.
TSIRIGOTI, D. & TSIKALOUDAKI, K. 2018. The effect of climate conditions on the relation between energy efficiency and urban form. *Energies,* 11**,** 582.
TZEMPELIKOS, A. & ATHIENITIS, A. K. 2007. The impact of shading design and control on building cooling and lighting demand. *Solar energy,* 81**,** 369-382.
U.S. CLIMATE DATA. 2021. *Climate Phoenix - Arizona* [Online]. Available: https://www.usclimatedata.com/climate/phoenix/arizona/united-states/usaz0166 [Accessed 2020].
UK GOVERNMENT. 2019. *UK becomes first major economy to pass net zero emissions law* [Online]. Department for Business, Energy & Industrial Strategy. Available: https://www.gov.uk/government/news/uk-becomes-first-major-economy-to-pass-net-zero-emissions-law [Accessed January 2021].
UK GOVERNMENT 2020. Vehicle mileage and occupancy. Department for Transport.
UNITED NATIONS. *Cities and Pollution* [Online]. Available: https://www.un.org/en/climatechange/climate-solutions/cities-pollution [Accessed 2020].

UNITED NATIONS 2014. World Urbanization Prospects: The 2014 Revision, Highlights. *Population Division.* United Nations.
UNITED NATIONS. 2015. *#Envision2030: 17 goals to transform the world for persons with disabilities* [Online]. Available: https://www.un.org/development/desa/disabilities/envision2030.html [Accessed 2021].
UNIVERSITY OF SOUTHAMPTON. *Research Group: Energy and Climate Change* [Online]. Available: https://www.southampton.ac.uk/engineering/research/groups/energy_and_climate_change_group.page#group_overview [Accessed 2020].
VAINIO, T., AIRAKSINEN, M. & VESANEN, T. 2017. Space heating measurement in apartment buildings. Espoo.
VANDEVYVERE, H. & STREMKE, S. 2012. Urban planning for a renewable energy future: Methodological challenges and opportunities from a design perspective. *Sustainability,* 4**,** 1309-1328.
WAIBEL, C., EVINS, R. & CARMELIET, J. 2016. Holistic Optimization of Urban Morphology and District Energy Systems. *Expanding Boundaries: Systems Thinking in the Built Environment***,** 70-76.
WAIBEL, C., EVINS, R. & CARMELIET, J. 2019. Co-simulation and optimization of building geometry and multi-energy systems: Interdependencies in energy supply, energy demand and solar potentials. *Applied Energy,* 242**,** 1661-1682.
WALTER, E. & KÄMPF, J. H. A verification of CitySim results using the BESTEST and monitored consumption values. Proceedings of the 2nd Building Simulation Applications conference, 2015. Bozen-Bolzano University Press, 215-222.
WAN, K. K., LI, D. H., LIU, D. & LAM, J. C. 2011. Future trends of building heating and cooling loads and energy consumption in different climates. *Building and Environment,* 46**,** 223-234.
WONG, N. H., JUSUF, S. K., SYAFII, N. I., CHEN, Y., HAJADI, N., SATHYANARAYANAN, H. & MANICKAVASAGAM, Y. V. 2011. Evaluation of the impact of the surrounding urban morphology on building energy consumption. *Solar Energy,* 85**,** 57-71.
WORLD POPULATION REVIEW. 2020a. *Helsinki Population* [Online]. Available: https://worldpopulationreview.com/world-cities/helsinki-population [Accessed December 2020].
WORLD POPULATION REVIEW. 2020b. *London Population* [Online]. World Population Review. Available: https://worldpopulationreview.com/world-cities/london-population [Accessed December 2020].
WORLD POPULATION REVIEW. 2020c. *Phoenix, Arizona Population* [Online]. Available: https://worldpopulationreview.com/us-cities/phoenix-az-population [Accessed December 2020].
WORLD POPULATION REVIEW. 2020d. *Singapore Population* [Online]. Available: https://worldpopulationreview.com/countries/singapore-population [Accessed December 2020].
WRIGHT, A. 2008. What is the relationship between built form and energy use in dwellings? *Energy Policy,* 36**,** 4544-4547.
WWF UK. *Reducing Carbon Emissions in the UK* [Online]. World Wide Fund for Nature. Available: https://www.wwf.org.uk/what-we-do/projects/reducing-carbon-emissions-uk?pc=AUT005007&gclsrc=aw.ds&&gclid=CjwKCAiAxp-ABhALEiwAXm6IycfdtCYdytBvNxYcgUW8tkgQ0sKoTv19urUcCc6R4tyuDPDHO77QCRoCwhQQAvD_BwE&gclsrc=aw.ds [Accessed January 2021].

YEO, I.-A., YOON, S.-H. & YEE, J.-J. 2013. Development of an Environment and energy Geographical Information System (E-GIS) construction model to support environmentally friendly urban planning. *Applied Energy,* 104**,** 723-739.
YIGITCANLAR, T., KAMRUZZAMAN, M., FOTH, M., SABATINI, J., DA COSTA, E. & IOPPOLO, G. 2019. Can cities become smart without being sustainable? A systematic review of the literature. *Sustainable cities and society*.
YOU, Y. & KIM, S. 2018. Revealing the mechanism of urban morphology affecting residential energy efficiency in Seoul, Korea. *Sustainable cities and society,* 43**,** 176-190.
ZANGHERI, P., ARMANI, R., PIETROBON, M., PAGLIANO, L., BONETA, M. F. & MÜLLER, A. 2014. Heating and cooling energy demand and loads for building types in different countries of the EU. *Polytechnic University of Turin, end-use Efficiency Research Group,* 3.
ZANON, B. & VERONES, S. 2013. Climate change, urban energy and planning practices: Italian experiences of innovation in land management tools. *Land use policy,* 32**,** 343-355.
ZCH 2009. Defining a fabric energy efficiency standard for zero carbon homes. *Task Group Recommendations.* London: Zero Carbon Hub.
ZHU, R., WONG, M. S., YOU, L., SANTI, P., NICHOL, J., HO, H. C., LU, L. & RATTI, C. 2020. The effect of urban morphology on the solar capacity of three-dimensional cities. *Renewable Energy,* 153**,** 1111-1126.
ZYGA, L. 2010. *White LEDs with super-high luminous efficacy could satisfy all general lighting needs* [Online]. Phys.org. Available: https://phys.org/news/2010-08-white-super-high-luminous-efficacy.html [Accessed 2020].

Appendix A

An exemplar Excel spreadsheet tool used for overlaying two different datasets on one graph for the chosen built form and cut-off angle.

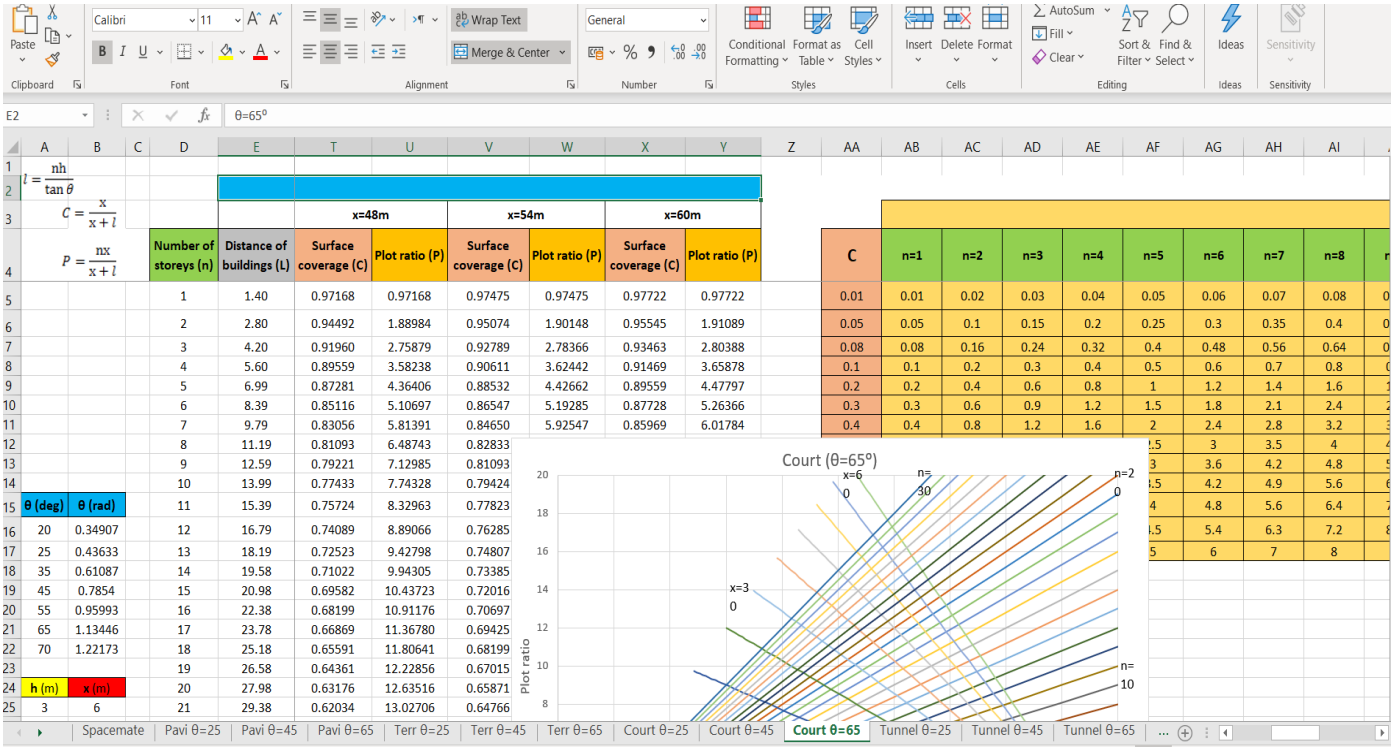

$$l = \frac{nh}{\tan\theta}$$

$$C = \frac{x}{x+l}$$

$$P = \frac{nx}{x+l}$$

Number of storeys (n)	Distance of buildings (L)	x=48m Surface coverage (C)	x=48m Plot ratio (P)	x=54m Surface coverage (C)	x=54m Plot ratio (P)	x=60m Surface coverage (C)	x=60m Plot ratio (P)
1	1.40	0.97168	0.97168	0.97475	0.97475	0.97722	0.97722
2	2.80	0.94492	1.88984	0.95074	1.90148	0.95545	1.91089
3	4.20	0.91960	2.75879	0.92789	2.78366	0.93463	2.80388
4	5.60	0.89559	3.58238	0.90611	3.62442	0.91469	3.65878
5	6.99	0.87281	4.36406	0.88532	4.42662	0.89559	4.47797
6	8.39	0.85116	5.10697	0.86547	5.19285	0.87728	5.26366
7	9.79	0.83056	5.81391	0.84650	5.92547	0.85969	6.01784
8	11.19	0.81093	6.48743	0.82833			
9	12.59	0.79221	7.12985	0.81093			
10	13.99	0.77433	7.74328	0.79424			
11	15.39	0.75724	8.32963	0.77823			
12	16.79	0.74089	8.89066	0.76285			
13	18.19	0.72523	9.42798	0.74807			
14	19.58	0.71022	9.94305	0.73385			
15	20.98	0.69582	10.43723	0.72016			
16	22.38	0.68199	10.91176	0.70697			
17	23.78	0.66869	11.36780	0.69425			
18	25.18	0.65591	11.80641	0.68199			
19	26.58	0.64361	12.22856	0.67015			
20	27.98	0.63176	12.63516	0.65871			
21	29.38	0.62034	13.02706	0.64766			

θ (deg)	θ (rad)
20	0.34907
25	0.43633
35	0.61087
45	0.7854
55	0.95993
65	1.13446
70	1.22173

h (m)	x (m)
3	6

C	n=1	n=2	n=3	n=4	n=5	n=6	n=7	n=8
0.01	0.01	0.02	0.03	0.04	0.05	0.06	0.07	0.08
0.05	0.05	0.1	0.15	0.2	0.25	0.3	0.35	0.4
0.08	0.08	0.16	0.24	0.32	0.4	0.48	0.56	0.64
0.1	0.1	0.2	0.3	0.4	0.5	0.6	0.7	0.8
0.2	0.2	0.4	0.6	0.8	1	1.2	1.4	1.6
0.3	0.3	0.6	0.9	1.2	1.5	1.8	2.1	2.4
0.4	0.4	0.8	1.2	1.6	2	2.4	2.8	3.2
					2.5	3	3.5	4
					3	3.6	4.2	4.8
					3.5	4.2	4.9	5.6
					4	4.8	5.6	6.4
					4.5	5.4	6.3	7.2
					5	6	7	8

Appendix B

A screenshot from an exemplar ‘XML’ file from CitySim that consists of 2494 lines.

```
<?xml version="1.0" encoding="ISO-8859-1"?>
<CitySim name="test">
    <Simulation beginMonth="1" endMonth="12" beginDay="1" endDay="31"/>
    <Climate location="" city="Unknown"/>
    <District>
        <FarFieldObstructions>
        </FarFieldObstructions>
        <Composite id="50" name=" Ehsan 0.18" category="Wall">
            <Layer Thickness="0.0200" Conductivity="0.8700" Cp="1101.59998" Density="1800" NRE="0" GWP="0" UBP="0"/>
            <Layer Thickness="0.1600" Conductivity="0.3500" Cp="900" Density="1100" NRE="0" GWP="0" UBP="0"/>
            <Layer Thickness="0.0310" Conductivity="0.0250" Cp="1000.79999" Density="1.23000002" NRE="0" GWP="0" UBP="0"/>
            <Layer Thickness="0.1300" Conductivity="0.0360" Cp="601.200012" Density="60" NRE="0" GWP="0" UBP="0"/>
            <Layer Thickness="0.1400" Conductivity="0.7000" Cp="1100" Density="1200" NRE="0" GWP="0" UBP="0"/>
            <Layer Thickness="0.0100" Conductivity="0.5800" Cp="900" Density="1200" NRE="0" GWP="0" UBP="0"/>
            <Layer Thickness="0.0200" Conductivity="0.7000" Cp="900" Density="1400" NRE="0" GWP="0" UBP="0"/>
        </Composite>
        <Composite id="40" name="Ehsan 0.13" category="Floor">
            <Layer Thickness="0.4000" Conductivity="1.6000" Cp="1000" Density="2200" NRE="0" GWP="0" UBP="0"/>
            <Layer Thickness="0.1900" Conductivity="0.0400" Cp="600" Density="120" NRE="0" GWP="0" UBP="0"/>
            <Layer Thickness="0.0001" Conductivity="0.2000" Cp="1400" Density="960" NRE="0" GWP="0" UBP="0"/>
        </Composite>
        <Composite id="37" name="Ehsan 0.13" category="Roof">
            <Layer Thickness="0.2000" Conductivity="1.4800" Cp="1100" Density="2400" NRE="0" GWP="0" UBP="0"/>
            <Layer Thickness="0.0200" Conductivity="0.2000" Cp="1600" Density="1200" NRE="0" GWP="0" UBP="0"/>
            <Layer Thickness="0.3000" Conductivity="0.0400" Cp="600" Density="120" NRE="0" GWP="0" UBP="0"/>
            <Layer Thickness="0.0100" Conductivity="0.2000" Cp="1400" Density="960" NRE="0" GWP="0" UBP="0"/>
            <Layer Thickness="0.4900" Conductivity="1.6000" Cp="1000" Density="2200" NRE="0" GWP="0" UBP="0"/>
        </Composite>
        <Composite id="21" name="Asphalt road" category="Ground">
            <Layer Thickness="0.0250" Conductivity="0.7000" Cp="1100" Density="2150" NRE="0" GWP="0" UBP="0"/>
            <Layer Thickness="0.0200" Conductivity="2.0000" Cp="1051.19995" Density="2000" NRE="0" GWP="0" UBP="0"/>
            <Layer Thickness="0.1000" Conductivity="2.0000" Cp="1051.19995" Density="2000" NRE="0" GWP="0" UBP="0"/>
            <Layer Thickness="3.8550" Conductivity="1.5000" Cp="2098.80005" Density="1500" NRE="0" GWP="0" UBP="0"/>
        </Composite>

        <OccupancyDayProfile id="0" name="empty day profile" p1="0" p2="0" p3="0" p4="0" p5="0" p6="0" p7="0" p8="0" p9="0" p10="0" p11="0" p12="0" p13="0" p14="0" p15="0" p16="0" p
        <OccupancyDayProfile id="1" name="House SIA2024" p1="1" p2="1" p3="1" p4="1" p5="1" p6="1" p7="0.8" p8="0.6" p9="0.4" p10="0.4" p11="0.4" p12="0.6" p13="0.8" p14="0.6" p15="

        <OccupancyYearProfile id="0" name="empty year profile" d1="0" d2="0" d3="0" d4="0" d5="0" d6="0" d7="0" d8="0" d9="0" d10="0" d11="0" d12="0" d13="0" d14="0" d15="0" d16="0"
        <OccupancyYearProfile id="1" name="Year Profile House" d1="1" d2="1" d3="1" d4="1" d5="1" d6="1" d7="1" d8="1" d9="1" d10="1" d11="1" d12="1" d13="1" d14="1" d15="1" d16="1"

        <DHWDayProfile id="0" name="empty day profile" p1="0" p2="0" p3="0" p4="0" p5="0" p6="0" p7="0" p8="0" p9="0" p10="0" p11="0" p12="0" p13="0" p14="0" p15="0" p16="0" p17="0"
```

Appendix C

MATLAB code developed to aggregate the data obtained from CitySim and generate yearly/monthly accumulative figures.

```
clc
Results=importdata('n=30.xlsx');
Heating_Consumption=Results.data(:,3);
Heating_Consumption = Heating_Consumption/1000;
%Heating_Consumption_annual_sum = sum(Heating_Consumption)
Cooling_Consumption=Results.data(:,4);
Cooling_Consumption = Cooling_Consumption/1000;
%Cooling_Consumption_annual_sum = sum(Cooling_Consumption)
Qi=Results.data(:,5);
Qi = Qi/1000;
Qi_annual_sum = sum(Qi)
PV_Generation=Results.data(:,12);
PV_Generation = PV_Generation*(-1);
PV_Generation_annual_sum = sum(PV_Generation)
Solar_Thermal_Production=Results.data(:,13);
%Solar_Thermal_Production = Solar_Thermal_Production/1000;
Qs=Results.data(:,6);
Qs=Qs/1000;
%%
Jan_Heating_Consumption = Heating_Consumption(1:744);
Jan_Heating_Consumption_sum = sum(Jan_Heating_Consumption);
Feb_Heating_Consumption = Heating_Consumption(745:1416);
Feb_Heating_Consumption_sum = sum(Feb_Heating_Consumption);
March_Heating_Consumption = Heating_Consumption(1417:2160);
March_Heating_Consumption_sum = sum(March_Heating_Consumption);
April_Heating_Consumption = Heating_Consumption(2161:2880);
April_Heating_Consumption_sum = sum(April_Heating_Consumption);
May_Heating_Consumption = Heating_Consumption(2881:3624);
May_Heating_Consumption_sum = sum(May_Heating_Consumption);
June_Heating_Consumption = Heating_Consumption(3625:4344);
June_Heating_Consumption_sum = sum(June_Heating_Consumption);
July_Heating_Consumption = Heating_Consumption(4344:5088);
July_Heating_Consumption_sum = sum(July_Heating_Consumption);
Aug_Heating_Consumption = Heating_Consumption(5089:5832);
Aug_Heating_Consumption_sum = sum(Aug_Heating_Consumption);
Sep_Heating_Consumption = Heating_Consumption(5833:6552);
Sep_Heating_Consumption_sum = sum(Sep_Heating_Consumption);
Oct_Heating_Consumption = Heating_Consumption(6553:7296);
Oct_Heating_Consumption_sum = sum(Oct_Heating_Consumption);
Nov_Heating_Consumption = Heating_Consumption(7297:8016);
Nov_Heating_Consumption_sum = sum(Nov_Heating_Consumption);
Dec_Heating_Consumption = Heating_Consumption(8017:8760);
Dec_Heating_Consumption_sum = sum(Dec_Heating_Consumption);
%%
Jan_Cooling_Consumption = Cooling_Consumption(1:744);
Jan_Cooling_Consumption_sum = sum(Jan_Cooling_Consumption);
Feb_Cooling_Consumption = Cooling_Consumption(745:1416);
Feb_Cooling_Consumption_sum = sum(Feb_Cooling_Consumption);
March_Cooling_Consumption = Cooling_Consumption(1417:2160);
March_Cooling_Consumption_sum = sum(March_Cooling_Consumption);
April_Cooling_Consumption = Cooling_Consumption(2161:2880);
April_Cooling_Consumption_sum = sum(April_Cooling_Consumption);
May_Cooling_Consumption = Cooling_Consumption(2881:3624);
May_Cooling_Consumption_sum = sum(May_Cooling_Consumption);
June_Cooling_Consumption = Cooling_Consumption(3625:4344);
June_Cooling_Consumption_sum = sum(June_Cooling_Consumption);
July_Cooling_Consumption = Cooling_Consumption(4344:5088);
July_Cooling_Consumption_sum = sum(July_Cooling_Consumption);
Aug_Cooling_Consumption = Cooling_Consumption(5089:5832);
Aug_Cooling_Consumption_sum = sum(Aug_Cooling_Consumption);
Sep_Cooling_Consumption = Cooling_Consumption(5833:6552);
Sep_Cooling_Consumption_sum = sum(Sep_Cooling_Consumption);
```

```
Oct_Cooling_Consumption = Cooling_Consumption(6553:7296);
Oct_Cooling_Consumption_sum = sum(Oct_Cooling_Consumption);
Nov_Cooling_Consumption = Cooling_Consumption(7297:8016);
Nov_Cooling_Consumption_sum = sum(Nov_Cooling_Consumption);
Dec_Cooling_Consumption = Cooling_Consumption(8017:8760);
Dec_Cooling_Consumption_sum = sum(Dec_Cooling_Consumption);
%%
Jan_Qi = Qi(1:744);
Jan_Qi_sum = sum(Jan_Qi);
Feb_Qi = Qi(745:1416);
Feb_Qi_sum = sum(Feb_Qi);
March_Qi = Qi(1417:2160);
March_Qi_sum = sum(March_Qi);
April_Qi = Qi(2161:2880);
April_Qi_sum = sum(April_Qi);
May_Qi = Qi(2881:3624);
May_Qi_sum = sum(May_Qi);
June_Qi = Qi(3625:4344);
June_Qi_sum = sum(June_Qi);
July_Qi = Qi(4344:5088);
July_Qi_sum = sum(July_Qi);
Aug_Qi = Qi(5089:5832);
Aug_Qi_sum = sum(Aug_Qi);
Sep_Qi = Qi(5833:6552);
Sep_Qi_sum = sum(Sep_Qi);
Oct_Qi = Qi(6553:7296);
Oct_Qi_sum = sum(Oct_Qi);
Nov_Qi = Qi(7297:8016);
Nov_Qi_sum = sum(Nov_Qi);
Dec_Qi = Qi(8017:8760);
Dec_Qi_sum = sum(Dec_Qi);
%%
Jan_PV_Generation = PV_Generation(1:744);
Jan_PV_Generation_sum = sum(Jan_PV_Generation);
Feb_PV_Generation = PV_Generation(745:1416);
Feb_PV_Generation_sum = sum(Feb_PV_Generation);
March_PV_Generation = PV_Generation(1417:2160);
March_PV_Generation_sum = sum(March_PV_Generation);
April_PV_Generation = PV_Generation(2161:2880);
April_PV_Generation_sum = sum(April_PV_Generation);
May_PV_Generation = PV_Generation(2881:3624);
May_PV_Generation_sum = sum(May_PV_Generation);
June_PV_Generation = PV_Generation(3625:4344);
June_PV_Generation_sum = sum(June_PV_Generation);
July_PV_Generation = PV_Generation(4344:5088);
July_PV_Generation_sum = sum(July_PV_Generation);
Aug_PV_Generation = PV_Generation(5089:5832);
Aug_PV_Generation_sum = sum(Aug_PV_Generation);
Sep_PV_Generation = PV_Generation(5833:6552);
Sep_PV_Generation_sum = sum(Sep_PV_Generation);
Oct_PV_Generation = PV_Generation(6553:7296);
Oct_PV_Generation_sum = sum(Oct_PV_Generation);
Nov_PV_Generation = PV_Generation(7297:8016);
Nov_PV_Generation_sum = sum(Nov_PV_Generation);
Dec_PV_Generation = PV_Generation(8017:8760);
Dec_PV_Generation_sum = sum(Dec_PV_Generation);
%%
Jan_Solar_Thermal_Production = Solar_Thermal_Production(1:744);
Jan_Solar_Thermal_Production_sum = sum(Jan_Solar_Thermal_Production);
Feb_Solar_Thermal_Production = Solar_Thermal_Production(745:1416);
Feb_Solar_Thermal_Production_sum = sum(Feb_Solar_Thermal_Production);
March_Solar_Thermal_Production = Solar_Thermal_Production(1417:2160);
March_Solar_Thermal_Production_sum = sum(March_Solar_Thermal_Production);
April_Solar_Thermal_Production = Solar_Thermal_Production(2161:2880);
April_Solar_Thermal_Production_sum = sum(April_Solar_Thermal_Production);
May_Solar_Thermal_Production = Solar_Thermal_Production(2881:3624);
May_Solar_Thermal_Production_sum = sum(May_Solar_Thermal_Production);
June_Solar_Thermal_Production = Solar_Thermal_Production(3625:4344);
```

```
June_Solar_Thermal_Production_sum = sum(June_Solar_Thermal_Production);
July_Solar_Thermal_Production = Solar_Thermal_Production(4344:5088);
July_Solar_Thermal_Production_sum = sum(July_Solar_Thermal_Production);
Aug_Solar_Thermal_Production = Solar_Thermal_Production(5089:5832);
Aug_Solar_Thermal_Production_sum = sum(Aug_Solar_Thermal_Production);
Sep_Solar_Thermal_Production = Solar_Thermal_Production(5833:6552);
Sep_Solar_Thermal_Production_sum = sum(Sep_Solar_Thermal_Production);
Oct_Solar_Thermal_Production = Solar_Thermal_Production(6553:7296);
Oct_Solar_Thermal_Production_sum = sum(Oct_Solar_Thermal_Production);
Nov_Solar_Thermal_Production = Solar_Thermal_Production(7297:8016);
Nov_Solar_Thermal_Production_sum = sum(Nov_Solar_Thermal_Production);
Dec_Solar_Thermal_Production = Solar_Thermal_Production(8017:8760);
Dec_Solar_Thermal_Production_sum = sum(Dec_Solar_Thermal_Production);
%%
Jan_Qs = Qs(1:744);
for i1 = 1:744
    if Jan_Qs(i1)>=0
        Jan_Qs_Pos(i1) = Jan_Qs(i1);
    else
        Jan_Qs_Pos(i1) = 0;
    end
    if Jan_Qs(i1)<0
        Jan_Qs_Neg(i1) = Jan_Qs(i1);
    else
        Jan_Qs_Neg(i1) = 0;
    end
end
Jan_Qs_sum_Pos = sum(Jan_Qs_Pos);
Jan_Qs_sum_Neg = sum(Jan_Qs_Neg);
Feb_Qs = Qs(745:1416);
for i2 = 1:672
    if Feb_Qs(i2)>=0
        Feb_Qs_Pos(i2) = Feb_Qs(i2);
    else
        Feb_Qs_Pos(i2) = 0;
    end
    if Feb_Qs(i2)<0
        Feb_Qs_Neg(i2) = Feb_Qs(i2);
    else
        Feb_Qs_Neg(i2) = 0;
    end
end
Feb_Qs_sum_Pos = sum(Feb_Qs_Pos);
Feb_Qs_sum_Neg = sum(Feb_Qs_Neg);
March_Qs = Qs(1417:2160);
for i3 = 1:744
    if March_Qs(i3)>=0
        March_Qs_Pos(i3) = March_Qs(i3);
    else
        March_Qs_Pos(i3) = 0;
    end
    if March_Qs(i3)<0
        March_Qs_Neg(i3) = March_Qs(i3);
    else
        March_Qs_Neg(i3) = 0;
    end
end
March_Qs_sum_Pos = sum(March_Qs_Pos);
March_Qs_sum_Neg = sum(March_Qs_Neg);
April_Qs = Qs(2161:2880);
for i4 = 1:720
    if April_Qs(i4)>=0
        April_Qs_Pos(i4) = April_Qs(i4);
    else
        April_Qs_Pos(i4) = 0;
    end
    if April_Qs(i4)<0
        April_Qs_Neg(i4) = April_Qs(i4);
```

```
    else
        April_Qs_Neg(i4) = 0;
    end
end
April_Qs_sum_Pos = sum(April_Qs_Pos);
April_Qs_sum_Neg = sum(April_Qs_Neg);
May_Qs = Qs(2881:3624);
for i5 = 1:744
    if May_Qs(i5)>=0
        May_Qs_Pos(i5) = May_Qs(i5);
    else
        May_Qs_Pos(i5) = 0;
    end
    if May_Qs(i5)<0
        May_Qs_Neg(i5) = May_Qs(i5);
    else
        May_Qs_Neg(i5) = 0;
    end
end
May_Qs_sum_Pos = sum(May_Qs_Pos);
May_Qs_sum_Neg = sum(May_Qs_Neg);
June_Qs = Qs(3625:4344);
for i6 = 1:720
    if June_Qs(i6)>=0
        June_Qs_Pos(i6) = June_Qs(i6);
    else
        June_Qs_Pos(i6) = 0;
    end
    if June_Qs(i6)<0
        June_Qs_Neg(i6) = June_Qs(i6);
    else
        June_Qs_Neg(i6) = 0;
    end
end
June_Qs_sum_Pos = sum(June_Qs_Pos);
June_Qs_sum_Neg = sum(June_Qs_Neg);
July_Qs = Qs(4344:5088);
for i7 = 1:745
    if July_Qs(i7)>=0
        July_Qs_Pos(i7) = July_Qs(i7);
    else
        July_Qs_Pos(i7) = 0;
    end
    if July_Qs(i7)<0
        July_Qs_Neg(i7) = July_Qs(i7);
    else
        July_Qs_Neg(i7) = 0;
    end
end
July_Qs_sum_Pos = sum(July_Qs_Pos);
July_Qs_sum_Neg = sum(July_Qs_Neg);
Aug_Qs = Qs(5089:5832);
for i8 = 1:744
    if Aug_Qs(i8)>=0
        Aug_Qs_Pos(i8) = Aug_Qs(i8);
    else
        Aug_Qs_Pos(i8) = 0;
    end
    if Aug_Qs(i8)<0
        Aug_Qs_Neg(i8) = Aug_Qs(i8);
    else
        Aug_Qs_Neg(i8) = 0;
    end
end
Aug_Qs_sum_Pos = sum(Aug_Qs_Pos);
Aug_Qs_sum_Neg = sum(Aug_Qs_Neg);
Sep_Qs = Qs(5833:6552);
for i9 = 1:720
```

```
    if Sep_Qs(i9)>=0
        Sep_Qs_Pos(i9) = Sep_Qs(i9);
    else
        Sep_Qs_Pos(i9) = 0;
    end
    if Sep_Qs(i9)<0
        Sep_Qs_Neg(i9) = Sep_Qs(i9);
    else
        Sep_Qs_Neg(i9) = 0;
    end
end
Sep_Qs_sum_Pos = sum(Sep_Qs_Pos);
Sep_Qs_sum_Neg = sum(Sep_Qs_Neg);
Oct_Qs = Qs(6553:7296);
for i10 = 1:744
    if Oct_Qs(i10)>=0
        Oct_Qs_Pos(i10) = Oct_Qs(i10);
    else
        Oct_Qs_Pos(i10) = 0;
    end
    if Oct_Qs(i10)<0
        Oct_Qs_Neg(i10) = Oct_Qs(i10);
    else
        Oct_Qs_Neg(i10) = 0;
    end
end
Oct_Qs_sum_Pos = sum(Oct_Qs_Pos);
Oct_Qs_sum_Neg = sum(Oct_Qs_Neg);
Nov_Qs = Qs(7297:8016);
for i11 = 1:720
    if Nov_Qs(i11)>=0
        Nov_Qs_Pos(i11) = Nov_Qs(i11);
    else
        Nov_Qs_Pos(i11) = 0;
    end
    if Nov_Qs(i11)<0
        Nov_Qs_Neg(i11) = Nov_Qs(i11);
    else
        Nov_Qs_Neg(i11) = 0;
    end
end
Nov_Qs_sum_Pos = sum(Nov_Qs_Pos);
Nov_Qs_sum_Neg = sum(Nov_Qs_Neg);
Dec_Qs = Qs(8017:8760);
for i12 = 1:744
    if Dec_Qs(i12)>=0
        Dec_Qs_Pos(i12) = Dec_Qs(i12);
    else
        Dec_Qs_Pos(i12) = 0;
    end
    if Dec_Qs(i12)<0
        Dec_Qs_Neg(i12) = Dec_Qs(i12);
    else
        Dec_Qs_Neg(i12) = 0;
    end
end
Dec_Qs_sum_Pos = sum(Dec_Qs_Pos);
Dec_Qs_sum_Neg = sum(Dec_Qs_Neg);
Qs_Pos_annual_sum = Jan_Qs_sum_Pos +
Feb_Qs_sum_Pos+March_Qs_sum_Pos+April_Qs_sum_Pos+May_Qs_sum_Pos+June_Qs_sum_Pos+Jul
y_Qs_sum_Pos+Aug_Qs_sum_Pos+Sep_Qs_sum_Pos+Oct_Qs_sum_Pos+Nov_Qs_sum_Pos+Dec_Qs_sum
_Pos
Qs_Neg_annual_sum = Jan_Qs_sum_Neg +
Feb_Qs_sum_Neg+March_Qs_sum_Neg+April_Qs_sum_Neg+May_Qs_sum_Neg+June_Qs_sum_Neg+Jul
y_Qs_sum_Neg+Aug_Qs_sum_Neg+Sep_Qs_sum_Neg+Oct_Qs_sum_Neg+Nov_Qs_sum_Neg+Dec_Qs_sum
_Neg
%%
```

```
a = [Jan_Heating_Consumption_sum, Feb_Heating_Consumption_sum,
March_Heating_Consumption_sum, April_Heating_Consumption_sum,
May_Heating_Consumption_sum, June_Heating_Consumption_sum,
July_Heating_Consumption_sum, Aug_Heating_Consumption_sum,
Sep_Heating_Consumption_sum, Oct_Heating_Consumption_sum,
Nov_Heating_Consumption_sum, Dec_Heating_Consumption_sum];
b = [Jan_Cooling_Consumption_sum, Feb_Cooling_Consumption_sum,
March_Cooling_Consumption_sum, April_Cooling_Consumption_sum,
May_Cooling_Consumption_sum, June_Cooling_Consumption_sum,
July_Cooling_Consumption_sum, Aug_Cooling_Consumption_sum,
Sep_Cooling_Consumption_sum, Oct_Cooling_Consumption_sum,
Nov_Cooling_Consumption_sum, Dec_Cooling_Consumption_sum];
c = [Jan_Qi_sum, Feb_Qi_sum, March_Qi_sum, April_Qi_sum, May_Qi_sum, June_Qi_sum,
July_Qi_sum, Aug_Qi_sum, Sep_Qi_sum, Oct_Qi_sum, Nov_Qi_sum, Dec_Qi_sum];
d = [Jan_PV_Generation_sum, Feb_PV_Generation_sum, March_PV_Generation_sum,
April_PV_Generation_sum, May_PV_Generation_sum, June_PV_Generation_sum,
July_PV_Generation_sum, Aug_PV_Generation_sum, Sep_PV_Generation_sum,
Oct_PV_Generation_sum, Nov_PV_Generation_sum, Dec_PV_Generation_sum];
e = [Jan_Solar_Thermal_Production_sum, Feb_Solar_Thermal_Production_sum,
March_Solar_Thermal_Production_sum, April_Solar_Thermal_Production_sum,
May_Solar_Thermal_Production_sum, June_Solar_Thermal_Production_sum,
July_Solar_Thermal_Production_sum, Aug_Solar_Thermal_Production_sum,
Sep_Solar_Thermal_Production_sum, Oct_Solar_Thermal_Production_sum,
Nov_Solar_Thermal_Production_sum, Dec_Solar_Thermal_Production_sum];
f =
[Jan_Qs_sum_Pos,Feb_Qs_sum_Pos,March_Qs_sum_Pos,April_Qs_sum_Pos,May_Qs_sum_Pos,Jun
e_Qs_sum_Pos,July_Qs_sum_Pos,Aug_Qs_sum_Pos,Sep_Qs_sum_Pos,Oct_Qs_sum_Pos,Nov_Qs_su
m_Pos,Dec_Qs_sum_Pos];
g =
[Jan_Qs_sum_Neg,Feb_Qs_sum_Neg,March_Qs_sum_Neg,April_Qs_sum_Neg,May_Qs_sum_Neg,Jun
e_Qs_sum_Neg,July_Qs_sum_Neg,Aug_Qs_sum_Neg,Sep_Qs_sum_Neg,Oct_Qs_sum_Neg,Nov_Qs_su
m_Neg,Dec_Qs_sum_Neg];
%%
% figure(1)
% bar(a)
% title('Heating Consumption')
% ylabel('kWh')
% figure(2)
% bar(b)
% title('Cooling Consumption')
% ylabel('kWh')
figure(1)
bar(c)
title('Qi')
ylabel('kWh')
figure(2)
bar(d)
title('PV Generation')
ylabel('kWh')
% figure(5)
% bar(e)
% title('Solar Thermal Production')
% ylabel('kWh')
figure(3)
bar(f)
title('Qs Positive')
ylabel('kWh')
figure(4)
bar(g)
title('Qs Negative')
ylabel('kWh')
```

Appendix D

Climate file generated by Meteonorm for London.

File Edit Format View Help

London UK
51.507,-0.1279,18,0

dm	m	h	G_Dh	G_Bn	Ta	Ts	FF	DD	RH	RR	N
1	1	1	0	0	12.7	9.9	1.4	218	79	4.6	8
1	1	2	0	0	13.3	10.3	1.0	252	73	0.3	8
1	1	3	0	0	13.0	9.9	0.8	249	73	0.4	8
1	1	4	0	0	12.9	10.0	1.1	265	73	0.2	8
1	1	5	0	0	12.8	9.8	1.1	263	73	0.1	8
1	1	6	0	0	12.7	9.9	1.4	252	61	0.0	8
1	1	7	0	0	12.6	9.6	1.1	276	73	0.1	8
1	1	8	0	0	12.5	9.9	1.8	237	58	0.0	8
1	1	9	2	0	12.5	11.9	1.4	214	60	0.0	8
1	1	10	10	0	12.4	12.0	3.3	298	62	0.1	8
1	1	11	18	0	12.4	12.0	2.4	185	73	0.2	8
1	1	12	23	0	12.4	12.1	2.4	226	73	0.0	8
1	1	13	25	0	12.4	12.1	2.8	235	57	0.0	8
1	1	14	20	0	12.4	12.0	3.1	148	56	0.1	8
1	1	15	12	0	12.4	11.9	2.6	190	58	0.0	8
1	1	16	3	0	12.3	11.8	4.0	221	73	0.3	8
1	1	17	0	0	12.1	10.0	2.6	126	73	0.6	8
1	1	18	0	0	11.9	10.0	3.1	200	78	1.1	8
1	1	19	0	0	11.5	9.3	2.4	187	78	2.2	8
1	1	20	0	0	11.7	9.5	2.4	236	73	0.7	8
1	1	21	0	0	11.4	9.2	2.4	249	78	1.5	8
1	1	22	0	0	11.4	8.8	1.6	210	73	0.9	8
1	1	23	0	0	11.4	8.5	1.1	265	73	0.5	8
1	1	24	0	0	11.4	8.4	1.0	216	78	0.0	8
2	1	1	0	0	11.2	8.3	1.2	247	78	0.0	8
2	1	2	0	0	10.8	8.6	2.4	220	73	0.8	8
2	1	3	0	0	10.8	9.1	3.7	235	73	0.2	8
2	1	4	0	0	10.7	8.9	3.3	155	78	0.0	8
2	1	5	0	0	10.6	9.0	4.0	187	78	0.0	8
2	1	6	0	0	10.5	8.6	3.1	125	78	0.0	8

Appendix E

The Excel tool for calculating the required data before and after simulation trials.

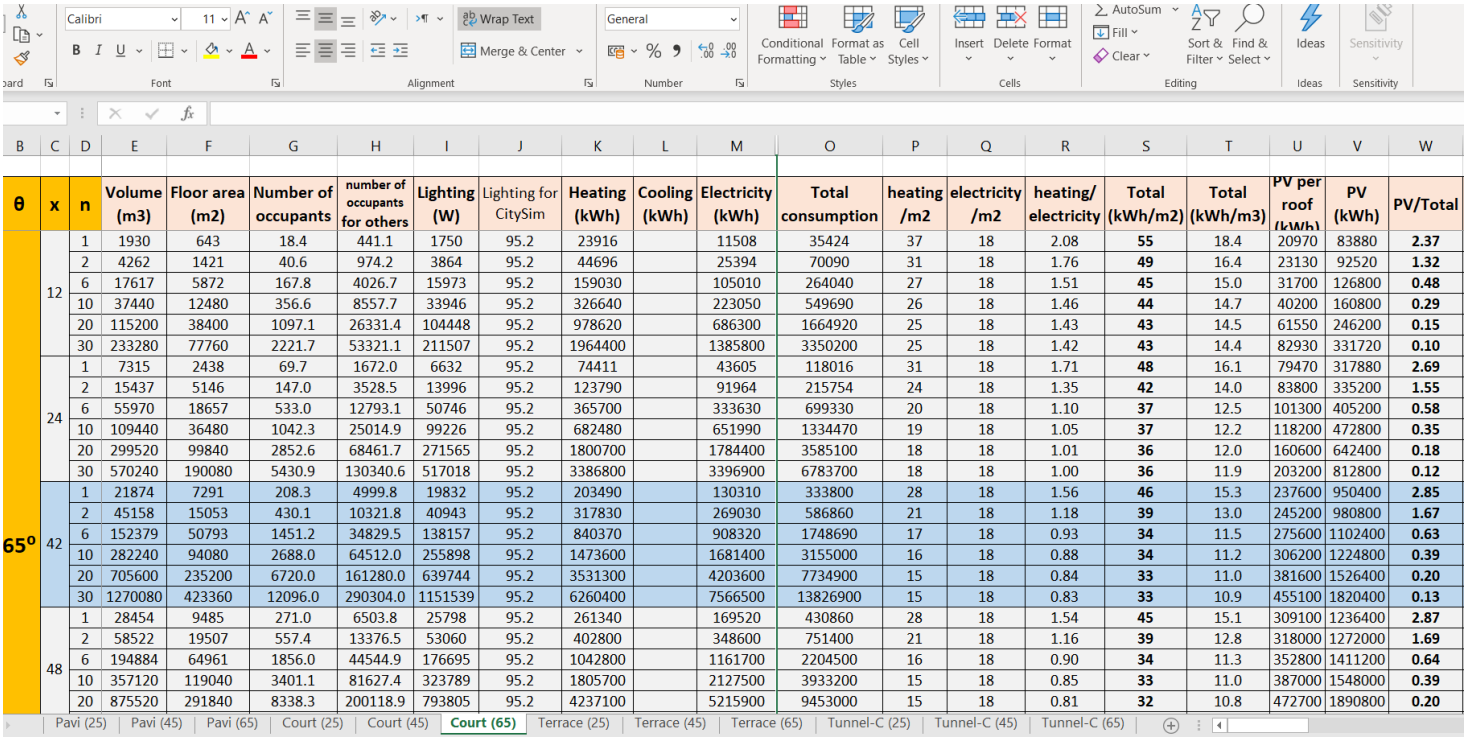

θ	x	n	Volume (m3)	Floor area (m2)	Number of occupants	number of occupants for others	Lighting (W)	Lighting for CitySim	Heating (kWh)	Cooling (kWh)	Electricity (kWh)	Total consumption	heating /m2	electricity /m2	heating/ electricity	Total (kWh/m2)	Total (kWh/m3)	PV per roof (kWh)	PV (kWh)	PV/Total
65°	12	1	1930	643	18.4	441.1	1750	95.2	23916		11508	35424	37	18	2.08	55	18.4	20970	83880	2.37
		2	4262	1421	40.6	974.2	3864	95.2	44696		25394	70090	31	18	1.76	49	16.4	23130	92520	1.32
		6	17617	5872	167.8	4026.7	15973	95.2	159030		105010	264040	27	18	1.51	45	15.0	31700	126800	0.48
		10	37440	12480	356.6	8557.7	33946	95.2	326640		223050	549690	26	18	1.46	44	14.7	40200	160800	0.29
		20	115200	38400	1097.1	26331.4	104448	95.2	978620		686300	1664920	25	18	1.43	43	14.5	61550	246200	0.15
		30	233280	77760	2221.7	53321.1	211507	95.2	1964400		1385800	3350200	25	18	1.42	43	14.4	82930	331720	0.10
	24	1	7315	2438	69.7	1672.0	6632	95.2	74411		43605	118016	31	18	1.71	48	16.1	79470	317880	2.69
		2	15437	5146	147.0	3528.5	13996	95.2	123790		91964	215754	24	18	1.35	42	14.0	83800	335200	1.55
		6	55970	18657	533.0	12793.1	50746	95.2	365700		333630	699330	20	18	1.10	37	12.5	101300	405200	0.58
		10	109440	36480	1042.3	25014.9	99226	95.2	682480		651990	1334470	19	18	1.05	37	12.2	118200	472800	0.35
		20	299520	99840	2852.6	68461.7	271565	95.2	1800700		1784400	3585100	18	18	1.01	36	12.0	160600	642400	0.18
		30	570240	190080	5430.9	130340.6	517018	95.2	3386800		3396900	6783700	18	18	1.00	36	11.9	203200	812800	0.12
	42	1	21874	7291	208.3	4999.8	19832	95.2	203490		130310	333800	28	18	1.56	46	15.3	237600	950400	2.85
		2	45158	15053	430.1	10321.8	40943	95.2	317830		269030	586860	21	18	1.18	39	13.0	245200	980800	1.67
		6	152379	50793	1451.2	34829.5	138157	95.2	840370		908320	1748690	17	18	0.93	34	11.5	275600	1102400	0.63
		10	282240	94080	2688.0	64512.0	255898	95.2	1473600		1681400	3155000	16	18	0.88	34	11.2	306200	1224800	0.39
		20	705600	235200	6720.0	161280.0	639744	95.2	3531300		4203600	7734900	15	18	0.84	33	11.0	381600	1526400	0.20
		30	1270080	423360	12096.0	290304.0	1151539	95.2	6260400		7566500	13826900	15	18	0.83	33	10.9	455100	1820400	0.13
	48	1	28454	9485	271.0	6503.8	25798	95.2	261340		169520	430860	28	18	1.54	45	15.1	309100	1236400	2.87
		2	58522	19507	557.4	13376.5	53060	95.2	402800		348600	751400	21	18	1.16	39	12.8	318000	1272000	1.69
		6	194884	64961	1856.0	44544.9	176695	95.2	1042800		1161700	2204500	16	18	0.90	34	11.3	352800	1411200	0.64
		10	357120	119040	3401.1	81627.4	323789	95.2	1805700		2127500	3933200	15	18	0.85	33	11.0	387000	1548000	0.39
		20	875520	291840	8338.3	200118.9	793805	95.2	4237100		5215900	9453000	15	18	0.81	32	10.8	472700	1890800	0.20

Appendix F

MATLAB code written for providing heat map of energy on the *Form Signature* graphs.

```
C_plot = [0.01 0.05 0.08 0.1 0.2 0.3 0.4 0.5 0.6 0.7 0.8 0.9 1];
Cn1_plot = [0.01 0.05 0.08 0.1 0.2 0.3 0.4 0.5 0.6 0.7 0.8 0.9 1];
Cn2_plot = [0.02 0.1 0.16 0.2 0.4 0.6 0.8 1 1.2 1.4 1.6 1.8 2];
Cn3_plot = [0.03 0.15 0.24 0.3 0.6 0.9 1.2 1.5 1.8 2.1 2.4 2.7 3];
Cn4_plot = [0.04 0.2 0.32 0.4 0.8 1.2 1.6 2 2.4 2.8 3.2 3.6 4];
Cn5_plot = [0.05 0.25 0.4 0.5 1 1.5 2 2.5 3 3.5 4 4.5 5];
Cn6_plot = [0.06 0.3 0.48 0.6 1.2 1.8 2.4 3 3.6 4.2 4.8 5.4 6];
Cn7_plot = [0.07 0.35 0.56 0.7 1.4 2.1 2.8 3.5 4.2 4.9 5.6 6.3 7];
Cn8_plot = [0.08 0.4 0.64 0.8 1.6 2.4 3.2 4 4.8 5.6 6.4 7.2 8];
Cn9_plot = [0.09 0.45 0.72 0.9 1.8 2.7 3.6 4.5 5.4 6.3 7.2 8.1 9];
Cn10_plot = [0.1 0.5 0.8 1 2 3 4 5 6 7 8 9 10];
Cn11_plot = [0.11 0.55 0.88 1.1 2.2 3.3 4.4 5.5 6.6 7.7 8.8 9.9 11];
Cn12_plot = [0.12 0.6 0.96 1.2 2.4 3.6 4.8 6 7.2 8.4 9.6 10.8 12];
Cn13_plot = [0.13 0.65 1.04 1.3 2.6 3.9 5.2 6.5 7.8 9.1 10.4 11.7 13];
Cn14_plot = [0.14 0.7 1.12 1.4 2.8 4.2 5.6 7 8.4 9.8 11.2 12.6 14];
Cn15_plot = [0.15 0.75 1.2 1.5 3 4.5 6 7.5 9 10.5 12 13.5 15];
Cn16_plot = [0.16 0.8 1.28 1.6 3.2 4.8 6.4 8 9.6 11.2 12.8 14.4 16];
Cn17_plot = [0.17 0.85 1.36 1.7 3.4 5.1 6.8 8.5 10.2 11.9 13.6 15.3 17];
Cn18_plot = [0.18 0.9 1.4 1.8 3.6 5.4 7.2 9 10.8 12.6 14.4 16.2 18];
Cn19_plot = [0.19 0.95 1.52 1.9 3.8 5.7 7.6 9.5 11.4 13.3 15.2 17.1 19];
Cn20_plot = [0.2 1 1.6 2 4 6 8 10 12 14 16 18 20];
Cn21_plot = [0.21 1.05 1.68 2.1 4.2 6.3 8.4 10.5 12.6 14.7 16.8 18.9 21];
Cn22_plot = [0.22 1.1 1.76 2.2 4.4 6.6 8.8 11 13.2 15.4 17.6 19.8 22];
Cn23_plot = [0.23 1.15 1.84 2.3 4.6 6.9 9.2 11.5 13.8 16.1 18.4 20.7 23];
Cn24_plot = [0.24 1.2 1.92 2.4 4.8 7.2 9.6 12 14.4 16.8 19.2 21.6 24];
Cn25_plot = [0.25 1.25 2 2.5 5 7.5 10 12.5 15 17.5 20 22.5 25];
Cn26_plot = [0.26 1.3 2.08 2.6 5.2 7.8 10.4 13 15.6 18.2 20.8 23.4 26];
Cn27_plot = [0.27 1.35 2.16 2.7 5.4 8.1 10.8 13.5 16.2 18.9 21.6 24.3 27];
Cn28_plot = [0.28 1.4 2.24 2.8 5.6 8.4 11.2 14 16.8 19.6 22.4 25.2 28];
Cn29_plot = [0.29 1.45 2.32 2.9 5.8 8.7 11.6 14.5 17.4 20.3 23.2 26.1 29];
Cn30_plot = [0.3 1.5 2.4 3 6 9 12 15 18 21 24 27 30];
Sc6_plot = [0.44444 0.25000 0.16000 0.11111 0.08163 0.06250 0.04938 0.04000 0.03306
0.02778 0.02367 0.02041 0.01778 0.01563 0.01384 0.01235 0.01108 0.01000 0.00907
0.00826 0.00756 0.00694 0.00640 0.00592 0.00549 0.00510 0.00476 0.00444 0.00416
0.00391 0.00367 0.00346 0.00327 0.00309 0.00292 0.00277 0.00263 0.00250 0.00238
0.00227];
P6_plot = [0.44444  0.50000 0.48000 0.44444 0.40816 0.37500 0.34568 0.32000 0.29752
0.27778 0.26036 0.24490 0.23111 0.21875 0.20761 0.19753 0.18837 0.18000 0.17234
0.16529 0.15879 0.15278 0.14720 0.14201 0.13717 0.13265 0.12842 0.12444 0.12071
0.11719 0.11387 0.11073 0.10776 0.10494 0.10226 0.09972 0.09730 0.09500 0.09280
0.09070];
Sc12_plot = [0.64000 0.44444 0.32653    0.25000 0.19753 0.16000 0.13223 0.11111
0.09467 0.08163 0.07111 0.06250 0.05536 0.04938 0.04432 0.04000 0.03628 0.03306
0.03025 0.02778 0.02560 0.02367 0.02195 0.02041 0.01902 0.01778 0.01665 0.01563
0.01469 0.01384 0.01306 0.01235 0.01169 0.01108 0.01052 0.01000 0.00952 0.00907
0.00865 0.00826];
P12_plot = [0.64000 0.88889 0.97959 1.00000 0.98765 0.96000 0.92562 0.88889 0.85207
0.81633 0.78222 0.75000 0.71972 0.69136 0.66482 0.64000 0.61678 0.59504 0.57467
0.55556 0.53760 0.52071 0.50480 0.48980 0.47562 0.46222 0.44953 0.43750 0.42608
0.41522 0.40490 0.39506 0.38568 0.37673 0.36818 0.36000 0.35217 0.34467 0.33748
0.33058];
Sc18_plot = [0.73469    0.56250 0.44444 0.36000 0.29752 0.25000 0.21302 0.18367
0.16000 0.14063 0.12457 0.11111 0.09972 0.09000 0.08163 0.07438 0.06805 0.06250
0.05760 0.05325 0.04938 0.04592 0.04281 0.04000 0.03746 0.03516 0.03306 0.03114
0.02939 0.02778 0.02630 0.02493 0.02367 0.02250 0.02142 0.02041 0.01947 0.01860
0.01778 0.01701];
P18_plot = [0.73469 1.12500 1.33333 1.44000 1.48760 1.50000 1.49112 1.46939 1.44000
1.40625 1.37024 1.33333 1.29640 1.26000 1.22449 1.19008 1.15690 1.12500 1.09440
1.06509 1.03704 1.01020 0.98454 0.96000 0.93652 0.91406 0.89256 0.87197 0.85224
0.83333 0.81519 0.79778 0.78107 0.76500 0.74955 0.73469 0.72039 0.70661 0.69333
0.68053];
```

```
Sc24_plot = [0.79012    0.64000 0.52893 0.44444 0.37870 0.32653 0.28444 0.25000
0.22145 0.19753 0.17729 0.16000 0.14512 0.13223 0.12098 0.11111 0.10240 0.09467
0.08779 0.08163 0.07610 0.07111 0.06660 0.06250 0.05877 0.05536 0.05224 0.04938
0.04675 0.04432 0.04208 0.04000 0.03807 0.03628 0.03461 0.03306 0.03160 0.03025
0.02897 0.02778];
P24_plot = [0.79012 1.28000 1.58678 1.77778 1.89349 1.95918 1.99111 2.00000 1.99308
1.97531 1.95014 1.92000 1.88662 1.85124 1.81474 1.77778 1.74080 1.70414 1.66804
1.63265 1.59810 1.56444 1.53174 1.50000 1.46924 1.43945 1.41061 1.38272 1.35573
1.32964 1.30440 1.28000 1.25640 1.23356 1.21147 1.19008 1.16938 1.14934 1.12992
1.11111];
Sc30_plot = [0.82645    0.69444 0.59172 0.51020 0.44444 0.39063 0.34602 0.30864
0.27701 0.25000 0.22676 0.20661 0.18904 0.17361 0.16000 0.14793 0.13717 0.12755
0.11891 0.11111 0.10406 0.09766 0.09183 0.08651 0.08163 0.07716 0.07305 0.06925
0.06575 0.06250 0.05949 0.05669 0.05408 0.05165 0.04938 0.04726 0.04527 0.04340
0.04165 0.04000];
P30_plot = [0.82645 1.38889 1.77515 2.04082 2.22222 2.34375 2.42215 2.46914 2.49307
2.50000 2.49433 2.47934 2.45747 2.43056 2.40000 2.36686 2.33196 2.29592 2.25922
2.22222 2.18522 2.14844 2.11203 2.07612 2.04082 2.00617 1.97224 1.93906 1.90664
1.87500 1.84414 1.81406 1.78475 1.75620 1.72840 1.70132 1.67497 1.64931 1.62432
1.60000];
Sc36_plot = [0.85207    0.73469 0.64000 0.56250 0.49827 0.44444 0.39889 0.36000
0.32653 0.29752 0.27221 0.25000 0.23040 0.21302 0.19753 0.18367 0.17122 0.16000
0.14984 0.14063 0.13223 0.12457 0.11755 0.11111 0.10519 0.09972 0.09467 0.09000
0.08566 0.08163 0.07788 0.07438 0.07111 0.06805 0.06519 0.06250 0.05998 0.05760
0.05536 0.05325];
P36_plot = [0.85207 1.46939 1.92000 2.25000 2.49135 2.66667 2.79224 2.88000 2.93878
2.97521 2.99433 3.00000 2.99520 2.98225 2.96296 2.93878 2.91082 2.88000 2.84703
2.81250 2.77686 2.74048 2.70367 2.66667 2.62966 2.59280 2.55621 2.52000 2.48424
2.44898 2.41428 2.38017 2.34667 2.31380 2.28158 2.25000 2.21908 2.18880 2.15917
2.13018];
Sc42_plot = [0.87111    0.76563 0.67820 0.60494 0.54294 0.49000 0.44444 0.40496
0.37051 0.34028 0.31360 0.28994 0.26886 0.25000 0.23306 0.21778 0.20395 0.19141
0.17998 0.16955 0.16000 0.15123 0.14317 0.13573 0.12886 0.12250 0.11660 0.11111
0.10600 0.10124 0.09679 0.09263 0.08873 0.08507 0.08163 0.07840 0.07536 0.07249
0.06978 0.06722];
P42_plot = [0.87111 1.53125 2.03460 2.41975 2.71468 2.94000 3.11111 3.23967 3.33459
3.40278 3.44960 3.47929 3.49520 3.50000 3.49584 3.48444 3.46722 3.44531 3.41965
3.39100 3.36000 3.32716 3.29291 3.25762 3.22156 3.18500 3.14813 3.11111 3.07409
3.03719 3.00049 2.96408 2.92802 2.89236 2.85714 2.82240 2.78816 2.75444 2.72125
2.68861];
Sc48_plot = [0.88581    0.79012 0.70914 0.64000 0.58050 0.52893 0.48393 0.44444
0.40960 0.37870 0.35117 0.32653 0.30440 0.28444 0.26639 0.25000 0.23508 0.22145
0.20898 0.19753 0.18700 0.17729 0.16831 0.16000 0.15229 0.14512 0.13845 0.13223
0.12642 0.12098 0.11589 0.11111 0.10662 0.10240 0.09842 0.09467 0.09114 0.08779
0.08463 0.08163];
P48_plot = [0.88581 1.58025 2.12742 2.56000 2.90249 3.17355 3.38752 3.55556 3.68640
3.78698 3.86283 3.91837 3.95719 3.98222 3.99584 4.00000 3.99633 3.98616 3.97061
3.95062 3.92695 3.90028 3.87114 3.84000 3.80726 3.77324 3.73824 3.70248 3.66617
3.62949 3.59258 3.55556 3.51853 3.48160 3.44483 3.40828 3.37202 3.33608 3.30050
3.26531];
Sc54_plot = [0.89751    0.81000 0.73469 0.66942 0.61248 0.56250 0.51840 0.47929
0.44444 0.41327 0.38526 0.36000 0.33715 0.31641 0.29752 0.28028 0.26449 0.25000
0.23667 0.22438 0.21302 0.20250 0.19274 0.18367 0.17523 0.16736 0.16000 0.15312
0.14667 0.14063 0.13494 0.12960 0.12457 0.11982 0.11534 0.11111 0.10711 0.10332
0.09972 0.09631];
P54_plot = [0.89751 1.62000 2.20408 2.67769 3.06238 3.37500 3.62880 3.83432 4.00000
4.13265 4.23781 4.32000 4.38293 4.42969 4.46281 4.48443 4.49633 4.50000 4.49671
4.48753 4.47337 4.45500 4.43308 4.40816 4.38075 4.35124 4.32000 4.28733 4.25351
4.21875 4.18326 4.14720 4.11073 4.07396 4.03702 4.00000 3.96298 3.92602 3.88920
3.85256];
Sc60_plot = [0.90703    0.82645 0.75614 0.69444 0.64000 0.59172 0.54870 0.51020
0.47562 0.44444 0.41623 0.39063 0.36731 0.34602 0.32653 0.30864 0.29218 0.27701
0.26298 0.25000 0.23795 0.22676 0.21633 0.20661 0.19753 0.18904 0.18108 0.17361
0.16660 0.16000 0.15379 0.14793 0.14240 0.13717 0.13223 0.12755 0.12311 0.11891
0.11491 0.11111];
P60_plot = [0.90703 1.65289 2.26843 2.77778 3.20000 3.55030 3.84088 4.08163 4.28062
4.44444 4.57856 4.68750 4.77502 4.84429 4.89796 4.93827 4.96713 4.98615 4.99671
5.00000 4.99703 4.98866 4.97566 4.95868 4.93827 4.91493 4.88909 4.86111 4.83132
```

```
4.80000 4.76740 4.73373 4.69918 4.66392 4.62810 4.59184 4.55525 4.51843 4.48147
4.44444];
plot(C_plot,Cn1_plot,'k','LineWidth',0.5);
t = text(1.2,8,'Energy demand (kWh/m2)','rotation',-90,'FontSize',14)
t = text(1.025,7,'Number of storeys','rotation',-90,'FontSize',14)
t = text(1.017,1,'1')
t = text(1.005,8,'8')
t = text(0.8,10.2,'12')
t = text(0.29,10.15,'30')
t = text(0.02,3.4,'Plan depth (m)','rotation',73,'FontSize',14)
t = text(-0.01,0.3,'6')
t = text(0.07,4.5,'60')
hold on
title('London-Pavilion (\theta=45°)','FontSize',14)
ylabel('Plot ratio','FontSize',14)
xlabel('Site coverage','FontSize',14)
plot(C_plot,Cn2_plot,'k','LineWidth',0.5);
hold on
plot(C_plot,Cn3_plot,'k','LineWidth',0.5);
hold on
plot(C_plot,Cn4_plot,'k','LineWidth',0.5);
hold on
plot(C_plot,Cn5_plot,'k','LineWidth',0.5);
hold on
plot(C_plot,Cn6_plot,'k','LineWidth',0.5);
hold on
plot(C_plot,Cn7_plot,'k','LineWidth',0.5);
hold on
plot(C_plot,Cn8_plot,'k','LineWidth',0.5);
hold on
plot(C_plot,Cn9_plot,'k','LineWidth',0.5);
hold on
plot(C_plot,Cn10_plot,'k','LineWidth',0.5);
hold on
plot(C_plot,Cn11_plot,'k','LineWidth',0.5);
hold on
plot(C_plot,Cn12_plot,'k','LineWidth',0.5);
hold on
plot(C_plot,Cn13_plot,'k','LineWidth',0.5);
hold on
plot(C_plot,Cn14_plot,'k','LineWidth',0.5);
hold on
plot(C_plot,Cn15_plot,'k','LineWidth',0.5);
hold on
plot(C_plot,Cn16_plot,'k','LineWidth',0.5);
hold on
plot(C_plot,Cn17_plot,'k','LineWidth',0.5);
hold on
plot(C_plot,Cn18_plot,'k','LineWidth',0.5);
hold on
plot(C_plot,Cn19_plot,'k','LineWidth',0.5);
hold on
plot(C_plot,Cn20_plot,'k','LineWidth',0.5);
hold on
plot(C_plot,Cn21_plot,'k','LineWidth',0.5);
hold on
plot(C_plot,Cn22_plot,'k','LineWidth',0.5);
hold on
plot(C_plot,Cn23_plot,'k','LineWidth',0.5);
hold on
plot(C_plot,Cn24_plot,'k','LineWidth',0.5);
hold on
plot(C_plot,Cn25_plot,'k','LineWidth',0.5);
hold on
plot(C_plot,Cn26_plot,'k','LineWidth',0.5);
hold on
plot(C_plot,Cn27_plot,'k','LineWidth',0.5);
hold on
```

```
plot(C_plot,Cn28_plot,'k','LineWidth',0.5);
hold on
plot(C_plot,Cn29_plot,'k','LineWidth',0.5);
hold on
plot(C_plot,Cn30_plot,'k','LineWidth',0.5);
hold on
plot(Sc6_plot,P6_plot,'k','LineWidth',0.5);
hold on
plot(Sc12_plot,P12_plot,'k','LineWidth',0.5);
hold on
plot(Sc18_plot,P18_plot,'k','LineWidth',0.5);
hold on
plot(Sc24_plot,P24_plot,'k','LineWidth',0.5);
hold on
plot(Sc30_plot,P30_plot,'k','LineWidth',0.5);
hold on
plot(Sc36_plot,P36_plot,'k','LineWidth',0.5);
hold on
plot(Sc42_plot,P42_plot,'k','LineWidth',0.5);
hold on
plot(Sc48_plot,P48_plot,'k','LineWidth',0.5);
hold on
plot(Sc54_plot,P54_plot,'k','LineWidth',0.5);
hold on
plot(Sc60_plot,P60_plot,'k','LineWidth',0.5);
hold on
xlim([0 1])
ylim([0 10])
xref = [0.640, 0.444, 0.160, 0.082, 0.028, 0.014, 0.790, 0.640, 0.327, 0.198,
0.082, 0.044, 0.852, 0.735, 0.444, 0.298, 0.141, 0.816, 0.907, 0.826, 0.592, 0.444,
0.250, 0.160];
yref = [0.640, 0.889, 0.960, 0.816, 0.556, 0.415, 0.790, 1.280, 1.959, 1.975,
1.633, 1.330, 0.852, 1.469, 2.667, 2.975, 2.813, 2.449, 0.907, 1.653, 3.550, 4.444,
5.000, 4.800];
zref = [64, 58, 53, 51, 50, 49, 52, 46, 41, 40, 39, 38, 48, 42, 37, 36, 35, 35, 46,
39, 34, 33, 33, 32];
edge_strength = 10;
% e.g. 400x400 image
resolution = 500;
%axis tight;
hold on;
colormap jet;
drawnow;
xlims = xlim;
ylims = ylim;
xstep = diff(xlims)./resolution;
ystep = diff(ylims)./resolution;
xs = xlims(1):xstep:xlims(2);
ys = ylims(1):ystep:ylims(2);
heatmap = zeros(size(xs,2),size(ys,2));
for xi=1:size(xs,2)
    x = xs(xi);
    for yi=1:size(ys,2)
        y = ys(yi);
        distances = sqrt( ((x-xref)./xstep).^2 + ((y-yref)/ystep).^2 );
        weights_unnormalized = (max(distances) - distances).^edge_strength;
        weights = weights_unnormalized./sum(weights_unnormalized);
        heatmap(xi,yi) = sum(weights.*zref);
    end
end
hm = image(xlim,ylim,heatmap');
hm.CDataMapping = 'scaled';
uistack(hm, 'bottom');
colorbar;
triangle = fill([0.008 1 1], [0 0 1], "white")
set(triangle,'EdgeColor','none')
hold off;
```